Investigating the role of Hu RNA-binding proteins in Neuroblastoma, Glioblastoma and Small cell lung cancer

Siverns, Sarah

Award date:
2019

Awarding institution:
Coventry University

Investigating the role of Hu RNA-binding proteins in Neuroblastoma, Glioblastoma and Small cell lung cancer

Sarah Rose Siverns

March 2019

A thesis submitted in partial fulfilment of the University's requirements for the Degree of Doctor of Philosophy

Certificate of Ethical Approval

Applicant:

Sarah Siverns

Project Title:

Involvement of Hu protein in Cancer

This is to certify that the above named applicant has completed the Coventry University Ethical Approval process and their project has been confirmed and approved as Medium Risk

Date of approval:

18 January 2016

Project Reference Number:

P39738

Abstract

There are a subset of cancers that since their initial discovery and early efforts to develop treatments, still have a poor prognosis. These include Small cell lung cancer, Neuroblastoma and Glioblastoma and together they contribute to a large percentage of human cancer deaths. Efforts now focus on identifying novel targets that drive the initiation and development of these cancers to advance therapeutics in an advance towards personalised cancer therapies.

Aberrant post-transcriptional gene regulation has been implicated in numerous diseases including Neurodegeneration and Cancer. The family of Hu proteins consists of the neuronal HuB, HuC and HuD and ubiquitously expressed HuR. They are proto-type RNA-binding proteins functioning in all aspects of RNA processing including RNA stability, alternative splicing, polyadenylation, localisation and nuclear export. Hu proteins that are ectopically expressed or overexpressed in Small cell lung cancer (SCLC), Neuroblastoma and Glioblastoma have been linked to tumour progression.

Little research has been done to analyse how Hu proteins contribute to the development and progression in the described cancers. Silencing Hu proteins using siRNA interference provides an opportunity to analyse the effect of decreased Hu expression on cellular properties and the change in post-transcriptional regulation of target RNA that may play a role tumour formation and progression.

Effects of cell migration and cell viability were assessed *in vitro* and revealed HuB and HuC proteins to be key regulators of these processes. A decrease of *HuB* gene expression by RNA interference resulted in an increase in migration, in Glioblastoma cells U87-MG and the Neuroblastoma cell lines SH-SY5Y and SK-N-AS. Whilst a decrease in *HuB* and *HuC* gene

expression showed an increase in viability and migration of the Neuroblastoma cells SH-SY5Y and Glioblastoma cells U87-MG suggesting these proteins act to control these factors in the cancers.

Individual and combined *Hu* gene knockdowns with siRNA also revealed regulatory and compensatory interactions of the Hu family members. HuR protein was found to positively regulate the expression of *HuC* in all cell models. In SH-SY5Y Neuroblastoma cells and U87-MG Glioblastoma cells, additional similarities were observed. HuR protein positively regulated *HuD* mRNA and HuC negatively regulated *HuR* mRNA. The HuR and HuC interactions suggests they can regulate each other's protein levels ensuring an abundance of each protein in cells.

Molecular screening of a set of mRNA targets that have been described to contribute to the development of each cancer revealed many changes. From the array of targets that changed after knockdowns, genes with a high expression fold-change and influenced by more than one Hu protein were chosen to confirm the regulation by Hu proteins. Many of these targets were identified as members of the MAPK signalling pathway.

Further analysis including a complete knockout of the Hu proteins is needed to confirm the role of Hu proteins in regulating members of the MAPK signalling pathway and how the knockout would affect upstream and downstream targets of this pathway.

Acknowledgements

First and foremost, I would like to thank my fantastic PhD supervisor Dr Irmgard Haussmann for providing me with this opportunity. Her continuous support, encouragement, time and experience has enabled me to broaden my scientific knowledge and passion for Cancer biology. Not only has she been an academic mentor, but a personal one too. For that I am truly grateful.

I would also like to thank my other supervisors, Dr Christopher Mee and Dr Helen Maddock who have supported me throughout my studies but also in the preparation of this thesis. I am extremely thankful to Chris for sparking my initial interest in Cancer Biology.

I have made many lifelong friendships in the laboratory to whom I am appreciative of their advice and support along the way. With special thanks to Dr Eliot Barson, Dr James Dayus and Dr Dani Craig-Meyer who were always helpful in my studies and made a more enjoyable atmosphere in the lab throughout this research.

I would also like to thank my wonderful partner Dr William Collier for believing in me and supporting me consistently. Also, for his time and patience whilst writing up this thesis.

Finally, I would like to dedicate this work to my amazing family without whom the completion of this dissertation would not have been possible. I am grateful of their unlimited support and for providing me with foundation that has made me the person I am today. You have always encouraged me to achieve my goals and dreams.

Table of Contents

List of Figures

List of Tables

List of Abbreviations

Abbreviation	Name
AREs	Adenylate/uridylate-rich elements
ARF	Alternate reading frame
BEGM	Bronchial epithelial cell growth medium
BSA	Bovine serum albumin
cDNA	Complementary DNA
CR	Coding region
CSC	Cancer stem cell
CSTF	Cleavage stimulatory factor
CT	Computed tomography
Ct	Mean threshold cycle values
CTG	Trinucleotide repeat
DAPI	4’,6-diamidino-2-phenylindole
DBPS	Dulbecco’s phosphate buffered saline
DEPC	Diethylpyrocarbonate
DGCR8	Microprocessor complex subunit DGCR8
DICER	Endoribonuclease dicer
DISC	Death-inducing signalling complex
DMEM	Dulbecco's modified eagle's medium
DMSO	Dimethyl sulfoxide
DNA	Deoxyribonucleic acid
EDTA	Ethylenediamine tetraacetic acid
ELISA	Enzyme-linked immunosorbent assay
EMEM	Eagle's minimum essential medium
EMT	Epithelial-mesenchymal transition
FBS	Fetal bovine serum
FISH	Fluorescence in situ hybridization
FITC	Fluorescein Isothiocyanate
GTP	Guanosine-5'-triphosphate
GU-rich	Guanosine uracil-rich
hnRNPs	Heterogeneous ribonucleoprotein particles
HNS	Nucleo-cytoplasmic shuttling sequences
HRP	Horseradish peroxidase
INRG	International Neuroblastoma Risk Group
LDCT	Low radiation dose Spiral computed tomography

Abbreviation	Name
MHC	Major histo-compatibility complex
miRNA	MicroRNA
MRI	Magnetic resonance imaging
mRNA	Messenger ribonucleic acid
NB	Neuroblastoma
ncRNAs	Non-coding Ribonucleic Acid
NSCLC	Non-small cell lung cancer
PAS2	Polyadenylation signal
PBST	Phosphate buffered saline with Tween 20
PCR	Polymerase Chain Reaction
PEM	Paraneoplastic encephalomyelitis
PSN	Paraneoplastic sensory neuropathy
PTGR	Post-transcriptional gene regulation
RBPs	RNA binding protein
RIPA	Radio Immuno-Precipitation Assay
RISC	RNA-induced silencing complexes
RNA	Ribonucleic Acid
RNP	Ribonucleoproteins
RQ	Relative Quantification
RRM	Ribonucleic acid recognition motif
RT-qPCR	Real-time Quantitative Polymerase Chain Reaction
S202	Serine 202
SCLC	Small cell lung cancer
SDS-PAGE	Sodium Dodecyl Sulphate-Polyacrylamide Gel electrophoresis
siRNA	Small interfering RNA
snRNA	Small nuclear ribonucleic acid
TAE	Tris/acetic acid/EDTA
TBE	Tris/Borate/EDTA
TBST	Tris-buffered saline with tween 20
TIC	Tumour initiating cells
TNF	Tumour necrosis factors
TSA	Tyramide signal amplification
UTR	Untranslated region
UV	Ultra Violet
WHO	World Health Organisation

List of Genes

Abbreviation	Gene Name
A2BP1	Muscle-specific splicing factor Fox-1
ABCB1	ATP binding cassette subfamily B member 1
ACTB	Beta-actin
AKT1	AKT serine/threonine kinase 1
ALK	Anaplastic lymphoma kinase
AMPK	AMP-activated protein kinase
APOE	Apolipoprotein E
APP	Amyloid precursor protein
ATM	ATM serine/threonine kinase
AURKA	Aurora kinase A
BACE1	β-site APP-cleaving enzyme 1
BCL-2	B-cell lymphoma 2
BDNF	Brain derived neurotrophic factor
BRCA1	Breast cancer 1
CCNA2	Cyclin A2
CCNB1	Cyclin B1
CCNB2	Cyclin B2
CCND1	Cyclin D1
CCND2	Cyclin D2
CD44	CD44 molecule (Indian blood group)
CDK1	Cyclin dependent kinase 1
CDK2	Cyclin dependent kinase 2
CDKN1A	Cyclin dependent kinase inhibitor 1A
CDKN2A	Cyclin dependent kinase inhibitor 2A
CHK2	Checkpoint kinase 2
CNS	Central nervous system
COL1A1	Collagen type I alpha 1 chain
COL1A2	Collagen type I alpha 2 chain
COX2	Cyclooxygenase-2
CPSF	Polyadenylation stimulatory factor
CPSF160	Multiprotein cleavage and polyadenylation specificity factor
CSTF	Cleavage stimulatory factor
CTBP2	C-terminal binding protein 2
CTGF	Connective tissue growth factor
CTNNB1	Catenin beta 1

Abbreviation	Gene Name
CUGBP1	CUG binding protein 1
CXCL12	C-X-C motif chemokine ligand 12
CXCR4	C-X-C motif chemokine receptor 4
dCK	Deoxycytidine kinase
DMPK	myotonic dystrophy protein kinase
E2F1	E2F transcription factor 1
EGFR	Epidermal growth factor receptor
EGR1	Early growth response 1
eIF4E	Eukaryotic translation initiation factor 4E
ELAV	Embryonic lethal abnormal vision
ELAVL	Embryonic Lethal, Abnormal Vision, Drosophila, Homolog-Like 1
EML4-ALK	Chinoderm microtubule-associated protein-like 4-anaplastic lymphoma kinase
ERBB2	Erb-b2 receptor tyrosine kinase 2
EZH2	Enhancer of zeste 2 polycomb repressive complex 2 subunit
FMR1	Fragile X mental retardation 1
FN1	Fibronectin 1
GAP43	Growth associated protein 43
GAPDH	Glyceraldehyde-3-phosphate dehydrogenase
GLUT1	Endogenous glucose transporter
GM-CSF	Granulocyte/macrophage-colony-stimulating factor
GSK3B	Glycogen synthase kinase 3 beta
GSTP1	Glutathione S-transferase pi 1
HIF1A	Hypoxia inducible factor 1 subunit alpha
HLA-DRB1	Major histocompatibility complex, class II, DR beta 1
HMOX1	Heme oxygenase 1
HNS	HuR nucleocytoplasmic shuttling sequence
HPRT1	Hypoxanthine phosphoribosyltransferase 1
HRAS	HRas proto-oncogene, GTPase
IFNG	Interferon gamma
IGF1	Insulin like growth factor 1

Abbreviation	Gene Name
IGF1R	Insulin like growth factor 1 receptor
IGFBP3	Insulin like growth factor binding protein 3
IGF-IR	Type-I insulin-like growth factor receptor
IL10	Interleukin 10
IL6	interleukin 6
IL8	Interleukin 8
iNOS	Inducible nitric oxide synthase
IRES	Internal ribosome entry site
ITGB1	Integrin subunit beta 1
KDR	Kinase insert domain receptor
KIT	KIT proto-oncogene receptor tyrosine kinase
KRAS	KRAS proto-oncogene, GTPase
MAP2K2	Mitogen-activated protein kinase kinase 2
MAPK	Mitogen-activated protein kinase
MAPK1	Mitogen-activated protein kinase 1
MAPK3	Mitogen-activated protein kinase 3
MBNL1	Muscle blind-like protein 1
MCL-1	Myeloid cell leukemia-1
MDM2	MDM2 proto-oncogene
MKI67	Marker of proliferation Ki-67
MKP-1	MAPK phosphatase-1
MLH1	MutL homolog 1
MMP1	Matrix metallopeptidase 1
MMP2	Matrix metallopeptidase 2
MMP7	Matrix metallopeptidase 7
MMP9	Matrix metallopeptidase 9
MSI1	Musashi1
MYC	MYC proto-oncogene, bHLH transcription factor
MYCN	N-myc proto-oncogene
NF1	Neurofibromin 1
NFKB2	Nuclear factor kappa B subunit 2
NOTCH1	Notch 1
NOVA-1	Neuro-oncological ventral antigen 1
$p21^{waf1}$	Cyclin-dependent kinase inhibitor 1
PCNA	Proliferating cell nuclear antigen
PIK3CA	Phosphatidylinositol-4,5-bisphosphate 3-kinase catalytic subunit alpha
PIK3R1	Phosphoinositide-3-kinase regulatory subunit 1

Abbreviation	Gene Name
PKC	Protein kinase C
PLAU	Plasminogen activator
PLAUR	Plasminogen activator, urokinase receptor
PRKCA	Protein kinase C alpha
PROM1	Prominin 1
PSA	Prostate-specific antigen
PTEN	Phosphatase and tensin homolog
QKI	Quaking I
RAF1	Raf-1 proto-oncogene, serine/threonine kinase
Rb	Retinoblastoma
RB1	RB transcriptional corepressor 1
RBM47	RNA binding motif protein 47
RBM9	c-Fos protein
RBP	RNA-binding protein
RRM	RNA recognition motif
RRM2	Ribonucleotide reductase regulatory subunit M2
SERPINE1	Serpin family E member 1
SIRT1	Sirtuin 1
SOD2	Superoxide dismutase 2
SP1	Sp1 transcription factor
SPP1	Secreted phosphoprotein 1
STAT3	Signal transducer and activator of transcription 3
TAP	Tip-associated protein
TBP	TATA-box binding protein
TCF7L2	Transcription factor 7 like 2
TERT	Telomerase reverse transcriptase
TGFB1	Transforming growth factor beta 1
TIMP1	TIMP metallopeptidase inhibitor 1
TIMP3	TIMP metallopeptidase inhibitor 3
TLR2	Toll like receptor 2
TNF	Tumour necrosis factor
TOP2A	DNA topoisomerase II alpha
TP53	Tumour protein 53
TSP1	Thrombospondin
TYMS	Thymidylate synthetase
UBB	Ubiquitin B
UBC	Ubiquitin C

Abbreviation	Gene Name
uPA	Urokinase-type plasminogen activator
uPAR	UPA receptor
UTR	Untranslated region
VCAM1	Vascular cell adhesion molecule 1
VEGF	Vascular endothelial growth factor
VEGFA	Vascular endothelial growth factor A
VIM	Vimentin
WNT5A	Wnt family member 5A
ZWINT	ZW10 interacting kinetochore protein

Chapter 1

Introduction

1.1 Gene regulation

The human genome encodes approximately 25,000 genes, organised into 23 chromosome pairs, made of over three billion deoxyribonucleic acid (DNA) base pairs. Whilst humans have the same sequence homology as plants and animals, there is greater diversity in appearance, properties and functions between organisms and within species due to differential ways genes are regulated (Phillips 2008).

The enormous complexity and dynamic structure of the human genome emphasises the need for its regulation. Regulation of eukaryotic gene expression is fundamental for synchronised synthesis, assembly and localisation of cells structure (Orphanides and Reinberg 2002). It is a multi-step process regulated at every level, from DNA to ribonucleic acid (RNA) and to protein. These processes begin in the nucleus and then continue in the cytoplasm following mRNA export.

These events regulate processes including transcription, RNA processing, mRNA transport, turnover, storage, and translation. Proteins also undergo post-translational regulatory mechanisms during modification events including phosphorylation, ubiquitination and methylation (Maniatis and Reed 2002).

The stages of gene regulation are displayed in Fig. 1.1.

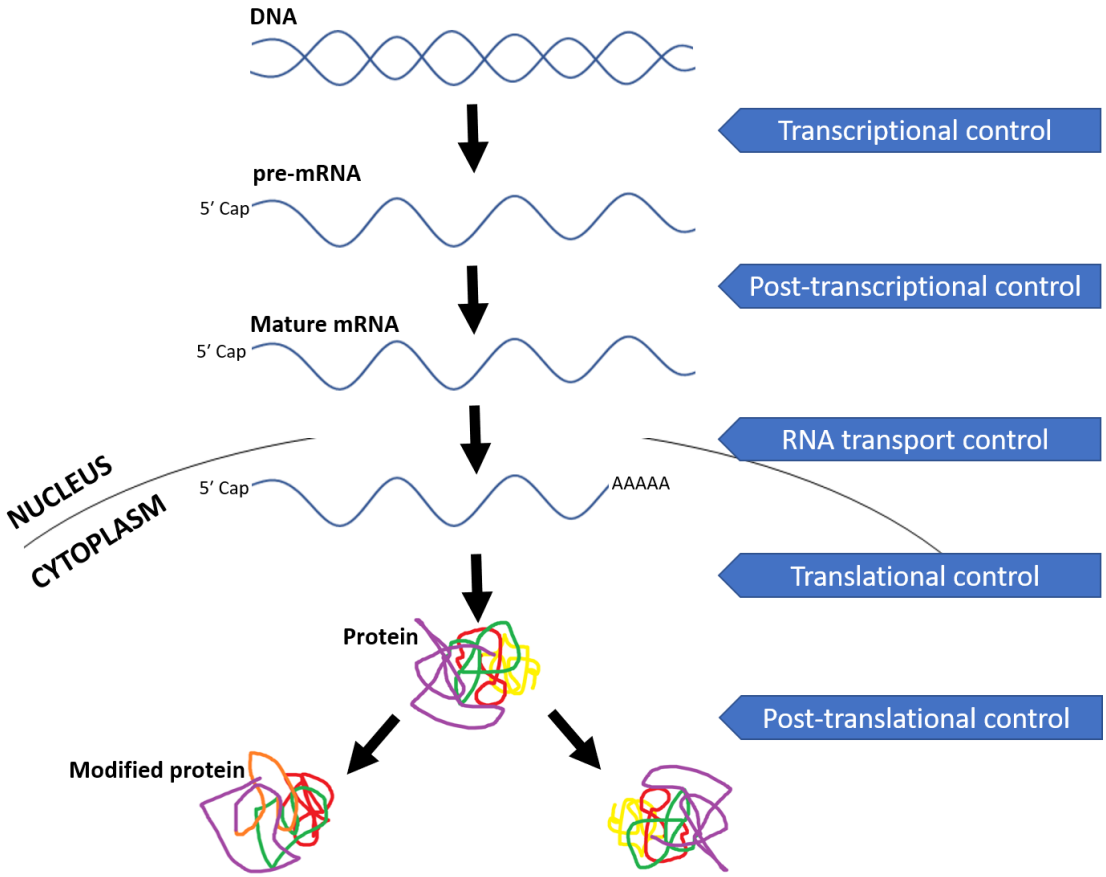

Figure 1.1. Gene regulation from DNA to protein. DNA is regulated at a transcriptional level, to ensure the quality and number of mRNA transcripts. The pre-mRNA is subjected to capping, splicing and polyadenylation during post-transcriptional control. The mature mRNA is then transported to the cytoplasm where it sustains translational regulatory events during protein production and further post-translational modifications.

In the nucleus, transcription factors recruit RNA polymerase II that bind upstream of a promoter in a gene sequence regulating RNA synthesis. The produced messenger RNA (mRNA) is processed by a large amount of RNA-binding proteins (RBPs) through post-transcriptional events which prepares the mRNA for export through nuclear pores. In the cytoplasm, the mRNA is localised to regions consistent with its fate. mRNA can be destined for exonuclease-mediated degradation or when colocalised to translation factors and ribosomes, is used as a template for protein synthesis. Following translation, proteins still

endure further modifications such as phosphorylation and methylation. These processes combined, allows cells to respond to physiological stimuli (Glisovic et al. 2008, Yao et al. 1993).

1.2 Post-transcriptional gene regulation

Post-transcriptional gene regulation is a highly-coordinated process controlled by multiple mechanisms to ensure cellular homeostasis and contribute to organismal complexity (Glisovic et al. 2008). Pre-mRNA produced from RNA synthesis undergoes post-transcriptional gene regulatory events including 5' capping, 3' polyadenylation, cleavage, pre-mRNA splicing, export, mRNA decay, and translation, ultimately increasing the diversity of a single gene. Several ubiquitous molecules and cell-specific trans-acting factors participate in the processes including RNA-binding proteins (RBPs), non-coding RNAs (ncRNAs) and microRNAs (miRNAs) (Khabar 2017). Modified pre-mRNA is then transported to the cytoplasm and translated into a protein (Glisovic et al. 2008).

1.2.1 5′ capping

The first modification the pre-mRNA experiences is 5'-capping where a 7-methylguanosine cap (5' m7G cap) is added to the beginning of the RNA transcript. The 5' m7G cap is evolutionarily conserved in eukaryotic mRNA. It allows the recruitment of cellular proteins that regulate pre-mRNA processing and nuclear export including c-myc, involved in cell proliferation (Ramanathan et al. 2016).

1.2.2 Alternative splicing

Alternative splicing occurs in all eukaryotes and is crucial for the development, differentiation and complexity of a cell. This diverse process determines the binding potential, intracellular localisation, enzymatic activity and protein stability of many proteins (Stamm et al. 2005). Alternative splicing allows the production of cell specific isoforms from a single gene in response to external stimuli (Roméria da Silva et al. 2015). A schematic diagram of this is shown in Figure 1.2.

All genes are composed of long non-protein coding sequences called introns and shorter untranslated/coding sequences called exons. Alternative splicing joins exons or portions of exons by removing intronic sequences in a pre-mRNA transcript. The diverse isoforms can differ in composition and function determined by which exons are spliced together and translated (David and Manley 2010).

Selection of alternative splice sites is determined by the spliceosome (Pagliarini et al. 2015). The spliceosome is a functionally dynamic, multi-megadalton ribonucleoprotein composed of small nuclear RNA (snRNA) and ribonucleoproteins (RNPs). c*is*-sequence transcripts in the core spliceosome bind to trans-acting RBPs that enlist factors and enzymes to initiate the removal of introns from the mRNA (Will and Lührmann 2011).

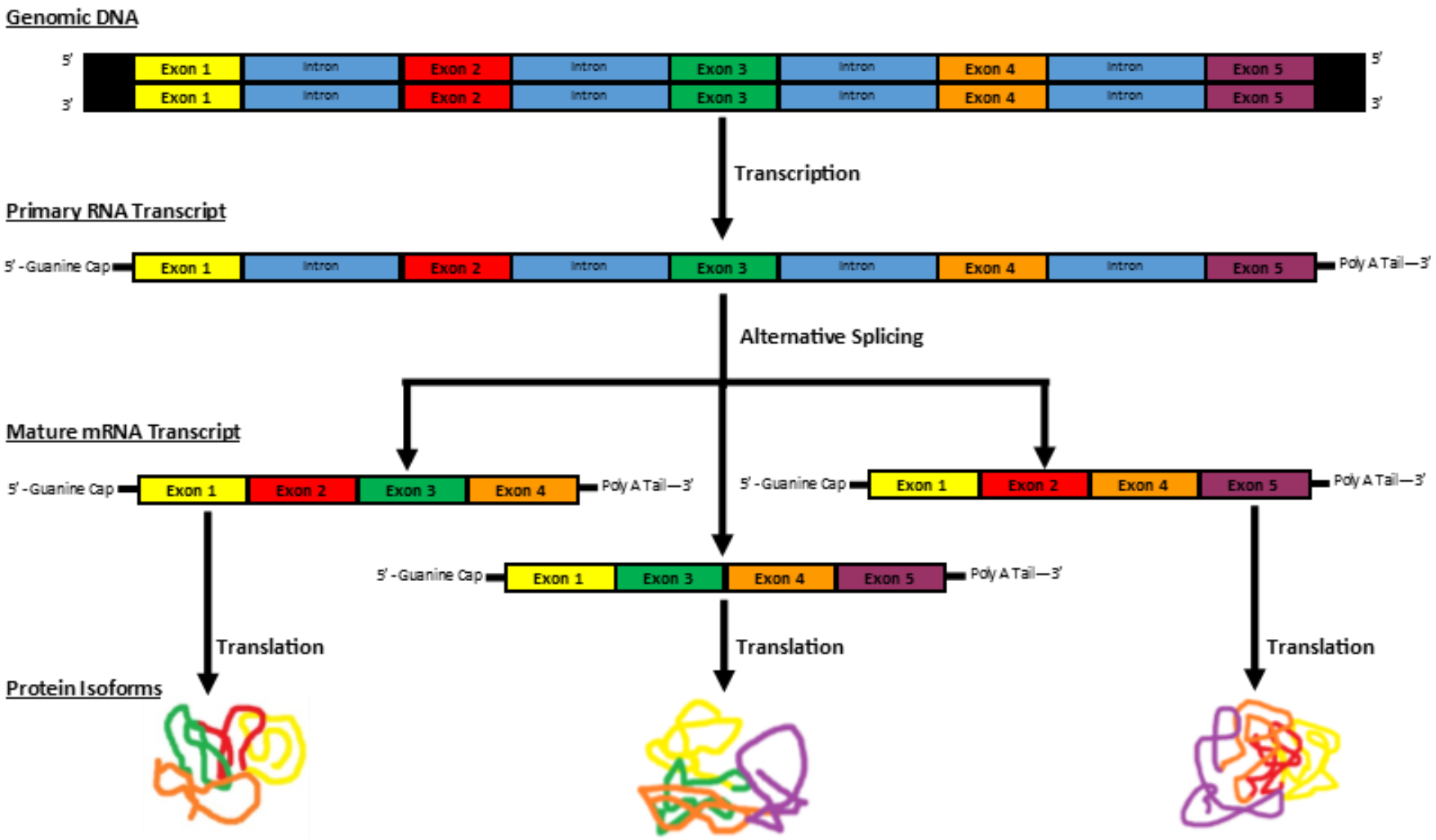

Figure 1.2: Alternative splicing of proteins. During transcription, a copy of DNA is made producing a pre-mRNA transcript. Alternative splicing of this transcript then joins different combinations of exons by the removal of introns forming a mature-mRNA transcript.

1.2.3 Polyadenylation

Polyadenylation is a complex mechanism to regulate gene expression in all eukaryotic mRNAs except histones. Polyadenylation occurs at the 3' end of pre-mRNA in the nucleus. It is a 2-step reaction involving the cleavage of the 3' end and addition of the poly (A) tail to the newly generated 3' end (Erson-Bensan 2016). Polyadenylate, also known as the poly(A) tail is around 100-200 nucleotides long and acts to protect the mRNA from degradation by phosphatases and nucleases (Ray and Fry 2015).

The process involves a multiprotein machinery consisting of subunits of cleavage factors; polyadenylation stimulatory factor (CPSF), cleavage stimulatory factor (CSTF) and several other cleavage factor complexes. CPSF is the main regulator of poly(A) signal selection, a 15-30 nucleotide sequence upstream of the cleavage site. The poly(A) signal sequence, AAUAAA, is highly conserved in mammals and present in 70% of human genes (Erson-Bensan 2016, Derti et al. 2012). Differential selection of poly(A) sites by polyadenylation and/or splicing factors can alter gene expression and implement significant physiological changes. RBPs play a crucial role in polyadenylation as they regulate the stability of the mRNA transcript during the process (Zhu 2009).

1.2.4 mRNA export

Transport of mRNA from the nucleus to the cytoplasm is crucial for the further processing of mRNA. The synthesised mature mRNA associates with various proteins forming a messenger ribonucleoprotein (mRNP) particle. The mechanism of nuclear mRNA export involves principal transport factors that allow only complete, functional mRNA to be transported to

the cytoplasm (Katahira 2015). Once in the cytoplasm, mRNA is either translated into protein, stored or recognised by degradation machinery depending on cell environmental signals (Zhu 2009).

1.2.5 mRNA stability

mRNA transcript stability is detrimental in the control of gene expression. It is mostly governed by AU-rich instability elements (AREs) and cis-acting elements located in the 3' untranslated region and their interactions with trans-acting factors including RBPs. These interactions are initiated by specific intra-cellular and extra-cellular signals. AREs are destabilised thereby increasing the stability and half-life of the mRNA (Caput et al. 1986). Stability can also be affected by polyadenylation, mRNA primary and secondary structure, rate of translation and intracellular location (Bolognani et al. 2012). Mutations in the coding region or nonsense mutation in 5'-UTR of mRNAs can result in truncated mRNAs that then contain an instability determinant affecting mRNA half-life (Ross 1995).

1.2.6 mRNA localisation

Eukaryotic cells contain various organelles that implement different functions. The localisation of mRNA depends on the transcript and its proteins function in certain specialised roles that relate to specific subcellular compartments (Martin and Ephrussi 2009). Some types of mRNA transcripts can re-enter the nucleus after being exported to the cytoplasm (Katahira 2015).

1.2.7 mRNA decay

RNA decay rate is dependent upon the mRNA sequence or structural elements within it. Poly-A tail protects mRNAs from rapid or indiscriminate degradation as the first step in mRNA decay is deadenylation. *cis*-acting regulatory sequences, like GU-rich elements can regulate RNA decay in a similar manner *trans*-acting sequences (Halees et al. 2011).

There are multiple RNA decay pathways and together they control the quality of gene expression. Pathways assesses properties crucial for functionality such as structural integrity or the presence of complete open reading frames. Upon initiation of mRNA decay, transcripts are degraded rapidly (Ghosh, Shubhendu and Jacobson 2010).

1.3 Aberrant gene regulation in the development of human disease

Maintenance of cell homeostasis including cellular growth, proliferation and differentiation are tightly managed processes activated when biological events occur including wound healing, blood cell formation, immune cell expansion and tissue regeneration (Campos-Melo et al. 2014). The intricate processes of cell homeostasis, the complex nature of gene regulation and its impact on cellular physiological development is rationale for the increased possibility for deleterious mutations, polymorphisms and deregulation to occur (Faustino et al. 2003). Mutations can lead to aberrant function of the gene expression regulators RBPs, microRNAs (miRNAs) and non-coding RNAs (ncRNAs). This results in altered gene expression levels and abnormal protein aggregation that impacts cellular function as displayed in Figure 1.3 (Fredericks et al. 2015, Lukong et al. 2008, Gerstberger et al. 2014). Aberrant gene regulation is implicated in the pathophysiology of diseases, including neurodevelopmental

disorders, neurological diseases and cancer (Cooper et al. 2009, Wurth 2012, Yano et al. 2016).

Aberrant splicing, a process controlled by RBPs, produce differential mRNA transcripts that translate to proteins with aberrant function. This allows inhibited cell death, uncontrolled proliferation and decreased response to anti-apoptotic factors in cancer, or excessive neuronal cell death in neurodegenerative diseases (Driver 2012, Zaharieva et al. 2012).

Alternative splicing contributes to functional complexity in normal cell homeostasis and influences tumour cell progression in cancer. Of all the post-transcription regulatory events, alternative splicing produces the most diverse outcomes. Whilst proto-oncogenes are largely associated with spontaneous mutation, activation of such genes can also occur through splicing events. The flexibility of remodelling the proteome is advantageous to cancer cells by producing proteins with antagonistic functions or excess expression levels that contribute to the growth and spread of the tumour (David and Manley 2010). Exon skipping produces truncated proteins with reduced or no function. Intron retention results in non-coding regions being translated, whilst use of alternative splice sites gives rise to a change in the protein composition or alteration to the proteome (Fredericks et al. 2015).

Alternative splicing in cancers is illustrated in Fig. 1.3.

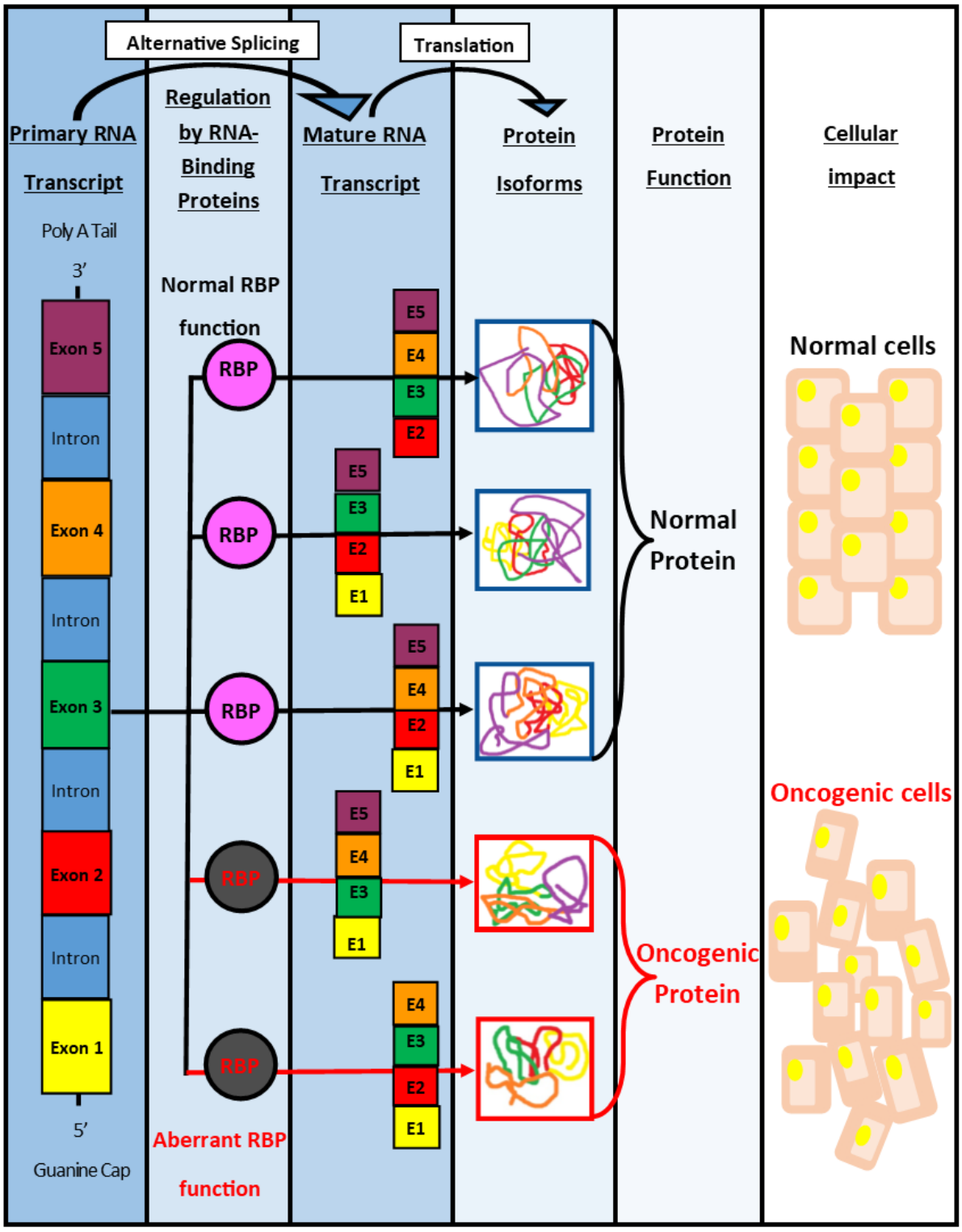

Figure 1.3: Deregulation of alternative splicing factors influences tumorigenesis. Aberrant changes in the regulation of alternative splicing can influence overexpression or aberrant function of splicing factors promoting the common traits of cancer formation and progression, angiogenesis, invasion, metastasis and evasion of cell death. Key: E-exon; RBP-RNA-binding protein.

Apoptosis is a result of many normal cellular pathways that many cancer cells are able to evade (Letai 2008). Alternative splicing of apoptosis-associated genes is regulated by RBPs. This results in isoforms with differentiated roles that are pro-apoptotic or anti-apoptotic proteins. A balance of these proteins achieves a regulatory mechanism for maintaining cell death in normal cells. In cancer cells, aberrant splicing patterns can result in fewer pro-apoptotic isoforms causing prolonged survival (Schwerk and Schulze-Osthoff 2005).

FOX-2 (*RBM9*) is an RBP paralog of the brain- and muscle-specific splicing factor FOX-1 (*A2BP1*). FOX-2 is an upstream master regulator of splicing regulators. In ovarian tumours, FOX-2 is down regulated three-fold compared to normal ovarian tissues resulting in disrupted splicing events. Consequently, this leads to increased cell proliferation. In breast cancer, FOX-2 influences 50% of splicing events particularly of genes involved in EMT (Venables et al. 2009).

Cyclin D1 is a key regulator of G1 phase progression of the cell-cycle. Cyclin D1 endures alternative splicing to produce Cyclin D1a and D1b, of which D1a is localised in the nucleus and the cytoplasm but D1b is found only in the nucleus (Betticher et al. 1995). Cyclin D1b is upregulated in breast and prostate cancer where nuclear Cyclin D1b expression is indicative of a more oncogenic form (Burd et al. 2006, Alt et al. 2000).

Caspase-2 is a highly conserved cysteine protease and regulator of apoptosis initiation and execution (Puccini et al. 2013). It is alternatively spliced to produce a proapoptotic isoform called exon 9-lacking caspase-2L, and a antiapoptotic isoform exon 9-containing caspase-2S. Aberrant splicing patterns lead to an imbalance of these two factors and in some cases, it favours the cancers growth (Iwanaga et al. 2005). Caspase 2 is often seen depleted in

Leukaemia, resulting in an increased survival of cells, particularly in response to chemotherapeutic agents (Ho et al. 2009).

The B-cell lymphoma (BCL2) family of proteins are responsible for the regulation of the mitochondrial or intrinsic apoptotic response. Increased expression of anti-apoptotic BCL-2 family proteins is observed in many cancers including breast and prostate cancer. Overexpression occurs due to chromosomal translocations, gene amplification, increased gene transcription, and/or altered post-translational processing (Hata et al. 2015). Alternative splicing of Bcl-*x* produces two distinct variants, Bcl-x_L and Bcl-x_S. Bcl-x_L has a longer sequence and inhibits apoptosis, whilst Bcl-x_S has a shorter sequence and activates apoptosis (Boise et al. 1993). Bcl- x_L is overexpressed in colorectal cancer (Scherr et al. 2016).

1.4 RNA-binding proteins

The family of RNA-binding proteins (RBPs) diversely function as primary regulators of gene expression, playing essential roles in RNA splicing, export to the cytoplasm, translation and stability ultimately controlling the fate of RNAs (Glisovic et al. 2008). Until 2014 1542 RBPs were documented in the mammalian genome (Gerstberger et al. 2014).

RBPs contain various structural motifs where RNA molecules interact directly with specific sequences or structures. There are several types of motifs, including K homology domain, Sm domain and zinc finger domain. The most abundant protein domain in eukaryotes is the RNA recognition motif (RRM) (Maris et al. 2005). The human genome has 497 genes coding for proteins containing RRMs. RRMs consist of 80-90 amino acid residues and can be present in single or multiple copies within a protein. RRMs are arranged specifically to achieve diverse functionality through their versatility and structural flexibility. This allows RBPs to control the

diversity of many different transcripts (Pereira et al. 2017). The target specificity of RBPs is influenced by the sequence length and type of ARE, the cellular environment and any posttranslational modifications to the RBP itself (Khabar 2017).

The localisation of the RBPs in the cell is also crucial to their regulatory role in post transcriptional gene regulation (Zaharieva et al. 2015a). RBPs can be found in the nucleus or cytoplasm and translocate by shuttling between the two (Fan and Steitz 1998). In the nucleus, RBPs exist as heterogeneous ribonucleoprotein particles (hnRNPs) that form complexes with pre-mRNA. In the cytoplasm, RBPs influence mRNA stability and turnover allowing cells to adapt to environmental changes and increase cell survival (Bronicki and Jasmin 2013).

RBPs can translocate between the nucleus and cytoplasm as a result of cellular stress including UV irradiation and hydrogen peroxide (H_2O_2) both of which induce oxidative stress (Wang et al. 2000), heat shock (Gallouzi et al. 2000), nutrient deficiency (Yaman et al. 2002) or energy depletion (Jeyaraj et al. 2005).

Proteins including importins and exportins facilitate the export of macromolecules including RNA and proteins across the nuclear membrane to the cytoplasm. Protein sequences can contain nuclear localisation signals. Importins and Exportins can bind to these sequences initiating translocation to or from the nucleus in a GTP-dependent reaction against a concentration gradient. This mechanism could explain the ability of RBP to shuttle between the nucleus and cytoplasm although further research would be required to clarify this (Lange et al. 2007).

miRNAs are a conserved family of about 22 nucleotide-long noncoding RNAs. In the human genome over 2000 miRNAs have been discovered. They regulate broad target networks and

influence diverse biological roles controlling one third of the genes in the genome (Hammond 2015). Like RBPs, miRNA bind directly to adenylate/uridylate-rich elements (AREs), controlling mRNA decay and translating RBPs (Agami 2010, Khabar 2017). RBPs and miRNAs interact with each other to cooperate in a complex or compete for specific binding sites on mRNA transcripts. This cooperation or antagonism regulates PTGR processes (Khabar 2017).

Another role of RBPs is as regulators of miRNA biogenesis (Fig. 1.4). RBPs function in every stage of miRNA formation from primary miRNA processing to formation of RNA-induced silencing complexes (RISC) (Loffreda et al. 2015).

RNA Polymerase II consists of 12 RBP subunits and is responsible for the synthesis of the primary-miRNA (pri-mRNA) (Ha and Kim 2014). The stem-loop structure of the pri-miRNA is cleaved by p68, a dimer composed of two subunits, the RNase III enzyme DROSHA and its essential cofactor DGCR8 (Denli et al. 2004). The released hairpin called precursor-miRNA (pre-miRNA) is exported to the cytoplasm by Exportin-5 (Yi et al. 2003). DICER converts the pre-miRNA into a mature 22nt miRNA of which one strand is integrated into the RNA-induced silencing complex (Hutvágner et al. 2001). RISCs are a family of ribonucleoprotein complexes that are programmed to target and silence any nucleic acid sequence (Pratt and MacRae 2009).

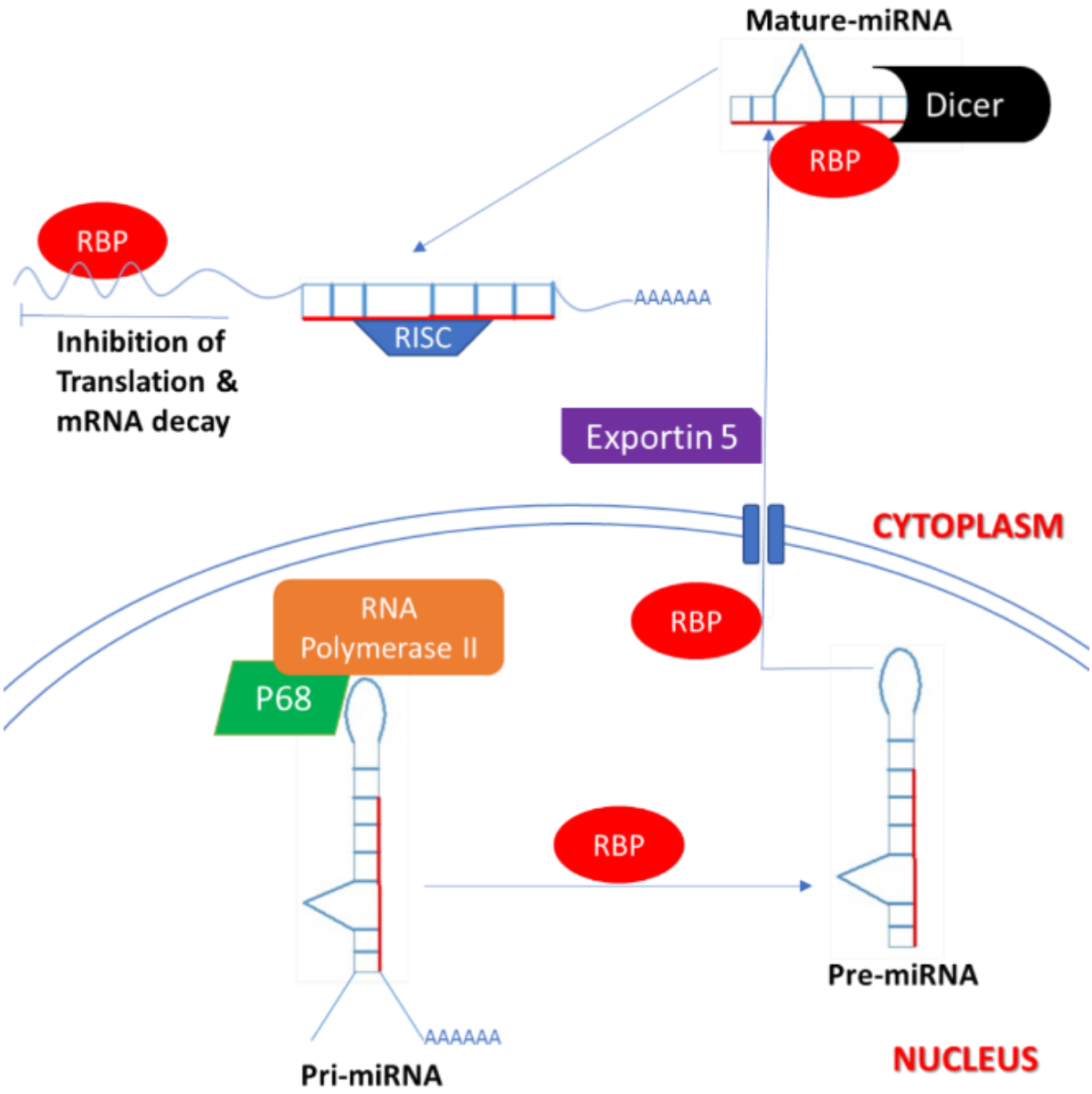

Figure 1.4: Biogenesis of canonical microRNAs. In the nucleus, pri-miRNA is cleaved by p68 aided by RNA polymerase II and RBPs. The pre-miRNA is then transported to the cytoplasm by Exportin 5. The miRNA experiences further processing by DICER and RBP. The mature miRNA associates with the RISC complex.

1.4.1 RNA-binding proteins implicated in disease

Human neurological disorders are often related to irregular function of RNA-binding proteins. For example, Fragile X syndrome is caused by a trinucleotide repeat (CGG) expansion in the 5' UTR of the fragile X mental retardation (*FMR1*) gene. This gene codes for the RNA-binding protein, FMR1 protein in which the mutation results in the loss of protein function (Chelly and Mandel 2001).

Similarly, Myotonic dystrophy is caused by a trinucleotide repeat (CTG) in the 3'UTR of the *DMPK* gene, coding for myotonic dystrophy protein kinase. *In vitro* experiments have shown that once the expanded trinucleotide repeat is transcribed, it folds into very stable and long RNA hairpin structures, that then accumulate in the nucleus. This alters the function of RBPs including Muscle blind-like protein 1 (MBNL) and CUG binding protein 1 (CUGBP1). MBNL was shown to have a loss of function (Lee and Cooper 2009), whilst the mutation causes hyper-phosphorylation and stabilisation of CUGBP1 initiating aberrant activation of the Protein kinase C pathway (Kuyumcu-Martinez et al. 2007).

NOVA-1 RBP has been implicated in paraneoplastic neurodegenerative disorders (Buckanovich and Darnell 1997). NOVA-1 expression is restricted to the brain. Therefore abnormal expression causes an immune response where auto-antibodies attack NOVA-1 in the normal expression areas of the brain and spinal cord (Yang et al. 1998).

Aberrant transcriptional events, deregulation of RBPs, abnormal gene amplifications and alterations to signalling events contribute towards cancer progression (Croce 2008, Wang et al. 2015). Gene regulatory events including splicing, polyadenylation, translation, mRNA and protein stability are altered during the development of cancers and can influence the diseases

initiation and progression. PTGR events are therefore considered a 'convergence point of oncogenic signalling' (Yan and Higgins 2013).

Several studies have highlighted correlation between aberrant RBP expression and cancer development. RBPs function as RNA regulatory factors in gene regulation is pathologically disrupted in cancer. Due to RBPs structurally flexible binding domains, they can regulate a wide range of mRNA sequences controlling their stability. Some of these transcripts can code for tumour-related proteins (Wang et al. 2015). They can therefore contribute to the complex network that enables tumour development (Eberhardt et al. 2016). Defects in RNA regulation include altered protein expression levels, abnormal aggregation, gene mutations and translocations and gain-of-function (oncogene). These changes deregulate important developmental pathways that drive cell proliferation, survival and differentiation, instead influencing invasion, metastasis and angiogenesis and avoiding cellular apoptosis (Abdelmohsen 2010, Wang et al. 2015, Wurth 2012).

The examples discussed below highlight the importance of identifying RBPs role in cancers also emphasising the significance of alternative mRNA processing in cancer (López de Silanes et al. 2005).

Musashi1 coded by the gene *MSI1* is an RBP. Sam68 belongs to a family of RBPs called Signal Transduction and Activation of RNA. Both these factors have been shown to target hundreds of genes, forming networks that control all aspects of homeostasis particularly ensuring a balance between self-renewal and differentiation (Glazer et al. 2012). Musashi1 and Sam69 have been shown to be upregulated in Glioblastoma, Breast and Colon cancer. In cancers, they regulate mRNA expression of oncogenic targets involved in cell adhesion, proliferation,

apoptosis, migration and invasion (Vo et al. 2012, Glazer et al. 2012, Plateroti et al. 2012, Busà et al. 2007, Richard et al. 2008).

Quaking I (QKI) is an RNA-binding protein essential for myelination of the central nervous system implicated in promoting oligodendrocyte lineage development (Chen et al. 2007). At a cellular level, QKI protein supresses cell proliferation and transformation thus their downregulation in lung cancers is associated with larger tumour growth (Zong et al. 2014).

1.5 Embryonic lethal abnormal vision

The Drosophila melanogaster (*D. melanogaster*) *Embryonic lethal abnormal vision (Elav)* gene was the first member of neuronal RNA-binding proteins to be identified and is a paradigm for a gene family present in all metazoans. The mammalian homolog of *elav is* therefore referred to as ELAV-like (ELAVL) more recently referred to as Hu. In *D.melanogaster*, *elav* resides in a family of three genes alongside *RNA-binding protein-9 (Rbp9)* and *found in neurons (Fne)* (Yao et al. 1993). The three genes share 59-68% sequence homology (Samson 2008).

Elav is one of the first neuronal proteins expressed during neurogenesis in Drosophila and continues to be expressed in all neurons throughout adulthood. It is essential for the differentiation, development and maintenance of post-mitotic neurons as well as and the development of the eyes (Robinow 1988). Fne also found exclusively in neurons but occurs later in *D. melanogaster* development than Elav. Fne is expressed in the cytoplasm suggesting a role in protein shuttling. Elav and Fne have been shown to interact with each other (Samson and Chalvet 2003). *Rbp9* is predominantly expressed in nerve cells. Rbp9 is expressed mainly in the nuclei of neuronal cells but has also been located in the cytoplasm of cystocytes during the production and development of ovum (Kim-Ha et al. 1999). A number of other proteins

homologous to *elav* have been identified in other species including *Xenopus laevis*, *Danio rerio* and *Mus musculus* (Good 1995). Figure 1.5 summarises the sequence homology of *elav* in different species.

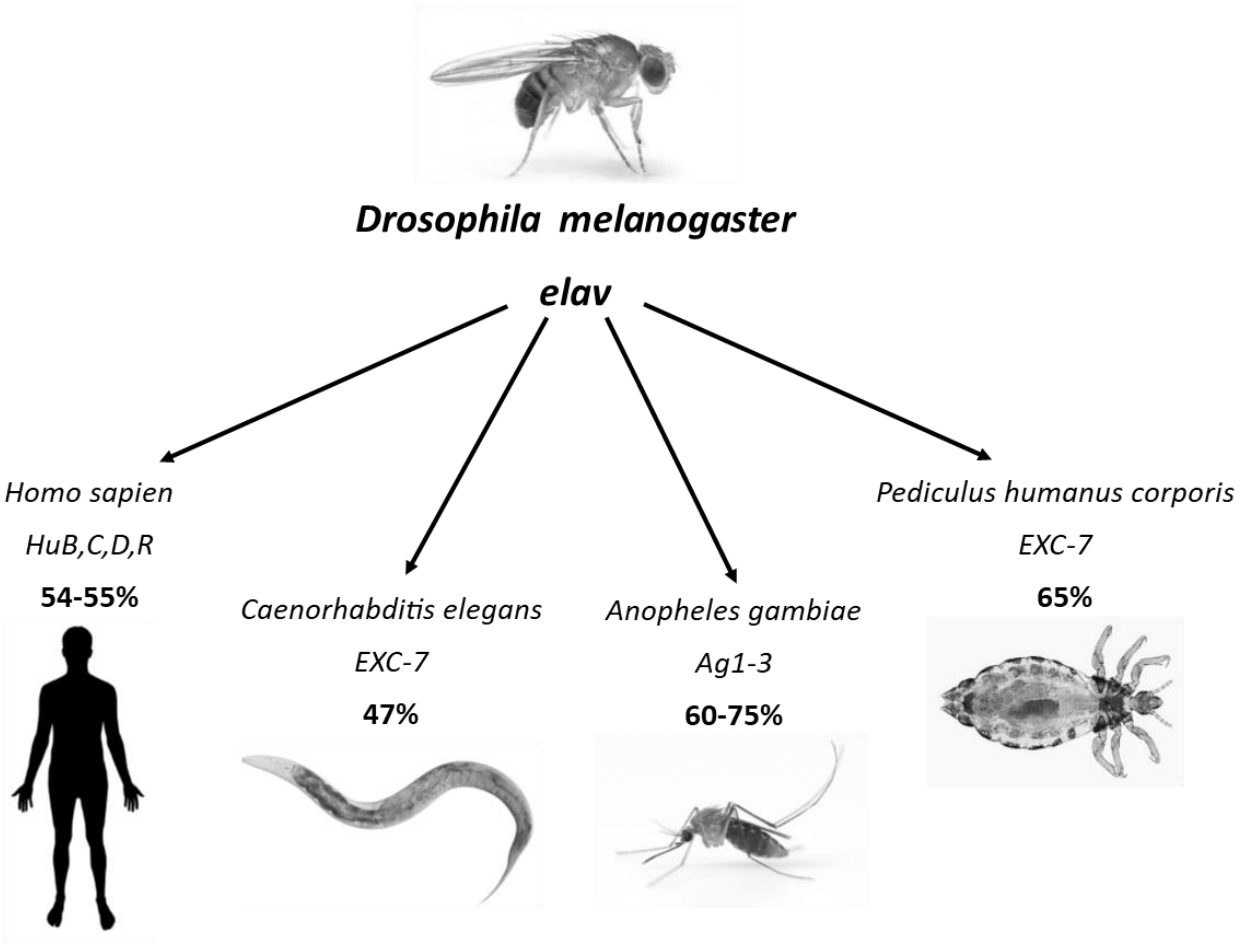

Figure 1.5: Sequence homology of *D. melanogaster* elav protein in other species. The elav family is conserved in 11 species. In *Homo sapiens*, the *Drosophila melanogaster* elav protein shares 55% sequence similarity with HuB, HuD and HuR whilst HuC shares 54% similarity. Elav in *C. elegans* called EXC-7 shares 47% protein identity. *A. gambiae* has three elav-like proteins called Ag-1, Ag-2 and Ag-3 that share 74%, 60% and 65% elav protein similarity. Like *C. elegans, P. humanus corporis* elav-like protein is called EXC-7 and shares 65% protein identity (Samson 2008).

In mice, the Hu homologue, ELAVL proteins, are expressed in neurons and shown to play a role in neuronal differentiation (Okano and Darnell 1997, Akamatsu et al. 2005). Studies have shown the direct binding of the mouse Hu homologues to target RNAs. Crosslinking immunoprecipitation and high-throughput sequencing of RNA (CLIP-seq), along with transcriptome profiling of *ELAVL3/4* knockout mice, showed that ELAVL binds to the U-rich elements with dispersed purine residues in 3'UTRs and introns within the mouse brain (Ince-Dunn et al. 2012). Knockout of *ELAVL3* and *ELAVL4* in mice causes problem in neuronal maturation as well as motor and sensory defects. Haploinsufficiency of ELAVL3 results in cortical hyper-synchronisation. These studies highlight the importance of *ELAVL* in mouse development but also a role in post-transcriptional events (Akamatsu et al. 2005, Ince-Dunn et al. 2012).

1.6 The human 'Hu' proteins

Human Hu proteins are a family of four RNA-binding proteins, HuB, HuC, HuD and HuR. They are highly conserved throughout evolution and the four human proteins share 74–91% identity (Samson, 2008). In humans, they were discovered due to their aberrant expression in paraneoplastic neurological syndromes (Darnell 1996). 'Hu' describes the first initials of the patient in which they were identified (Bronicki and Jasmin 2013). In the disease, autoantibodies are released by the immune system in response to the tumour that. These autoantibodies cross the blood-brain barrier and target healthy tissue causing severe neurological defects defined as paraneoplastic syndrome (Szabo et al. 1991, Darnell 2010, DeLuca et al. 2009). More on this topic is discussed in Section 1.8.

The *HuB* gene is located on chromosome 9p21.3 and contains 20 exons. This was determined by chromosome microdissection polymerase chain reaction (PCR) and fluorescence in situ hybridization (FISH) (Han et al. 1996).

The *HuB* gene encodes a protein of 39.60kDa (D'Alessandro et al. 2008). In older studies, *HuB* is often referred to as Hel-N1. It has three transcript variants encoding two different isoforms. Alternative 5' splicing of *HuB* mRNA containing 20 exons, creates two isoforms Hel-N1 (HuB) and Hel-N2. Hel-N2 is characterised by the insertion of a 91-bp exon and has a larger N-terminal region of 29 amino acids than Hel-N1. Both isoforms are predominantly localised to the cytosol although they can be in the nucleus too. The Hel-N2 isoform is expressed in different cell lines including neuronal precursors however, it is absent in mature neurons (Gao et al. 1994, King, 1994). Two isoforms also exist in rat neural tissue, *Rel-N1* and *Rel-N2* and share 96% nucleotide conservation between the two isoforms (King 1994).

The HuB protein is localised in the cytoplasm of gonadal tissue and undifferentiated neurons. In neurons HuB co-localises with ribosomes facilitating mRNA metabolism and neuronal differentiation, ultimately influencing mRNA homeostasis in the dendrites of maturing neurons (Gao and Keene 1996). If the HuB-bound mRNAs associate with microtubules of the cytoskeleton, the complex binds with polysomes forming large β complexes that associate with the microfilament framework of the cytoskeleton (Antic and Keene 1998).

Van Tine et al. (1998) used the tyramide signal amplification (TSA)-FISH technique, a molecular tool for visualising specific amplified DNA sequences in chromosome preparations, and radiation hybrid mapping of chromosomes for *HuC* localisation studies. *HuC* is localised to chromosome 19p13.2.

HuC encodes a protein of 39.55kDa (D'Alessandro et al. 2008). It is expressed in the cytoplasm of differentiated neurons. Four alternatively spliced transcript variants encode for two protein isoforms of HuC. The first is 367 nucleotides and the second is 360 nucleotides in length, the loss of nucleotides from RRM3 (Hinman et al. 2013, Kasashima et al. 1999).

HuD was found to be located on 1p34 by Fluorescent in-situ hybridisation (FISH) (Muresu et al. 1994). The *HuD* gene spans 146kb of DNA and has eight coding exons, E1 to E8, each containing 44kb of DNA (Sekido et al. 1994, Inman et al. 1998, Bronicki et al. 2012). *HuD* gene contains multiple promoters that may provide considerable variation and complexity, further supporting its ability to be ectopically expressed in some cancers (Bronicki et al. 2012).

HuD encodes a protein of 40.50kDa(D'Alessandro et al. 2008). *HuD* is alternatively spiced producing three isoforms called as HuD, HuDmex and HuDpro, with HuD being the more prominent transcript (Sekido et al. 1994). HuDpro is the largest variant due to the inclusion of an additional 42 nucleotides from the HuD isoform whilst, HuDmex is the smallest isoform characterised by a deletion of 13 amino acids (Liu et al. 1995).

In mature neurons, HuD protein is present in axons and dendrites including pre- and post-neurite terminals (Aronov et al. 2002). It is localised to the cytoplasm in neurons (Kasashima et al. 1999). Contrary to previous thoughts that HuD protein was only expressed in neurons, immunohistochemical analysis of HuD expression in a human tissue arrays reveals traces of HuD in in several non-neuronal tissues including lung, testes, liver, heart, pituitary gland and skeletal muscle (Abdelmohsen et al. 2010). Additionally, HuD is located in Beta-cells of the pancreas facilitating insulin expression (Lee et al. 2012).

Like *HuC*, *HuR* is also localised to chromosome 19p13.2. HuR and HuC each have distinct loci with HuC centromeric to HuR (Van Tine et al. 1998, Ma and Furneaux 1997).

HuR encodes a protein of 36.00kDa (D'Alessandro et al. 2008). HuR exists as three isoforms which differ in 3' UTR length. Each variant has differential AU-rich element involvement and stability. Each variant differs in size and in their tissue distribution. The 2.4kb transcript is ubiquitously expressed, the 1.5kb variant is localised in the testes with minor expression in heart and spleen, whilst the rarer, less-stable 6.0kb isoform is induced during neuronal differentiation and is expressed only in neurons (Mansfield and Keene 2012). The RNA binding specificity of HuR is similar to that of HuD and Hel-N1 (Ma et al. 1996).

HuR protein is expressed ubiquitously including in the adipose tissue, intestines, spleen and testes (Wang et al. 2013). Its expression is predominantly seen in the nucleus of cells (Good 1995).

1.6.1 Structure of Hu proteins

Th Hu protein family range between 326 and 380 amino acids with the sequence similarity between 74–91%. Thus, the four Hu proteins are of a similar size (Samson 2008). Hu proteins belong to the RNA recognition motif (RRMs) superfamily. Hu proteins have three, RRM1, RRM2 and RRM3, as shown in Fig 1.6, with each RRM containing 60-100 amino acid residues (Lunde et al. 2007). The RRM are structurally flexible allowing the binding of a large range of transcripts. Sequence alignment indicates that all three RRMs have the same canonical β1α1β2β3α2β4 fold (Maris et al. 2005). All three RRMs are highly conserved in vertebrates with the hinge domain less conserved. The N-terminal fragment is the most diverse domain among the ELAVL proteins (Liu et al. 1995). It is 117-amino acids long and carries RRM1 (Pulido

et al. 2016). HuR's N-terminus has a small sequence homology to HuB, HuC or HuD. However, HuR's N-terminus is most similar to the *Xenopus* homologue, elrA (Good 1995).

RRM1 and RRM2 are consecutively arranged near the N-terminus followed by a hinge domain and RRM3 near the C-terminus (Fig 1.6) (Antic and Keene 1997). A nucleocytoplasmic shuttling sequence (HNS) is in the hinge region of Hu proteins. It is around 60-residues long and essential for nuclear export and subcellular localisation (Keene 1999, Fan and Steitz 1998a).

Figure 1.6: Structure of Hu Proteins. The generalised structure of Hu proteins displays three RNA Recognition Motifs (RRMs). RRM1 and RRM2 are separated from RRM3 by a hinge region.

RRM1 and RRM2 of Hu proteins have been shown to specifically bind to the cis-acting elements, typically in the 3'UTR (Uren et al. 2011). RRM3 functions to block polyadenylation and binds with high specificity to long poly(A) tails stabilising RBP-mRNA complexes (Zhu et al. 2007, Brennan and Steitz 2001). RRM3 assembles HuR oligomers on RNA transcripts to support stabilisation (Fialcowitz-White et al. 2007). HuR's RRM3 preferably binds to Uracil-rich sequences rather than AUUUA motifs (Scheiba et al. 2014).

The first two RRMs of HuD interact with the primary general mRNA export receptor complex, nuclear RNA export factor 1 (NXF1) also called tip-associated protein (TAP) in humans. HuD therefore acts as a regulator for efficient export of ARE-containing mRNAs in neuronal cells (Saito et al. 2004). HuD has also been shown to bind and regulate cell cycle regulator p21 (Joseph et al. 1998), neuronal mRNAs including N-*myc* (Lazarova et al. 1999) and growth-controlling proteins including c-fos (Fig. 1.7) (Chung et al. 1996).

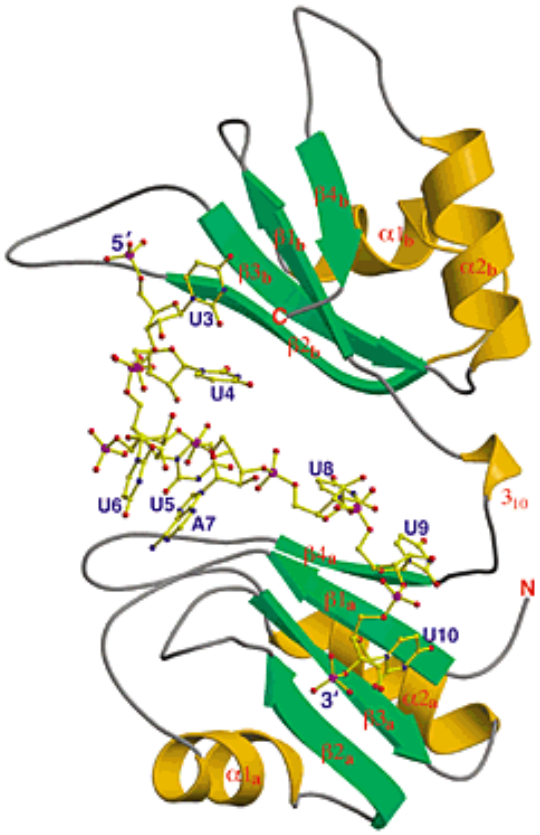

Figure 1.7: Interaction of *c-fos* mRNA with HuD. This ribbon diagram displays an 11 nucleotide fragment of *c-fos* 3'UTR binding with the β-sheets (green) of the first two RRM's of HuD. A-helix of the protein structure are shown in yellow. This image is reproduced from (Wang and Hall 2001).

The versatility and flexibility of Hu proteins' structure allows them to bind to many RNA targets and regulate their fate through different mechanisms (Wurth 2012, López de Silanes et al. 2004).

1.7 Function of Hu proteins

The family of Hu proteins are part of an intricate network where they are collaboratively responsible for many biological functions including the regeneration and development of the nervous system, neuronal specific RNA processing, differentiation, synaptic plasticity and learning and memory (Akamatsu et al. 2005, Deschênes-Furry et al. 2007). It also plays a crucial role in neuronal plasticity controlling the response to axonal injury and increasing learning and memory (Bronicki and Jasmin 2013).

Both *in vitro* and tissue culture studies have shown that neuronal Hu proteins regulate gene expression at a post-transcriptional level typical of RNA-binding proteins. They influence all aspects of RNA processing including RNA stability, alternative splicing, polyadenylation, localisation and nuclear export as displayed in Fig 1.8. They are therefore essential in maintaining the cell homeostasis (Zhu 2009).

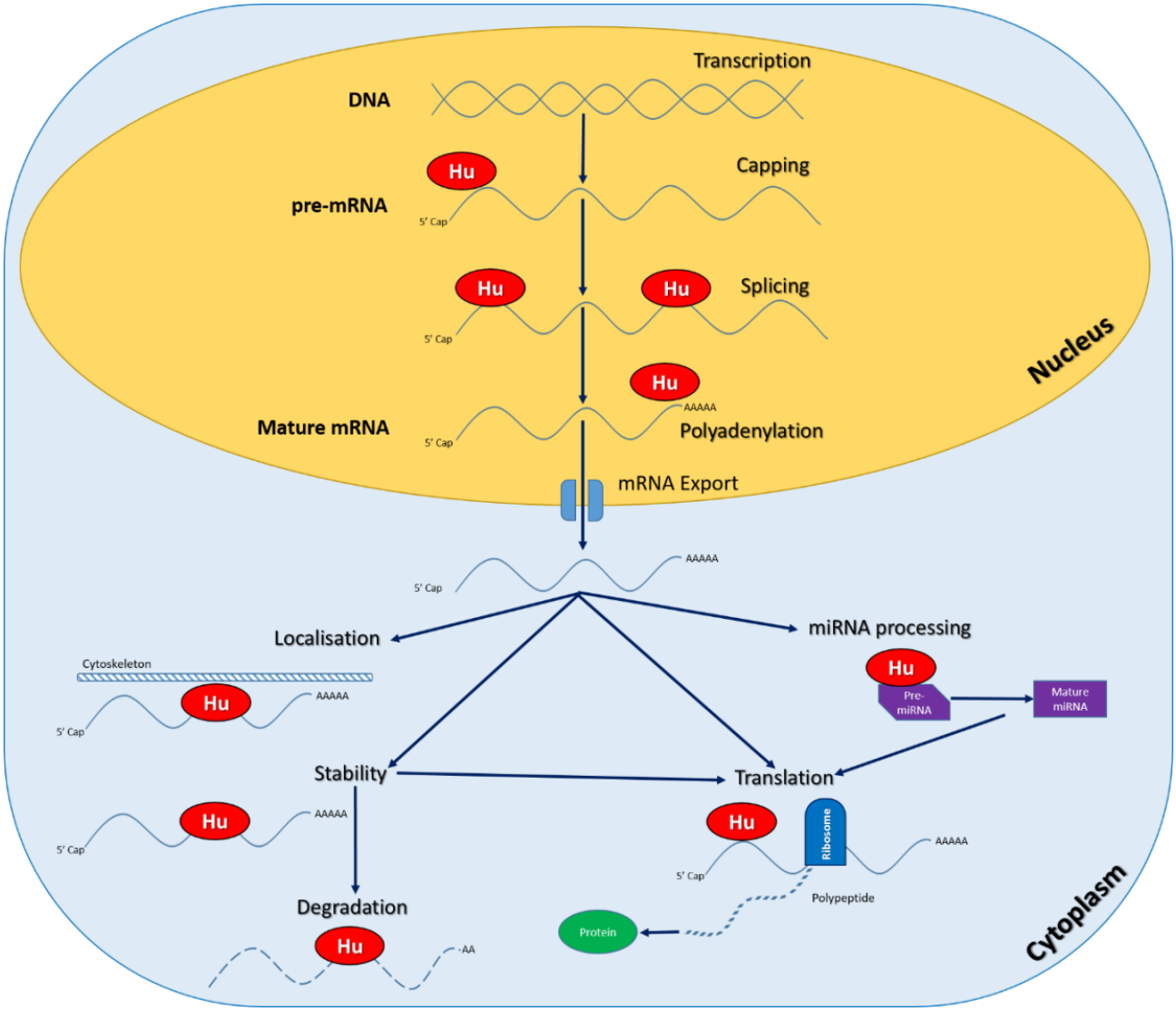

Figure 1.8 Hu proteins influence on gene regulation. Hu proteins mediate many aspects of core-transcription and post-transcriptional events. In the nucleus, Hu proteins regulate 5' capping, alternative splicing, 3' poly-A tail addition and mRNA export. In the cytoplasm, they regulate mRNA localisation, stability and degradation.

miRNAs have been shown to regulate RBP expression. Abdelmohsen et al. (2008) reported miR-519 binds directly to *HuR* mRNA decreasing *HuR*-regulated gene expression. HuR contains two binding sites for miR-519, one located in the coding regions and the other in its 3'UTR. By measuring HuR translation and *HuR* mRNA association with polysomes, in several cancers over expressing miR-519 including, cervical, colon and ovarian, it was found that miR-519 does not alter *HuR* mRNA abundance but decreases HuR biosynthesis. This thereby reduces HuR translation, *HuR*-regulated gene expression and cell division.

Hu RNA-binding proteins promote skipping of alternative exons by inducing local histone hyperacetylation through interactions with pre-mRNAs and alternative exons (Wang et al. 2010). The neuronal proteins, HuB, HuC and HuD are mostly implicated in alternative splicing, which allows cells to adapt to different stimuli by altering protein compositions (Wurth 2012). This significantly impacts neurophysiological mechanisms including neurotransmission, cell recognition and receptor specificity (Zhu 2009).

Another role that Hu proteins regulate is polyadenylation. During this process, cleavage of the 3' end of the sequence and addition of the poly (A) tail to the newly generated 3' end occurs producing mature mRNA as previously described in Section 1.2.3 (Erson-Bensan 2016). Hu proteins bind directly to sequence in cleavage sites preventing polyadenylation signals being transmitted. Hu proteins particularly target poly(A) sites that contain U-rich sequences near cleavage sites and the third RNA-recognition motif of Hu proteins is required to block polyadenylation. Interplay between Hu proteins and two poly(A) factors, the multiprotein cleavage and polyadenylation specificity factor (CPSF160) and the Cleavage stimulation factor (CstF64) is known. CPSF160 interacts with poly(A) polymerase initiating cleavage and poly(A)

addition whilst CstF64 is directly involved in binding to pre-mRNAs on 3' non-coding sites (Zhu et al. 2007).

Neurofibromatosis type I or von Recklinghausen neurofibromatosis is one of the most common dominant inherited autosomal disorders affecting 1 in 3,500 individuals worldwide. Neurofibromin 1, (*NF1*) gene codes for neurofibromin protein. This protein acts a tumour suppressor. *NF1* gene mutations result in multiple abnormalities, including development of neurofibromas and gliomas and abnormal distribution of melanocytes (Bernards 1995). Exon 23a of the *NF1* gene is an in-frame exon that is included during alternative splicing. In the presence of HuC protein, exon23a of *NF1* is skipped by binding to AU-rich sequences located either side of the regulated exon. This results in a defective NF1 protein. Deletions of HuC proteins RRMs resulted in exon 23a inclusion in *NF1*, whilst deletion of the hinge region only reduced *NF1* exon 23a inclusion. This confirms HuC's role as a polyadenylation regulator (Zhu et al. 2008).

Hu proteins are essential in the cytoplasm for regulating mRNA stability by binding to AU-rich elements (AREs) of many short-lived mRNAs. AREs are typically found in non-coding regions of the transcripts, particularly the introns and the 3' untranslated regions (UTR). By binding directly to AREs, Hu proteins influence the translation rate of targets RNA, preventing their degradation and enhancing protein production (Zhu et al. 2007). Hu proteins target an array of RNA transcripts coding for transcription factors, cytokines, growth factors and proto-oncogenes (Wang et al. 2015).

Jain et al. (1997) show that overexpression of HuB in preadipocytes elevated the expression of endogenous glucose transporter (GLUT1) protein 10-fold. This resulted in increased the uptake of glucose. HuB binding occurred directly to the U-rich region of *GLUT1* mRNAs 3'-UTR

increasing *GLUT1* at both translational and post-transcriptional levels confirming a role of HuB in mRNA stabilization and accelerated formation of translation initiation complexes.

Although most neurons express HuC with HuB and/or HuD proteins, cerebellar Purkinje cells and hippocampal granule cells express only HuC protein. Studies in mice showed that HuC protein deficiency caused progressive motor deficits resulting in severe cerebellar ataxia and eventual axonal degeneration. This demonstrates that HuC protein is required for the maintenance of Purkinje neuron axons (Ogawa et al. 2018).

HuD plays a critical role in Protein kinase C (PKC)-mediated neurite outgrowth through stabilising growth-associated protein-43 (*GAP-43*) mRNA. HuD protein binds to *GAP-43* mRNA regulating its transcript. GAP-43 regulates axon growth in neurons (Beckel-Mitchener et al. 2002). Overexpression of HuD results in delayed degradation of GAP-43 due to decrease in the rate of mRNA de-adenylation. PKC phosphorylates GAP-43, regulating neurite formation, regeneration and synaptic plasticity (Mobarak et al. 2000).

p21 gene is highly regulated enabling cells to progress through the cell cycle. HuD protein binds with high affinity to a 42-nucleotide sequence within a U-rich region of the 3'UTR of cyclin-dependent kinase inhibitor 1 (*p21^{waf1}*) mRNA. p21^{waf1} causes cell cycle arrest at the transition from G1 to S phase of the cell cycle through inhibition of cyclin-dependent kinases and proliferating cell nuclear antigens. G1 to S phase is essential in cell differentiation (Joseph et al. 1998). HuR was also shown to bind in the same manner to *p21^{waf1}* (Giles et al. 2003). Binding of Hu proteins enhances the transcripts stability. This example indicates how Hu proteins role in binding to targets involved in the regulation of the cell cycle, influences cell differentiation, mRNA stability, and the termination of the cell cycle.

HuR was first discovered in 1997 and is the most broadly studied in the Hu protein family (Ma and Furneaux 1997). Many of HuR mRNA targets encode proteins responsible for cell growth, proliferation, the immune response and the cellular response to stress and embryonic development and survival (Mansfield and Keene 2012, Hinman and Lou 2008). Specific mRNA targets are discussed in more detail in Chapter 1.10.

HuR functions in energy depletion through interactions with the mRNA target V-ATPases. These are multi-subunit membrane proteins that use ATP binding and hydrolysis to pump protons across cellular membranes against a concentration gradient. They also function in acidification of internal components in mechanisms including endocytosis and are therefore are required by all eukaryotes. V-ATPases are regulated at a post-transcriptional level. When ATP depletion is caused by cellular stress, HuR binds directly to AREs within the V-ATPase mRNA and stabilises the transcript, ultimately protecting the cell from loss of V-ATPase protein (Jeyaraj et al. 2005).

1.7.1 Hu protein expression during development

HuB, HuC and HuD proteins are expressed at different levels in embryonic neurons in comparison to adult neurons. HuB proteins are initially expressed in neurogenic progenitor cells and stays continuously expressed in mature neurons (Marusich et al. 1994, Yano et al. 2016). HuC and HuD expression begins slightly later in development during cortical neuron development (Yano et al. 2016). In developing neurons, HuD is found in the growth cones of extending neurites (Aranda-Abreu et al. 1999).

Akamatsu et al. (2005) showed that a triple knockdown of the neuronal *Hu* genes is lethal in mice. A single knockdown of *HuC* and *HuD* gene showed mice survive to adulthood but they

do display some neurological defects including poor hind-limb reflexes and decreased proliferative activity in the neural progenitor cells (Akamatsu et al. 2005). Interestingly, a knockdown of *HuR* in mice resulted in death of progenitor cells in the bone marrow, thymus, and intestine, loss of intestinal villi and obstructive inflammation of the small intestine and the colon. Death occurred within 10 days showing that in mice, HuR is required for organism survival (Ghosh et al. 2009).

1.7.2 Homo- and hetero-dimerisation of Hu proteins

Hu proteins are known to bind to themselves and other Hu protein family members to form complex assemblies (Kasashima et al. 2002). In situ chemical crosslinking assays revealed HuB can form dimers but not trimers. It also found HuD forms dimers, trimers and multimers in cells. The multimer maintains its ability to regulate mRNA transcripts and bind with additional Hu proteins. Additionally, HuR can form dimers but not trimers (Kasashima et al. 2002).

Using immunoprecipitation and RT-PCR, it was found that the hinge region and the first 24 amino acids of RRM3 of HuC are required for HuC homo-dimerisation. All four splice variants of the HuC hinge region were able to form HuC-self interactions highlighting alternative splicing does not affect homodimerization (Hinman et al. 2013).

Similar to HuC, the third RRM and the hinge region of HuR play a role in homo-multimerization (Fialcowitz-White et al. 2007). HuR binds the 2.4kb ubiquitously expressed transcript of *HuR* mRNA sequences containing an ARE and stabilises its own transcript. This results in increased HuR expression (Pullmann et al. 2007, Al-Ahmadi et al. 2009).

1.7.3 Hu proteins participate in nucleo/cytoplasmic shuttling

The subcellular location of Hu proteins determines the role in which they function. Hu proteins must become localised in the nucleus for pre-mRNA splicing to occur (Zhu 2009).

HuR has been shown to shuttle between the nucleus and cytoplasm and can therefore be assumed the neuronal proteins HuB, HuC and HuD could have the same ability. The cytoplasmic trafficking of HuR and mRNA cargo is poorly understood although there are many proposed mechanisms. HuR contains nucleo-cytoplasmic shuttling sequences (HNS) in the hinge region of the protein spanning residues 205–237. It is thought this region is responsible for translocation (Fan and Steitz 1998). The HNS is phosphorylated by kinases including protein kinase Cα (Doller et al. 2007), protein kinase Cβ (Amadio et al. 2010), protein kinase Cδ (Doller et al. 2008), checkpoint kinase 2 (Abdselmohsen et al. 2007), cyclin dependant kinase 5 (Filippova et al. 2012) and cyclin dependent kinase 1 (Kim et al. 2008).

The binding activity of HuR and its localisation is dependent on the kinase phosphorylating the HNS but also the position within the HNS that is phosphorylated (Kim and Gorospe 2008). For example, protein kinase C phosphorylates HuR at serine 158 and serine 221 and increasing its cytoplasmic expression (Doller et al. 2007). Cyclin dependent kinase 1 phosphorylates HuR at serine 202 (S202) ensuring HuR remains in the nucleus where it regulates polyadenylation and splicing. Unphosphorylated HuR-S202 complex is actively transported to the cytoplasm confirming phosphorylation of the complex changes its cellular location (Kim et al. 2008).

Doller et al. (2013) proposed the involvement of actin-myosin in *HuR* mRNA trafficking. Angiotensin II initiates translocation of protein-kinase Cδ, which in turn phosphorylates nuclear HuR at serine 318 located within RRM3. This process increases HuR's binding potential

to mRNAs. The HuR-bound mRNA complex interacts with motile transport ribonucleoproteins and cytoskeleton bound polysomes to translocate to the cytoplasm through myosin-driven transport along filamentous actin. HuR-bound mRNA is protected from degradation by exonucleases increasing the transcript stability. Once in the cytoplasm, HuR releases itself from the bound mRNA and returns to the nucleus (Fan and Steitz 1998a).

Translocation of Hu proteins is modulated by cellular stress induced by UV-light, heat shock and nutrient deficiency derived translocation are described here.

P21 protein is an inhibitor of cyclin-dependent kinase and known target of HuR protein. Human colorectal carcinoma, RKO cells were stimulated by Ultraviolet C-irradiation. HuR cytoplasmic localisation was enhanced, more HuR-*p21* complexes were observed resulting in enhanced stability of *p21* mRNA and its consequential upregulation. In the same study, western blot confirmed that when treating RKO cells with damaging agents including actinomycin D, hydrogen peroxide, an alkylating agent, and a cyclopentenone, p21 protein and cytoplasmic protein HuR levels increased (Wang et al. 2000).

Immunofluorescence and cell fractionation studies revealed that following a heat-shock of HeLa cells, cytoplasmic HuR expression increased. Although cytoplasmic HuR is usually associated with upregulation of mRNA transcripts containing AREs, this was not observed and instead the only function of cytoplasmic HuR was sequestration of mRNA transcripts in the nucleus (Gallouzi et al. 2000). This highlights that a large cytoplasmic presence of HuR is not necessarily functioning to upregulate transcripts expression that would disrupt the homeostasis of the cell.

1.7.4 Self-regulation of Hu proteins

Similar to its Drosophila homologue, members of the Hu family can bind their own mRNA and auto-regulate themselves or other Hu proteins (Bolognani et al. 2009, Mansfield and Keene 2012). HuR protein has been shown to auto-regulate its own expression through a negative feedback loop. Nuclear HuR protein binds *HuR* mRNA sequences containing a GU-rich element that overlaps the HuR major polyadenylation signal, PAS2. Increased expression of HuR protein initiates the expression of the 2.4KB *HuR* mRNA that contains an ARE to destabilize the *HuR* mRNA and therefore reduce its protein production. Reduced recruitment of the Cleavage stimulating factor CstF-64 in the GU-rich region on *HuR* mRNA, resulted in activated PAS2. This mechanism results in a definite expression of HuR protein and allows a stable nucleocytoplasmic distribution and HuR homeostasis in proliferating cells (Dai et al. 2012)

Hu proteins can also function as splicing enhancers on their own family transcripts. An example is their ability to promote the inclusion of an alternative exon, called exon 6 of the *HuD* pre-mRNA. This exon contains an ARE in which HuD and other Hu proteins can bind to resulting in an abundance of HuD protein expression (Wang et al. 2010). All three HuC RRMs are critical for the regulation of reporter *HuD* exon 6 inclusion (Kasashima et al. 2002). This confirms Hu proteins role as splicing regulators of their own transcripts but also allows them to self-regulate their own expression.

1.8 Hu Proteins Implicated in Disease

Since Hu proteins regulate many aspects of RNA regulation and the complex nature of the processes involved, there are many opportunities for deregulation to occur. This then causes disease in humans (Bronicki and Jasmin 2013).

Paraneoplastic encephalomyelitis and/or a sub-acute sensory neuropathy (PEM/SN) are collectively known as paraneoplastic neurological diseases (Anderson et al. 1987). These are disorders caused by an elicit Hu-specific humeral immune system response to Hu antigens produced ectopically by a primary tumour or metastasis in the brain. The body recognises these as foreign and releases autoantibodies that target all Hu proteins for degradation, this includes those that occur naturally in the body and those that are oncogenic, ectopically expressed. Normal tissue as well as cancerous tissue is targeted for degradation (Fisher et al. 1994, Graus et al. 1997). This produces systemic symptoms resulting in dementia, cerebellar degeneration, brainstem encephalitis, or myelitis. The presence of paraneoplastic disorders has shown a more promising cancer-related prognosis due to the body destroying the Hu proteins in the tumour. However, the patients quality of life remains diminished as they suffer non-reversible, debilitating neurological syndromes (Manley et al. 1995, Dalmau, Josep and Furneaux 1992, Graus et al. 1997). The presence of these neuropathies is considered symbolic of a Small cell lung cancer tumour or Neuroblastoma (Szabo et al. 1991, Fisher et al. 1994).

HuD was originally discovered by Szabo et al. (1991) due to its presence in patients with both Small cell lung cancer and paraneoplastic diseases. Patient's antiserum was screened against a cerebellar expression library and found to have Hu autoantibodies present. This disorder was later described as the 'Hu syndrome,' after the name of the patient in which the antibody was first discovered (Graus et al. 1997). All SCLC tumours aberrantly expressed neuronal HuD protein and the tumour-initiated immune response can be detected in up to 20% of those patients however PEM/SN is thought to develop in 1% of SCLC patients (Dalmau, Josep and Furneaux 1992, DeLuca et al. 2009). Posner and Dalmau (1997) determined the

other neuronal members of the Hu family, HuB and HuC were also autoimmune antigens of the Hu syndrome.

A study by Dalmau and Furneaux (1992) of patients with PEM/SN and a raised level of Hu-antibodies had tumours that were localised and small and this remained unchanged until death. Hu-autoantibodies are protective against tumour development and may aid eradication of tumour cells or at least improve patient survival (Graus et al. 1997). Research by Darnell and DeAngelis (1993) showed patients positive for anti-Hu antibodies showed spontaneous regression of Small cell lung cancer. This finding suggests the HuD-antigen might provide a molecular target for immunotherapy against HuD positive tumours but also provides a potential target for screening as a biomarker (Ehrlich et al. 2014). However, current efforts with systemic immunotoxin therapy and solid tumours is relatively unsuccessful due to poor penetration into the tumour mass because of large molecular size of the therapy, chemical instability or immunogenicity (Shan et al. 2013).

Some Neuroblastoma patients also present with anti-HuD antibodies that initiate neuronal apoptosis resulting in enteric nervous system impairment underlying paraneoplastic gut dysmotility (De Giorgio et al. 2003). In one of the first reported cases, a child with Neuroblastoma, showed paraneoplastic symptoms of progressive hearing loss, areflexia, and seizures following removal of the tumour. Analysis of serum and cerebrospinal fluid discovered anti-Hu antineuronal antibodies (Fisher et al. 1994).

Whilst aberrant expression of antigens by tumours can initiate an immune response, it is unusual for it to develop into a paraneoplastic disease therefore understanding the mechanism at which this occurs could be of value in the development of tumour detection,

diagnosis and new treatments, including immunotherapy (Kazarian, Meleeneh and Laird-Offringa 2011).

A recent study by Pulido et al (2016), identified isoaspartylation as a potential mechanism. Isoaspartylation is a naturally-occurring post-translational modification generating immunogenic protein damage. Isoaspartyl compounds are normally processed in the body causing no harm however abnormal isoaspartylation is implicated in several autoimmune diseases. Antibodies against isoaspartylated Hu would cross-react eliciting an immunological stimulus and an autoimmune response. Isoaspartyl linkages in proteins have been linked to aging and arise under physiological condition causing cellular stress (Mamula et al. 1999). HuD contains four canonical isoAsp-prone sites. The N-terminal region containing RRM1 contains three of those isoAsp conversion sites suggestive of RRM1's role in the auto-immune response of paraneoplastic disease in SCLC (Pulido et al. 2016, Manley et al. 1995, Graus et al. 1997). Additionally, the deregulated expression of neuronal protein in non-neuronal cell types, like that of the neuronal Hu proteins in the lung, can induce isopartylated proteins (Pulido et al. 2016).

Neurofibromatosis type I or von Recklinghausen neurofibromatosis is one of the most common dominant inherited autosomal disorders affecting 1 in 3,500 individuals worldwide. Neurofibromin 1, (*NF1*) gene codes for neurofibromin protein. This protein acts a tumour suppressor. *NF1* gene mutations result in multiple abnormalities, including development of neurofibromas and gliomas and abnormal distribution of melanocytes (Bernards 1995). Exon 23a of the *NF1* gene is an in-frame exon that is included during alternative splicing. In the presence of HuC protein, exon23a of *NF1* is skipped by binding to AU-rich sequences located either side of the regulated exon. This results in a defective NF1 protein. Deletions of HuC

proteins RRMs resulted in exon 23a inclusion in *NF1*, whilst deletion of the hinge region only reduced *NF1* exon 23a inclusion. This confirms HuC's role as a polyadenylation regulator (Zhu et al. 2008).

Aberrant expression of Hu proteins is also thought to play a role in Neurodegeneration (Doxakis 2014, Okano and Darnell 1997). Within the nervous system, the role of RBPs in brain function is essential for the architectural complexity of the neurons (Campos-Melo et al. 2014). Hu proteins have been shown to play important roles in neurite outgrowth, synapse formation and plasticity. HuD's role in neural development and regeneration means its aberrant role results in in multiple neurological disorders including Parkinson's disease, Alzheimer's disease, schizophrenia, epilepsy and spinal muscular ataxia (Perrone-Bizzozero and Bird 2013). HuD was shown to bind to mRNA transcripts of *APP* encoding amyloid precursor proteins and *BACE1* encoding β-site APP-cleaving enzyme 1, connected to Alzheimer's disease pathogenesis. HuD upregulated transcript stability by binding to the 3' UTR enhancing production of Aβ peptides that are related to the neurotoxicity of Alzheimer's disease (Kang et al. 2014). Genome-wide association study (GWAS) of Japanese and Chinese populations found SNPs in *HuB* to contribute to the pathogenesis of schizophrenia (Yamada et al. 2011).

Neurodegeneration is caused by disruptions of pathways involved in cell survival, cell death and the cell cycle resulting in a decrease in regulatory functions that impact on progressive neuronal cell death in neurodegenerative diseases (Driver 2012). A homeostatic balance between cell survival and cell death is dependent on the preservation of DNA integrity and repair. Additionally, deregulation to RNA metabolism is also considered a key feature in Neurodegeneration since it is essential for the molecular processes of RNA transcription,

maturation, transport, stability, degradation and translation in normal cells (Campos-Melo et al. 2014). HuR stabilises the mRNAs transcripts coding for cyclins D1, E1, A2, B1 each of which favour cell cycle progression. Therefore deregulation of HuR protein may influence neurodegeneration progression (Wurth 2012).

Commonly seen in neurodegenerative diseases is the ectopic expression of proteins and accumulation of cytoplasmic protein aggregates that initiates cell death and neurotoxicity due to protein inspecificity (Zaharieva et al. 2012). Hu proteins are reportedly ectopically and overexpressed in many cancers and therefore their role in neurodegeneration should be further analysed.

1.9 Cancer

Cancer is a heterogeneous group of diseases characterised by growth, invasion and metastasis defined through changes at cellular, genetic, and epigenetic levels and abnormal cell division. In the process of cancer development, normal cells evolve progressively to a neoplastic, malignant state forming complex tissues called tumours (Fig. 1.9).

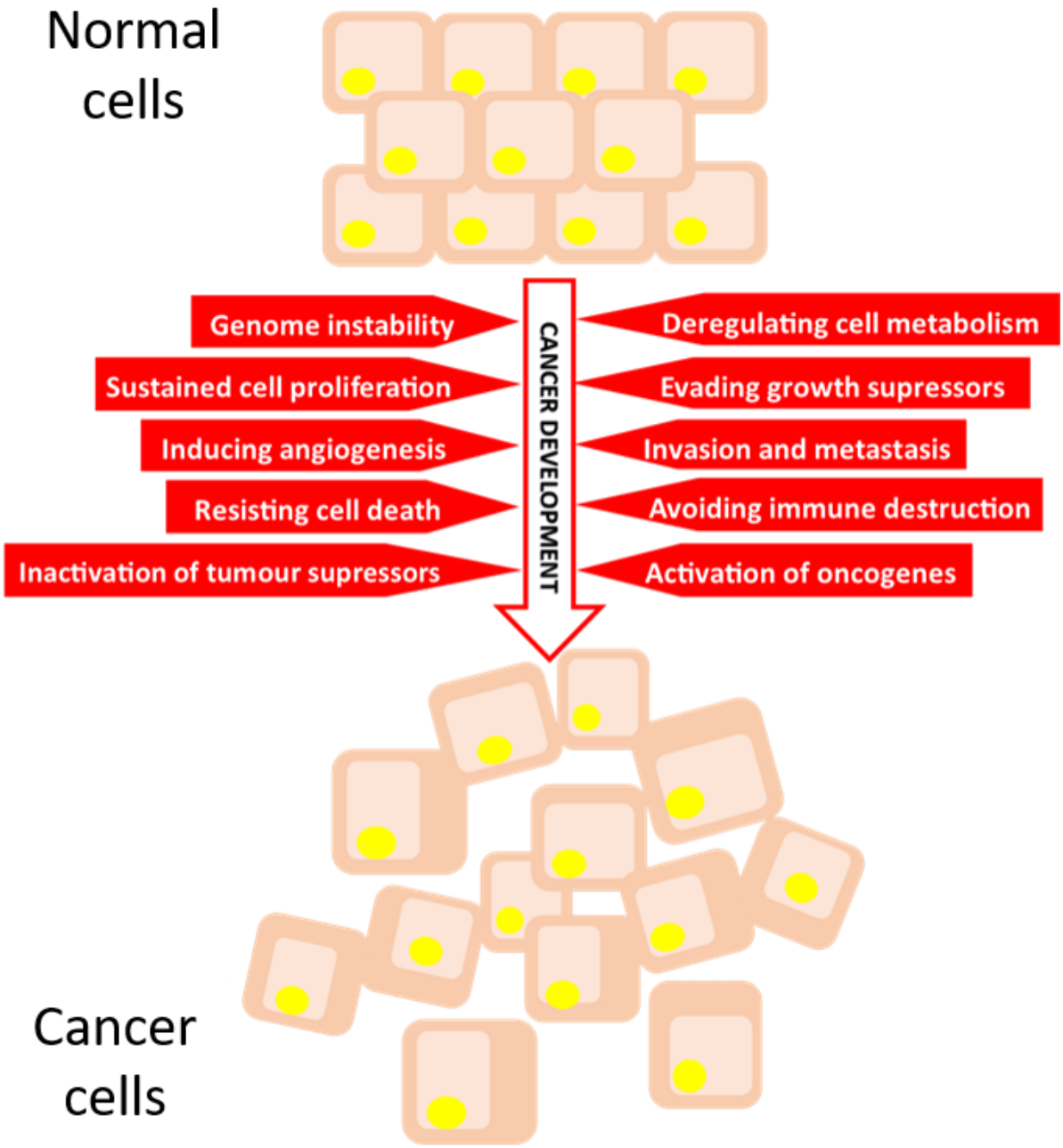

Figure 1.9: Hallmarks of cancer development. Normal cells evolve into oncogenic cells through a series of mechanisms that ultimately results in mutated cells and formation of tumours.

Inflammation and energy metabolism also play an extensive role in cancer progression. Ultimately cancer is caused by an activation of oncogenes or decreased expression of tumour suppressors (Hanahan and Weinberg 2011). Tumours develop from cell populations including

inflammatory cells, vascular cells and support cells. Interactions between these cells is critical for the cancers maintenance and survival from the body's immune defences and any additional treatments (Bissell and Labarge 2005). Cancer initiation and development is dependent on the reprogramming of cellular metabolism networks. This occurs through oncogenic mutations that allow the cancer cells to access nutrients from a nutrient-enriched environment and use them to sustain growth and vitality. Ultimately changes occur to glucose uptake, nutrient retrieval, glycolysis, nitrogen demand, gene regulation, and metabolic interactions with the microenvironment (Pavlova and Thompson 2016).

For normal homeostasis, cells experience regulated cell death called apoptosis. Cancer cells that become mutated due to DNA damage, form a secondary tumour in an extrinsic area or are targeted by cancer therapy, should go through apoptosis as a method to supress tumour formation. Unfortunately cancer cells are able to evade apoptosis following these events (Lopez and Tait 2015). Apoptosis is triggered through two pathways; the extrinsic and intrinsic pathways. The extrinsic pathway is induced when tumour necrosis factors (TNF) bind to cell surface death receptors which initiates the death-inducing signalling complex (DISC) and the apical caspase 8. The intrinsic pathway is started by interference with the mitochondrial outer membrane function and is the most common deregulated pathway involved in cancer apoptosis. It is regulated by a balance of pro- and antiapoptotic members of the Bcl-2 family of proteins (Reed 2000).

Another cellular process affected in cancer is the epithelial to mesenchymal transition (EMT). This is a dynamic set of processes during which cells transition from a polarised epithelial cells into migratory, invasive mesenchymal phenotypes and was first described by Hay and Zuk (1995). In the human body it is essential for the formation of the body plan and differentiation

of tissues and organs as well as processes including tissue repair. During cancer, EMT is stimulated in epithelial-derived cancer cells allowing cells to dissociate from the primary tumour, invade blood vessels and initiate the formation of a secondary tumour (Thiery et al. 2009, Goossens et al. 2017). EMT is controlled by a series of transcription factors including the families of Snail, Zeb and Twist, as well as microRNAs and epigenetic and post-transcriptional gene regulators. During cancers, these factors and process can be aberrantly affected also contributing to a carcinogenic phenotype.

Despite huge advances in our understanding into the mechanisms by which metastatic cells arise from primary tumours and the reasons that certain tumour types tend to metastasize to specific organs, it still accounts for around 90% of all cancer-related deaths. This mechanism was first described by an English surgeon called Stephen Paget in 1889. He hypothesised that metastasis relies on homeostatic interactions between the cancer cells, 'the seeds', and the organ microenvironment, 'the soil'. Research has continued to evolve this theory (Fidler 2003).

1.10 Hu proteins, their presence and function in carcinogenesis

Hu proteins interact and stabilise many mRNA targets that code for proto-oncogenes, cytokines and lymphokines each of which influence carcinogenesis. Regulation consists of multiple tightly controlled processes, consequently the complexity of each step increases the chance for deregulation to occur. Modifications to expression levels and function of RBPs and their mRNA targets can augment the effects of cancer driver genes by accelerating tumour progression and promoting aggressiveness (Bronicki and Jasmin 2013).

Radio-labelled transcripts and binding studies revealed HuB interacts and forms multimers with c-myc. This binding occurs directly to AUUUG, AUUUA, and GUUUUU sequences in the 3' UTR of *c-MYC* mRNA. Deletion analysis determined HuB's RRM3 binds to those sequences (Levine et al. 1993). c-Myc functions as a transcription factors in many cancers, activating autonomous proliferation and growth, increasing DNA replication, upregulating cellular metabolism and has therefore been considered a molecular hallmark of cancer (Gabay et al. 2014). *c-FOS* is also a target of HuB (Levine et al. 1993). c-Fos functions in proliferation and differentiation of normal tissue as well as in oncogenic transformation and tumour progression (Mahner et al. 2008).

Each Hu proteins are known to have complementary mRNA target that once bound effects their stability. Brennan and Steitz (2001) have shown that HuR achieves stabilisation by competing with destabilizing ARE-binding proteins for the same mRNA binding sites or through actively protecting the mRNA transcript from degradation. HuR's stabilising function correlates with its cytosolic presence which is often seen overexpressed in high grade tumours (Brennan and Steitz 2001, Bolognani et al. 2012). HuR binds to mRNA transcripts coding for proto-oncogenes, cytokines, growth factors and invasion factors increasing stability and translation. The corresponding proteins then influence various stages of tumour development including over-proliferation through c-Myc upregulation, evasion of apoptosis via apoptosis factors p27, p21, Bcl-2, sustained angiogenesis by upregulating VEGF and tissue invasion and metastasis by affecting the expression of MMP-9 and Snai1 (Wang et al. 2013, Vo et al. 2012, Wurth 2012, Filippova et al. 2011, Dong et al. 2007, 2014). Further details of these mRNA targets of the Hu family of RBP are described in Table 1.1.

Cancer Hallmark	mRNA Target	Hu protein	Expression change	Reference
Tumour Formation	*ER*	HuR	Upregulated	(Calaluce et al. 2010)
	GLUT1	HuB	Upregulated	(Jain et al. 1997)
	Wnt5a	HuR	Downregulated	(Leandersson et al. 2006)
Proliferation	*BCL-2*	HuR	Upregulated	(Filippova et al. 2011)
	p21	HuD HuR	Upregulated	(Joseph et al. 1998) (Wurth 2012)
	p27	HuR	Upregulated	(Wang et al. 2013)
	Msi-1	HuR	Upregulated	(Vo et al. 2012)
	c-fos	HuD HuR HuB	Upregulated	(Chung et al. 1996) (Nabors et al. 2001) (Levine et al. 1993)
	Cyclin A	HuR	Upregulated	(Guo and Hartley 2006)
	Cyclin B1	HuR	Upregulated	(Cho et al. 2006)
	Cyclin E1	HuR	Upregulated	(Guo and Hartley 2006)
	N-myc	HuD	Upregulated	(Lazarova et al. 1999)
	C-myc	HuB HuC HuD HuR	Upregulated	(Levine et al. 1993) (King 2000) (King 2000) (Milne et al. 2006)
	NP53	HuR	Upregulated	(Yan et al. 2012)
Invasion and Metastasis	*B-Actin*	HuR	Upregulated	(Dong, R. et al. 2007, Dormoy-Raclet et al. 2007)
	uPA	HuR	Upregulated	(López de Silanes et al. 2004)
	Snai1	HuR	Upregulated	(Dong, R. et al. 2007)
	MMP-9	HuR	Upregulated	(Dong, R. et al. 2014)
Angiogenesis	*VEGF*	HuC HuD HuR	Upregulated	(King 2000) (King 2000) (Nabors et al. 2003)
	Hif-1 α	HuR	Upregulated	(Dong, R. et al. 2014)
	COX-2	HuR	Upregulated	(Nabors et al. 2001)
Immunomodulation	*TNF-ß*	HuR	Upregulated	(Nabors et al. 2001)
	TNF-α	HuR	Upregulated	(Nabors et al. 2003)
	IL-8	HuR	Upregulated	(Nabors et al. 2001)
	IL-6	HuR	Upregulated	(Nabors et al. 2001)

Table 1.1: mRNA targets of Hu proteins. Table 1.1 shows the variation of effects Hu proteins can have influencing the expression of other protein factors involved in tumour growth, tumorigenesis, invasion and metastasis, angiogenesis and tumour inflammation.

In cancer, cellular polarity and senescence are disrupted, these cellular processes are influenced by Hu proteins. HuR regulates Tumour protein 63 (*ΔNp63*) transcript that maintains cell proliferation and polarity in normal mammary epithelial cells. RNA electrophoretic mobility shift assays performed on immortalized mammary epithelial cells, MCF10A, identified HuR binding regions in *p63* transcript. HuR binds directly to one of two U-rich elements in the 3'-UTR of the *ΔNp63* mRNA inhibiting ΔNp63 protein expression through translation. Thus, HuR maintains cell proliferation and polarity of MCF10A cells at least in part via regulating ΔNp63 expression (Yan et al. 2012).

During cell senescence cells reach their replicative life span *in vitro* and ultimately experience irreversible growth arrest. In humans, the Ink4a-Rb pathway plays a crucial role in senescence. HuR destabilises *Ink4a* mRNA in human diploid fibroblasts as well as controlling the regulation of other genes that function in senescence notably *p53, p21* and *cyclin D1*. HuR is also known to repress the alternative reading frame (ARF) tumour suppressor of the $p14^{ARF}$ pathway which allows the replicative potential of the cells to increase (Kawagishi et al. 2013). Cellular senescence potentially acts as an anti-cancer mechanism whereas microglial senescence is thought to contribute towards Neurodegeneration. During cellular replicative senescence, HuR expression is suppressed and this is linked to a decreased capability of the protein to stabilise mRNA of pro-survival factors (Campos-Melo et al. 2014).

Hu proteins regulate alternative splicing and polyadenylation. The complex nature of alternative splicing, polyadenylation and their deregulation is thought to initiate or contribute to many human diseases (Faustino et al. 2003). HuR regulates pre-mRNA splicing of *FAS,* an apoptotic-promoting receptor. When *FAS* endures alternative splicing, exclusion of exon 6 results in an isoform that prevents programmed cell death. HuR promotes the exon 6 skipping

by binding to an exonic spicing silencer. This confirms HuR's role in alternative splicing and in influencing cell fate (Izquierdo 2008). This is particularly significant in hepatocellular carcinoma where HuR restricts translation of *FAS* mRNA obstructing Fas-mediated apoptosis. Ultimately this results in an increase in cell survival and proliferate increasing the growth of the tumour (Zhu et al. 2015).

Zaharieva et al. (2015) shows that specificity of RBPs binding patterns on mRNA transcripts are relative to its concentration, activity and localization. An interrelationship between Hu ectopic or over-expression and larger malignant tumours, advanced stage disease, positive lymph nodes, chemo resistance to standard cancer treatments and consequently poor survival rates (Denkert et al. 2004). Table 1.2 details Hu proteins aberrant or overexpression in cancers.

Calaluce et al. (2010) described how HuR controls genes in different stages of cancer and hypothesized *HuR* is a tumour-maintenance gene, allowing for cancer progression once it is established. Its overexpression and cytoplasmic presence in many cancers suggests it could be used as a prognostic marker and a target in therapeutic treatments. Since these proteins share similar structure and function, it can be assumed that the other Hu proteins also can in this manner. Additionally, in mammals, *Hu* genes are alternatively spliced to produced different protein isoforms. Most variation occurs due to alternative splicing coding for the hinge region (Keene 1999). HuR isoforms often have different functions and are expressed based on their need and this may influence aberrant Hu protein expression in cancers, depending on the need and conditions within the tumour microenvironment.

Hu Protein	Cancer	Expression	Subcellular Location	Reference
HuB	Small cell lung cancer	Aberrant expression		(King 1997)
	Medulloblastoma	Aberrant expression	Cytoplasmic	(Gao and Keene 1996)
HuC	Large cell neuroendocrine carcinoma	Aberrant expression		(Matsumoto et al. 2012)
	Small cell lung cancer	Aberrant expression		(Matsumoto et al. 2012)
HuD	Small cell lung cancer	Aberrant expression		(King 1997)
	Neuroblastoma	Aberrant expression		(Dalmau, J et al. 1995)
HuR	Oral cancer	Over-expression	Cytoplasmic	(Kakuguchi et al. 2010)
	Oesophageal cancer	Over-expression	Cytoplasmic	(Zhang et al. 2014)
	Cervical cancer	Over-expression		(Cho et al. 2006)
	Colon cancer	Over-expression	Both	(López de Silanes et al. 2003)
	Small cell lung cancer	Over-expression		(Wurth 2012)
	Non-small cell lung cancer	Over-expression	Cytoplasmic	(Wang et al. 2011)
	Breast cancer	Over-expression	Cytoplasmic	(Hostetter et al. 2008)
	Renal cancer	Over-expression	Cytoplasmic	(Datta et al. 2005)
	Merkel cell carcinoma (Skin)	Over-expression	Cytoplasmic	(Koljonen et al. 2008)
	Mesothelioma	Over-expression	Cytoplasmic	(Stoppoloni et al. 2008)
	Ovarian cancer	Over-expression	Cytoplasmic	(Prislei et al. 2013)
	Urinary tract urothelial carcinoma		Cytoplasmic	(Liang et al. 2012)
	Bladder cancer	Over-expression	Cytoplasmic	(Miyata et al. 2013)
	Glioblastoma	Over-expression	Cytoplasmic	(Nabors et al. 2003)
	Gastric cancer	Over-expression	Nuclear	(Milne et al. 2006)
	Pancreatic cancer	Over-expression	Cytoplasmic	(Jimbo et al. 2015)
	Prostate cancer	Over-expression	Cytoplasmic	(Niesporek et al. 2008)
	Thyroid cancer	Over-expression		(Danilin et al. 2009)
	Medulloblastoma	Over-expression		(Nabors et al. 2001)

Table 1.2: Association of Hu protein expression in Cancer. Summary of Hu proteins and their implication in cancer. This data particularly highlights a correlation between cytoplasmic over-expression of HuR in cancer.

The localisation of RBPs within cells importantly influences its role in gene regulation events and its target mRNA transcripts. Although HuR protein is predominantly localised to the nucleus of normal cells, in response to environmental stimuli HuR can in an adaptive response translocate to the cytoplasm whereby it can participate in cytoplasmic gene regulation events (Atasoy et al. 1998, Nabors et al. 2001). In the cytoplasm, Hu proteins influence aberrant regulation of many mRNA transcripts. They can decrease the stability of tumour suppressor genes but more commonly increase the stability and translation of proto-oncogenes, cyclins, kinases, inflammatory factors, apoptosis-related factors that each have a direct influence of tumour formation and development(Wang et al. 2013). It is also important to consider the level of expression of Hu proteins in human cells since overexpression of the Hu homologue ELAV protein in *Drosophila Melanogaster* has shown to be lethal or produce cellular defects. This concentration-based functionality has also been observed in other RBPs (Zaharieva et al. 2015b).

Both the HuB protein isoforms are discussed in more detail in Section 1.6, are expressed in human Medulloblastoma cells and display different expression patterns in human brain and tumour cells (Gao et al. 1994). In Medulloblastoma cells extracted from a brain tumour, HuB proteins were found predominantly expressed in the cytoplasm. HuB proteins reside in granular structures that contain multiple protein molecules bound to each mRNA forming a multimeric RNP that then associates with polysomes. This highlights their involvement in translation or mRNA stability. Additionally, both HuB isoforms are also expressed in Small-cell lung carcinoma (Gao and Keene 1996).

As discussed in Section 1.7.4, HuR proteins auto-regulation occurs through a negative feedback loop. This feature allows a stable nucleocytoplasmic distribution in normal cells (Dai

et al. 2012). In cancer, cytoplasmic HuR expression is related to the ability to bind and upregulate the stability of cancer-related mRNA transcripts, this helps accelerate the cancers progression. This is thought to occur in oesophageal cancers where upregulated cytoplasmic HuR expression is observed and associated with positive lymph node metastasis, deep tumour invasion, high-grade malignancy and poor survival rates during diagnosis (Zhang et al. 2014). Similarly, HuR cytoplasmic overexpression is seen in in breast cancer with characteristic large tumours, p53 positivity and oestrogen and progesterone receptor negativity (Heinonen et al. 2007, Calaluce et al.2010). Knockdown of HuR in HeLa, a cervical carcinoma cell line, revealed HuR is a suppressor of apoptosis. Cellular stress caused by UV-radiation in HeLa cells showed upregulation of HuR and therefore extreme survival under stress (Lal et al. 2005). The role of HuR in transcript stabilisation is seen with *Vascular endothelial growth factor-A* (*VEGF-A*) and cyclooxygenase-2 (*COX-2*) mRNA. HuR bind specifically to AU-rich sequences in the 3' UTR of *VEGF* and *COX-2* transcripts. In tumour microenvironments, cytoplasmic HuR protein responds to hypoxia by stabilising of the mRNA transcripts of *VEGF-A* and *COX-2* (Levy et al. 1998, Kurosu et al. 2011). Under normal conditions, VEGF protein participates in a variety of physiological and pathological processes including stimulating the formation of blood vessels particularly during embryo development and wound healing. Overexpression of VEGF and its receptors, VEGFR-1, VEGFR-2, neuropilin-1, are associated with poor prognosis in Breast cancer (Ghosh et al. 2008).

Recent research suggests RBPs influence miRNAs activity and stability and vice versa indicating a combined contribution towards regulating gene expression. HuR functions alongside miRNAs to aid the stabilisation process (Wurth 2012). For example, in breast cancer, HuR upregulates cyclin E1 expression by interacting directly within its transcript. Additionally,

miR-16 represses cyclin E1 through similar binding. This concludes that miR-16 can override HuR upregulation of cyclin E1 without affecting HuR expression and direct association with the *cyclin E1* mRNA (Guo and Hartley 2006).

1.11 Lung cancers

Lung cancers are one of the leading causes of cancer-related deaths worldwide (Matsumoto et al. 2012). Lung cancer accounts for 12.7% of all cancer registrations in England and is the second most common malignant cancer for both females and males, after breast cancer in females and prostate cancer in males (King and Broggio 2018).

Lung cancers are divided into two categories, Small cell lung cancer (SCLC) and Non-small cell lung cancer (NSCLC) which includes Squamous cell carcinoma, Large cell carcinoma and Adenocarcinoma (Van Meerbeeck et al. 2011). Whilst treatments for NSCLC have improved vastly in recent years, SCLC treatment is limited. This highlights the need for a deeper understanding of the disease, identification of novel targets and discovery of treatments (Lovly and Carbone 2011).

1.11.1 Small cell lung cancer

Small cell lung cancer (SCLC) is highly malignant and one of the most aggressive pulmonary neoplasms, with a rapid onset of symptoms (Ehrlich et al. 2014). Patients diagnosed with limited disease survive for 15-20 months with treatment. Patients with extensive disease at diagnosis survive between 7-11 months with treatment and without the median survival time is 2-4 months (Lampaki et al. 2016). Metastases are commonly found upon diagnosis in the liver, adrenals, bone, bone marrow and brain (Ehrlich et al. 2014, Glisson and Byers 2015).

SCLC originates from neuroendocrine cells (Glisson and Byers 2015). It was first referred to as 'Oat cell carcinoma' when it was identified in 1936 in a asbestosis patient (Roodhouse Gloyne 1936).

SCLC shows a considerable degree of morphological histopathological variability. SCLC cells are small round, oval or spindle shaped cells with scanty cytoplasm (Brambilla et al. 2001). Of all lung cancers diagnosis, tumours with less than 10% of large cells is classified as pure SCLC by the World Health Organisation (WHO). Within the tumour, the size of the cells can vary however finely granulated chromatic, no prominent nucleoli and the lack of cell boarders are typical for SCLC morphology (Travis et al. 2015, Rekhtman 2010). SCLC is distinguished from NSCLC physiologically due to aggressive nature, fast growth and easily developed metastases (Glisson and Byers 2015).

Since 1970, there has been over 40 clinical trials conducted on SCLC patients with no significant change therefore the combination of chemotherapeutic drugs remain the same (Lampaki et al. 2016). Current research supports the idea that identifying a set of new novel antibody markers, more specific to the biology and behaviour of the SCLC will allow the development of a national screening program, improved targeted diagnosis and monitoring and specific treatments to overall improve the survival rate.

SCLCs initiation and progression is a complex multi-step procedure. Progressive genetic alterations involving proto-oncogenes include the myc family, *c-myb, c-kit, c-jun* and *c-src.* Additionally two tumour suppressor genes that are affected are *p53* and Retinoblastoma-associated (*Rb*) (Cook et al. 1993). The use of paraffin-embedded tissue, highly polymorphic markers and PCR-based analysis revealed allelic loss on chromosomes 3p, 5q, 13q, and 17p

was found in 75-100% of SCLCs tumours obtained at autopsy. The 13q is typically significant of alteration to the *Rb* tumour suppressor gene (Merlo et al. 1994).

Drug resistance often develops in SCLC. Early studies of the NCI-H69 SCLC cell line revealed amplification and expression of the P-glycoprotein encoded by *MDR-1* and highlighted this as a cause of multidrug resistance in some SCLC tumours (Reeve et al. 1989).

1.11.2 Non-small cell lung cancer

Non-small cell lung cancer describes a series of Lung cancers including Adenocarcinoma (38%), Squamous cell carcinoma (20%), Large-cell carcinoma (5%), and other poorly differentiated variants (Goldstraw et al. 2011). In comparison to SCLC, it is seen to have better survival rates and clinically more manageable disease.

Non-small cell tumours are defined by cells that are large, have a low nuclear to cytoplasmic ratio, have vesicular, coarse or fine chromatin and frequent nucleoli. Not all non-small cell lung tumour meet this criteria but are still considered NSCLC due to their large size and abundant cytoplasm (Travis et al. 1999).

NSCLC is typically characterised by several genetic changes downregulating tumour suppressor genes and upregulating oncogenes. Research has sought to identify susceptibility genes that predispose Lung cancer. Of interest is 15q24–25, this region contains several genes of interest, including three genes that encode nicotinic acetylcholine receptor subunits (Thorgeirsson et al. 2008). Genes of interest in NSCLC include the tumour suppressors, tumour protein-53 (*TP53*), retinoblastoma-associated 1 (*RB1*), that govern two complementary regulatory pathways of proliferation control. Additional genes of interest are those including

epidermal growth factor receptor (*EGFR*), echinoderm microtubule-associated protein-like 4-anaplastic lymphoma kinase (*EML4-ALK*) and cyclin-dependant kinase (*p16INK4a*). Genetic alterations including allelic loss of heterozygosity at chromosomes 3p and 17p are frequent in Lung cancers and has been shown to correlate with clinical parameters and poor prognosis (Chmara et al. 2004).

Treatments targeting genetic alterations or the pathways they influence are in development. In NSCLC treatment, targeted gene therapies have focussed on mutations in *EGFR* and rearrangements in *ALK*. *EGFR* mutations are seen more commonly in Asian patients accounting for 30-50% of NSCLC cases in this population. Clinical trials using tyrosine-kinase inhibitors targeting EGFR proteins in patients positive for the *EGFR* mutation have shown promising results (Rosell et al. 2012). Alterations to the oncogenic fusion genes *EML4-ALK* is often seen in non-smokers and younger patients representing 2-7% of tumours (Reck et al. 2013). ALK protein inhibition of EML4-ALK rearrangement-positive tumours saw a reduction in tumour size and a more stable disease in most patients (Kwak et al. 2010).

1.12 Hu proteins in Small cell lung cancer

The Hu protein family are considered tumour antigens in Small cell lung cancer (SCLC) (D'Alessandro et al. 2008). The neuronal Hu family members, HuB, HuC and HuD are ectopically expressed in SCLC tumours, but not in Non-small cell lung cancers. An over-expression of HuR is common in both cancers (Manley et al. 1995). Paraneoplastic encephalomyelitis/sensory neuropathy (PEM/PSN) which accounts for 3-5% of all SCLC patients, although lower titres of Hu antibodies can be seen in about 15-20% of SCLC patients without autoimmune symptoms (Dalmau, Josep and Rosenfeld 2008, Kanaji et al. 2014).

As discussed in Section 1.12, the presence of Hu proteins in SCLC specifically is often symbolic of a more favourable cancer prognosis. Hu antigens initiate a humeral immune response producing an autoimmune attack on the nervous system where autoantibodies destroy Hu tumour antigens and normal immune antigens in the nervous system resulting in non-reversible neurological paraneoplastic syndromes (Harmsma et al. 2013). Although a higher survival rate is predicted, the patients quality of life is reduced due to the symptoms of the paraneoplastic syndrome (Graus et al. 1997).

Kazarian et al. (2009) showed in mice, anti-Hu levels rise before the cancer is chemically detectable. D'Alessandro et al. (2008) showed that in newly diagnosed SCLC patients, low anti-Hu-Ab are detected. Hu proteins could be used as biomarkers for this tumour type especially. Harmsma et al. (2013) summarised that the presence of Hu and anti-Hu autoantibodies is a good indicator of SCLC particularly since the immune response to Hu proteins may occur whilst the cancer is still small, asymptomatic and undetectable by routine methods. The cancer diagnosis could then be confirmed using imaging methods. Hu mRNA was detectable in the peripheral blood of SCLC patients, using RT-qPCR technologies suggesting a method to prompt further tests and secondly as monitoring tool (D'Alessandro et al. 2008). The immunoreactive regions of HuD protein have been mapped to the N-terminal region and in the first and second RRMs (Manley et al. 1995, Kazarian et al. 2009).

A study looked at the role of MHC proteins in SCLC and the role they play in regulating the anti-Hu immune response. MHC Class I molecules are required for the presentation of viral or tumour antigens to cytotoxic T lymphocytes. MHC Class I proteins are found to be lowly expressed in SCLC, which is associated with a poor prognosis and increased metastatic potential. It was concluded that co-expression of Class I MHC and Hu antigen by tumours may

play a role in the development of anti-Hu associated paraneoplastic disorders (Dalmau et al. 1995).

Analysis of 20 primary human neuroendocrine lung tumour tissues revealed HuD ectopic expression. Sequencing revealed two inactivating somatic mutations in the coding sequence of *HuD* mRNA in 7 of the tumours. A stop codon mutation, (c.655C>T), resulting in a truncated protein and a frameshift caused by c.424delA. Loss of heterozygosity is common in cancer and results in the loss of gene function. This was seen in seven of the tumours studied (D'Alessandro et al. 2010). In the same study, genetic analysis of five SCLC cell lines revealed one mutation that was previously documented by Sekido et al. (1994). *HuD* mRNA experiences alternative splicing of its 5'-coding region resulting in an additional 87 base pairs of sequence and a termination codon. This codes for a small truncated protein of 11 amino acids but its function was undetermined.

SCLC is associated with overexpression of c-myc protein and this contributes towards the cancers malignant and aggressive nature (Little et al. 1983). As previously described in Section 1.10, HuD has additionally been shown to bind to AU-rich stability sequences of *c-Myc* mRNA, upregulating its expression (Cook et al. 1993, Liu et al. 1995).

RT-qPCR and Western blot studies revealed *HuC* mRNA and HuC protein in 5 of 6 SCLC cell lines and 2 of 2 Large cell neuroendocrine carcinoma (LCNEC) cell lines which is a rare pulmonary tumour. Of SCLC patients with and without PEM/SN, 12.9% displayed anti-HuC antibodies (Matsumoto et al. 2012).

1.13 Neuroblastoma

Neuroblastoma (NB) is an embryonal tumour of the peripheral sympathetic nervous system characterized by a substantial phenotypic diversity. NB is the most common extra-cranial solid tumour diagnosed in children and represents 15% of all childhood cancer deaths (Maris et al. 2007). NB has an average 5-year survival rate of less than 50% (Ehrlich et al. 2014). The severity of this disease highlights the need to yield actionable therapeutic targets for the highly fatal cancer (Louis and Shohet 2015).

Neuroblastoma is a heterogenous disease in its pathology and in its molecular profile. This heterogeneity is responsible for the exceptional phenotypic diversity resulting in contrasting clinical presentations and varied treatment responses (Louis and Shohet 2015). At one end of the spectrum, it is possible that the cells reach maturity and even spontaneous regression. On the contrary, significant disease progression irrespective of treatment can be fatal due to the transient state of neuronal crest cells.

Screening of thousands of NB cases have not found a single homogenous genetic or epigenetic mutation further supporting the molecular heterogeneity. Familial NB accounts for 1-2% of cases with the primary cause identified as a germline mutation in the anaplastic lymphoma kinase (*ALK*) gene (Mossé et al. 2008). Patients with an increased expression of N-myc proto-oncogene (*MYCN)* have showed to have a poorer prognosis. N-Myc protein is a transcriptional regulator expressed in the peripheral neural crest. In normal cells it controls proliferation, migration and stem cell homeostasis (Westermark et al. 2011). The molecular profile of this cancer might provide an insight into development of the disease and give rise to new novel targets for new therapies.

Neuroblastoma provides an ideal disease model to study functional cellular hierarchy in solid tumours in relation to the cancer stem cell (CSC) theory, due to its embryonal origin and heterogeneity (Hansford et al. 2007). Additionally, its wide range of clinical behaviours that can show spontaneous regression or a very aggressive metastatic disease, with limited response to treatment also supports the CSC model (Monclair et al. 2009). The CSC model describes a functional cellular hierarchy for malignancy or clonal evolution within the tumour which is entirely supported by tumour initiating cell (TICs) (Kreso and Dick 2017, Coulon et al. 2011). Hansford et al. (2007) investigated characteristics including self-renewal through sequential sphere-forming cells, tumorigenicity, drug resistance and the ability to differentiate towards distinct lineages to identify tumour initiating cells. They concluded NB cells contain cancer stem cell properties adequate in tumour-initiating ability. Coulon et al. (2011) later confirmed and showed that the CSC model correlated with NB tumour-initiating cells which was suggestive of functional stem cell-like characteristics and contributors of tumour progression.

1.14 Hu proteins in Neuroblastoma

Hu proteins and their corresponding antibodies have been found in Neuroblastoma. In 1992, Dalmau and Furneaux, showed HuD protein is aberrantly expressed in over 50% of Neuroblastoma cells. Later in 1997, Ball and King described HuD and HuB proteins as excellent neuronal markers of Neuroblastoma. Their study on 36 primary tissue samples and 11 cultured cell lines, showed HuB or HuD were expressed in 98% of their test samples.

Cytoplasmic protein aggregates causes cell death and neurotoxicity in Neurodegenerative diseases, however in cancer, increased protein expression has no effect showing their ability

to tolerate these aggregates and continue proliferation (Zaharieva et al. 2012). Also, seen in neurodegeneration is ectopic expression of proteins which leads to protein inspecificity and function and therefore cell death (Zaharieva et al. 2015b).

In a third of all Neuroblastoma cases, over expression of the proto-oncogene, *MYCN*, is observed. The level of *MYCN* expression can be used to determine the clinical behaviour of the Neuroblastoma since its expression correlates with rapid disease progression. HuD is known to modulate the expression of n-Myc protein through post-transcriptional events (Lazarova et al. 1999). HuB is predominantly expressed in Neuroblastoma tumours with unamplified n-Myc status. HuD specifically was associated with a clinically favourable prognosis since it's expression is associated with single copy n-Myc status and limited disease progression (Ball and King 1997).

A study identifying the presence of Hu antigens in Neuroblastoma patients found them present in 78% cases with less than 4% having clinically detectable titres anti-Hu antibodies in their blood serum. This suggests the measure of Hu antigens is a good indicator of tumour presence. Neuroblastoma tumours expressing little or no Class I MHC proteins were more aggressive and had more metastasis. Correlation between expression of MHC Class I proteins and the anti-Hu immune response in Neuroblastoma was suggestive of an additional T-cell mediated cytotoxic response but this would need further clarification (Dalmau et al. 1995).

1.15 Glioblastoma multiforme

Glioblastoma Multiforme also known as Glioblastoma, are very aggressive tumours of the central nervous system (Nabors et al. 2003). Brain tumours are classified according to their origin including astrocytic tumours, oligodendrogliomas, ependymomas, and mixed gliomas.

Glioblastoma are a type of astrocytoma and have an extremely poor prognosis (Schwartzbaum et al. 2006).

Todays grading system is based on the initial findings of Bailey and Cushing (1926) and Glioblastomas are always graded IV due to their high malignancy, invasiveness and growth rate and the tumours contain undifferentiated cells (Ferguson and Lesniak 2005). Glioblastomas are easily distinguished from low-grade astrocytic tumours, due to their distinct histopathological features including cellular atypia, mitotic figures, necrotic foci with peripheral cellular pseudopalisading and microvascular hyperplasia.

Glioblastomas are the most common primary malignant brain tumour accounting for 16% of primary brain and central nervous system neoplasms. Generally it is considered a rare tumour with an incidence of less than 10 in 100,000 people globally (Thakkar et al. 2014).

Glioblastoma develop by two different mechanisms, and although the tumours are not morphologically different, they contain different patterns of promoter methylation and expression profiles at both RNA and protein levels (Ohgaki and Kleihues 2007). 90% of Glioblastoma cases develop *de novo* where normal glial cells endure multistep tumorigenesis and are termed primary Glioblastoma. Genetically 70% are characterised by loss of heterozygosity 10q, 36% have epidermal growth factor receptor (*EGFR*) amplification, 31% have a $p16^{INK4a}$ deletion and 25% have phosphate and tensin homologue (*PTEN*) mutations. Tumours display rapid growth developing in 3 months on average and manifests in older people (Ohgaki and Kleihues 2007). Secondary Glioblastomas develop through progression from low-grade tumours including low-grade glial tumours or anaplastic glial tumours. Genetic mutations in the *TP53* gene, amplification of platelet-derived growth factor receptors and loss of heterozygosity at 17p, 19q, and 10q are often found. Secondary Glioblastomas

develop over time but generally present in younger patients (Kleihues and Ohgaki 1999). Previously, it was thought Glioblastoma only developed from glial cells. However, it was recently shown that it can develop from multiple cell types if they have neural stem-cell like properties. The cells in these tumours vary in stages of differentiation with their phenotypic variations induced by alterations to the Akt and Notch signalling pathways (Phillips et al. 2006).

The cause of Glioblastoma is under consideration. One factor known to increase the risk of glioma is ionising radiation exposure. This typically appears years later following treatment for a different tumour or condition where the risk of developing Glioblastoma following radiotherapy is estimated at 2.5% (Johnson et al. 2015, Salvati et al. 2003). Other environmental factors are thought to include exposure to pesticides, smoking, electromagnetic fields, formaldehyde, and nonionizing radiation from mobile phones although evidence is limited for these factors (Alifieris and Trafalis 2015).

Development of Gliomas is correlated with some genetic diseases including Neurofibromatosis 1 and 2, Tuberous sclerosis, Li-Fraumeni syndrome, Retinoblastoma, and Turcot syndrome. However, these genetic diseases account for less than 1% of all Glioblastoma patients (Ellor et al. 2014).

Genome studies of the U87-MG Glioblastoma cell line highlighted 512 genes with homozygous mutations. The mutations included an array of different types including single nucleotide polymorphisms, small insertions and deletions, microdeletions and interchromosomal translocations (Clark et al. 2010). A further study of more than 200 tumour samples and 600 genes produced a genetic profile where three key signalling pathways that were commonly activated. These were the p53 pathway, the receptor tyrosine

kinase/Ras/phosphoinositide 3-kinase signalling pathway, and the retinoblastoma pathway. Activation of these pathways results in uncontrolled cell proliferation and enhanced cell survival, essentially driving the process of gliomagenesis (Chen et al. 2012).

Glioblastoma is associated with a significantly poor prognosis which is preliminary determined by the patients age and the histological type of their tumour as described above (Schwartzbaum et al. 2006, Thakkar et al. 2014). The two-year survival rate for adults between 46-64 years of age is 7.7% and for people over 65, it is 2.1% which emphasises the aggressive nature of the disease (Bolognani et al. 2012). More recently, gene expression studies have given rise to genetic profiling allowing a prediction of patient outcome and response to treatment through the relationships of implicated genes in tumour biology (Sulman et al. 2009).

Glioblastoma are particularly challenging to treat because they embed in deep, specialised areas of the brain that control aspects of speech, motor function and the senses. The tumours proliferate and invade other tissues very quickly and there are no effective treatments available (Ware et al. 2003). Initially, seizures can be treated with antiepileptic drugs. Whilst corticosteroids help control vasogenic oedema and its symptoms. The ability of surgical resection has improved over the years, however the survival rate is still low (Thakkar et al. 2014). Chemotherapy is an additional option and often follows surgical resection. Despite maximal initial resection and multimodality therapy, recurrence of GBM is common affecting around 70% of patients (Stupp et al. 2009).

1.16 Hu proteins in Glioblastoma multiforme

In the brain, RBPs ensure RNA regulation by performing roles both within the nucleus and at distant sites (Darnell and DeAngelis 1993). RBPs also regulate protein translation at synapses possibly providing an insight into learning and long-term memory (McKee et al. 2005).

In normal glial cells, HuR is in the nucleus whilst in Gliomas HuR experiences nucleoplasmic shuttling to the cytoplasm where it upregulates growth factors and promotes neoplastic progression. Another common feature in malignant Gliomas is that HuR is expressed in excessive amounts (López de Silanes et al. 2005, Wang et al. 2013, Nabors et al. 2003).

HuR's target-mRNA transcripts decay rates were analysed in Gliomas and it was determined to be slower than in astrocytes (Bolognani et al. 2012). Disruption to the cell cycle is a common feature in most Gliomas including apoptosis, proliferation and migration (Schwartzbaum et al. 2006, Ware et al. 2003). Glioblastoma has been identified to have *TP53* mutation and *EGFR* amplification. HuR is known to stabilise and regulate the transcription of mRNA transcripts *TNF-α*, *VEGF* and *IL-8* in Glioblastoma as they contain a 3' untranslated region (UTR) with an AU- or U- rich cis-regulatory sequence optimal for the binding of Hu proteins. Stabilisation of these oncogenes promotes a higher grade tumour and poorer prognosis (Nabors et al. 2003). Filippova et al. (2011) determined that in Glioma cells, HuR increased cell proliferation, anchorage-independent growth and chemoresistance to regular glioma treatments. They also identified that the known oncogenic *BCL-2* family are target sequences for HuR increasing Bcl-2 protein expression levels.

As previously mentioned, Musashi1 (*MSI1*) gene encodes an oncogenic protein that is found aberrantly expressed in high quantities in Glioblastoma but also Lung and Colon cancer. Msi1

protein regulates gene expression involved in cancer-related processes including cell proliferation, apoptosis, cell cycle and differentiation. *MSI1*'s 3'UTR contains AU- or U- rich cis-regulatory sequences to which Hu proteins can bind. HuD has previously been implicated as a post-transcriptional regulator of *MSI1* in normal stem cells influencing differentiation (Bolognani et al. 2012). Whilst Vo et al's (2012) study provided evidence that high expression of *MSI1* was partially influenced by HuR through direct binding to and increasing stability leading to an increased protein expression of Msi1 proteins. This highlights the importance of HuR in Gliomagenesis (Vo et al. 2012).

1.17 Aims of this study

The fact that Hu proteins are ectopically or overexpressed in Small cell lung cancer, Neuroblastoma and Glioblastoma raises the question about their role in these cancers. Therefore, the main aim of this study is to identify which of the four Hu proteins are expressed in the three different cancers and if a knockdown of Hu expression can identify specific targets that may contribute to the cancerous phenotype.

To address this overall aim the following objectives were established:

- RT-qPCR will determine the expression levels of *HuB*, *HuC*, *HuD* and *HuR* genes in the human cancer cell lines; SK-N-AS and SH-SY5Y for Neuroblastoma and U87-MG for Glioblastomas and NCI-H69, NCI-H345 and CorL88 for Small cell lung cancer.
- After the initial expression level of the four Hu proteins in the cancer cell lines is analysed, a siRNA knockdown will be established. The efficiency of the knockdown will be confirmed at RNA expression level as well as at protein level through RT-qPCR, western blotting and immunofluorescence techniques.
- MTS assay, migration assays and microscopy will be used to analyse cell viability, migration and morphology following siRNA knockdown
- To characterise the role of *Hu* genes on a molecular level, expression levels of target genes described to play a role in the cancer development of Neuroblastoma and Glioblastoma will be analysed before and after the knockdown.
- MTS assay, migration assays and microscopy will allow analysis of viability, migration and morphology following siRNA knockdown
- To characterise the role of *Hu* genes on a molecular level, RT-qPCR of genes involved in each cancer's development will be analysed to determine Hu proteins mRNA targets and identify any pathways involved in Hu activity

Chapter 2

Methods & Materials

2.1 Cell culture

All cell culture was performed in a Category 2 laminar flow cabinet (Nuaire) to prevent airborne contamination. Cell lines were maintained in T25 and T75 tissue culture flasks (Fisher Scientific) and passaged regularly to maintain growth of cells by avoiding contact inhibition. Cells were incubated under standard conditions in a humidified incubator (Nuaire) at 37°C and 5% CO_2.

2.1.1 Cancer cell lines

The human Glioblastoma, astrocytoma cell line, Uppsala 87 Malignant Glioma (U87-MG) were cultured as a monolayer in Dulbecco's Modified Eagle's Medium (DMEM) (Lonza, Switzerland) supplemented with Penicillin 100U/ml, Streptomycin 100µg/ml, 10% heat-inactivated Foetal Bovine Serum (FBS) (Fisher), Glucose, 2mM L-Glutamine and non-essential amino acids. U87-MG is one of the most commonly studied Glioblastoma vitro cell line models. It was derived from a male of unknown age (ATCC 2016h).

The human Neuroblastoma cell lines, SK-N-AS and SH-SY5Y were cultured in DMEM (Lonza, Switzerland) supplemented with Penicillin 100U/ml, Streptomycin 100µg/ml, 10% heat inactivated FBS, Glucose, 2mM L-Glutamine and non-essential amino acids. Both cell lines derived from the metastatic site of the bone marrow. SK-N-AS is fully adherent and was

obtained from a six-year-old Caucasian female (ATCC 2016f), whilst SH-SY5Y is semi-adherent and was obtained from a four-year-old Caucasian female (ATCC 2016e).

Human Small-Cell Lung Carcinoma (SCLC) cell lines, NCI-H69, NCI-H345 and CorL88 are suspension cell lines maintained in Roswell Park Memorial Institute medium (X GI 1640) also complete with Penicillin 100U/ml, Streptomycin 100µg/ml, 10% heat inactivated FBS, Glucose, 2mM L-Glutamine and non-essential amino acids. NCI-H345 was derived from the metastatic site of the bone marrow from a 64-year-old Caucasian male (ATCC 2016b). NCI-H69 was taken directly from the lung as floating aggregates from a 55-year-old Caucasian male (ATCC 2016d). NCI-H345and NCI-H69 grow as clumps in suspension. COR-L88 was derived from the pleural effusion of a 55-year-old Caucasian male and grows semi-adherent (Sigma-Aldrich 2017a).

Human Non-Small Cell Lung Carcinoma (NSCLC) cell lines, NCI-H322 and NCI-H358 were maintained in X GI 1640 complete with Penicillin 100U/ml, Streptomycin 100µg/ml, 10% heat inactivated FBS, 2mM Glucose, L-Glutamine and non-essential amino acids. NCI-H322 derived from a primary bronchioalveolar carcinoma of the lung from a 52-year-old male taken prior to treatment (Sigma-Aldrich 2017b). NCI-H358 was isolated from a primary bronchioalveolar carcinoma of the lung from a Caucasian male taken prior to treatment (ATCC 2016c). Both cell lines grow as an adherent monolayer.

2.1.2 Normal cell lines

The human normal lung cell line BEAS-2B was maintained in Bronchial Epithelial Cell Growth Medium Bullet Kit (BEGM™) (Lonza, Switzerland) not including the gentamycin-amphotericin B mix (GA1000) provided with the BEGM kit. This media was supplemented with Penicillin

100U/ml, Streptomycin 100µg/ml. BEAS-2B cells were derived from normal bronchial epithelium obtained from autopsy of non-cancerous individuals (ATCC 2016a). These cells grow as an adherent monolayer.

The normal human brain cell line SVG p12 was cultured in Eagle's Minimum Essential Medium (EMEM) (Lonza, Switzerland) supplemented with 10% FBS and Penicillin 100U/ml, Streptomycin 100µg/ml. This cell line grows as an adherent monolayer. These cells were extracted from the brain of healthy patients (ATCC 2016g).

2.1.3 Cell harvesting

Harvesting of cells from tissue culture flasks of 80% confluency was completed for general passaging, preparation for experiments or cryopreservation of cells.

To subculture the adherent cell lines, the nutrient-depleted growth media was discarded, the cells were washed once with 10ml Dulbecco's Phosphate Buffered Saline (DPBS) (2.7mM potassium chloride, 137mM sodium chloride, and 1.76mM potassium phosphate per litre in H_2O, pH7.4) to remove any traces of serum, Calcium and Magnesium that inhibit the trypsin process. 1ml of Trypsin (0.5%) enzyme was added and incubated for 5 minutes at 37°C to detach the cells from the flask. Tapping of the flask allowed any final attached cells to be released. Fresh growth medium, warmed to 37°C in a heated water bath (Clifton) was added to re-suspend detached cells which could then be split into additional flasks for continued growth or transferred to a 20ml universal tube, pelleted at 1500x g in an Eppendorf centrifuge 5702 (Eppendorf), counted and used in further experiments.

Suspension cells line were split by transferring nutrient-depleted media containing cells to a new flask and adding sufficient fresh media to allow further growth. Alternatively, for experiments, the cells in media were transferred to a 20ml universal tube and centrifuged at 1500x g for 5 minutes in an Eppendorf centrifuge 5702. The pelleted cells were then re-suspended in fresh media. The method of cell counting follows in Section 2.4.1.

2.1.4 Cell counting

Harvested cells were transferred to a 20ml universal tube and centrifuged for 5 minutes at 1500x g to obtain a cell pellet. After the supernatant was discarded, the pellet was suspended in 10ml fresh medium and mixed by pipetting. A 200µl aliquot of the new cell suspension was mixed 1:1 dilution with 0.4% Trypan Blue stain (Gibco) once again ensuring sufficient mixing. Live unstained cells were counted by loading 15 µl to the bottom of a coverslip loaded on a haemocytometer, which is evenly distributed along the counting chamber by capillary action. Using a microscope set on the 10X objective, the corner sixteen squares of the haemocytometer were counted using a hand tally counter.

2.1.4.1 Calculating viable cell number

An average of the corner 16 squares was calculated, multiplied by 2, the dilution factor to allow for the trypan blue stain (Gibco), and further multiplied (10^4), the standard conversion factor for the haemocytometer. The calculated number is the number of viable cells/ml of the original suspension.

2.1.5 Cryopreservation of cells

In preparation for long-term storage, cells were harvested from 80% confluent cell culture flasks and pelleted by centrifugation for 5 minutes at 1500x g then the supernatant was discarded. Cell pellets were then re-suspended in 1.5ml of cold freezing-media (complete media containing an extra 20% FBS and 10% Dimethyl sulfoxide). Dimethyl sulfoxide (DMSO) lowers the freezing temperature of the medium allowing it to cool more slowly, reducing the chance of ice crystals forming therefore preventing cell death. The cell suspension was transferred to polypropylene cryovials (Sarstedt, Germany). To preserve cells for long term storage, cell lines were stored in the gas stage above liquid nitrogen, whilst for short term storage, cell lines were kept at -80°C in a freezer (Sanyo, Japan).

2.1.5.1 Thawing of cryopreserved cells

Frozen cell aliquots were thawed quickly by agitating the cryovials in a 37°C water bath (Clifton) to avoid DMSO-related cell death. The cells were then transferred to a T25 flask containing warmed complete cell culture medium. Following a 24-hour incubation at 37°C and 5% CO_2, cells were either sub-cultured or the medium replaced.

2.1.6 Microscopy

Cells were assessed for confluency using the Eclipse II inverted fluorescent microscope. Cell images were obtained by a Microtec camera for single images. More information

2.2 Gene studies

Polymerase Chain Reaction (PCR) was used to determine the expression level of each *Hu* gene in each cancer cell line and non-cancerous control cell lines and additionally, confirm the annealing temperature of each primer set. Real-time quantitative PCR (RT-qPCR) was then performed as a more accurate method of gene expression. In preparation for all PCR reactions, the following steps occur: RNA isolation, RNA quantification, RNA purity analysis by gel electrophoresis and reverse transcription for the conversion of RNA to synthesis complementary DNA (cDNA).

2.2.1 Total RNA isolation

Total RNA from all the cell lines was extracted using the TRIsure reagent following the manufacturer's guidelines with addition steps detailed below (Sigma-Aldrich). Cells were harvested from flasks using 1ml TRIsure or from a well-plate using 0.5ml TRIsure and a cell scraper. The contents were then transferred to an Eppendorf tube and mixed by pipetting to lyse the cells. This suspension was then transferred to an Eppendorf tube and incubated at room temperature for 5 minutes before 0.2ml of chloroform was added. Following vigorous mixing for 15 seconds, a further incubation for 3 minutes at room temperature followed by centrifugation for 15 minutes at 12,000g. The contents separated into three layers, a lower organic phase, an interphase that contain proteins and deoxyribonucleic acid (DNA) and an upper aqueous phase containing the RNA. The aqueous layer was carefully transferred to a new Eppendorf tube. To further eliminate traces of the TRIsure reagent, the chloroform step was repeated. An equal volume of ice-cold isopropanol allows the RNA to precipitate out of the aqueous phase. Samples were incubated at room temperature for 10 minutes and

centrifuged for 10 minutes at 12,000g. Additionally, for smaller samples with a lower RNA yield, 1µl glycogen was added at this stage. Glycogen acts as a carrier and improves the visibility of the RNA pellet. The pellet was washed with 70% ethanol by vortex mixing and undergoes a final centrifuge of 7500g for 5 minutes. The RNA pellet was air-dried and eluted in 12-20µl of Diethylpyrocarbonate (DEPC)-treated water dependent of the size of the starting sample. RNA was either stored in the -80°C or kept on ice ready for cDNA preparation.

2.2.1.2 Removal of genomic DNA contamination

All RNA samples were treated to remove any traces of DNA. This process was done using the Invitrogen TURBO DNA-*free*™ kit. 0.1 volume of 10X buffer and 1µl of TURBO DNase was added to the RNA. Following mixing by pipetting, the samples were incubated for 30 minutes at 37°C. 0.1 volume of DNase Inactivation reagent was added, and the samples mixed well. The samples were incubated at room temperature for 5 mins to allow the inactivation to work and finally the samples were centrifuged for 90 seconds at 10,000g to pellet the inactivation reagent and contained contaminants and the RNA transferred to a new tube.

To further purify the RNA sample, 200µl of phenol and 180µl of DEPC-treated water were added to the samples. The samples were mixed via vortex and spun for 10 minutes at 13,000g. The samples separated to three phases of which the upper phase was transferred to a new tube. To the new tube, 200µl of 24:1 chloroform-isoamylalcohol was added and a further centrifuge for spin 5 minutes at 13,000g. The aqueous phase was transfer to a new tube. To this tube 20µl of 10% sodium acetate, 1µl of glycerol and 500µl of Ethanol were added. The samples were mixed thoroughly then incubated at -20°C for 20 minutes. A spin of 30 minutes at 10,000g was performed. The supernatant was removed then 200µl 75% ethanol was added

and a final spin of 10 minutes at 10,000g. The supernatant was discarded, and the RNA pellet was resuspended in 20µl of DEPC-treated water.

2.2.2 RNA quantification

The quality and quantity of the extracted RNA samples was analysed using a Nanodrop One™ spectrophotometer (Thermo Fisher Scientific) set at 260nm. 2µl of the RNA sample was loaded onto the pedestal of the spectrophotometer. RNA Purity was measured by a ratio of absorbance at 260 nm and 280 nm.

2.2.3 Gel electrophoresis for RNA Integrity

Agarose gel electrophoresis was used to analyse the integrity of the RNA, absence of other nucleic acid contamination and visualise ribosomal RNA subunits. Tris/acetic acid/EDTA (TAE) buffer (40mM Tris, 20mM acetic acid, 1mM Ethylenediamine tetraacetic acid (EDTA) buffer and 1.5% gel was used. RNA samples were mixed with 1x loading dye (2.5% Ficoll®-400, 11mM EDTA, 3.3mM Tris-HCl, 0.017% SDS, 0.015% bromophenol blue) and FastRuler™ Middle Range DNA Ladder (10mM Tris-HCl (pH 7.6), 0.03% bromophenol blue, 60% glycerol and 60mM EDTA) with the band sizes 100, 400, 850, 2000 and 5000bp. To visualise separated nucleic acids under ultraviolet (UV) light, 2µl GelRed™, a nucleic acid intercalating dye was added to melted agarose. 40V was applied to the gel (Bio-Rad) and then analysed using a UV Analyser (Bio-Rad) at 302nm and Bio-Rad Image Lab 4.1 software.

2.2.4 cDNA synthesis

RNA was reverse-transcribed using the Tetro cDNA synthesis kit (Bioline) following the manufacturer's protocol. 1500ng of RNA was used for all cDNA reactions. Mastermix consisting of oligo $(dT)_{18}$ primers, 10mM dNTP mix, 5x RT buffer, 1 u/µl Ribosafe RNase Inhibitor, 200u/µl Tetro Reverse Transcriptase and DEPC-treated water was made to total 20µl. Samples are incubated for 45°C for 30 minutes followed by a termination incubation of 85°C for 5 minutes. The temperature changes were controlled by the Eppendorf Mastercycler Gradient (Eppendorf). The cDNA samples were chilled on ice and used immediately or stored at -20°C.

2.2.5 Polymerase chain reaction

PCR analysis was undertaken to test for primer specify and to confirm the product size determined primer blast software (NCBI 2017).

For each reaction, 0.6µl dNTP, 3.0µl buffer, 0.2µl Taq, 1.5µl of each primer set for each *Hu* gene and β-Actin housekeeping gene and 300ng cDNA together with water to total 25µl. Samples were run in triplicate with a negative control for each primer set. For PCR, the Eppendorf Mastercycler Gradient machine was used. The cycling conditions are shown in Table 2.1.

PCR Stage	Temperature	Time
Initial Denaturation	97ºC	5 minutes
Denaturation	94ºC	1 minute
Annealing	56ºC	1 minute
Extension	72ºC	1 minute
Repeat for 39 Cycles		
Final Extension	72ºC	10 minutes
Hold	4 ºC	

Table 2.1: Benchtop PCR protocol. The cycling temperature and time period used at each PCR stage.

The optimal annealing temperatures were determined by a gradient temperature PCR with temperatures ranging from 55°C to 61°C increasing 1°C every cycle. Initially two primer sets for each Hu protein were used alongside one ß-Actin primer as a positive control. Following optimisation one primer set for each Hu protein was selected and used in further PCR applications. The primers for HuB, HuC, HuD, HuR, GAPDH and β-Actin were purchased from Invitrogen and the sequences are detailed in Table 2.3.

2.2.5.1 Gel electrophoresis for PCR band analysis

The PCR products were analysed using 1.5% agarose Tris/Borate/EDTA (TBE) gel electrophoresis described in Section 2.2.3 and a PCR marker (New England Biolabs) displaying bands of 50, 150, 300, 500 and 766bp. TBE buffer consists of 89mM tris base, 89mM boric acid, 2mM EDTA.$NA_2 2H_2 0$ per 1 litre, pH8.

2.2.6 Real time-quantitative polymerase chain reaction

Real time quantitative PCR (RT-qPCR) was performed using Hard-Shell® 96-Well, low profile, semi-skirted, green PCR Plates (Bio-Rad) sealed by a Microseal® Adhesive film (Bio-Rad) and the Bio-Rad CFX96 PCR Detection System (Bio-Rad). For each reaction, 0.4µM of each primer, 300ng of cDNA and milli-Q water was added to 5µl of iTaq™ universal SYBR® Green supermix (x2) (Bio-Rad) creating a 10µl reaction. Primer sequences are listed below in Table 2.3.

The amplification protocol is detailed in Table 2.2. *β-actin* served as a positive control and to normalise expression levels in analysis. Negative controls containing extra Milli-Q water in replace of cDNA were used. Each sample had three replicates.

PCR Stage	**Temperature**	**Time**
Initial Denaturation	95°C	3 minutes
Denaturation	95°C	20 seconds
Annealing	60°C	30 seconds
Extension	72°C	30 seconds
Repeat for 39 Cycles		
Melt Curve	55°C – 95°C	5 seconds

Table 2.2: RT-qPCR cycling. The cycling conditions showing temperature and time period used at each RT-qPCR stage.

2.2.6.1 Real time-quantitative polymerase chain reaction analysis

Quantitative PCR data was initially interpreted by the Bio-Rad CFX manager software. The mean threshold cycle values (Ct) were determined for each *Hu* gene and *β-actin*. For general

gene expression, the relative quantification (RQ) method, the expression change in fold-difference was calculated using the formula:

$$\Delta CT = Ct\ target - Ct\ \beta\text{-}Actin$$

This determines the quantification of the target gene against the housekeeping gene to investigate physiological changes in gene expressions levels.

When comparing fold gene expression before and after small interfering RNA (siRNA) knockdown experiments, I used the normalised expression analysis for which the formula is:

$$RQ = 2^{-\Delta\Delta CT}$$

$$\text{Where, } \Delta\Delta CT = \Delta CT\ treated - \Delta CT\ control$$

The normalised quantification analysis shows any changes to expression levels of target genes following treatment.

Melting curve analysis was conducted to measures the dissociation of double-stranded DNA during the heating process described in Table 2.2, by recording the absorbance intensity of fluorescent probes.

2.2.7 Primer design for qualitative polymerase chain reaction

All primers were designed using Primer-BLAST: a tool to design target-specific primers for polymerase chain reaction (Ye et al. 2012). Primer sequences are listed in Table 2.3.

Gene	Size	Primer	Sequence
HuB(1)	75bp	Forward	5’- TGGGAGAACTGCACCGTTAC -3’
		Reverse	5’- TGGCAGCAATTACCTGCTTT -3’
HuB(2)	396bp	Forward	5’- AAACCTTAAGGGAGAAAGCAGG -3’
		Reverse	5’- AGAAGCTGAACTTGGGCGAG -3’
HuC(1)	526bp	Forward	5’- ACAAGATCACAGGGCAGAGC -3’
		Reverse	5’- CCGTAGGCCATGTTGAGCA -3’
HuC(2)	318bp	Forward	5’- GACCAGGTCACAGGTGTCTC -3’
		Reverse	5’- GATGGCGATCGGCGAGAA -3’
HuD(1)	585bp	Forward	5’- GGTTTCAGCTCACTGCTCCT -3’
		Reverse	5’- GGACGGGCATATGAGACCTTT -3’
HuD(2)	592bp	Forward	5’- ATCGGGGGTTTCAGCTCACT -3’
		Reverse	5’- CGGACGGGCATATGAGACCTTT -3’
HuD(3)	359bp	Forward	5’- GTCTCTTCGGGAGCATTGGT -3’
		Reverse	5’- CCTCTTATCAAAGCGGAT -3’
HuD(4)	112bp	Forward	5’- CCAGGCCCTGCTGTCCC -3’
		Reverse	5’- AGGCTTCTCATTCCATC -3’
HuD(5)	245bp	Forward	5’- AGCCAATTTCAGCAAGGCTC -3’
		Reverse	5’- GCAGAGCTTCGACTCTTCTG -3’
HuD(6)	73bp	Forward	5’- ACACATACACGAAAGAGAGAGAAACAA -3’
		Reverse	5’- AACACTGGCTTATAAAGTCCATGGT -3’
HuR(1)	302bp	Forward	5’- CGGGATAAAGTAGCAGGACACA -3’
		Reverse	5’- CGGATAAACGCAACCCCTCT -3’
HuR(2)	277bp	Forward	5’- GAAGACCACATGGCCGAAGA -3’
		Reverse	5’- GGCGAGCATACGACACCTTA -3’
ß-Actin	168bp	Forward	5’- CTGGAACGGTGAAGGTGACA -3’
		Reverse	5’- AAGGGACTTCCTGTAACAATGCA -3’

Table 2.3: Hu primer sequences. Sequences and target amplicon size for each primer.

2.2.8 PrimePCR™ assays

To study individual genes affected by the Hu proteins, PrimePCR™ pathway plates with primers for specific genes already loaded in were purchased from Bio-Rad. For Glioma, we used the plate, Human Glioma Tier 1 and for Neuroblastoma we used Human Neuroepithelial Neoplasms Tier 1. The PCR plates also include general PCR controls. The Plates were loaded the same as normal PCR plates but without primers.

2.7.9 Statistical analysis of transfections

All results represent the mean ± standard deviation from three independent experiments. An unpaired two-tailed T-test was used to evaluate the differences between the control cells and Hu knockdown cells in GraphPad prism software. Significant significance is displayed as *P ≤ 0.05, **P ≤ 0.01, ***P ≤ 0.001.

2.3 Western blotting

Western blotting allows the detection of specific proteins with in a cell line. Firstly, protein is extracted from a cell line, it is then quantified and prepared for western blotting.

2.3.1. Cell lysis

Whole cell lysates were prepared from all cell lines by adding 1ml of ice-cold RIPA (Radio Immuno-Precipitation Assay) buffer containing 150mM NaCl, 1.0% IGEPAL CA-630, 0.5% sodium deoxycholate, 0.1% SDS, 50mM Tris with pH 8.0, directly to a 75cm^2 confluent flask which has been washed with PBS. For 6-well plates a smaller volume of 0.5ml RIPA buffer was used. Cell scrapers aided detaching of the cells from the flask and collection into an Eppendorf tube. The

suspension was left rocking for 30 minutes at 4°C. The samples were then centrifuged at 13,000g for 20 minutes to pellet cell debris and the supernatant was transferred to a new tube. Samples were stored on ice prior to protein spectrophotometry, Western blotting or storage at -20°C for longer periods of time.

2.3.2 Protein quantification

2.3.2.1 Spectrophotometry

The protein concentrations were initially determined using a spectrophotometer at 280nm using RIPA buffer as a blank. Aliquots were stored at -20°C.

2.3.2.2 Bradford assay

To optimise the protein quantification, the Bradford assay was used. A series of standard Bovine Serum Albumin (BSA) concentrations were prepared from 100 to 1000µg/ml with a blank sample at 0µg/ml. The BSA was diluted in deionised water. At the same time, five dilutions of the unknown protein isolations were diluted also in deionised water to create a range between 0 and 1:15. All dilutions were performed in cuvettes to which 1ml of Bradford reagent was added, mixed and incubated at room temperature for five minutes. The absorbance of the standards and unknown samples were read at 595nm.

2.3.3 Protein preparation

The proteins were mixed 1:1 ratio with SDS loading buffer (1M TrisHCl pH 6.8, 10% SDS, 0.2% Bromophenol blue, 1M DTT and Glycerol in MilliQ water). The samples were boiled at 95ºC for 5 minutes in a heating block to ensure denaturation.

2.3.4 Sodium dodecyl sulphate-polyacrylamide gels

A 12% SDS-PAGE gel composed of a 4% stacking gel (30% Acrylamide, 1m Tris HCl pH6.8, 10% SDS and water) and a 12% separating gel (4x Lower gel buffer (1.5M Tris Base, 0.5% SDS and H2O), 30% acrylamide, 10% ammonium persulphate, TEMED and water) was used to separate proteins of different samples.

To improve the efficiency and manage time restraints, 12-well Mini-Protean® TGX Stain-free™ Any kD™ Precast Gels (Bio-Rad) were also used.

2.3.5 Separation of proteins

The Mini-PROTEAN® electrophoresis tank (Bio-Rad) was filled with 1L protein running buffer (3.5mM SDS, 25mM Tris, 192mM Glycine and water) ensuring both inside and outside of the chambers were filled. Once the gel combs were removed, the wells were loaded with 20µl of sample and at least one well contained 5 µl Precision Plus Protein™ Dual Colour Standard (Bio-Rad) which has stained bands ranging between 10-250kD.

Current was applied to the SDS-PAGE gel at 20mA for 10 minutes, followed by 25mA (until the gel had run to the end) for a single gel to allow the separation of proteins. The current was increased on the addition of more gels into the tank.

2.3.6 Transfer to nitrocellulose membrane

On completion of the electrophoresis, the gels were released from the plates and proteins were transferred from the gel to a nitrocellulose membrane, either by a wet blot system or later a semi dry blotting. For the wet blot method, a sandwich of Grade 3MM Chromatography blotting paper (Fisher), gel and Amersham Protran 0.45 nitrocellulose membrane (Fisher Scientific) was held tightly in a holder and 70V was applied to the tank containing Transfer buffer (25mM Tris, 192mM glycine, 20% (v/v) methanol, 0.1% SDS in water) for approximately 1 hour at room temperature. For the semi-dry blot method, a Trans-Blot® Turbo™ Midi PVDF Transfer Pack (Bio-Rad) and Trans-Blot®Turbo™ Blotting System (Bio-Rad) were used. The gel was placed onto a nitrocellulose membrane directed towards the anode. The Bio-Rad pre-defined method for a mixed molecular weight turbo mode which runs for 7 minutes at 55V, 1.3A was used for all membranes.

2.3.7 Membrane blocking

The membrane was blocked in 5% semi-skimmed milk powder diluted in Tris-buffered saline with/Tween solution (50mM Tris-HCl, pH 7.6; 150mM NaCl, H20 and 0.05% Tween20) (TBST) for 30 minutes on a Gyro-rocker (Stuart Scientific Bibby). The remaining binding surface of the membrane is blocked to prevent nonspecific binding of the antibodies. The milk was removed ready for the addition of antibodies.

2.3.8 Immunolabelling

The primary Hu Antibodies were sourced from Santa Cruz Biotechnology. Anti-HuB (N-15): sc-5982 goat polyclonal IgG, anti-HuC (G-15): sc-5981 goat polyclonal IgG, anti-HuD (E-1): sc-28299

mouse monoclonal IgG, anti-HuR (G-8): sc-365816 mouse monoclonal IgG. Anti-GAPDH (14C10) rabbit monoclonal IgG was purchased from Cell Signalling. Primary antibodies were added to membranes at a 1:1000 dilution in TBST containing 10% semi-skimmed milk powder. The membranes were left in the antibody solution on the gyro-rocker (Stuart Scientific Bibby) overnight at 4°C.

The non-bound primary antibody was removed by washing the membrane in TBST for three times for 10 minutes on the gyro rocker (Stuart Scientific Bibby). Horse-radish peroxidase (HRP)-conjugated secondary antibodies, goat anti-mouse IgG (H+L) Poly-HRP conjugated antibody (Life technologies) at a concentration of 1:10000 or goat anti-rabbit fluorescent HRP-conjugated antibody (Cell signalling), Rabbit anti-goat IgG (H+L) Secondary Antibody HRP conjugate (Life Technologies) 1:2000 in TBST 0.5% semi-skimmed milk powder was added to the membrane and left to incubate at room temperature for 1 hour with constant rocking. Three final washes of 10 minutes in TBST occurred to remove unbound secondary antibody.

2.3.9 Immunodetection

To develop the membrane, Supersignal® West Femto Maximum Sensitivity Substrate Chemiluminescent kit (Thermo Fisher Scientific) was used following the manufacturer's instructions, of which 1ml of luminol enhancer solution and 1ml of stable peroxide buffer was added and left to develop for two minutes. Immunodetection of Hu proteins and controls were performed using the chemi-doc UV analyser (Bio-Rad) and Bio-Rad Image Lab version 4.1 software.

2.4 Immunofluorescence protein labelling

Cells were double-immunostained to confirm the presence and localisation of Hu proteins and the cell nucleus.

2.4.1 Adherent cell lines

The cell lines were seeded into sterile 6-well plates containing 19mm glass cover slips at $0.5x10^5$/ml. Cells were incubated overnight at 37ºC and 5% CO_2. The adhered cells were washed with PBS three times for 10 minutes and fixed with cold 4% paraformaldehyde for 20 minutes. Cells were washed to remove the fix, three times for 10 minutes with PBST (1x PBS, 10% FBS, 0.1% Triton X100). Primary antibody anti-HuB goat polyclonal IgG, anti-HuC goat polyclonal IgG, anti-HuD mouse monoclonal IgG, anti-HuR mouse monoclonal IgG (Santa Cruz Biotechnology) was added to the well diluted in Phosphate buffered saline with Tween 20 (PBST). The plates were left overnight at 4°C in the dark. The wells were then washed with three times with PBST again. The secondary mouse anti-goat Alexa Green 488 Fluorescein isothiocyanate (FITC) IgG (Invitrogen) or goat anti-mouse Alexa 488 FITC IgG (Fisher) was applied to the wells 1:250 dilution 4',6-diamidino-2-phenylindole (DAPI) nucleus stain 1:1000 in PBST and incubated for 1 hour. Cells were washed a final three times for 10 minutes in PBST. Analysis is described below in section 2.4.3.

2.4.2 Suspension cell lines

Cells were seeded into 6-well plates at a concentration of $1x10^5$/ml. Following 24 hours' incubation, the cells were transferred to an Eppendorf tube, to pellet the cells, the tube was spun at 800rcf for 3 minutes and the media discarded. The pellet was re-suspended in 160µl of

PBS and 20µl of 3.7% paraformaldehyde was added to the suspension. Following incubation at room temperature for 15 minutes, the suspension was centrifuged for 3 minutes at 800rcf and the supernatant was discarded. 1ml of PBS was added and the tube was spun at 800rcf for 3 minutes and the supernatant discarded, and the wash step repeated. To permeabilise the cells, the pellet was re-suspended in 500µl of 0.3% Triton X100 in PBS. The tube was centrifuged at 800rcf for 3 minutes and the supernatant removed. 1µl primary antibody for anti-HuB, anti-HuC, anti-HuD or anti-HuR suspended in PBST was then added and incubated at room temperature overnight. The cells were centrifuged for 3 minutes at 800rcf followed by a wash with 500µl PBST and a spin for 3mins at 800rcf twice. The secondary antibodies were added along with 1µl DAPI nucleus stain. This suspension was left for 1 hour at room temperature. The tube was spun at 800rcf for 3 minutes and the supernatant removed. Two final washes in PBT spun at 800rcf for 3 minutes occurred. Following the discard of the final supernatant the cells were transferred to a coverslip.

2.4.3 Analysis of immunofluorescence

Before fluorescence microscope analysis, all the coverslips were mounted on a microscope slide using Vectashield (Vectorlabs) to protect the fluorescent labelled samples from photobleaching the presence and cellular localisation of the different proteins were visualised and photographed using the Nikon Eclipse II fluorescent microscope, Microtec camera with the DAPI - 358nm and Fluorescein isothiocyanate (FITC) - 495nm filters and imaged using the SOFTWARE. Images were then overlaid using the software Image-J (National Institute of Health, US).

2.5 Cell migration assays

Cell movement was recorded on a CytoSMART™ microscope camera (Lonza, Switzerland) set to image every 15 minutes until the migration is complete or a given time. Due to malfunction of this equipment mid-project, cell movement was recorded using the Nikon Eclipse II fluorescent microscope and Microtec camera.

2.5.1 Agarose-gel migration

Prior to cells seeding, a 10µl droplet of 0.5% solution of electrophoresis grade agarose gel was created in 24-well opening. After 15 minutes' cells were seeded into 24-well plate at a concentration of $5x10^4$ in 500µl of fresh media. Cells were incubated for 24-hours to allow the cells to adhere to the wells before imaging began. Images were captured every 15 mins. The images analysed were every 6 hours over a 42-hour period. Images were acquired by a CytoSMART™ camera.

2.5.2 Scratch-wound assays

Cells were seeded into 6-well plates SK-N-AS $0.7x10^5$/ml, SH-SY5Y $1x10^5$/ml and U87-MG $0.65x10^5$/ml, 72-hours post transfection once protein knockdown was confirmed, multiple wounds were made per well using a sterile metal syringe edge to disturb the monolayer. Detached cells were removed by replacing the media. The wound was imaged every 24 hours for 96 hours. Between imaging cells were incubated under normal conditions.

2.5.3 Data analysis of migration assay

All imagery analysis of migration assays was achieved using the software Image-J (National Institute of Health, US). Percentage area of cell migrated into agarose gel and percentage area of cells invading an man-made gap was calculated.

2.6 Cell metabolism assay

To determine any changes in cell growth before and after transfection, CellTiter 96® AQ_{ueous} One Solution Cell Proliferation Assay (MTS) (Promega, US) was used. All studies were under normal cell culture conditions.

This cell proliferation assay focuses on the reduction of the tetrazolium compound [3-(4,5-dimethyl-2-yl)-5-(3-carboxymethoxyphenyl)-2-(4-sulfophenyl)-2H-tetrazolium, inner salt also known as MTS. Like the MTT assay described above, NADPH and NADH produced by dehydrogenase enzymes in metabolically active cells aid the reduction process. Phenazine ethosulfate (PES) combines with MTS to form a stable solution. 48-hour post-transfection, 20µl of the CellTiter 96® AQ_{ueous} One Solution Reagent was added to each well of the 96-well plate containing cells in 100µl of medium. The plate was then incubated under normal conditions for 2 hours. The absorbance of the plate was then read at 490nm using the fluorescent plate reader.

From the absorbance readings, we could calculate the percentage of cell growth and cell growth inhibition using the following equations.

2.6.1 Data analysis of proliferation assays

Changes were calculated as percentage of control cell growth using the formula:

$$\text{Change in proliferation (\%)} = \frac{\text{Mean absorbance of Hu siRNA transfection}}{\text{Mean absorbance of Hu siRNA control transfection}} \times 100$$

Significance was calculated by a two-tailed t-test. This analysis allows the linear relationship between cell number and signal produced to be documented.

2.7 Transfection

Each cell line was tested to derive the most suitable cell seeding, incubation periods, transfection reagent and concentrations of those transfection regents and siRNAs.

2.7.1 Small-interfering RNAs

All siRNA was purchased in a stock of 10nmol which was suspended in 500ul of 1X siRNA buffer (Thermo Fisher Scientific) to produce a 20uM stock. Further dilutions of this stock were made depending on the requirements of individual transfection protocols.

ON-TARGETplus SMARTpool siRNA sequences	Sequence
HuB ELAVL-2	UCACAAUAUGGACGCAUUA CAAUAUGGCUUAUGGAGUA GGUGUAGGGUUUAUUCGAU GAAAUAGAGUCCUGUAAGC
HuC ELAVL-3	CCUCAACGGCCUCAAAUUA GCGAACAACCCAAGUCAGA GCAAGUUGGUUCGGGACAA UCAAGGUCAUCCGUGAUUU
HuD ELAVL-4	GGUAUGGAUUUGUUAACUA GGAACUGGGUGGUGCAUCU CUACGGAACCGAUUACUGU CAGGGAUGCUAACCUCUAU
HuR ELAVL-1	GACAAAUCUUACAGGUUU GACAUGUUCUCGGUUUG ACAAAUAACUCGCUCAUGC GCUCAGAGGUGAUCAAAGA
GAPDH Control Pool	GUCAACGGAUUUGGUCGUA CAACGGAUUUGGUCGUAUU GACCUCAACUACAUGGUUU UGGUUUACAUGUUCCAAUA
Non-targeting Pool	UGGUUUACAUGUCGACUAA UGGUUUACAUGUUGUGUGA UGGUUUACAUGUUUUCUGA UGGUUUACAUGUUUUCCUA

Table 2.4: Sequences of siRNAs. The sequences of the siRNA constructs are shown in the table.

2.7.2 JETprime transfection

JETprime (Polyplus transfection) regent was determined the most suitable for SK-N-AS transfection. SK-N-AS cells were seeded at $1.4x10^5$ for RNA or $1.3x10^5$ for protein analysis in 6-well plates and left under normal cell culture conditions for 24 hours. siRNAs were diluted to give a final concentration of 50nM and 4ul of JETprime was added. After a quick vortex and spin, it was left to incubate at room temperature for 15 minutes for the JETprime/siRNA complexes to form. To mix was then added dropwise to the wells containing 2ml Antibiotic-free media and incubated for 48 hours at 37ºC and 5% CO_2. After transfection, cells were harvested for RT-PCR at 48 hours' post-transfection or protein analyses at 72-hour post-transfection.

2.7.3 DharmaFECT I transfection

DharmaFECT I (Dharmacon) reagent was used for both U87-MG and SH-SY5Y cell lines. For a 6-well plate, cells were seeded at SH-SY5Y $1x10^5$/ml and U87-MG $0.65x10^5$/ml for RNA analysis and SH-SY5Y $0.95x10^5$/ml and U87-MG $0.6x10^5$/ml for protein analysis into media containing no serum and incubated for 24 hours under normal conditions. For each Hu protein and controls, two separate solutions were prepared in sterile Eppendorf tubes. The first containing siRNA to a to a final concentration of 25nM and the second containing 6ul of DharmaFECT I in 200ul of serum-free media. The two tubes were mixed on a vortex and spun for several seconds followed by an incubation for 15 minutes at room temperature to allow the DharmaFECT I/siRNA complexes to form. The tubes were combined and mixed by vortex and centrifugation and incubated for a further 20 minutes. After this time, 1600ul of antibiotic free-media was added to the mix and the whole solution applied to the well of the cells. Cells

were incubated in the transfection mix for 48 hours at 37ºC and 5% CO_2 before harvesting RNA and or for 72 hours for harvesting protein for analysis.

2.7.4 Lipofectamine RNAi MAX

Lipofectamine RNAi MAX (Invitrogen) was used during initial testing of siRNA knockdown experiments. Different concentrations of Lipofectamine RNAi MAX and all *Hu* genes siRNA were trialled following the manufacturers guidelines. In one Eppendorf tube, Lipofectamine RNAi MAX was diluted in 150µl of Gibco™ Opti-MEM™ - Reduced Serum Media (ThermoFisher Scientific). In a second Eppendorf tube, the siRNA was diluted also in 150µl Gibco™ Opti-MEM™. The two tubes were mixed together and incubated at room temperature for 20 minutes to allow the Lipofectamine/siRNA complex to form. 250µl of the solution was added to each well followed by 2250µl of antibiotic-free media. Incubation at 37ºC and 5% CO_2 for 48 hours before harvesting protein and RNA.

2.7.5 Statistical analysis of transfections

All results represent the mean ± standard deviation from three independent experiments. The T-test was used to evaluate the differences between the control cells and Hu knockdown cells in Graphpad Prism software. Significant significance is displayed as *P ≤ 0.05, **P ≤ 0.01, ***P ≤ 0.001.

Chapter 3

Results

Part I: Expression of Hu proteins in Small cell lung cancer, Non-small cell Lung Cancer and normal bronchial epithelial cells

Hu protein expression was first identified in patients with Small cell lung cancer (SCLC) and paraneoplastic encephalomyelitis and/or a sub-acute sensory neuropathy (PEM/SN) (Szabo, a et al. 1991). All SCLC tumours aberrantly express neuronal HuD protein and the tumour-initiated immune response can be detected in up to 20% of those patients, however PEM/SN is thought to occur in only 1% of all SCLC patients (Dalmau and Furneaux 1992, DeLuca et al. 2009).

The aim of this study was to investigate the presence of Hu RNA-binding proteins in lung cancer cells and normal bronchial epithelial cells as a control. A detailed analysis of Hu expression could potentially be used to detect SCLC at an early stage of disease and improve treatment options that are currently very limited. Detection could be done through blood screening for Hu antibodies or following tissue extraction (D'Alessandro et al. 2008). The development of molecular markers for targets of drug therapies could improve the low survival rates associated with SCLC.

To investigate the expression of HuB, HuC, HuD and HuR in Small cell lung cancer the NCI-H345, NCI-H69 and CorL88 cell lines were used. Additionally, the normal bronchial epithelial cell line BEAS2B was used as a control, whilst Non-small cell lung cancer cell lines NCI-H322 and NCI-H358 allowed the comparison of these characteristically different lung cancers.

In addition to Hu gene and protein expression and localisation, a comparison of the morphology of the normal lung and cancerous lung cell lines and the motility of the NSCLC cells compared to the normal bronchial epithelial cells. These particular cell lines have not previously been examined for this property.

3.1 *Hu* gene and protein expression and localisation in Small cell lung cancer, Non-small cell lung cancer and normal bronchial epithelial cells

The aberrant expression of *Hu* genes is often recognised within cancers. To build an expression profile, each *Hu* gene and protein was analysed separately in all cell lines for gene expression, protein expression and protein localisation.

Investigations into *HuB* gene expression levels in the normal bronchial epithelial cells, NSCLC and SCLC cell lines were performed by real time-quantitative polymerase chain reaction (RT-qPCR) (described in Section 2.26) measuring mRNA levels. Primers sequences are listed in Table 2.3 in Section 2.27.

Gene expression studies at RNA level do not necessarily reflect on the abundance of the gene product. Therefore, Western blot was used to determine the protein expression level. There is much evidence to suggest the localisation of Hu proteins within a cell determine its function therefore immunofluorescent staining confirmed protein localisation within the cells (Kasashima, K et al. 1999).

3.1.1 *HuB* expression

RT-qPCR analysis of *HuB* gene expression in the normal bronchial epithelial cells, NSCLC and SCLC cell lines used the primers HuB (1) and *β-Actin* that are described in Table 2.3. The mRNA expression of *HuB* in SCLC, NSCLC and normal bronchial epithelial cells is displayed in Fig. 3.1.

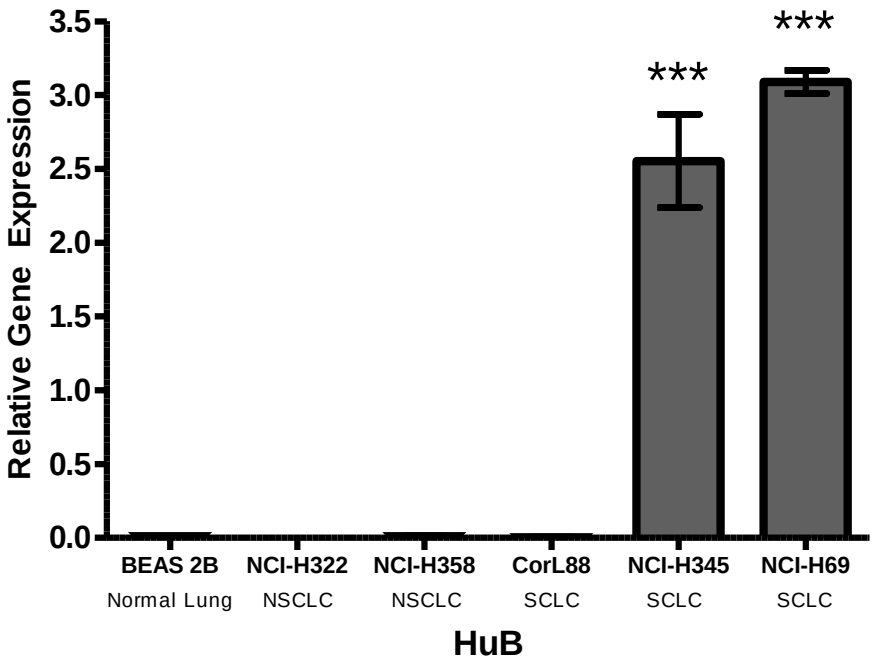

Figure 3.1: *HuB* gene expression in SCLC, NSCLC and normal bronchial epithelial cell lines. *HuB* gene expression was analysed by RT-qPCR in Small cell lung cancer cell lines, CorL88, NCI-H345 and NCI-H69, Non-small cell lung cancer cell lines, NCI-H322 and NCI-H358 and normal bronchial epithelial cells BEAS2B. The ΔCt results shown are an average of three replicates normalised to *β-Actin* gene expression, relative to zero. Error bars display ± standard error of the mean (SEM). Statistical significance was calculated by a two-tailed t-test and is displayed by *P ≤ 0.05, **P ≤ 0.01, ***P ≤ 0.001. (n=3).

The examined gene, *HuB*, is a member of the Hu RNA-binding protein family and normally exclusive to the neurons and gonads. The expression of *HuB* gene was absent in the normal bronchial epithelial cells, NSCLC cells and CorL88 SCLC cells. Significant *HuB* expression was

observed in two of the SCLC cell lines, NCI-H345 and NCI-H69 when compared to the control normal bronchial epithelial cells. A 2.6-fold-increase of *HuB* gene expression was seen in NCI-H345 cells when compared to the control BEAS2B cells. Whilst a 3.1-fold-increase of *HuB* gene expression was observed in NCI-H69 cells. These results indicate aberrant expression of *HuB* gene in the NCI-H345 and NCI-H69 SCLC cell lines.

To further analyse if the gene expression of the HuB RNA-binding protein could be detected at protein level, western blotting was performed (Figure 3.2). Each cell line derived from normal bronchial epithelial cells, Small cell lung cancer and Non-small cell lung cancer was blotted and stained for HuB protein. Glyceraldehyde 3-phosphate dehydrogenase (GAPDH) was used as a loading control.

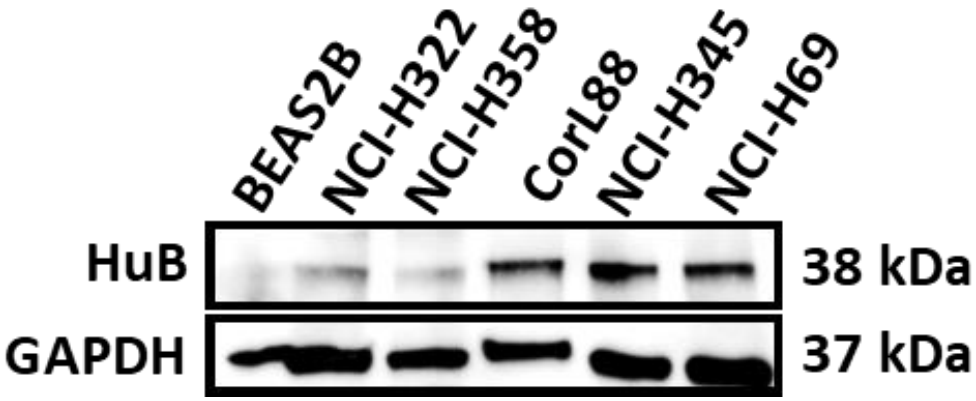

Figure 3.2: Representative example of HuB protein expression detected by western blot. HuB protein expression in normal bronchial epithelial cell line BEAS2B, Non-small cell lung cancer cell lines, NCI-H322 and NCI-H358 and Small cell lung cancer cell lines, CorL88, NCI-H345 and NCI-H69. GAPDH protein expression was used as a loading control (n=3).

The strongest HuB expression was observed in the SCLC cell lines CorL88, NCI-H345 and NCI-H69 represented by darker bands that are less than the loading control. Weaker expression

was observed in the NSCLC cell lines NCI-H322 and NCI-H358 displayed by fainter bands showing less expression than the loading control. Only GAPDH protein could be detected in the lane containing protein extracted from the normal bronchial epithelial cells BEAS2B, confirming an absence of HuB protein expression.

Whilst there was an absence of *HuB* gene expression in both NSCLC cell lines and SCLC cell line CorL88 (Fig. 3.2), a low level of *HuB* gene expression must be present to produce these proteins that is detected when the gene expression data is normalised.

To determine the subcellular localisation of HuB proteins, immunofluorescent staining was performed with primary anti-HuB IgG and secondary Alexa green 488 FITC IgG (Fig 3.3). Cells were counterstained with DAPI for nuclear localisation.

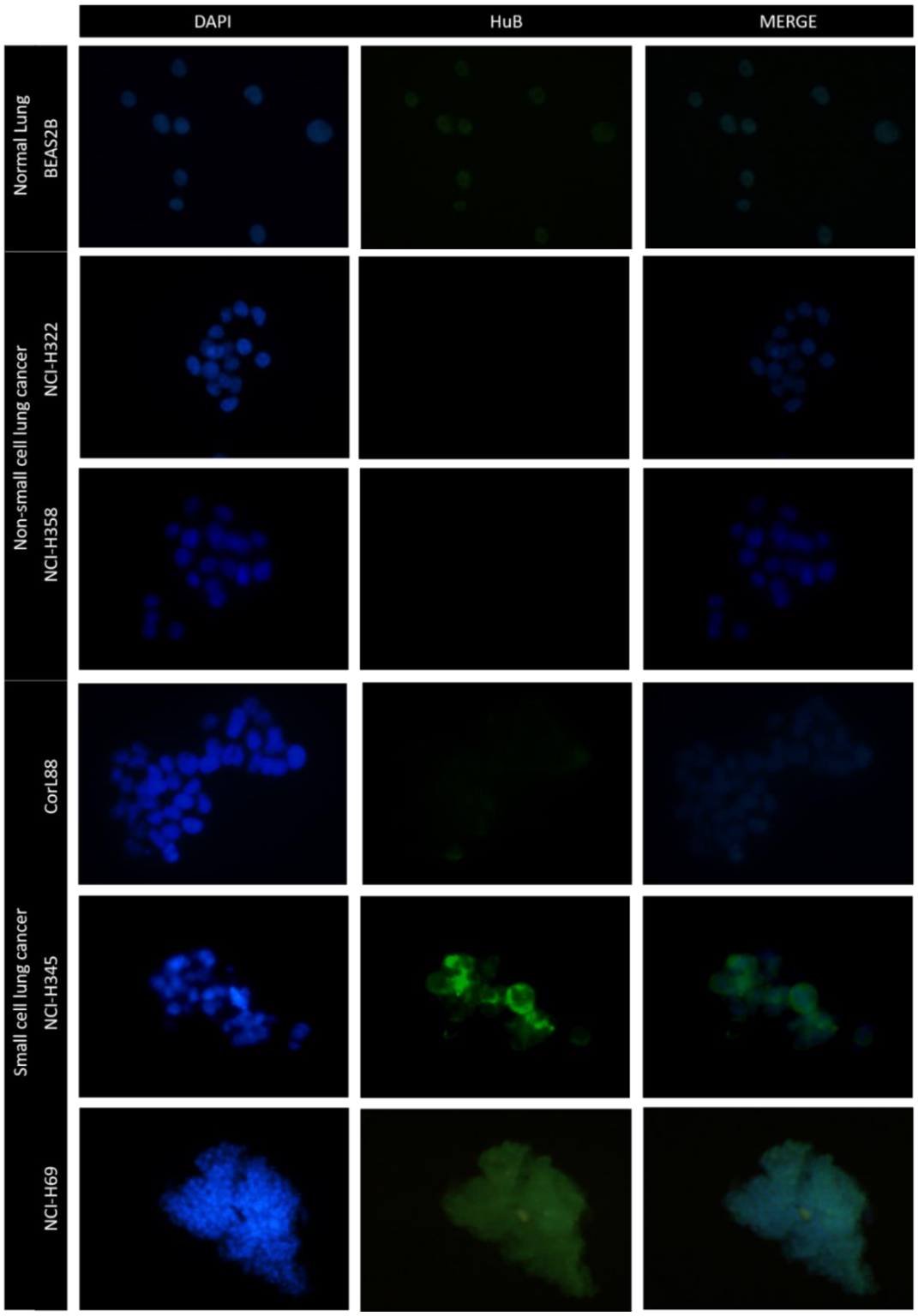

Figure 3.3: Representative example of HuB protein localisation in SCLC, NSCLC and normal bronchial epithelial cells. Cellular localisation of HuB in the normal bronchial epithelial cells BEAS2B, Non-small cell lung cancer cell lines, NCI-H322 and NCI-H358 and Small cell lung cancer cell lines, CorL88, NCI-H345 and NCI-H69. The left column showed staining of nuclei with DAPI (blue), the is middle column with anti-Hu (green) and the right column displays merged pictures. Magnification 20x. (n=3).

A low signal was detected for HuB protein in BEAS2B however, there was no *HuB* gene expression detected (Fig. 3.1) and it was absent from the western blot protein analysis (Fig. 3.2). An explanation for this is that it is background noise arising from fluorescence or nonspecific staining. Lack of fluorescent anti-Hu staining confirmed HuB was absent in the NSCLC cell lines NCI-H322 and NCI-H358. Whilst, two of the SCLC cell lines, NCI-H345 and NCI-H69 showed HuB protein expression consistent with the gene expression data (Fig. 3.1) and western blot protein determination shown in Fig. 3.2. CorL88 displayed some HuB protein expression in some of the cells that localised in the cytoplasm.

In NCI-H69 cells, anti-HuB staining co-localised with the DAPI nucleus stain therefore confirming HuB protein is localised in the nucleus of these cells. NCI-H345 showed stronger HuB expression than NCI-H69 however, in this cell line HuB protein was clearly localised in the cytoplasm.

3.1.2 *HuC* expression

Next, analysis of *HuC* gene expression in cell lines representative of the normal bronchial epithelial cells, NSCLC and SCLC was performed using RT-qPCR. The mRNA expression of *HuC* in SCLC, NSCLC and normal bronchial epithelial cells is shown in Fig. 3.4.

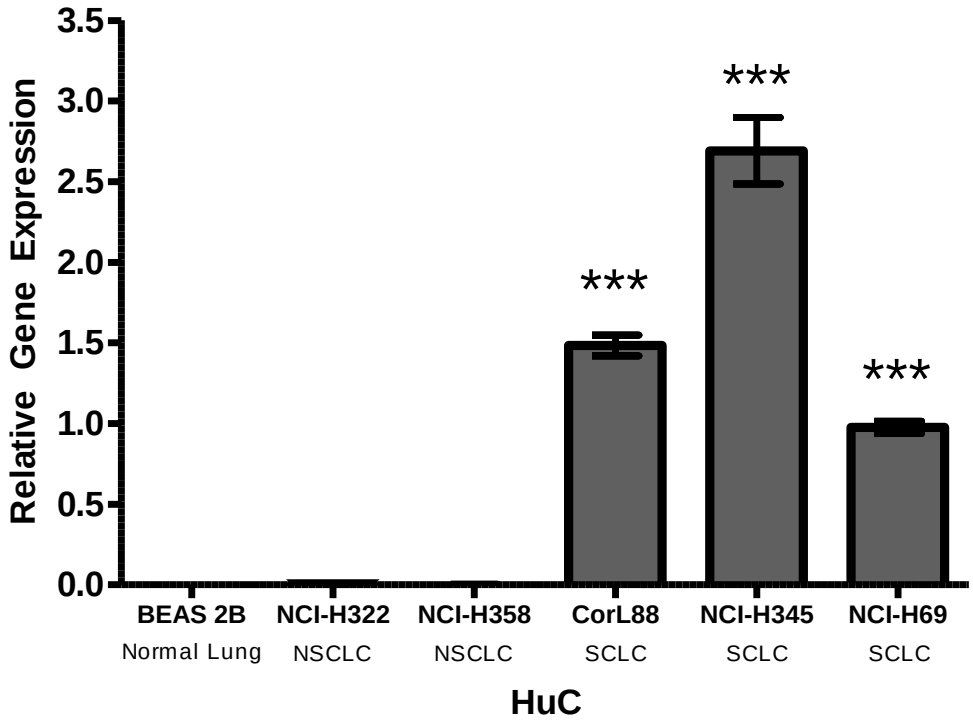

Figure 3.4: Gene expression of *HuC* in SCLC, NSCLC and normal bronchial epithelial cells. *HuC* gene expression was analysed by RT-qPCR in Small cell lung cancer cell lines, CorL88, NCI-H345 and NCI-H69, Non-small cell lung cancer cell lines, NCI-H322 and NCI-H358 and normal bronchial epithelial cells BEAS2B. The ΔCt results shown are an average of three replicates normalised to *β-Actin* gene expression relative to zero. Error bars display ± standard error of the mean (SEM). Statistical significance was calculated by a two-tailed t-test and is displayed by *P ≤ 0.05, **P ≤ 0.01, ***P ≤ 0.001. (n=3).

The expression of *HuC* was absent in the NSCLC and normal bronchial epithelial cells. *HuC* gene expression was observed in CorL88, NCI-H345 and NCI-H69 confirming significant aberrant expression of *HuC* in SCLC when compared to the normal bronchial epithelial cells. A 1.55-fold-increase of *HuB* gene expression was observed in CorL88 compared to the normal bronchial epithelial cells, BEAS2B. A 2.7-fold-increase of *HuC* expression was observed in NCI-H345 and a 1.0-fold-increase of *HuC* was shown in NCI-H69.

To detect if the gene expression was present at a protein level, western blotting (Section 2.3) of HuC protein using anti-HuC IgG was performed in each cell line derived from normal bronchial epithelial cells, Small cell lung cancer and Non-small cell lung cancer. GAPDH was used as a control protein with anti-GAPDH IgG to compare protein expression. Horse-radish peroxidase (HRP)-conjugated secondary antibodies were used to allow a detectable signal. The protein expression of HuC, RNA-binding protein in SCLC, NSCLC and normal bronchial epithelial cells is shown in Fig. 3.5.

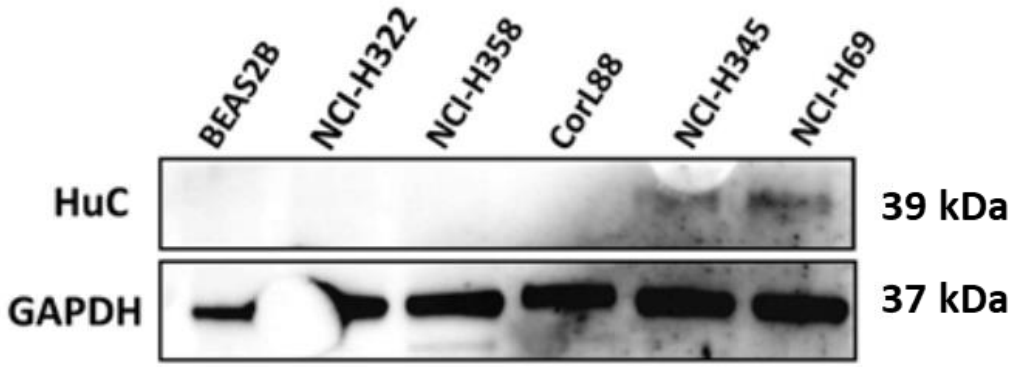

Figure 3.5: Representative example of HuC protein detected by western blot. HuC protein expression in normal bronchial epithelial cells BEAS2B, Non-small cell lung cancer cell lines, NCI-H322 and NCI-H358 and Small cell lung cancer cell lines, CorL88, NCI-H345 and NCI-H69. GAPDH protein expression was used as a loading control (n=3).

The results confirm an absence of HuC protein expression in the cell extracts of the normal bronchial epithelial cell line BEAS2B and NSCLC cell lines, NCI-H322 and NCI-H358. HuC protein was detected in the SCLC cell lines NCI-H345 and NCI-H69, correlating with the gene expression profile (Fig. 3.4). The bands detected for HuC protein in NCI-H345 and NCI-H69 are

less than the loading control. Interestingly, *HuC* gene was expressed in CorL88, but could not be detected at protein level.

Immunofluorescence staining was performed to confirm the HuC protein presence in the normal and cancer cell lines and to identify its subcellular localisation using anti-HuC and secondary Alexa green 488 FITC IgG (Fig 3.6).

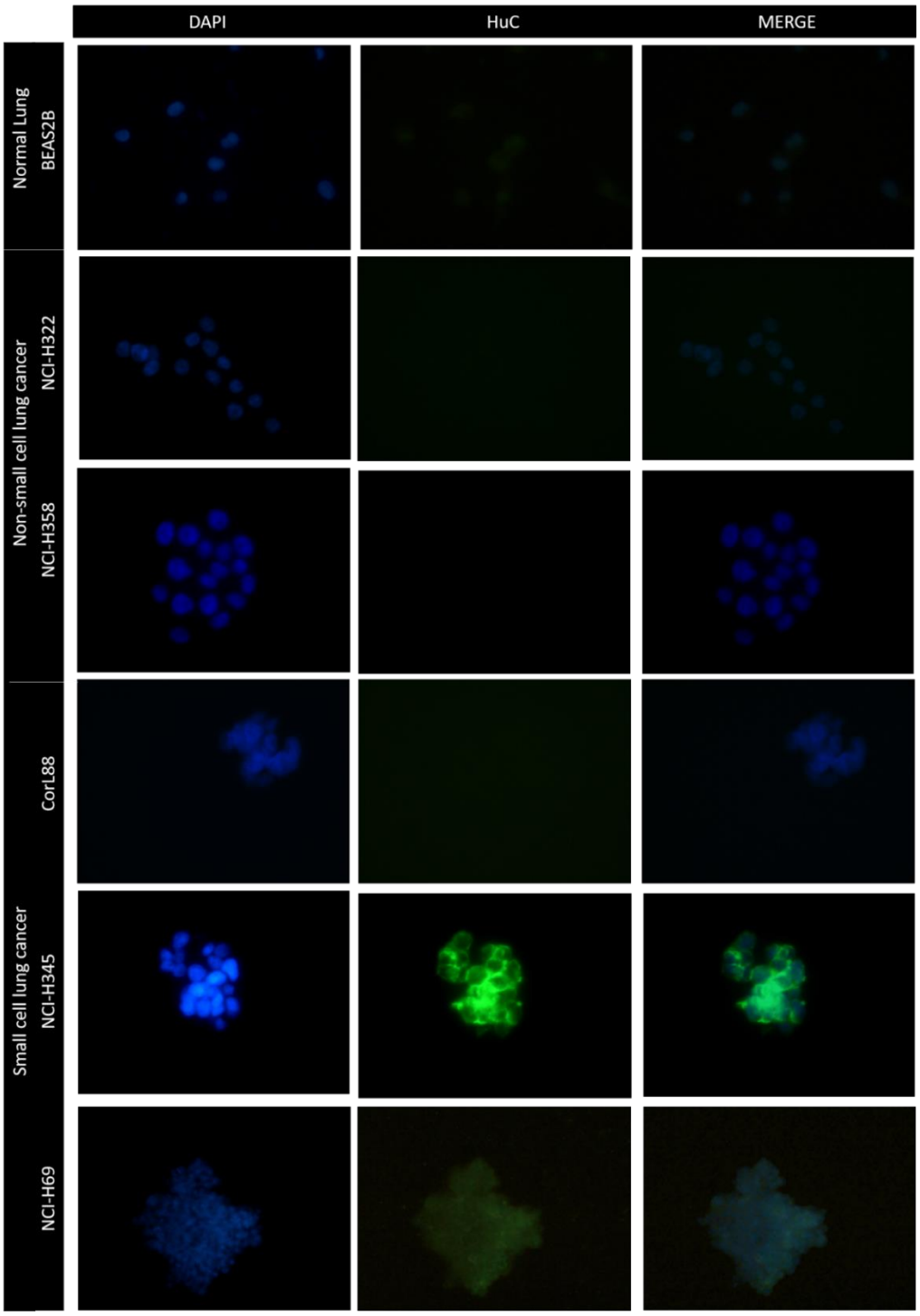

Figure 3.6: Example of HuC protein localisation in SCLC, NSCLC and normal bronchial epithelial cells. Cellular localisation of HuC in the normal bronchial epithelial cells BEAS2B, Non-small cell lung cancer cell lines, NCI-H322 and NCI-H358 and Small cell lung cancer cell lines, CorL88, NCI-H345 and NCI-H69. The left column showed staining of nuclei with DAPI (blue), the is middle column with anti-Hu (green) and the right column displays merged pictures. Magnification 20x. (n=3).

A very low fluorescence of HuC protein in BEAS2B cells was observed. However, since there was no *HuC* gene expressed (Fig. 3.4) and it was absent in the western blot protein analysis (Fig. 3.5), this must therefore be background fluorescence. This background fluorescence was also detected in staining of HuB protein in the BEAS2B cells strongly suggesting these cells autofluorescence.

HuC was absent from both NSCLC cell lines, NCI-H358 and NCI-H322 as expected. Two of the three SCLC cell lines, NCI-H345 and NCI-H69 showed HuC protein expression which differs from the gene expression results where all three SCLC cell lines including CorL88 showed *HuC* gene expression (Fig. 3.4).

NCI-H69 displays HuC protein that co-localises with the DAPI nucleus stain, therefore confirming HuC protein was localised to the nucleus of these cells. NCI-H345 showed stronger HuC protein expression than NCI-H69 and the staining was inconsistent with the DAPI nucleus stain. This concludes HuC protein was localised to the cytoplasm in these cells. These findings highlight variation of Hu protein localisation in SCLC cell lines.

Additionally, correlation was seen between the varied localisation of aberrantly expressed HuB and HuC proteins in the NCI-H345 and NCI-H69 cell lines individually. Like HuB protein in Fig 3.3, Fig3.6 showed HuC protein was present in the cytoplasm of NCI-H345 whereas HuB and HuC proteins were present in the nucleus of NCI-H69.

3.1.3 *HuD* expression

HuD gene expression analysis in cell lines representative of the normal bronchial epithelial cells, NSCLC and SCLC was performed by RT-qPCR described in Section 2.2.6. The mRNA

expression of HuD RNA-binding protein in SCLC, NSCLC and normal bronchial epithelial cells is shown in Fig. 3.7.

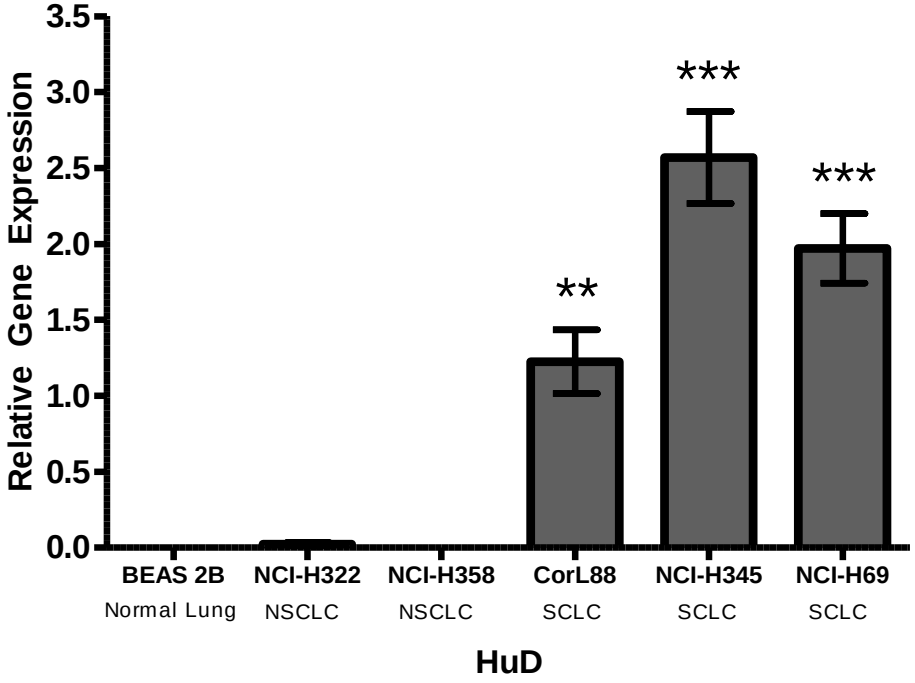

Figure 3.7: Gene expression of *HuD* in SCLC, NSCLC and normal bronchial epithelial cells. *HuD* gene expression was analysed by RT-qPCR in Small cell lung cancer cell lines, CorL88, NCI-H345 and NCI-H69, Non-small cell lung cancer cell lines, NCI-H322 and NCI-H358 and normal bronchial epithelial cells BEAS2B. The ΔCt results shown are an average of three replicates normalised to *β-Actin* gene expression relative to zero. Error bars display ± standard error of the mean (SEM). Statistical significance was calculated by a two-tailed t-test and is displayed by *P ≤ 0.05, **P ≤ 0.01, ***P ≤ 0.001. (n=3).

The expression of *HuD* gene was absent in the normal bronchial epithelial cells, BEAS2B and NSCLC cells, NCI-H322 and NCI-H358. *HuD* gene was expressed in all SCLC cell lines CorL88, NCI-H345 and NCI-H69, highlighting significant aberrant expression of *HuD* in this cancer

compared to the normal bronchial epithelial cells. A 1.2-fold-increase of *HuD* gene expression was observed in CorL88 compared to the normal bronchial epithelial cells, BEAS2B. A 2.6-fold-increase of *HuD* gene expression was observed in NCI-H345 and a 2.0-fold-increase of *HuD* gene expression was observed in NCI-H69.

To confirm if the *HuD* gene expression is effectively translated to a protein, western blot analysis (Section 2.3) was performed. Anti-HuD IgG was used for the detection of HuD protein in each cell lines derived from normal bronchial epithelial cells, Small cell lung cancer and Non-small cell lung cancer. GAPDH expression was also detected using anti-GAPDH IgG and used as a loading control. The protein expression of HuD, RNA-binding protein in normal bronchial epithelial cells, NSCLC and SCLC cell lines is displayed in Fig. 3.8.

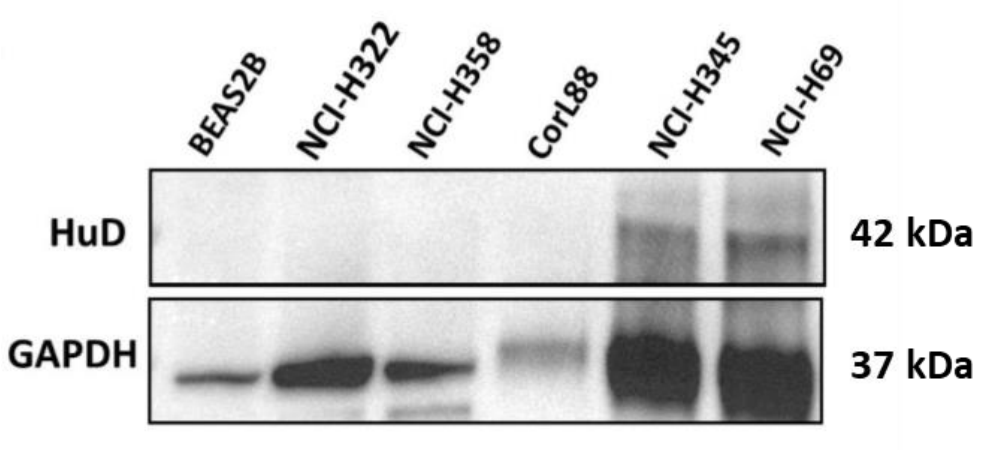

Figure 3.8: Representative western blot of HuD protein with anti-HuD antibody. HuD protein expression in normal bronchial epithelial cells BEAS2B, Non-small cell lung cancer cell lines, NCI-H322 and NCI-H358 and Small cell lung cancer cell lines, CorL88, NCI-H345 and NCI-H69. GAPDH protein expression was used as a loading control (n=3).

An absence of HuD protein expression was observed in the normal bronchial epithelial cell line BEAS2B and NSCLC cell lines, NCI-H322 and NCI-H358 correlating with gene expression results where HuD mRNA was not expressed (Fig. 3.7). HuD protein was detected in two of the three SCLC cell lines. NCI-H345 and NCI-H69 cells show faint bands indicating HuD protein expression whilst no band is present in the CorL88 cells. This differs from *HuD* gene expression shown in Fig. 3.7 where CorL88 also expressed *HuD* mRNA.

To clarify the data above and identify HuD's subcellular localisation in SCLC cell NCI-H345 and NCI-H69, immunofluorescence staining was performed. Anti-HuD IgG was used with the secondary Alexa 488 FITC IgG. Cells were also counterstained with DAPI nucleus stain for nuclear localisation.

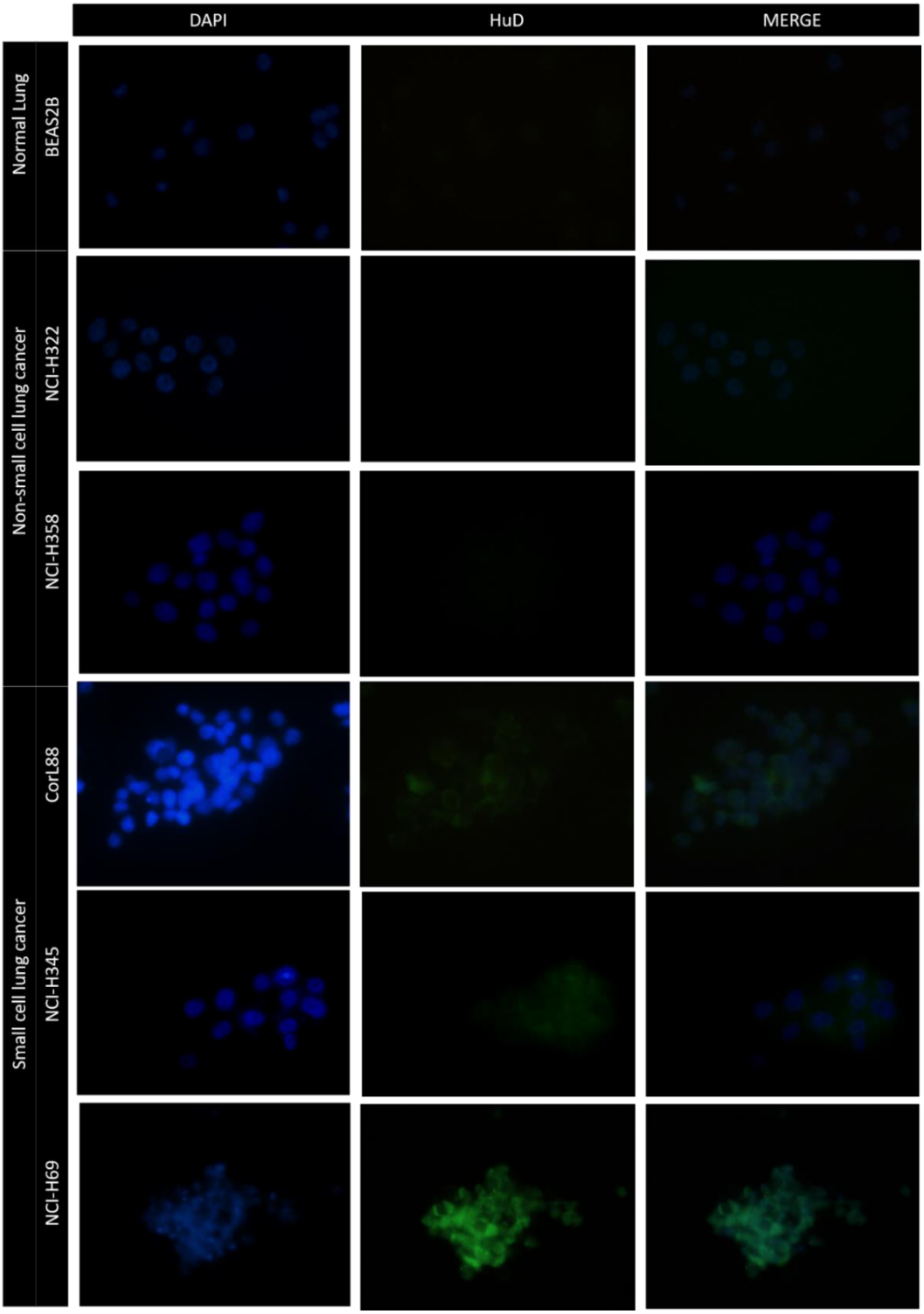

Figure 3.9: Representative localisation of HuD protein in SCLC, NSCLC and normal bronchial epithelial cells. Cellular localisation of HuD in the normal bronchial epithelial cells BEAS2B, Non-small cell lung cancer cell lines, NCI-H322 and NCI-H358 and Small cell lung cancer cell lines, CorL88, NCI-H345 and NCI-H69. The left column showed staining of nuclei with DAPI (blue), the is middle column with anti-Hu (green) and the right column displays merged pictures. Magnification 20x. (n=3).

The Immunofluorescence staining shown in Fig. 3.9 collaborates gene expression (Fig. 3.7) and western blot data (Fig. 3.8), where an absence of *HuD* gene and protein is shown in the normal bronchial epithelial cell line BEAS2B and the NSCLC cell lines NCI-H322 and NCI-H358.

HuD gene expression (Fig. 3.7) in CorL88 is confirmed at a protein level by immunofluorescence confirms a protein expression with a low signal observed in CorL88 SCLC cells. HuD protein expression in CorL88 was not detected during western blot (Fig. 3.8) and low protein expression level was most likely the cause of this. Additionally, low fluorescence of HuD protein was detected in the SCLC NCI-H345 cells, contrasting the strong fluorescence observed in SCLC NCI-H69 cells.

The HuD staining in CorL88 and NCI-H345 cells was inconsistent with the DAPI nucleus stain ultimately showing HuD was localised in the cytoplasm in these cells. NCI-H69 has HuB staining that co-localises with the DAPI nucleus stain and confirming its expression there.

3.1.4 *HuR* expression

Analysis of *HuR* gene expression in cell lines representative of the normal bronchial epithelial cells, NSCLC and SCLC was performed by RT-qPCR (Section 2.2.6). The fold-change of gene expression was calculated comparing expression to the normal bronchial epithelial cells BEAS2B. The data was normalised to the housekeeping gene *β-Actin*. HuR (2) and β-Actin primers are listed in Table 2.3. Statistical significance was calculated by a two-tailed t-test.

The mRNA expression of HuR RNA-binding protein in normal bronchial epithelial cells, BEAS2B cell line, NSCLC cell lines NCI-H322 and NCI-H358 and SCLC cell lines CorL88, NCI-H345 and NCI-H69 is shown in Fig. 3.10.

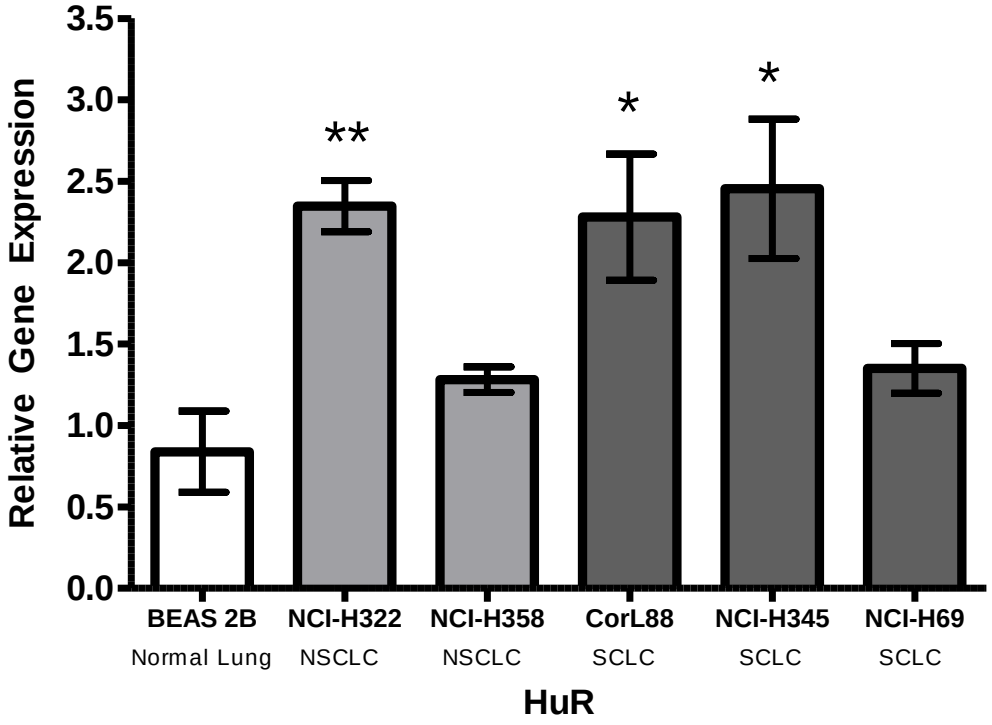

Figure 3.10: Gene expression of *HuR* in SCLC, NSCLC and normal bronchial epithelial cells. *HuR* gene expression was analysed by RT-qPCR in Small cell lung cancer cell lines, CorL88, NCI-H345 and NCI-H69, Non-small cell lung cancer cell lines, NCI-H322 and NCI-H358 and normal bronchial epithelial cells BEAS2B. The ΔCt results shown are an average of three replicates normalised to *β-Actin* gene expression relative to zero. Error bars display ± standard error of the mean (SEM). Statistical significance was calculated by a two-tailed t-test and is displayed by *P ≤ 0.05, **P ≤ 0.01, ***P ≤ 0.001. (n=3).

HuR gene is ubiquitously expressed in human cells and this was confirmed by RT-qPCR where HuR gene expression was confirmed in all cell lines (Wang et al. 2013). Overall, a higher $2^{-\Delta\Delta Ct}$ *HuR* mRNA expression was observed in the cancer cell lines in comparison to the normal bronchial epithelial cells control with a significant increase observed in the NSCLC cell line NCI-H322 and SCLC cell line CorL88 and NCI-H345. Of the two NSCLC cell lines, a 1.51 fold-increase was observed for NCI-H322 whilst a 0.44 fold-increase was observed in NCI-H358,

the latter was not significant. The three SCLC cell lines revealed a 1.44 fold-increase in *HuR* expression for CorL88, a 1.61 fold-increase in NCI-H345 and a 0.51 fold-increase in NCI-H69, again the latter was not significant.

To confirm if the *HuR* gene was present at a protein level, western blot analysis using anti-HuR IgG was carried out in each cell line derived from normal bronchial epithelial cells, Small cell lung cancer and Non-small cell lung cancer was compared. Anti-GAPDH IgG was also used for the detection of GAPDH as a loading control. Horseradish peroxidase (HRP)-conjugated secondary antibodies were used to allow a detectable signal.

The protein expression of HuR, RNA-binding protein in normal bronchial epithelial cells, NSCLC and SCLC cell lines is displayed in Fig. 3.11.

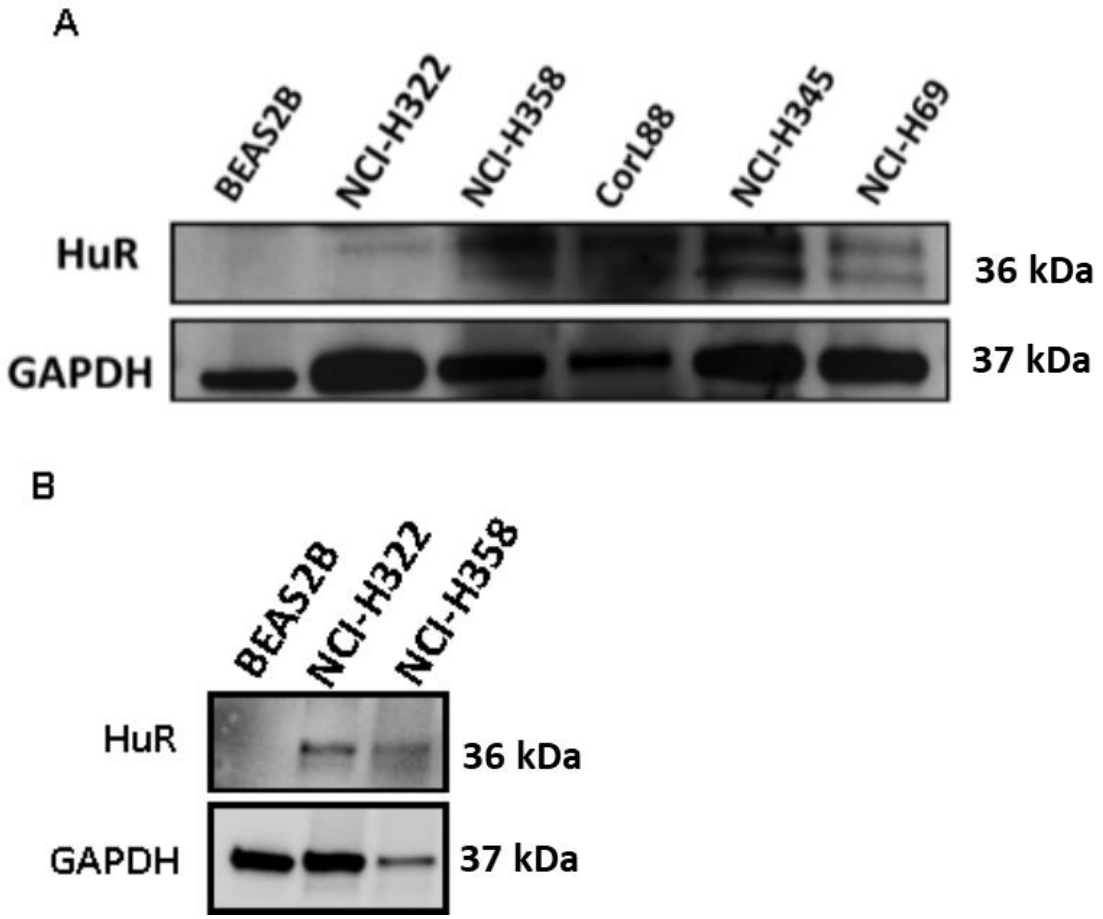

Figure 3.11: Example western blot analysis of HuR protein with anti-HuR antibody. A) HuR protein expression in normal bronchial epithelial cell line and different NCLC and SCLC cell lines. B) HuR protein expression in the normal bronchial epithelial cells and NSCLC cell lines only. GAPDH protein expression was used as a loading control in both blots. (n=3).

HuR protein was detected in the cell extracts from NSCLC cell lines NCI-H322 and NCI-H358, and SCLC cell lines CorL88, NCI-H69 and NCI-H345 cell lines represented by two distinct bands around 36kDa, the expected size of HuR. A possible explanation for the two bands is that HuR has experienced posttranslational modifications such as phosphorylation resulting in two slightly different sized proteins. GAPDH protein was detected at the expected size of 37kDa.

Strongest staining was observed in the NSCLC NCI-H358 cell line and SCLC cell lines CorL88 and NCI-H345. The SCLC protein expression matches the gene expression data (Fig. 3.10) where CorL88 and NCI-H345 cells showed the highest HuR mRNA expression. However, for the NSCLC cells, the protein expression varies from the gene expression data (Fig. 3.10) that showed more *HuR* mRNA expressed in the NSCLC NCI-H322 than the NCI-H358 cell line. This could be explained by post-transcriptional modifications resulting in more HuR gene translated in some cell lines than others although there is no evidence to support this.

Whilst the normal bronchial epithelial cell line, BEAS2B, displayed no HuR protein expression, *HuR* gene expression was previously shown to be expressed in the lungs in Fig. 3.10. To confirm if HuR protein lied under the detection level due to the high level of detection of the other bands shown in Fig. 3.11A, a second western blot with only NSCLC and normal bronchial epithelial cells was performed. This confirmed an absence of HuR protein expression in the BEAS2B cell lines.

To confirm the HuR protein presence and identify the location of the proteins in all the analysed cell lines, immunofluorescence staining was performed using anti-HuR mouse IgG and secondary Alexa 488 FITC IgG. Cells were counterstained with DAPI nucleus stain for nuclear localisation.

HuR protein fluorescence shown in Fig. 3.12 was observed in all cell lines BEAS2B, NCI-H322, NCI-H358, CorL88, NCI-H345 and NCI-H69 correlating with gene expression data in Fig. 3.10.

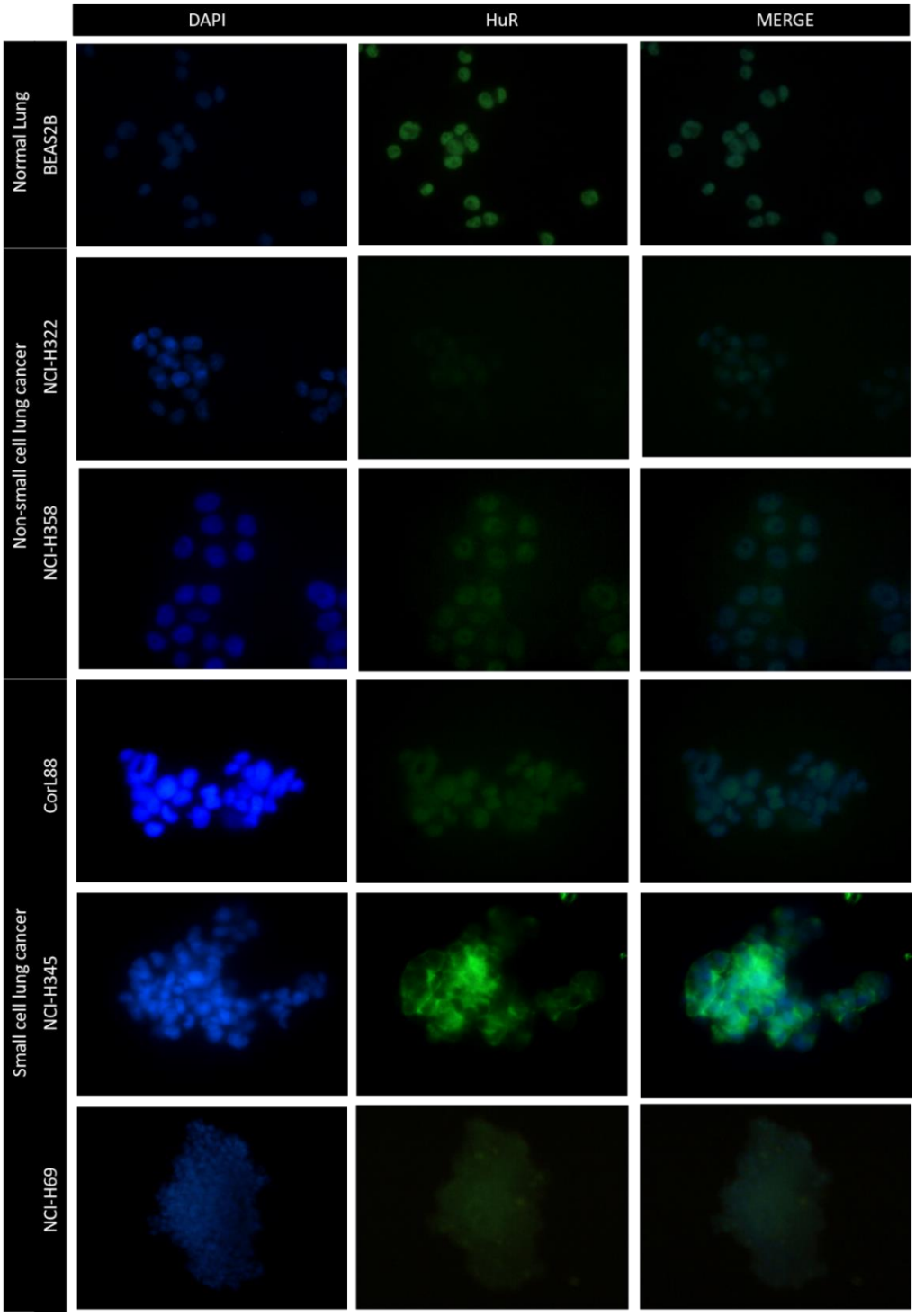

Figure 3.12: Representative localisation of HuR protein in normal bronchial epithelial cells and NSCLC and SCLC cell lines. Cellular localisation of HuR in the normal bronchial epithelial cells BEAS2B, Non-small cell lung cancer cell lines, NCI-H322 and NCI-H358 and Small cell lung cancer cell lines, CorL88, NCI-H345 and NCI-H69. The left column showed staining of nuclei with DAPI (blue), the is middle column with anti-Hu (green) and the right column displays merged pictures. Magnification 20x. (n=3).

In NCI-H322 cells, only a weak signal could be detected for HuR protein in the nucleus. This was consistent with western blot results where only a weak band could be detected in NCI-H322 cell extract.

The fluorescence of HuR protein in the normal bronchial epithelial cell line BEAS2B was co-localised with the DAPI nucleus stain therefore HuR protein was localised to the nucleus. Strong fluorescence in the nucleus was also observed in both NSCLC cell lines NCI-H322 and NCI-H358. Two of the SCLC cell lines also display HuR nuclear localisation CorL88 and NCI-H69. The remaining SCLC cell line NCI-H345 displayed strong cytoplasmic localisation of HuR.

3.2 Morphology of lung cell lines

Lung cancers are easily distinguishable into Non-small cell lung cancers and Small cell lung cancer due to their size. A tumour with less than 10% of large cells is classified as SCLC by WHO (Travis et al. 2015). Often cellular changes to the morphology or lung cells is how lung cancers are observed through biopsies during diagnosis.

SCLC showed a considerable degree of morphological histopathological variability during *in-vitro* studies. SCLC cells are small, round, oval or spindle shaped cells with scanty cytoplasm (Brambilla et al. 2001). Their nucleus contain granular nuclear chromatin and very faint or absent nucleoli and lack of cell boarders (Travis et al. 1999). Krohn et al. (2014) reports of two cells types. Some cells float in clusters, are smaller, round and have small nuclei. Attached cells are larger (although still smaller than three lymphocytes defining cells ‘small’) and grow in little clumps with less cell-cell contacts and a large cytoplasm-to-nucleus ratio.

Non-small cell lung cancer tumours contain large cells, that have a small nuclear to cytoplasmic ratio, also contain vesicular, coarse or fine chromatin and common nucleoli. Not all NSCLC tumours meet this criteria but are still considered NSCLC due to their bigger size and large cytoplasm (Travis et al. 1999).

To observe difference in the morphology of cell lines derived from the lung cell images were obtained using an Eclipse II fluorescent inverted microscope and Microtec camera as described in Section 2.1.6. These are shown in Fig. 3.13.

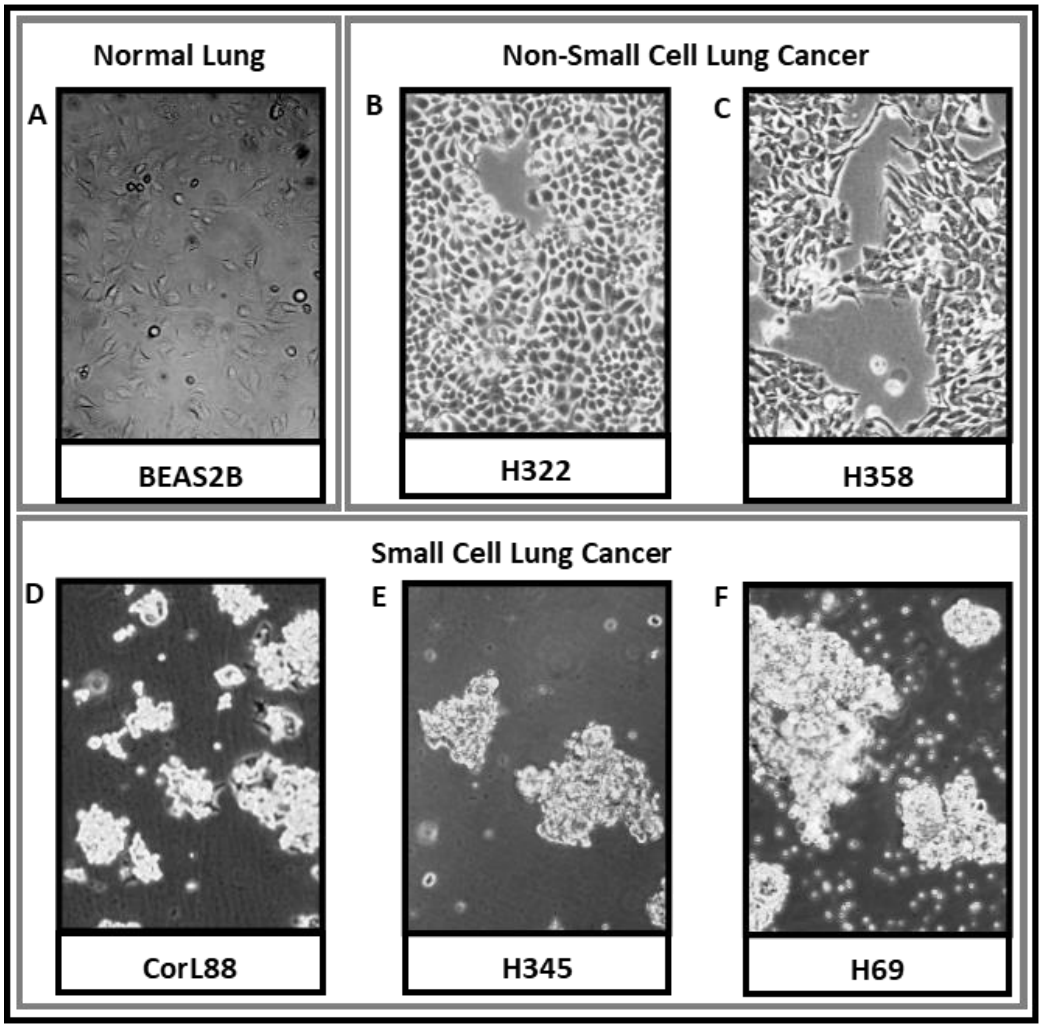

Figure 3.13: Microscopy images of each lung cell line. Inverted microscopy at x20 Objective. A) Normal lung cell line, BEAS2B. B) NSCLC cell line, NCI-H322. C) NSCLC cell line, NCI-H358. D) SCLC cell line, CorL88. E) SCLC cell line, NCI-H345. F) SCLC cell line, NCI-H69.

The normal bronchial epithelial cells (Fig. 3.13A) grew with similar properties to that of the two NSCLC cell lines NCI-H322 (Fig. 3.13B) and NCI-H358 (Fig. 3.13C). These are adherent cells that grow as a single monolayer. They have an epithelial-like shape.

In contrast, the three SCLC cells lines studied, collectively feature both semi-adherent and suspension cells described by Krohn et al. (2014). The CorL88 (Fig. 3.13D) is a semi-adherent cell line whilst the NCI-H345 (Fig. 3.13E) and NCI-H69 (Fig. 3.13F) cell lines are grow in suspension. All SCLC cell lines grow in multi-cellular aggregates and have a visually similar morphology. NCI-H345 and NCI-H69 are solely suspension cell lines that grow in large clumps and are very similar. CorL88 also feature these large clumps in suspension however, as a semi-adherent cell line, the adherent cells form small clumps that anchor to the cell culture flask rather than float in suspension. These anchored cells often show a fibroblast-like appearance, while suspended cells attached to this clump are round. The SCLC cells are distinctly smaller than NSCLC cells.

3.3 Motility of lung cells

An assessment of cell motility was made to compare the normal bronchial epithelial cells and NSCLC cells. This aimed to determine the invasiveness of NSCLC cells in culture, since a key characteristic of cancer cells is the ability to invade into distant tissues. Unfortunately, a measure of SCLC invasiveness could not be determined by this method as two of the SCLC cell lines grow in suspension in culture and the other is semi-adherent.

The cell motility was analysed in normal bronchial epithelial cells BEAS2B and NSCLC, NCI-H322 and NCI-H358 cell lines. It was measured by the ability of the cells to invade into a 0.5% agarose gel matrix captured through several microscopy imaging equipment. The images

below show time-lapse photography by a CytoSMART™ camera, described in Sections 2.5 and 2.5.1.

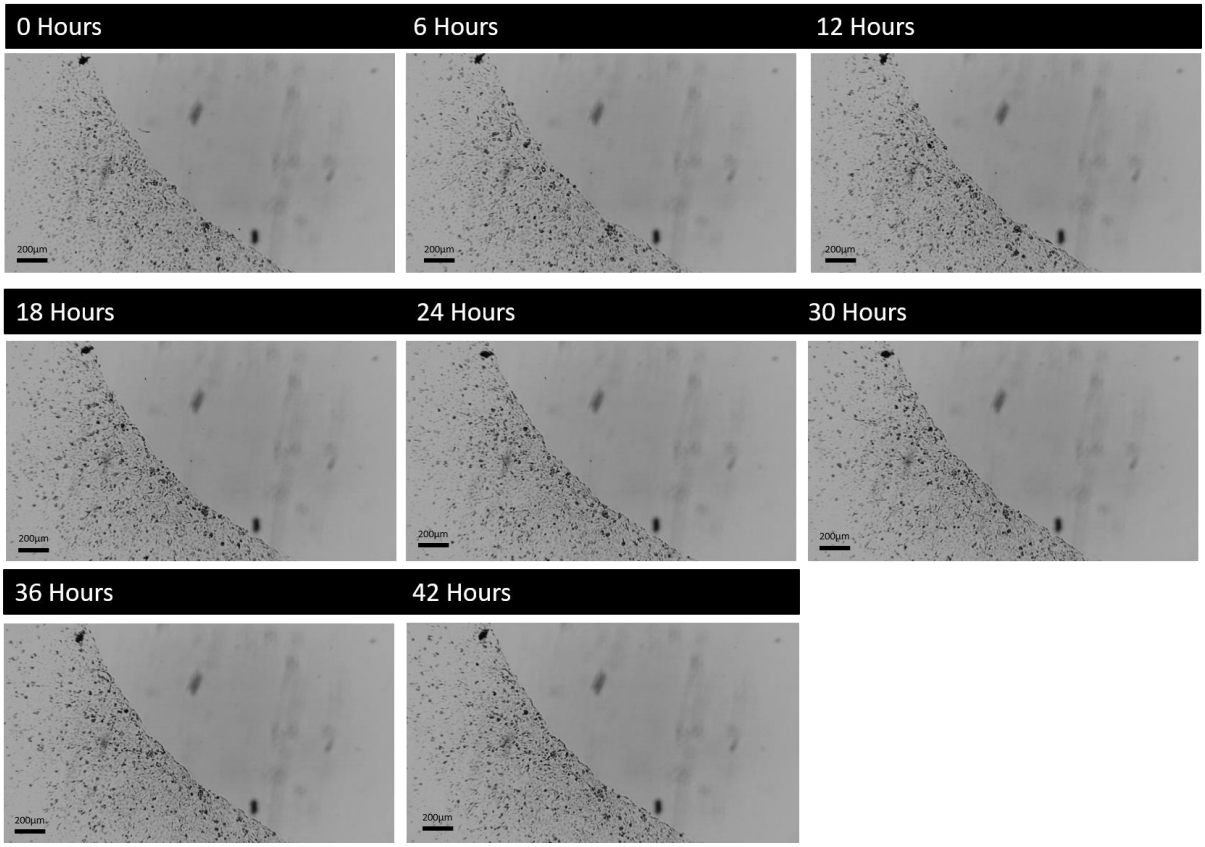

Figure 3.14: The non-migration of BEAS2B, normal bronchial epithelial cells into an agarose gel matrix. During the observed 42-hour period, no migration into the gel matrix was detected. Time-lapse photography of the cell migration can be viewed at: https://cytomate.com/access/Project_main/main.php?DiD=238&PiD=19712&ac1=149416767a375353f51632463fb10382a640ba0896cb9b42bd7d545ad26b5e1b&ac2=880daacfc972a8ab4d37a6ff5a3c82f587f08552a7ed72cafb0c4c4ac2e8894d

The normal bronchial epithelial cells, BEAS2B, did not move into the agarose gel during the observed 42-hours as expected for a non-cancer cell line. Instead they grew densely in a line surrounding the agarose.

When the NSCLC, NCI-H322 cells, were observed for their motility over 42 hours, they too, did not migrate into the agarose. These cells also grew in a line around the outside of the agarose gel.

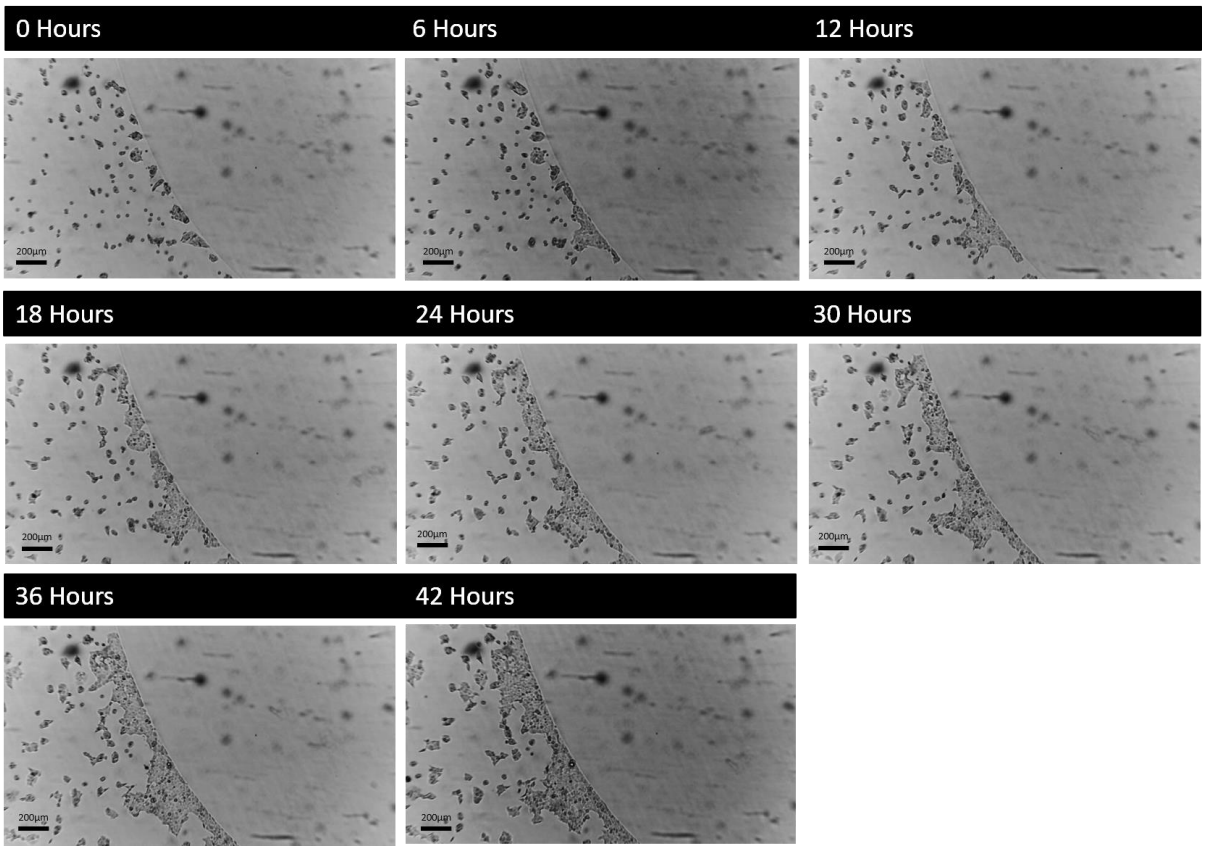

Figure 3.15: The non-migration of NCI-H322, Non-small cell lung cancer cells into an agarose gel matrix. Over the observed 42-hour period, no migration into the gel matrix was detected. Time-lapse photography of the cell migration can be viewed at: https://cytomate.com/access/Project_main/main.php?DiD=238&PiD=9757&ac1=711ef18fe2c9639658912d0e6549cbfa07b511b3dc550fd92d290f069aa92db9&ac2=efc7fe8945b0c64aead79e94ca96cfee4147a02bebbd4081979f4a4047ba5c1c

Next, the second NCSLC NCI-H358 cell line was analysed for their migrative ability. In contrast to the BEAS2B and NCI-H322 cell lines, the NCI-H358 cells moved into the agarose gel matrix.

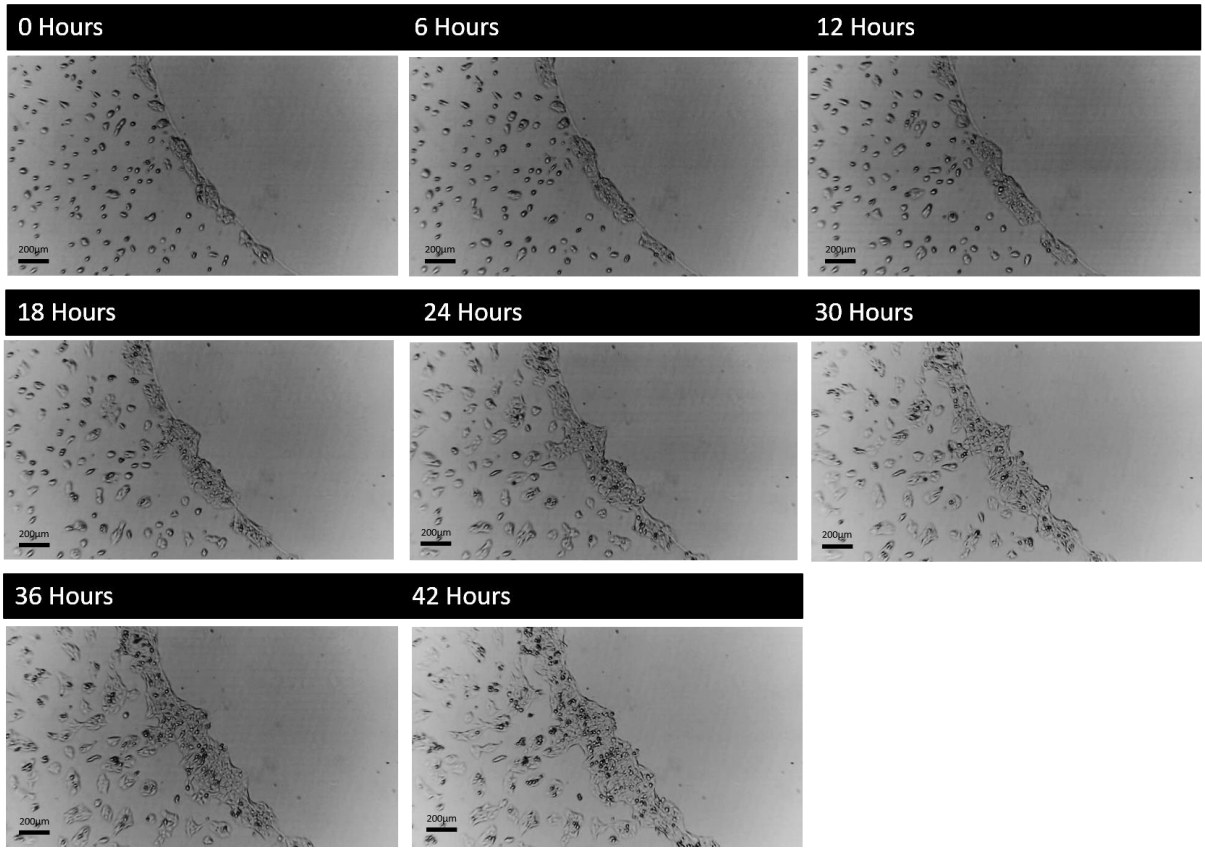

Figure 3.16: The migration of NCI-H358, Non-small cell lung cancer into an agarose gel matrix. Over the observed 42-hour period, cells migrated into the gel matrix. Time-lapse photography of the cell migration can be viewed at: https://cytomate.com/access/Project_main/main.php?DiD=233&PiD=9876&ac1=c81bf7110ff48994eda221f058f3b2b551a0a584726303de3164645b899f6839&ac2=008c9d6d9c1a69de50192aac15c1eea44c463735f0044aea87f10ed2f698eef1

As seen in Fig. 3.16, the NCI-H358 cells can be seen collecting around the agarose gel at 0 hours. From 6 hours the cells began to migrate into the gel matrix.

Imagery analysis displayed above is representative of one attempt although consistently observed was the ability of the NCI-H358 cells to migrate into the gel whilst NCI-H322 and BEAS2B cells were not able to.

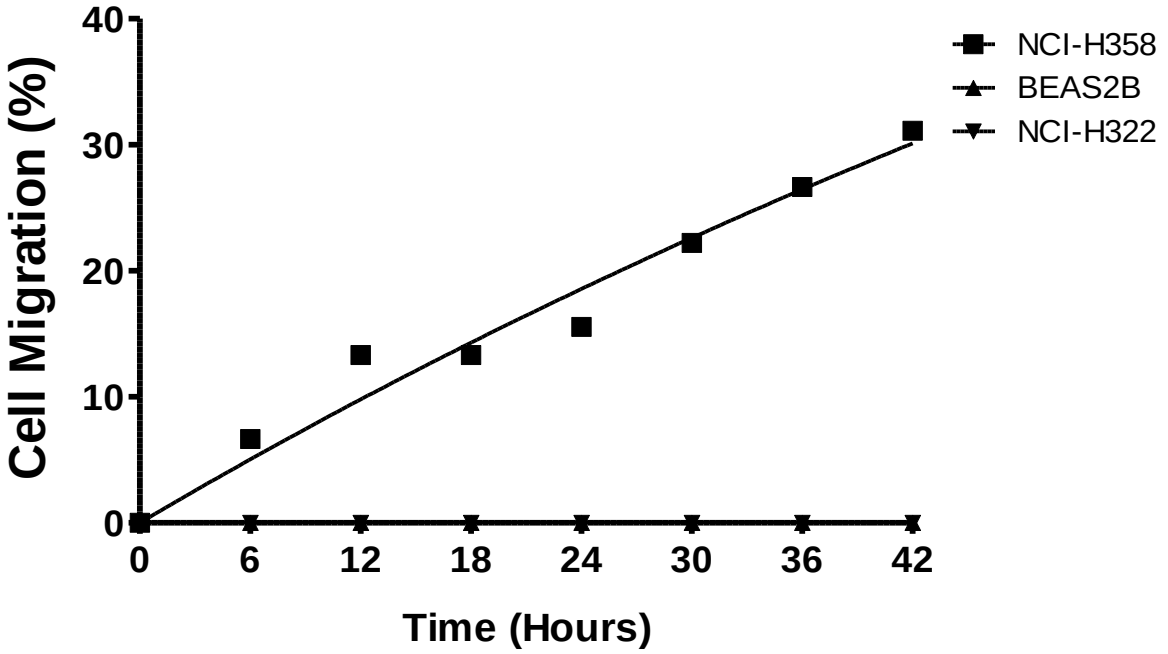

Figure 3.17: The migration of NCI-H358 NSCLC cells compared to the non-migration of normal bronchial epithelial cells BEAS2B and NSCLC NCI-H322. Percentage area of the gel matrix invaded by NCI-H358 cells.

As seen in Fig. 3.17, NCI-H358 cells were able to invade into the gel matrix potentially replicating their invasiveness in the body. Over a 42-hour period cells invaded 31.11% of the observed section of gel matrix (Fig. 3.17).

3.4 Summary

For the first time, an expression profile comparing Hu expression in different lung cancer cell lines has been established. Concluded in Table 3.1 is the Hu protein expression detected in each cell line following different methods for mRNA and protein analysis.

		Hu Protein											
Cell type	Cell line	HuB			HuC			HuD			HuR		
		PCR	WB	IF	PCR	WB	IF	PCR	WB	IF	PCR	WB	IF
Bronchial epithlia	BEAS2B												N
Non-Small Cell Lung Cancer	NCI-H322												N
	NCI-H358												N
Small Cell Lung Cancer	CorL88									C			N
	NCI-H345			C			C			C			C
	NCI-H69			N			N			N			N

Table 3.1: Overall expression of HuB, HuC, HuD and HuR proteins in cell lines of normal bronchial epithelial cells, Non-Small Cell Lung Cancer and Small Cell Lung Cancer cells. Each method of analysis including RT-qPCR (PCR), western blotting (WB) and immunofluorescent staining (IF) is shown. Green represents a positive result. Also shown is the localisation of the proteins determined through immune fluorescence cytoplasm is shown by C and the nucleus is represented by N.

There are several conclusions that can be drawn from the investigation into the presence of Hu RNA-binding proteins in lung cancers. Gene expression analysis showed a difference between the expression of the neuronal Hu protein family members *HuB*, *HuC* and *HuD* in the normal bronchial epithelial cells and different lung cancer groups. All neuronal *Hu* genes were expressed in the Small cell lung cancer cell lines apart from HuB in CorL88. This is significant since HuB, HuC and HuD are not naturally expressed within lung tissue. Additionally, there was an absence of the neuronal *Hu* genes in the normal bronchial epithelial cells and NSCLC cell lines. This data confirms these genes are only present in SCLC providing an insight into a functional role required for the development of the cancer.

HuR gene was detected in all the lung cell lines which was expected since it is ubiquitously expressed in all tissues in the human body. In each cancer, at least one cell line showed significant upregulated *HuR* gene expression in comparison to the normal bronchial epithelial cell line BEAS2B supporting the idea that *HuR* is functionally upregulated in cancers.

Whilst gene expression is important in cancer studies, the active status of a gene and its ability to translate into a functional protein is of equal significance. Western blot studies interestingly showed, HuC and HuD proteins were only present in two of the SCLC cell lines NCI-H345 and NCI-H69 despite CorL88 also expressing these genes at an RNA level. Conversely, *HuB* gene was detected at a high level though RT-qPCR in NCI-H345 and NCI-H69 cell lines yet at a protein level, it was detected at high levels in all three SCLC, NCI-H345, NCI-H69 and CorL88 cell lines. Interestingly, CorL88 differs from NCI-H69 and NCI-H345 in its morphology in culture. CorL88 is semi-adherent whilst NCI-H345 and NCI-H69 grows in suspension, suggestive of alternative characteristics within SCLC tumours.

Despite the aberrant and over expression of these Hu proteins that has been described in this study at both gene and protein levels, the location of the Hu proteins within the cell has been shown to influence the pathogenicity of some cancers.

Anti-Hu fluorescent staining revealed all the Hu proteins present in the nucleus of the NCI-H69 cells, whilst all Hu proteins were detected in the cytoplasm in the NCI-H345 cells. CorL88 cells revealed HuD protein localises in the cytoplasm and HuR protein in the nucleus. HuD protein was previously undetected by western blot and whilst the fluorescent staining is weak, it does confirm HuD protein is actively translated in this cell line. However, during the western blot, the strong bands of the HuD in the other two SCLC cell lines NCI-H345 and NCI-H69, CorL88 HuD fluorescence remained undetected. Interestingly, western blot of HuR

detected two bands significant of a phosphorylation event of HuR resulting in two differently sized HuR protein monomers. This has previously been described by (Kim and Gorospe, 2008).

During western blot studies in comparison to the loading control GAPDH, the NSCLC cell line NCI-H358, showed a strong expression of HuR. Whilst NCI-H322 did display weak staining despite HuR gene expression being significantly higher in NCI-H322. HuR immunofluorescence studies showed its expression was localised to the nucleus in both NSCLC cells lines.

HuR protein expression could not be detected in normal bronchial epithelial cells using western blotting however, antibody staining methods did and confirmed its localisation in the nucleus. During the western blot, HuR protein expression was most likely missed due its expression remaining under the detection level.

In summary, all Hu proteins are found expressed in two of the SCLC cell line NCI-H69 and NCI-H345. CorL88, also a SCLC cell line showed HuD and HuR expression at both RNA and protein levels. HuC was expressed at RNA level but not at a protein level. In the normal bronchial epithelial cells and NSCLC cell lines NCI-H322 and NCI-H358, only HuR was present at both gene and protein level.

Cell culture observations show a similarity in the morphology of the different lung cancer groups in comparison to the normal bronchial epithelial cells suggestive of similar characteristics within the named cancers and potentially their pathogenicity. The differences in size, growth as a monolayer or as multicellular aggregates, nuclear to cytoplasm ratio, nucleoli presence and chromatin structure aids diagnosis and the ability to distinguish between SCLC and NSCLC.

When determining the invasive potential of the NSCLC cell lines, interestingly only one of the cell lines NCI-H322 cells managed to penetrate the gel matrix. This is clinically significant of the ability for cells to migrate into other organs and form tumour growth and highlights a difference in migrative potential within the NSCLC cell types.

Overall, there are several conclusions that can be drawn from the results in this Chapter. Firstly, the ectopic presence of the neuronal genes in SCLC is established and an overexpression of HuR expression in both NSCLC and SCLC is shown. Within this expression there was still distinct differences within protein expression and localisation within the cells despite cell morphology similarities. In summary, this highlights differences within tumour types at both a genetic and protein level.

Chapter 4

Results

Part II: Expression of Hu proteins, their role and mRNA targets in Neuroblastoma

Hu proteins were first described in Neuroblastoma by Dalmau, Josep and Furneaux (1992), whereby analysis of neuroendocrine tumours such as Small cell lung cancer, Neuroblastoma, Sarcoma, and Prostate carcinoma revealed about 50% of Neuroblastoma tumours express Hu proteins. Later is was described that specifically HuB and HuD were identified in some Neuroblastoma patients (Ball, N. S. and King, Peter H. 1997). In these patients and similar to the effect in SCLC, the triggered immune response initiates neuronal apoptosis resulting in enteric nervous system impairment underlying paraneoplastic gut dysmotility (De Giorgio et al. 2003). However, the extent of all Hu proteins expression and their biological function of Hu proteins in Neuroblastoma has not been established.

The general expression of each *Hu* gene and protein in Neuroblastoma was determined through studies on two Neuroblastoma cell lines SK-N-AS and SH-SY5Y compared to a normal astrocyte cell line SVG p12. Next, knockdown studies of *Hu* genes were established to ultimately define how Hu expression may influence a cancerous phenotype through tumour initiation and development characteristics. Finally, these studies analysed mRNA transcripts targeted by the Hu RNA-binding protein family and sought to determine the Hu protein family's overall influence on molecular pathways and the downstream effects of these pathways in cancer development.

4.1 *Hu* gene expression in Neuroblastoma and normal astrocytes

The gene expression of all Hu proteins in two Neuroblastoma cell lines SH-SY5Y and SK-N-AS and in normal astrocytes SVG p12 was determined using quantitative RT-PCR. The fold-change of expression was analysed by comparing expression levels to the normal astrocyte cell line SVG p12. *β-Actin* was the housekeeping gene to which the data was normalised. Statistical significance was calculated by a two-tailed t-test. The relative transcript expression levels of all *Hu* genes in the two Neuroblastoma cell lines in comparison to the normal astrocyte cell line is displayed in Fig. 4.1.

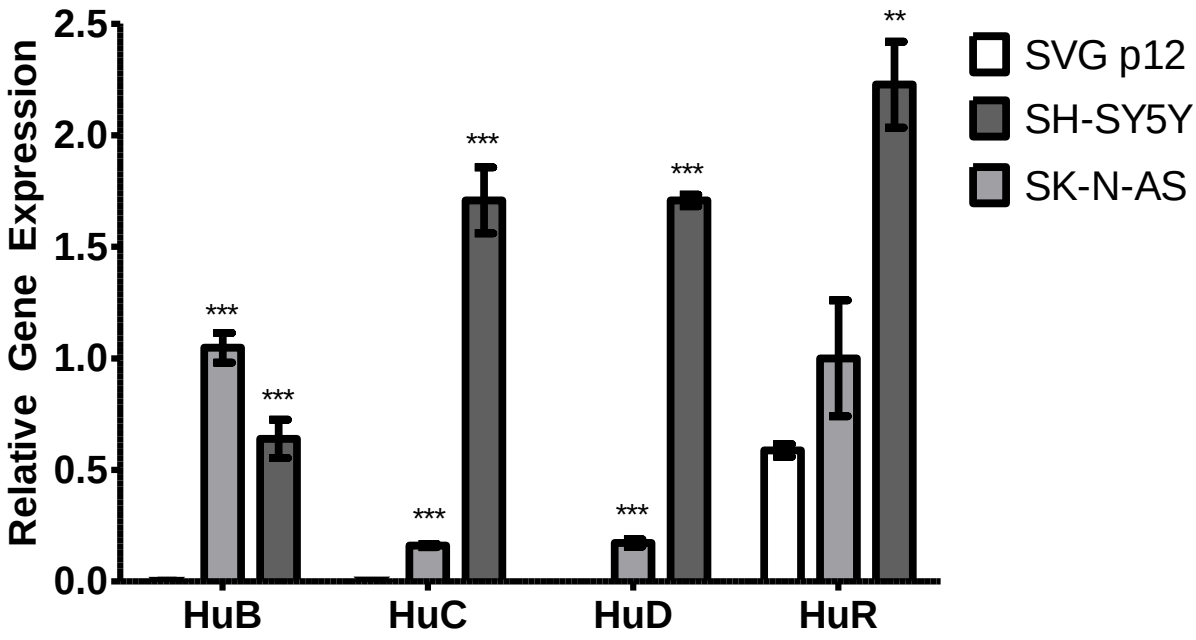

Figure 4.1: Gene expression of all the *Hu* protein family members in normal astrocytes and Neuroblastoma cells. *HuB*, *HuC*, *HuD* and *HuR* gene expression was analysed by RT-qPCR in normal astrocytes, SVG p12 and Neuroblastoma cell lines, SH-SY5Y and SK-N-AS. The ΔCt results shown are an average of three replicates normalised to *β-Actin*, relative to zero. Error bars display ± SEM. Statistical significance was calculated by a two-tailed t-test and is displayed by *P ≤ 0.05, **P ≤ 0.01, ***P ≤ 0.001. (n=3).

The normal astrocyte cell line SVG p12 expressed *HuB*, *HuC* or *HuD* mRNA in very low levels that upon normalisation of the data, is not displayed on the graph. SVG p12 cells do express *HuR* gene. All *Hu* genes was expressed in the Neuroblastoma cell lines SH-SY5Y and SK-N-AS. All upregulated gene expression values were statistically significant except HuR expression in SK-N-AS Neuroblastoma cells.

A 1.05 fold-increase of *HuB* gene expression was observed for SK-N-AS in comparison to the normal astrocyte line SVG p12, whilst a 1.05 fold-increase of *HuB* gene expression was observed for SH-SY5Y. *HuC* and *HuD* gene expression was seen upregulated the most in SH-SY5Y cells with a 1.71 fold-increase in *HuC* expression and a 1.71 fold-increase also in HuD expression. In SK-N-AS cells, *HuC* was increased by 0.16 fold-change whilst *HuD* was increased 0.17 fold-change. The gene expression of *HuR* only showed a small increase of 0.15 in SK-N-AS cells. A 1.42 fold-increase in *HuR* expression was observed in the SH-SY5Y cells.

4.2 Hu protein expression and localisation in Neuroblastoma and normal astrocytes

Gene expression does not always reflect the amount of protein expressed due to post-transcription gene regulation. Therefore, the presence of Hu proteins in the normal astrocytes SVG p12 and Neuroblastoma cells SK-N-AS and SH-SY5Y was determined using Western Blotting (Section 2.3). Whilst subcellular localisation of Hu proteins was determined by immunofluorescent staining methods (Section 2.41).

4.2.1 HuB protein expression and localisation

HuB protein expression in SK-N-AS and SH-SY5Y Neuroblastoma cells and SVG p12 normal astrocytes was determined by western blot analysis (Fig. 4.2). Blots were probed for the presence of HuB protein with anti-HuB IgG. Anti-GAPDH IgG, was used to detect GAPDH as a loading control.

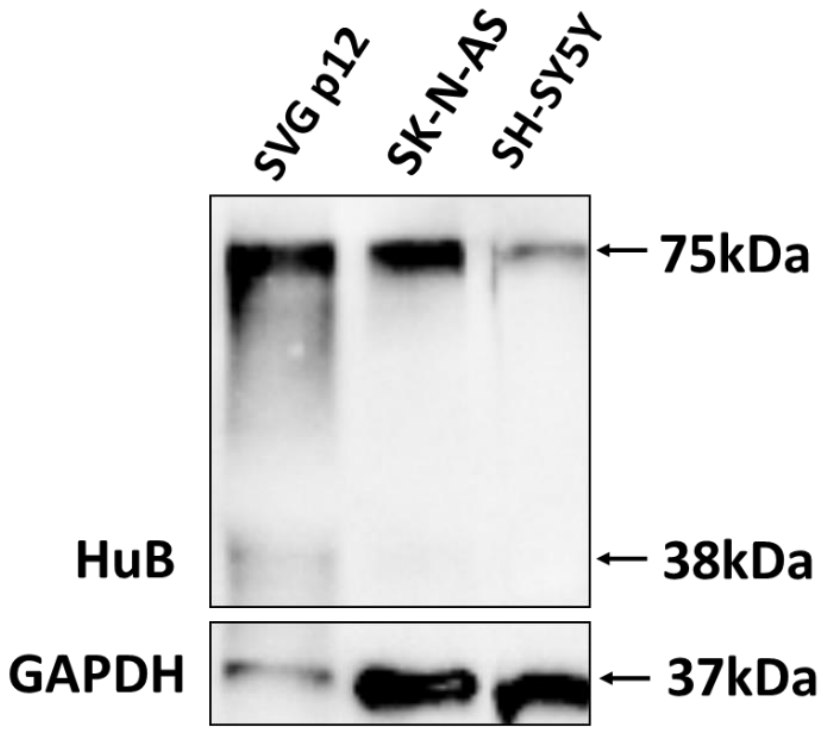

Figure 4.2: Representative western blot of HuB protein with anti-HuB antibody. HuB and GAPDH protein expression in normal astrocytes SVG p12, and Neuroblastoma cells SK-N-AS and SH-SY5Y. GAPDH protein expression was used as a loading control (n=3).

HuB protein was detected in the normal astrocytes, SVG p12 at the expected size of 38kDa. A higher migrating band was detected in all cell lines, SVG p12, SK-N-AS and SH-SY5Y at around 75kDa. Since this is about double the expected size of the HuB protein and the Hu family is

known to form dimers (Kasashima et al. 2002), this leads to the conclusion it is a result of dimerisation. GAPDH was detected at the expected size of 37kDa.

Western blot analysis showed that *HuB* gene is expressed in very high amounts in normal astrocytes in comparison to the Neuroblastoma cell lines. At a protein level, HuB is expressed more than GADPH protein expression. The western blot and RT-qPCR results suggest that HuB is translated very efficiently in the normal astrocytes cells, SVG p12 since there was very little HuB gene expression (Fig 4.1).

Of the two Neuroblastoma cell lines, *HuB* gene expression was highest in the SK-N-AS cells (Fig. 4.1) and this was also observed at the protein expression level (Fig. 4.2). HuB protein expression was comparable to GAPDH protein expression whilst in SH-SY5Y cells, HuB protein was less than the GAPDH expression.

Subcellular Hu protein localisation was determined for all Neuroblastoma and normal astrocytes cell lines using immunofluorescent staining (Section 2.4.1). To detect HuB protein, anti-HuB IgG was used with the secondary Alexa green 488 FITC IgG and counterstained with DAPI nucleus stain.

As seen in Fig. 4.3, HuB fluorescence is observed in all cell lines, SVG p12, SK-N-AS and SH-SY5Y. This aligns with the HuB protein detected during western blotting displayed in Fig. 4.2.

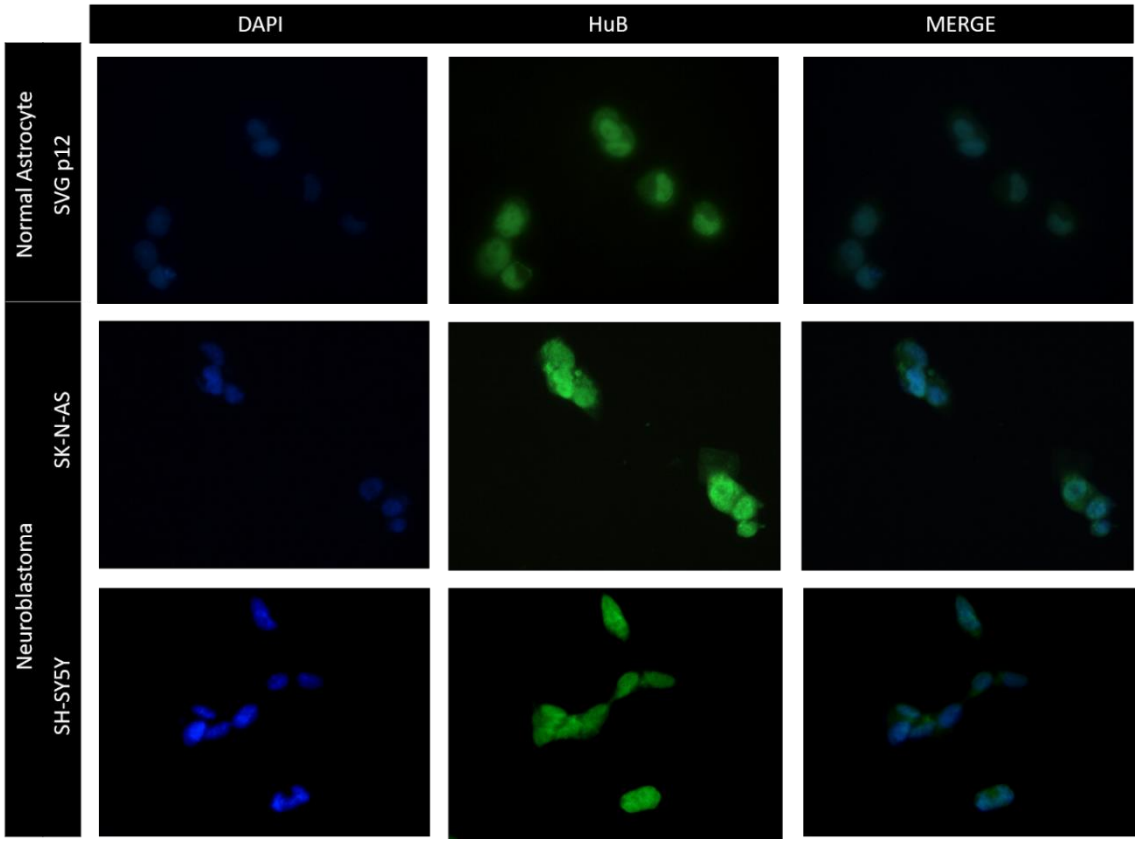

Figure 4.3: Example of cellular localisation of HuB protein in normal astrocytes SVG p12 and Neuroblastoma cells SK-N-AS and SH-SY5Y. The left column displays staining of nuclei with DAPI (blue), the middle column is stained with anti-HuB (green) and the right column displays a merged picture of DAPI and anti-HuB staining. Magnification x20. (n=3).

HuB protein expression was observed in both the nucleus and the cytoplasm of all cell lines. The strongest HuB protein fluorescence was observed in regions co-localised to the DAPI nuclei counterstain confirming HuB is predominantly nuclear.

4.2.2 HuC protein expression and localisation

HuC protein expression and localisation was determined through western blot analysis (Section 2.3) and anti-HuC immunofluorescence (Section 2.4.1).

Detection of HuC protein was carried out in each cell line derived from normal astrocytes and Neuroblastoma by western blot (Fig. 4.4). GAPDH was used as a control protein to compare protein expression to. Anti-HuC IgG detected HuC protein whilst anti-GAPDH IgG detected GAPDH, used as a loading control.

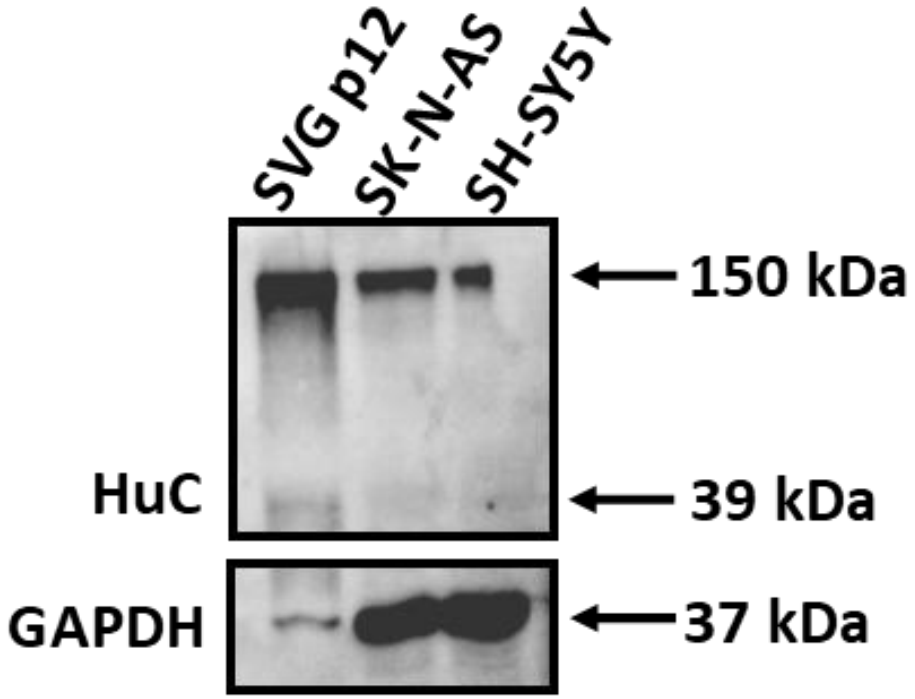

Figure 4.4: Representative western blot of HuC protein with anti-HuC antibody. HuC and GAPDH protein expression in normal astrocytes SVG p12, and Neuroblastoma cells SK-N-AS and SH-SY5Y. GAPDH protein expression was used as a loading control. (n=3).

Like HuB protein, HuC protein was detected in the normal astrocytes at its expected size of 39kDa and an additional migrating band was observed in all cell lines for normal astrocytes and Neuroblastoma at around 150kDa. As this is four times the expected band size, it is most likely due to HuC multimerisation. With this observation, Fig. 4.4 displays the astrocytes and

both Neuroblastoma cell line express HuC protein. GAPDH, used as a loading control was detected at 37kDa as expected for its molecular weight.

HuC expression at RNA level (Fig. 4.1) showed *HuC* gene is expressed in very low amounts in normal astrocytes in comparison to the Neuroblastoma cell lines, yet western blot analysis reveals HuC protein is expressed more than GADPH protein. The western blot results suggest that like HuB, HuC is very efficiently translated in normal astrocytes.

Immunofluorescent HuC protein labelling (Section 2.4.1) was performed to identify its subcellular localisation. Anti-HuC IgG was used with the secondary Alexa green 488 FITC IgG. Cells were counterstained with DAPI nucleus stain. The stains are shown in Figure 4.5.

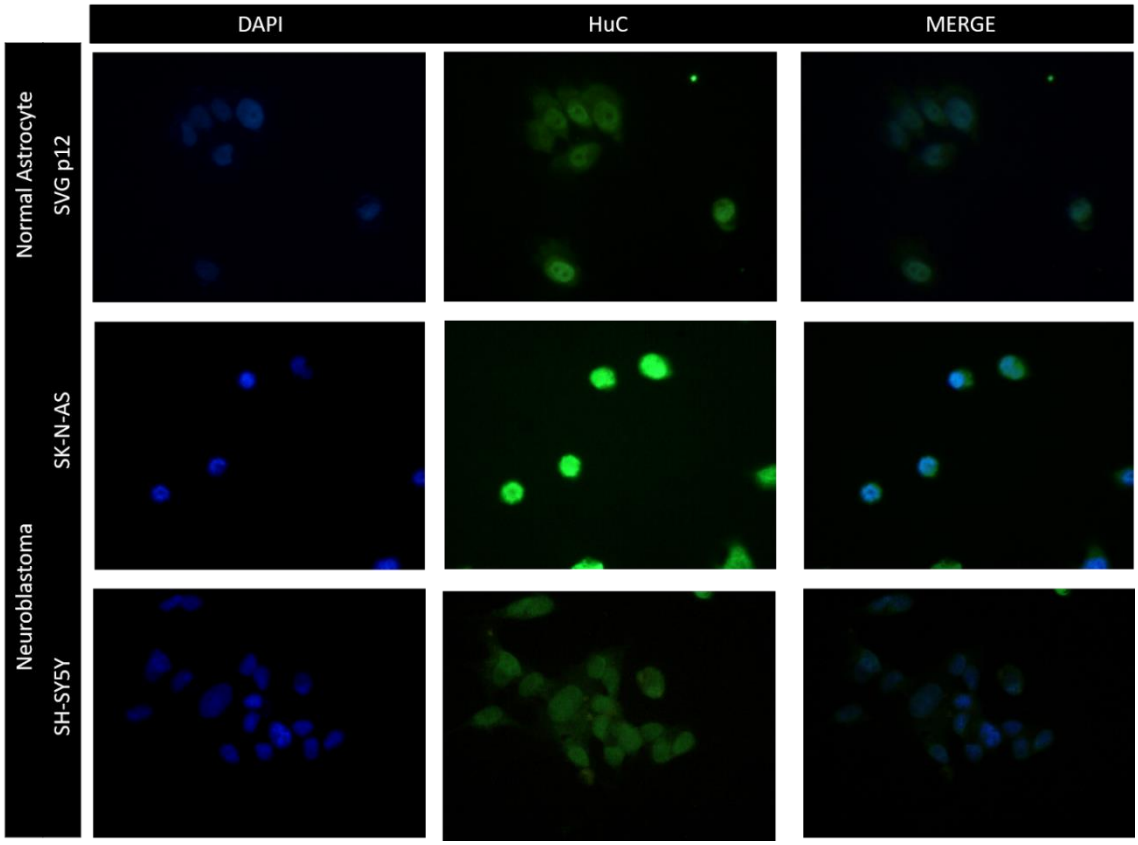

Figure 4.5: Example of cellular localisation of HuC protein in normal astrocytes SVG p12 and Neuroblastoma cells SK-N-AS and SH-SY5Y. The left column showed staining of nuclei with DAPI (blue), the middle column is stained with anti-HuC (green) and the right column displays a merged picture of DAPI and anti-HuC staining. Magnification x20. (n=3).

As seen in Fig. 4.5, HuC protein expression was observed in SVG p12, SK-N-AS and SH-SY5Y cell lines, confirming western blot data shown in Fig. 4.4. The strongest HuC protein fluorescence was observed in SVG p12 cell line which is co-localising with the DAPI nucleus stain indicating its localisation in the nucleus. A weaker staining was also observed in the cytoplasm. In the SH-SY5Y and SK-N-AS Neuroblastoma cell lines, HuC protein labelling was inconsistent with the DAPI nucleus stain concluding HuC was localised to the cytoplasm in the Neuroblastoma cells.

4.2.3 HuD protein expression and localisation

To confirm if the *HuD* gene expression is effectively translated to a protein, western blot (Section 2.3) was performed using anti-HuD to detect HuD protein in each cell line derived from normal astrocytes SVG p12 and Neuroblastoma cells SK-N-AS and SH-SY5Y.

As shown in Fig. 4.6, HuD protein was detected at its expected molecular weight of 42kDa in both Neuroblastoma cell lines SK-N-AS and SH-SY5Y. A distinct absence of HuD protein was observed in the normal astrocyte cell line SVG p12.

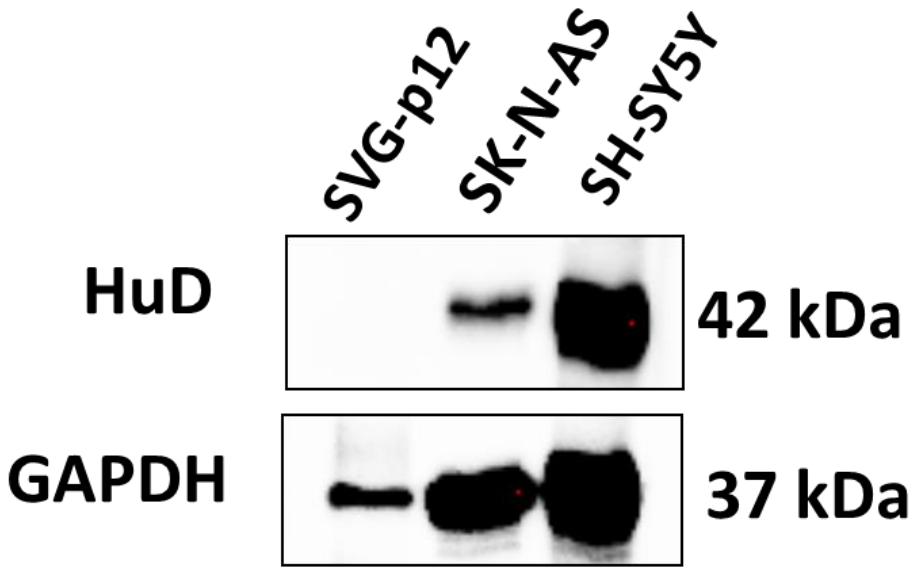

Figure 4.6: Representative western blot of HuD protein with anti-HuD antibody. HuD and GAPDH protein expression in normal astrocytes SVG p12, and Neuroblastoma cells SK-N-AS and SH-SY5Y. GAPDH protein expression was used as a loading control. (n=3).

HuD expression at RNA level displayed in in Fig. 4.1 showed more *HuD* gene expression in the SH-SY5Y cells followed by SK-N-AS cells with little or no expression of HuD in the normal astrocyte cell line SVG p12 strongly correlating the protein expression shown in Fig. 4.6.

GAPDH protein detection was used as a loading control and was detected at the expected size of 37kDa. HuD protein expression level in SH-SY5Y cells was comparable to that of the GAPDH protein expression. The HuD protein expression in the SK-N-AS Neuroblastoma cell line was less than the GAPDH protein expression.

The prominent expression of HuD protein was comparable to *HuD* gene expression and an indication of a relative translation rate of the upregulated *HuD* gene in Neuroblastoma.

To identify the subcellular localisation of HuD proteins in normal astrocytes and Neuroblastoma, immunofluorescence staining was performed as described in Section 2.4.1. Anti-HuD IgG was used with secondary Alexa 488 FITC IgG and counterstaining with DAPI was used for nuclear localisation. The immunofluorescent images are shown in Figure 4.7.

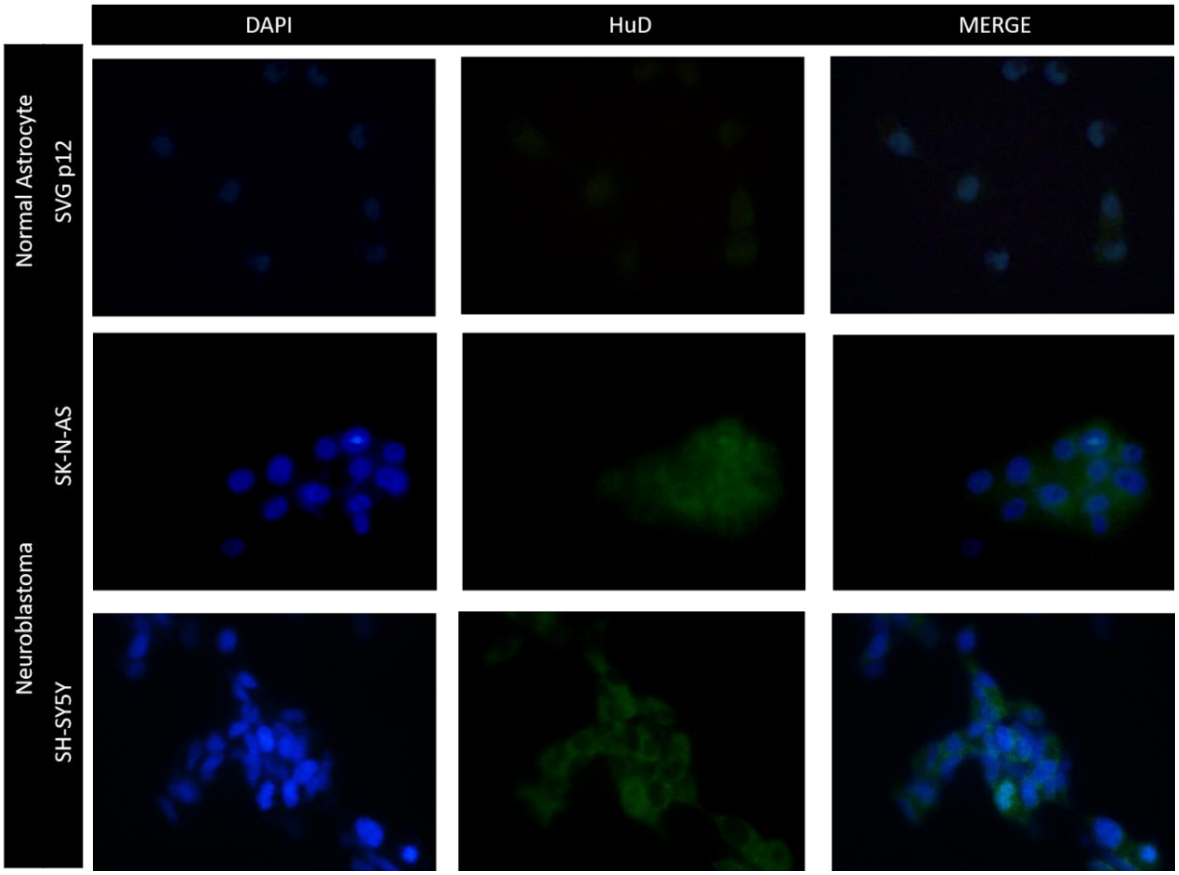

Figure 4.7: Example of cellular localisation of HuD protein in normal astrocytes SVG p12 and Neuroblastoma cells SK-N-AS and SH-SY5Y. The left column showed staining of nuclei with DAPI (blue), the middle column is stained with anti-HuD (green) and the right column displays a merged picture of DAPI and anti-HuD staining. Magnification x20. (n=3).

No HuD protein expression could be detected by immunostaining in SVG p12 normal astrocytes. Strong fluorescence was observed in both Neuroblastoma cell lines SK-N-AS and SH-SY5Y. These findings agree with western blot data of HuD protein expression (Fig. 4.6) and *HuD* gene expression profile (Fig. 4.1) in these cell lines.

HuD expression in both Neuroblastoma cell lines SK-N-AS and SH-SY5Y did not show a co-localisation with nuclear DAPI staining therefore argues a cytoplasmic localisation of HuD protein in these cells.

4.2.4 HuR protein expression and localisation

Finally, the protein expression level and cellular localisation of ubiquitously expressed HuR was analysed. Western blot was performed as described in section 2.3. Anti-HuR IgG and loading control anti-GAPDH IgG were used for detection of HuR and GAPDH proteins respectively. As seen in Fig. 4.8, HuR protein was detected at its expected size of 36kDa and the loading control, GAPDH was observed at 37kDa.

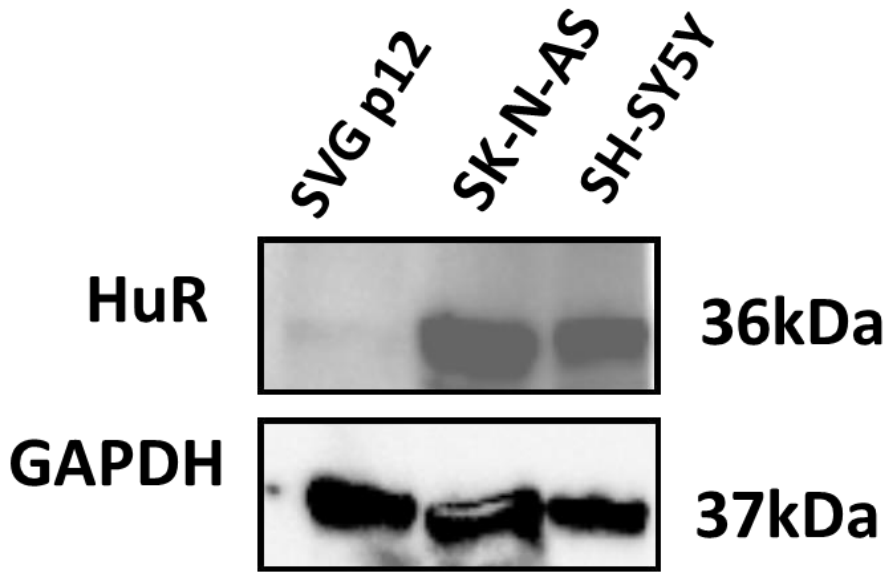

Figure 4.8: Representative western blot of HuR protein with anti-HuR antibody. HuR and GAPDH protein expression in normal astrocytes SVG p12, and Neuroblastoma cells SK-N-AS and SH-SY5Y. GAPDH protein expression was used as a loading control. (n=3).

HuR protein expression was faintly observed in the normal astrocyte cell line SVG p12. The gene expression profile in Fig. 4.1 displayed a large expression of *HuR* mRNA in the SVG p12 cell line. This shows that the *HuR* gene to protein translation is low and could be explained by

post-transcriptional modifications and post-translational regulatory events. HuR expression at RNA-level (Fig. 4.1) revealed *HuR* was upregulated in Neuroblastoma cells in comparison to the normal astrocyte. The highest expression was observed in the SH-SY5Y cells.

HuR protein was detected by western blot in both Neuroblastoma cell lines and was expressed slightly higher than the GAPDH control. SH-SY5Y cell line showed HuR expression higher than the control whilst SK-N-AS cells showed a higher expression.

To identify the location of the Hu RNA-binding proteins in all the analysed cell lines, immunofluorescent staining (Section 2.4.1) was performed (Fig. 4.9). Anti-HuR IgG was used with the secondary Alexa 488 FITC IgG and the counterstain DAPI for nuclear localisation.

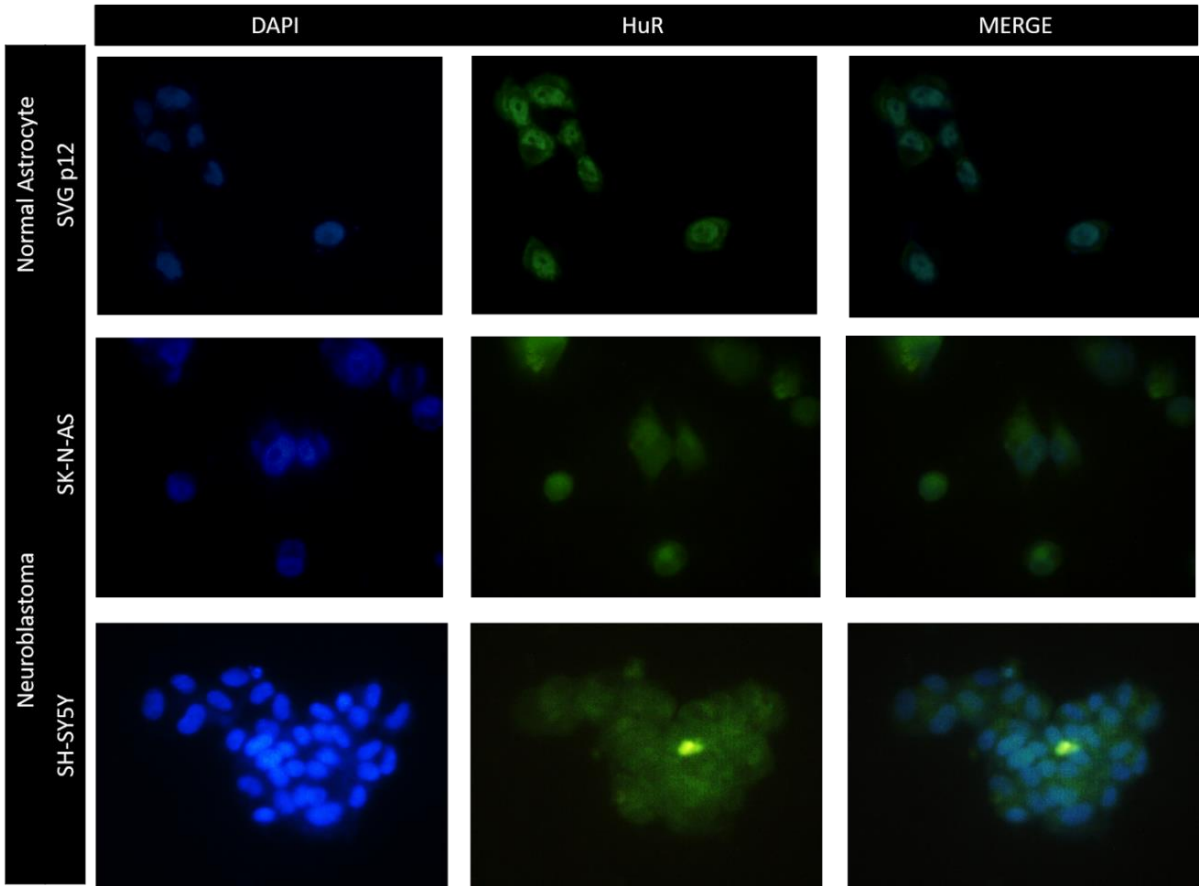

Figure 4.9: Example of cellular localisation of HuR protein in normal astrocytes SVG p12 and Neuroblastoma cells SK-N-AS and SH-SY5Y. The left column showed staining of nuclei with DAPI (blue), the middle column with anti-HuR (green) and the right column displays a merged picture of DAPI and anti-HuR. Magnification x20. (n=3).

Displayed in Fig. 4.9, HuR protein expression is observed in normal astrocytes SVG p12 and Neuroblastoma cells SK-N-AS and SH-SY5Y. In SVG p12 cells, strong nucleus staining of HuR protein was observed with a weaker staining in the cytoplasm. In SK-N-AS cells, HuR protein was only localised to the nucleus whilst in the second Neuroblastoma cell line SH-SY5Y, HuR expression was predominantly observed in the cytoplasm.

4.3 Establishing *Hu* gene knockdowns using siRNA interference in Neuroblastoma cells

To gain an insight into the molecular role of Hu protein expression and its contribution to a cancerous phenotype, siRNA interference was established to downregulate *Hu* gene expression in the Neuroblastoma cell lines, SK-N-AS and SH-SY5Y. Each cell line was tested for the most efficient transfection by trialling different transfection reagents, concentration of siRNAs and different time periods. Following RT-qPCR, all samples were analysed using the $2^{-\Delta\Delta CT}$ method.

4.3.1 *Hu* gene knockdown in SH-SY5Y Neuroblastoma cells

For each individual *Hu* gene in the SH-SY5Y Neuroblastoma cell line, a knockdown was established through transfection with ON-TARGETplus SMARTpool small-interfering RNA (siRNA). These commercially available siRNAs were purchased to interfere with the genes *HuB*, *HuC*, *HuD*, *HuR*, *GAPDH* and a non-targeting siRNA. Each siRNA contained a pool of four interfering sequences listed in Table 2.4.

The optimum transfection in SH-SY5Y Neuroblastoma cells was achieved using DharmaFECT I transfection reagent over 48 hours for which the protocol is provided in Section 2.7.3.

RT-qPCR was performed to confirm *Hu* gene knockdowns. The cycling and reactions of RT-qPCR are described in Section 2.26. HuB (1), HuC (1), HuD (6), HuR (2) and β-Actin primer sequences are listed in Table 2.3 of Section 2.27. The fold-change of expression was analysed by comparing expression levels to the control non-targeting siRNA. *β-Actin* was the housekeeping gene to which the data was normalised. Statistical significance was calculated by a two-tailed t-test.

Figure 4.10 displays the mRNA-transcript levels that were determined by RT-qPCR 48-hours post-transfection with DharmaFECT I.

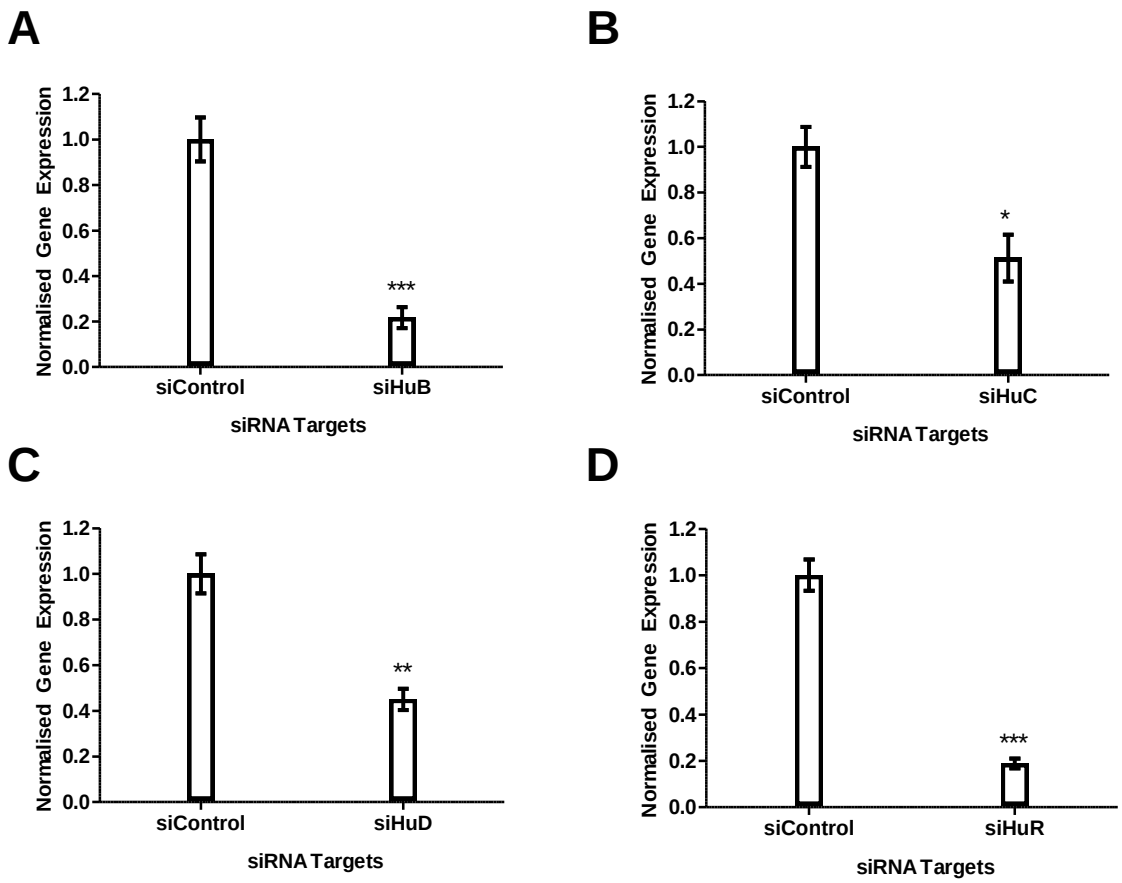

Figure 4.10: Knockdown efficiency of *Hu* genes after individual *Hu* siRNA interference in the Neuroblastoma cell line SH-SY5Y. *HuB* (A), *HuC* (B), *HuD* (C) and *HuR* (D) gene expression following *Hu* gene knockdowns was analysed by RT-qPCR in the Neuroblastoma cell line, SH-SY5Y. The $2^{-\Delta\Delta Ct}$ results shown are an average of three replicates normalised to *β-Actin* gene expression and compared with the control set at 1.00. Error bars display ± SEM. Statistical significance was calculated by a two-tailed t-test and is displayed by *P ≤ 0.05, **P ≤ 0.01, ***P ≤ 0.001. (n=3).

In the Neuroblastoma cell line, SH-SY5Y, the knockdown decreased 4.7-fold for *HuB*, 2.0-fold for *HuC*, 2.2-fold for *HuD* and 5.5-fold for *HuR*.

To observe the effects of a combined *Hu* gene family knockdown in Neuroblastoma, SH-SY5Y cells were transfected with all *Hu* gene siRNAs in a single attempt using the same methods described above. The results of this combined knockdown are shown in Fig. 4.11.

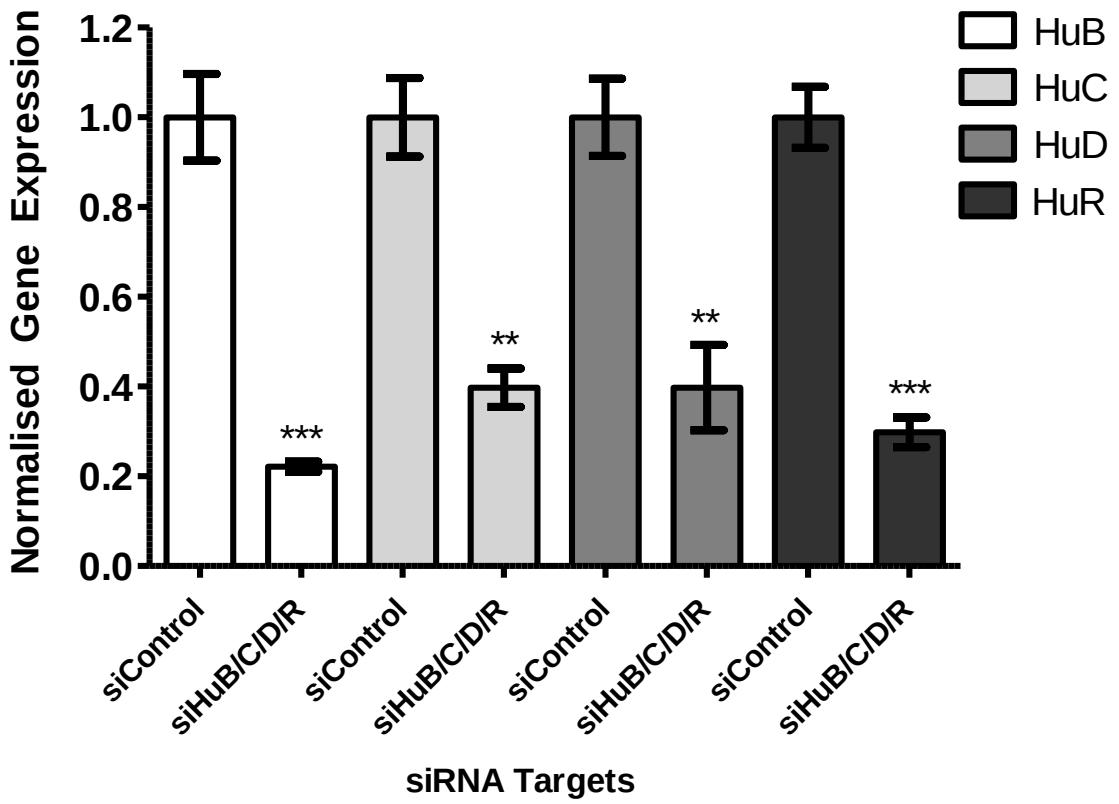

Figure 4.11: Combined siRNA interference of all *Hu* genes in the Neuroblastoma cell line SH-SY5Y. *HuB*, *HuC*, *HuD* and *HuR* gene expression following a full knockdown of each *Hu* gene in a single attempt in the SH-SY5Y Neuroblastoma cells. Samples were analysed by RT-qPCR. The $2^{-\Delta\Delta Ct}$ results shown are an average of three replicates normalised to *β-Actin* gene expression and compared with the control set at 1.00. Error bars display ± SEM. Statistical significance was calculated by a two-tailed t-test and is displayed by *P ≤ 0.05, **P ≤ 0.01, ***P ≤ 0.001. (n=3).

A combined knockdown of all four *HuB*, *HuC*, *HuD* and *HuR* genes was successful. The gene expression profile showed the mRNA expression of each *Hu* gene in the control non-targeting siRNA sample and its reduced expression in the combined siRNA transfection attempt.

When comparing the knockdown of each *Hu* gene individually and in combination, the combined knockdown increased the knockdown efficiency of *HuC* and *HuD* gene when compared to single siRNA knockdown attempts.

Single *HuB* gene knockdown and combined *Hu* gene family knockdown achieved a 4.76- fold decrease and 4.54-fold decrease in *HuB* gene expression respectively showing little difference.

Interestingly, *HuC* knockdown efficiency increased by 0.5-fold from a 2.0-fold decrease following single *HuC* knockdown to a 2.5-fold *HuC* gene decrease in combined *Hu* gene family knockdown. *HuD* efficiency increased by 0.3-fold from a 2.2-fold *HuD* gene reduction in single *HuD* gene knockdown to 2.5-fold following combined *Hu* gene family knockdown. Surprisingly, *HuR* gene expression revealed a decrease in knockdown efficiency of 1.9-fold from a 5.3-fold decrease by single *HuR* knockdown to a 3.4-fold decrease following combined *Hu* family knockdown attempts.

Since the knockdown amounts differ between single knockdowns and combined knockdown, this suggests an external factor may influence *Hu* gene expression when other Hu members expression is compromised.

4.3.2 *Hu* gene knockdown in SK-N-AS Neuroblastoma cells

Hu gene knockdown was achieved in the SK-N-AS Neuroblastoma cell line using jetPRIME transfection reagent over 48 hours described in Section 2.7.2. ON-TARGETplus SMARTpool siRNAs targeted the *HuB*, *HuC*, *HuD*, *HuR*, *GAPDH* genes and a non-targeting siRNA was used as a control.

RT-qPCR was performed to confirm *Hu* gene knockdown with the primers HuB (1), HuC (1), HuD (6), HuR (2) and β-Actin (Sequences listed in Table 2.3 of Section 2.27). The fold-change of expression was analysed by comparing expression levels to the control non-targeting siRNA transfection. *β-Actin* was the housekeeping gene to which the data was normalised. Statistical significance was calculated by a two-tailed t-test.

Displayed in Fig. 4.12, gene expression was analysed by RT-qPCR 48-hours post-transfection and showed the knockdown efficiency was 2.0-fold for *HuB*, 2.6-fold for HuC, 2.2-fold for *HuD* and 18.6-fold for *HuR*.

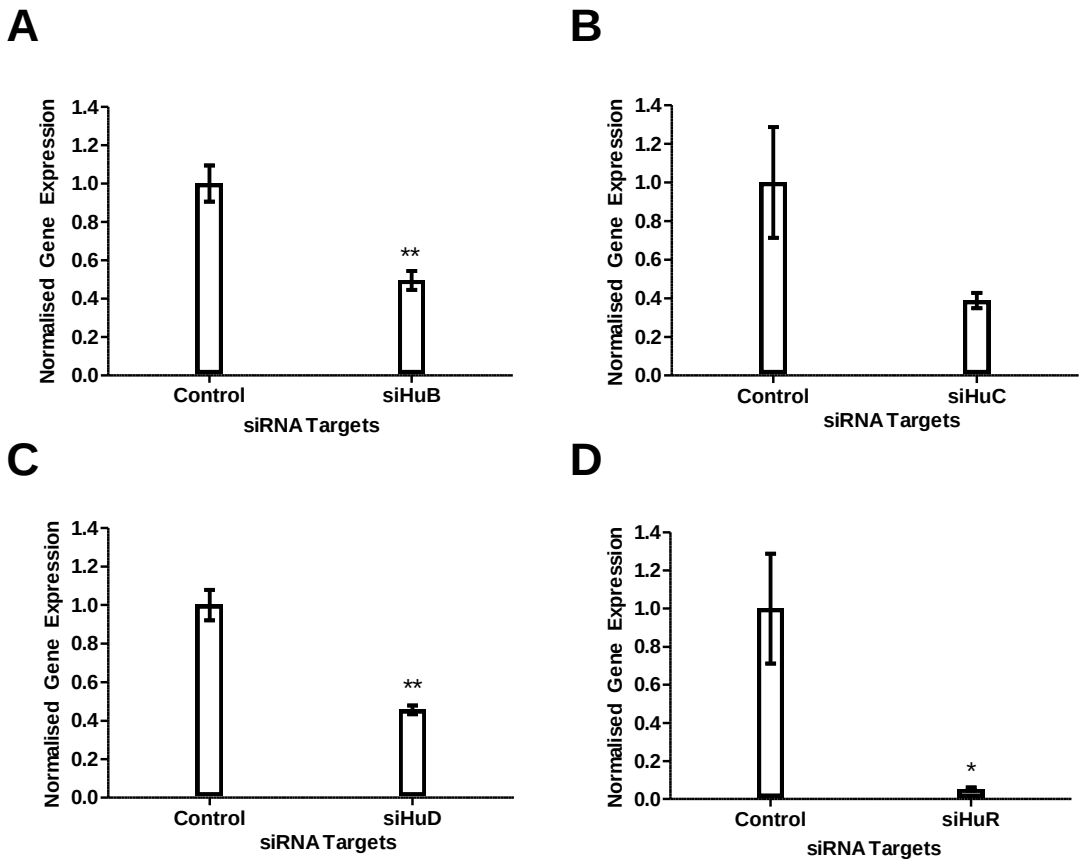

Figure 4.12: *Hu* gene expression levels in the Neuroblastoma cell line SK-N-AS following individual *Hu* RNA interference. *HuB* (A), *HuC* (B), *HuD* (C) and *HuR* (D) gene expression was analysed by RT-qPCR

in SK-N-AS Neuroblastoma cells. The $2^{-\Delta\Delta Ct}$ results shown are an average of three replicates normalised to *β-Actin* gene expression and compared with the non-targeting control set at 1.00. Error bars display ± SEM. Statistical significance was calculated by a two-tailed t-test and is displayed by *P ≤ 0.05, **P ≤ 0.01, ***P ≤ 0.001. (n=3).

Overall, the knockdown efficiency in SK-N-AS cells compared to SH-SY5Y cells was lower, however *HuB*, *HuD* and *HuR* gene reductions were still statistically significant.

A combined knockdown of each *Hu* gene family member was established using siRNAs for each *Hu* gene in a combined attempt. The results as analysed by RT-qPCR are shown in Fig. 4.13.

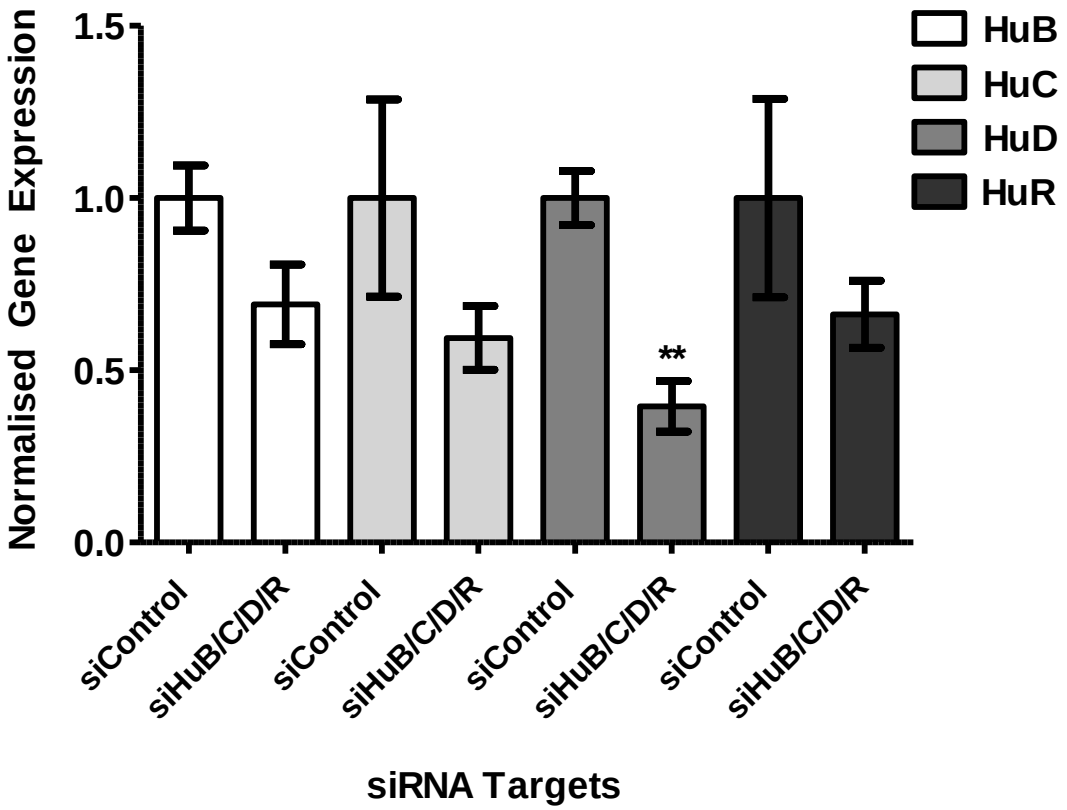

Figure 4.13: Combined siRNA interference of all *Hu* genes in the Neuroblastoma cell line SK-N-AS. *HuB*, *HuC*, *HuD* and *HuR* gene expression following a single knockdown in the SK-N-AS Neuroblastoma

cells. Samples were analysed by RT-qPCR. The $2^{-\Delta\Delta Ct}$ results shown are an average of three replicates normalised to *β-Actin* gene expression and compared with the non-targeting control set at 1.00. Error bars display ± SEM. Statistical significance was calculated by a two-tailed t-test and is displayed by *P ≤ 0.05, **P ≤ 0.01, ***P ≤ 0.001. (n=3).

The combined knockdown off all *Hu* genes in SK-N-AS resulted in a 1.4-fold reduction of a *HuB* expression, a 1.7-fold reduction in *HuC* expression, a 2.5-fold reduction in *HuD* expression and a 1.5-fold reduction in *HuR* expression however only the reduction in *HuD* was statistically significant.

When all *Hu* genes were knocked down, the mRNA expression of *HuB*, *HuC* and *HuR* showed a smaller reduction compared to individual knockdowns.

HuB transfection decreased by 0.6-fold from a 2.0-fold decrease achieved during single knockdown to a 1.4-fold decrease during combined *Hu* knockdown. *HuC* expression decreased from 2.6-fold during single *HuC* knockdown to a 1.7-fold decrease following transfection with all *Hu* siRNAs, a difference of 0.9-fold. *HuR* transfection decreased by 17.1-fold from an 18.6-fold decrease with single HuR knockdown to a 1.5-fold decrease with combined *Hu* family knockdown. *HuD* transfection increased slightly by 0.3-fold from a 2.2-fold decrease during single knockdown to a 2.5-fold decrease when all *Hu* genes were knocked down.

4.3.3 *Hu* gene knockdowns confirmed at a protein level

To confirm the *Hu* genes knockdowns and the impact at protein-level, protein expression levels were analysed by western blot analysis (Section 2.3). Cellular target protein levels may

remain in the cell following gene expression knockdown, dependent upon protein half-life. Protein expression was therefore analysed 96-hours post-transfection.

Each *Hu* gene knockdown both individually and in combination in each Neuroblastoma cell line SK-N-AS and SH-SY5Y was blotted and stained for Hu proteins. The primary antibodies anti-HuB IgG, anti-HuC IgG, anti-HuD IgG, anti-HuR IgG and anti-GAPDH IgG were used along with Horse-radish peroxidase (HRP)-conjugated secondary antibodies. GAPDH was used as a control protein to normalise expression.

SH-SY5Y Neuroblastoma cells with siRNAs targeting *HuB*, *HuC* and *HuR* individually and in combination were probed for the target proteins. The results are displayed in Figure 4.14. *Hu* family siRNA interference show varied results at protein level.

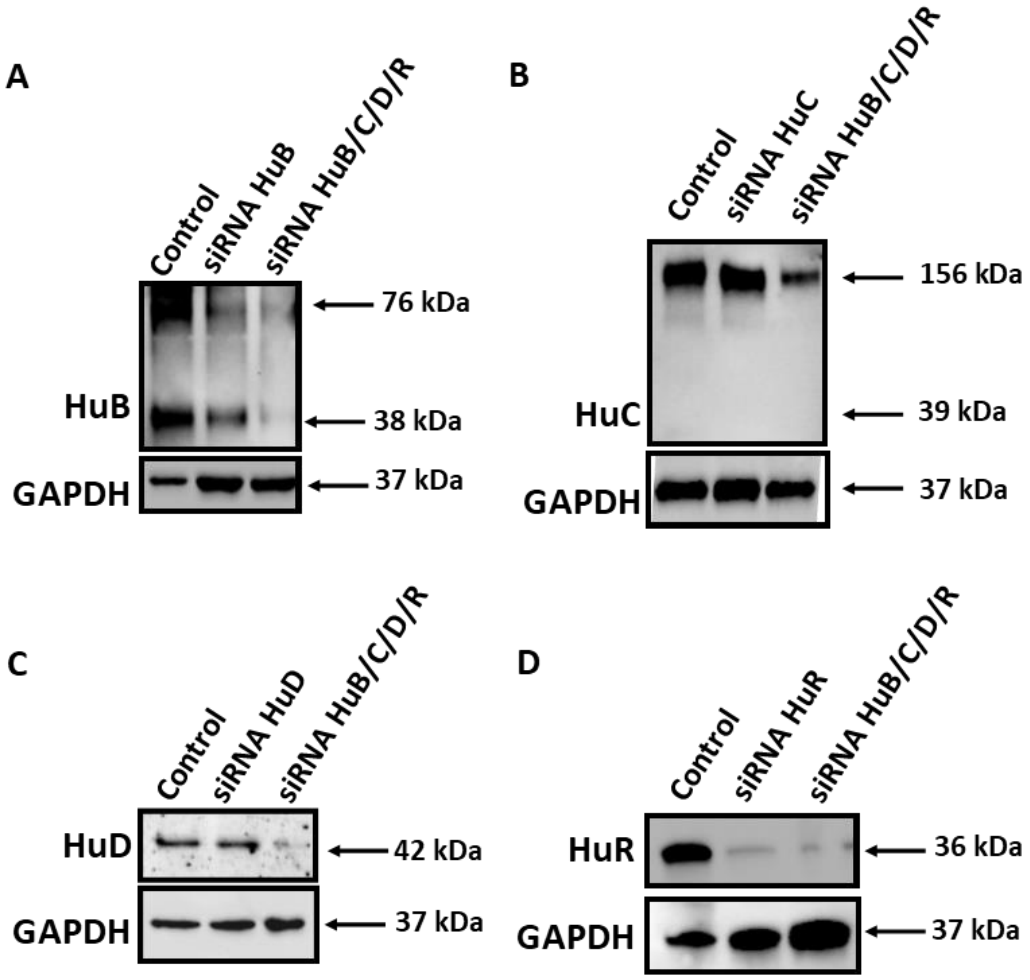

Figure 4.14: Hu protein expression during single and combined *Hu* knockdowns in SH-SY5Y Neuroblastoma cells. A) HuB protein expression following single *HuB* and combined *Hu* family knockdown. B) HuC protein reduction following single *HuC* and combined *Hu* knockdown. C) HuD protein partial reduction following single *HuD* and combined *Hu* knockdown. D) HuR protein knockdown following single *HuR* and combined *Hu* family knockdown. GAPDH protein expression was used as a loading control.

As previously described in Section 4.2.1, HuB protein was detected as a dimer (Fig. 4.2) and that is also observed here. The HuB protein both in monomer and dimer complex show a 50% depletion following individual *HuB* knockdown and a 90% knockdown following combined *Hu* family knockdown (Fig. 4.14A). The same effect is seen for HuD protein expression that was detected at 42kDa (Fig. 4.14C).

The previously described HuC multimer at 156kDa (Fig. 4.4) shows little change following the single *HuC* gene knockdown and a 50% reduction following the combined *Hu* knockdown. *HuR* individual knockdown was effective in knocking down HuR protein which was detected at 36kDa in the non-targeting control sample. These protein results correlate with *Hu* gene expression data following gene knockdowns displayed in Fig. 4.10 and Fig. 4.11.

Figure 4.15 displays Hu protein knockdown confirmation following siRNA interference.

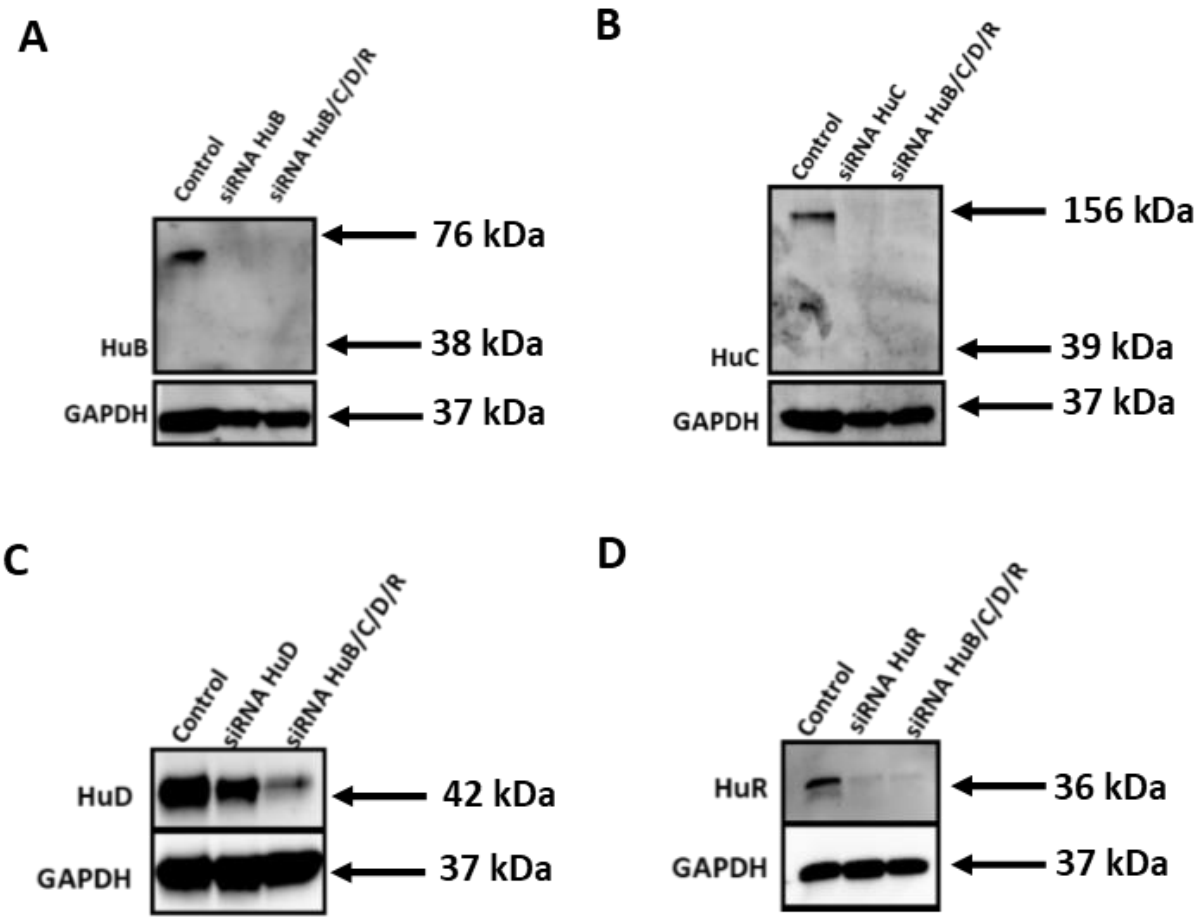

Figure 4.15: Hu protein expression during single and combined *Hu* knockdowns in SK-N-AS Neuroblastoma cells. A) HuB protein expression following single *HuB* and combined *Hu* family knockdown. B) HuC protein reduction following single *HuC* and combined *Hu* knockdown. C) HuD protein partial reduction following single *HuD* and combined *Hu* knockdown. D) HuR protein knockdown following single *HuR* and combined *Hu* family knockdown. GAPDH protein expression was used as a loading control.

As previously described in Section 4.2.1, HuB protein was detected as a dimer (Fig. 4.2) and that is also observed here. The HuB dimer at 75kDa is present in the control non-targeting siRNA interference sample yet absent in the single and combined siRNA transfections. Additionally, the HuC multimer at 156kDa (Fig. 4.4) first observed in Section 4.2.2 is present in the control but absent in the single and combined Hu knockdown. *HuR* individual knockdown was enough to knockdown HuR protein which was detected at 36kDa in the non-targeting control sample. All these results of full protein knockdowns are despite a lower knockdown efficiency observed in the combined gene knockdowns displayed in Fig. 4.13.

A 50% reduction of HuD protein (42kDa) was observed through single *HuD* siRNA interference. In the combined *Hu* siRNA interference, HuD protein expression decreased by 90% when compared to HuD control and comparable GAPDH expression in all samples.

At protein level, in *HuD* single and combined knockdown attempts there was a difference in Hu proteins expression when individual Hu knockdown efficiency was compared to the combined knockdown. This may be due to complex interplay between the Hu family members in that they are able to influence expression or translational efficiency by targeting their own or family members sequences and up-regulating their expression although further studies look to confirm this hypothesis below in Section 4.4.

4.4 Differential gene expression of Hu proteins following individual and combined *Hu* gene knockdowns

Due to the described differences in gene and protein expression following single and combined knockdowns and the known ability of HuR to -regulate its own expression, a gene expression profile was established to explore the possibility of a regulatory mechanism within

the Hu family of RNA-binding proteins. The level of all *Hu* genes individual expression following individual *Hu* gene knockdowns was analysed.

4.4.1 *Hu* gene expression profiling in SH-SY5Y Neuroblastoma cells

RT-qPCR (Section 2.26) was performed to confirm *Hu* gene knockdowns and to determine any changes to the expression levels of other *Hu* genes. The primers HuB (1), HuC (1), HuD (6), HuR (2) and β-Actin were used. *β-Actin* was the housekeeping gene to which the data was normalised and compared to the non-target control. Statistical significance was calculated by a two-tailed t-test.

Figure 4.16 displays the effect on other Hu genes expression level following individual Hu knockdown. Here, the original knockdown levels are those initially described in Fig. 4.10.

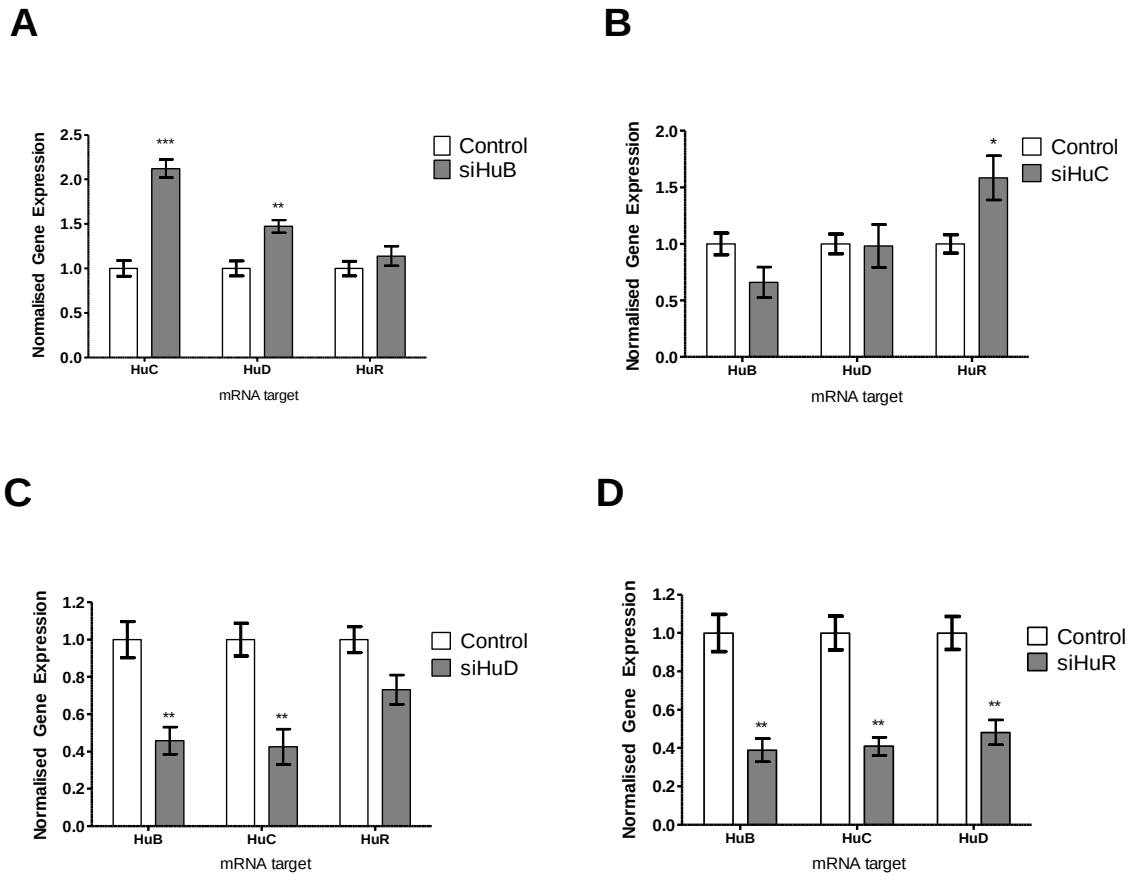

Figure 4.16: Influence of individual *Hu* gene knockdowns on other *Hu* family members gene expression in SH-SY5Y Neuroblastoma cells. A) *HuB* Knockdown B) *HuC* Knockdown C) *HuD* Knockdown D) *HuR* Knockdown. The $2^{-2\text{-}\Delta\Delta Ct}$ results shown are an average of three replicates normalised to *β-Actin* gene expression and compared with the non-target control. Error bars display ± SEM. Statistical significance was calculated by a two-tailed t-test and is displayed by *P ≤ 0.05, **P ≤ 0.01, ***P ≤ 0.001. (n=3).

In Fig. 4.16A, a 4.6-fold knockdown of *HuB* gene expression resulted in a significant increase of *HuC* and *HuD* by 1.1-fold and 0.5-fold respectively. No significant change was observed for *HuR* gene expression.

A 2-fold interference of *HuC* expression also showed a significant 0.6-fold increase in *HuR* expression. No significant change was observed for *HuB* and *HuD* gene expression following *HuC* knockdown.

Interestingly, a 2.2-fold decrease of *HuD* gene expression showed an opposite effect to *HuB* and *HuC* siRNA knockdown and a significant decrease in gene expression of *HuB* and *HuC* was observed. *HuB* gene expression decreased by 2.18-fold, whilst *HuC* gene expression decreased by 2.3-fold. No significant change was observed for *HuR* gene expression.

HuR knockdown significantly decreased the expression of the other three family members. A 5.3-fold reduction of *HuR* gene expression resulted in *HuB* gene expression decrease of 2.6-fold, *HuC* gene expression decrease of 2.4-fold and *HuD* gene expression decrease of 2.1-fold.

To provide a clearer visual representation, highlight key characteristics and gain a better understanding of the effect of each *Hu* gene knockdown, a full expression profile was established. This data shown is Figure 4.17 is a combination of that shown in Fig. 4.10, Fig. 4.11 and Fig. 4.16. The data is normalised to the same non-target controls of the siRNA interference transfection.

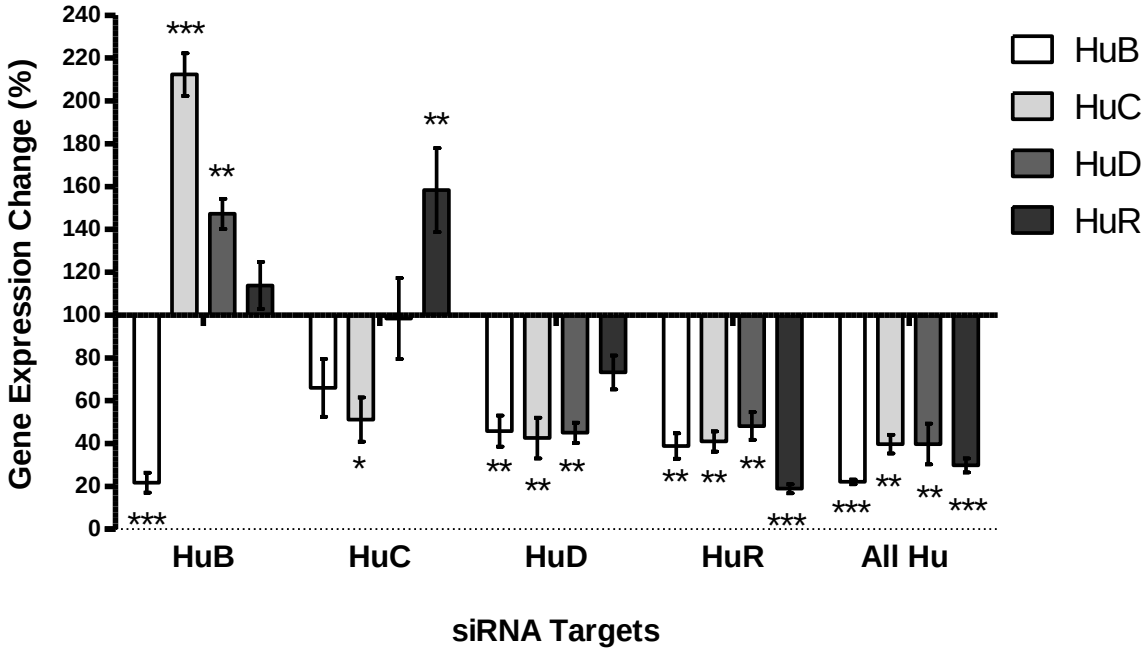

Figure 4.17: The complete profile of *Hu* gene expression in Neuroblastoma cell line SH-SY5Y, after knockdown of each individual Hu protein individually and combined. *HuB*, *HuC*, *HuD* and *HuR* expression following knockdown of each *Hu* gene both individually and in combination was analysed by RT-qPCR in SH-SY5Y cells. The $2^{-\Delta\Delta Ct}$ results shown are an average of three replicates normalised to *β-Actin* gene expression and compared with the non-targeting control. Error bars display ± SEM. Statistical significance was calculated by a two-tailed t-test and is displayed by *P ≤ 0.05, **P ≤ 0.01, ***P ≤ 0.001. (n=3).

The effect of the individual and combined knockdowns on *Hu* gene expression is shown in displayed in Fig. 4.17. Here it is clear that generally, *HuB* knockdown results in an increase of the other *Hu* family members. *HuC* knockdown decreases the expression of *HuB* and increases the expression of *HuR*. Similarities are highlighted between *HuD*, *HuR* and combined *Hu* knockdown in that all other Hu family members are also decreased upon their reduced expression. This suggests HuD and HuR may be major players in the reduction of *Hu* genes and therefore also responsible for the results observed in the combined *Hu* knockdown.

The overall knockdown profile is summarised as percentages in a heatmap is displayed in Fig. 4.18.

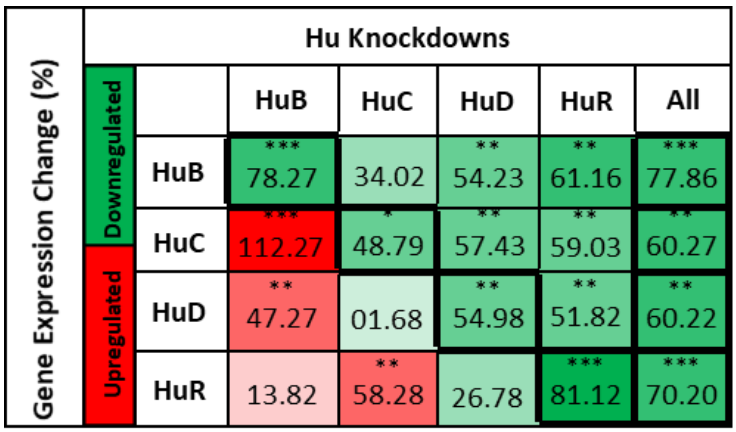

Figure 4.18: Heatmap summarising *Hu* gene expression change after single and combined knockdown experiments in SH-SY5Y Neuroblastoma cells. Colour intensity proportional to the amount. Statistical significance was calculated by a two-tailed t-test and is displayed by *P ≤ 0.05, **P ≤ 0.01, ***P ≤ 0.001. (n=3).

In summary, a similar *Hu* gene expression profile is observed when all *Hu* genes are knocked down in combination, with that of HuD and HuR knockdowns. Upregulation of *Hu* gene family members only occurs during HuB and HuC knockdowns.

The changes in expression levels of the different *Hu* family members following knockdown of single *Hu* genes could be explained in three ways. A compensatory effect through which other *Hu* genes become more expressed to compensate for the reduced expression of a different Hu family member. A second interpretation is a regulatory effect whereby Hu family members actively target each other's transcripts affecting its stability and ultimately controlling its expression. A third idea is that there may be off-target effects of the *Hu* gene downregulation. This is explained by different mRNA targets that *Hu* genes normally regulate form part of a

pathway that upon *Hu* gene knockdown, a series of downstream effects result in other *Hu* gene family members subsequent upregulation or downregulation.

The model in Fig. 4.19 displays how different Hu family members can regulate each other's expression in the Neuroblastoma cell-line SH-SY5Y.

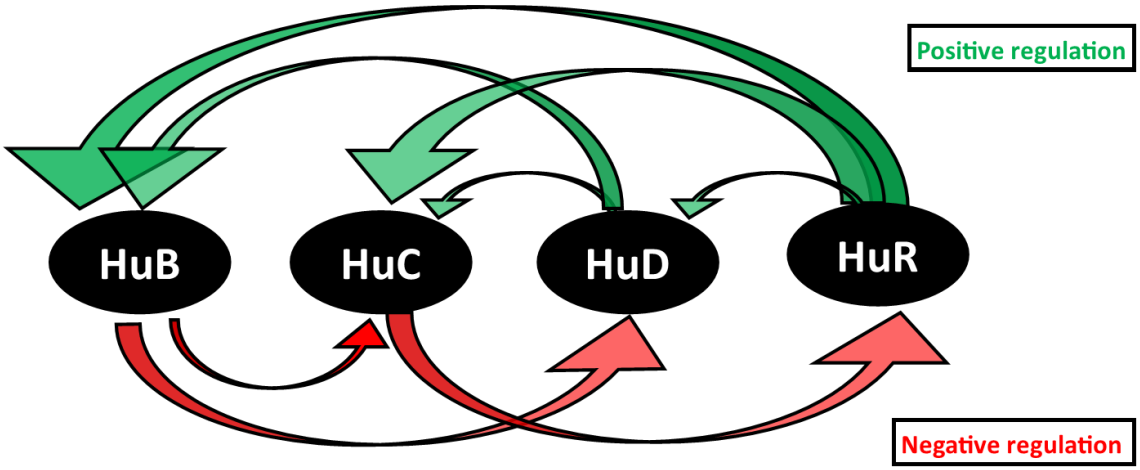

Figure 4.19: A model representing the regulation of the Hu protein family in the Neuroblastoma cell-line SH-SY5Y. Colour intensity proportional to the change in regulation.

The model in Fig. 4.19 is based only on significant changes in gene expression determined by a two-tailed T-test. This data indicates that *HuB* knockdown increased the gene expression of *HuC* and *HuD*. *HuC* knockdown increased the gene expression of HuR. Whilst individual *HuD* knockdown decreased *HuB* and *HuC* gene expression and *HuR* knockdown significantly decreased the gene expression of all the other Hu family members.

Based on the three theories described above of compensatory expression, regulatory influences within the Hu family or off-target effects, there are several conclusions that can be drawn in the SH-SY5Y Neuroblastoma cell model.

4.4.2 *Hu* gene expression profiling in SK-N-AS Neuroblastoma cells

For the second Neuroblastoma cell line SK-N-AS, a RT-qPCR expression profile (Section 2.2.6) was established to identify the general expression of *Hu* genes and any regulatory influences between the family members. RT-qPCR was performed to confirm *Hu* gene knockdowns and changes in the gene expression of other *Hu* family members (Fig. 4.20) using the primers HuB (1), HuC (1), HuD (6), HuR (2) and β-Actin. *β-Actin* was the housekeeping gene to which the data was normalised. Statistical significance was calculated by a two-tailed t-test.

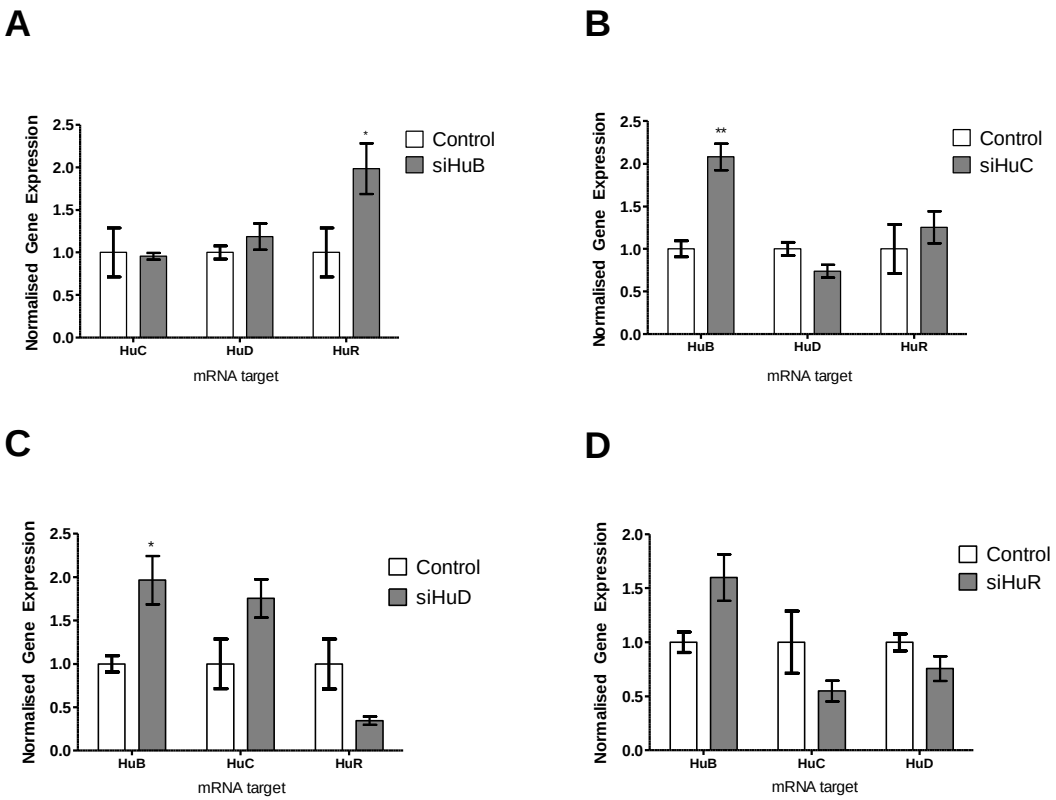

Figure 4.20: Influence of individual *Hu* gene knockdowns on other *Hu* gene family members expression levels in SK-N-AS, Neuroblastoma cells A) *HuB* Knockdown B) *HuC* Knockdown. C) *HuD* Knockdown. D) *HuR* Knockdown. The $2^{-2\text{-}\Delta\Delta Ct}$ results shown are an average of three replicates normalised to *β-Actin* gene expression and compared with the control. Error bars display ± SEM. Statistical significance was calculated by a two-tailed t-test and is displayed by *P ≤ 0.05, **P ≤ 0.01, ***P ≤ 0.001. (n=3).

The amount of gene expression change was calculated and normalised to the non-target siRNA control. A *HuB* knockdown of 2.0-fold resulted in a 1.0-fold increase in *HuR* gene expression (Fig. 4.20A). No significant change was observed in *HuC* and *HuD* gene expression.

HuC siRNA decreased *HuC* gene expression by 2.57-fold. As seen in Fig. 4.20B, this reduction in *HuC* gene expression resulted in a 1.1-fold increase of *HuB* gene expression. No significant change was observed for *HuD* and *HuR* gene expression levels.

A *HuD* knockdown of 2.2-fold resulted in a 1.0-fold increase in *HuB* gene expression. No statistical change was observed for *HuC* and *HuR* gene expression.

siRNA transfection of *HuR* resulted in a decrease of *HuR* gene expression by 18.6 fold. As seen in Fig. 4.20D, this gene knockdown did not result in any significant change to the other Hu family members expression.

To provide a clearer visual representation, highlight key characteristics and gain a better understanding of the effect of each *Hu* gene knockdown, a full expression profile was established. Fig. 4.24 is a summary of the results presented in Fig. 4.12, Fig. 4.13 and Fig. 4.20. The data is normalised to the same non-target siRNA controls of the transfection.

A complete *Hu* gene expression profile in SK-N-AS Neuroblastoma cells following individual and combined *Hu* siRNA knockdowns is displayed in Fig. 4.21.

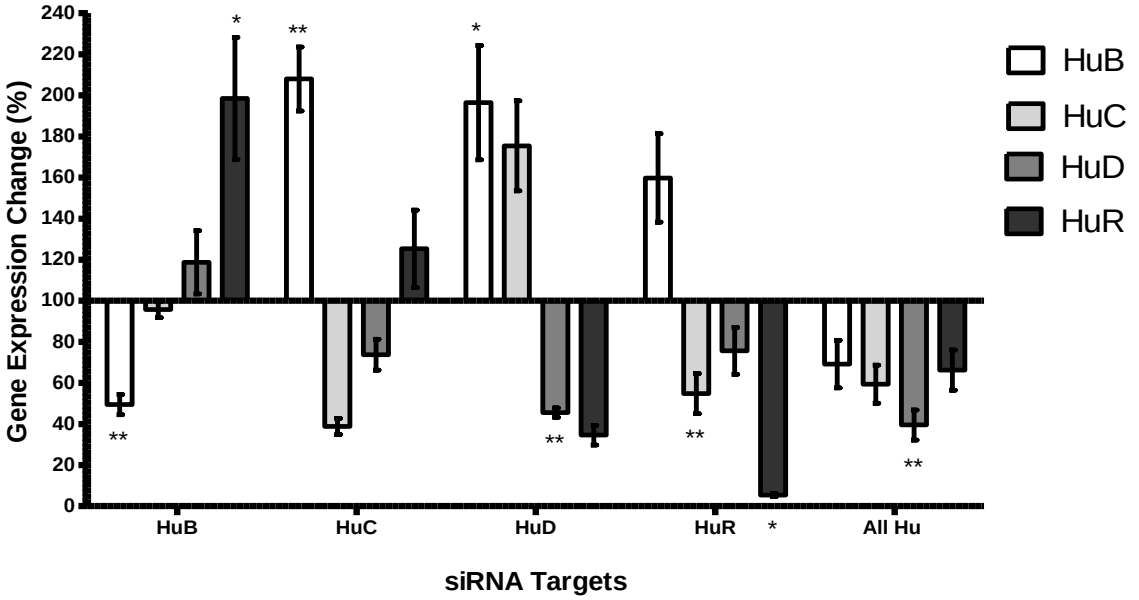

Figure 4.21: The complete profile of *Hu* gene expression in Neuroblastoma cell line SK-N-AS, after knockdown of each individual Hu protein individually and combined. *HuB*, *HuC*, *HuD* and *HuR* expression knockdown of each *Hu* gene individually and following combined knockdown was analysed by RT-qPCR in SK-N-AS cells. The $2^{-\Delta\Delta Ct}$ results shown are an average of three replicates normalised to *β-Actin* gene expression and compared with the non-targeting control. Error bars display ± SEM. Statistical significance was calculated by a two-tailed t-test and is displayed by *P ≤ 0.05, **P ≤ 0.01, ***P ≤ 0.001. (n=3).

Generally, *HuB* knockdown results in an increase of *HuR* expression. *HuC* knockdown increased *HuC* and *HuR* expression but decreased *HuD* expression. *HuD* siRNA interference results in an increased in *HuB* and *HuC* expression whilst a decrease of *HuR* expression is observed. *HuR* siRNA interference results in an increase of *HuB* gene expression and a decreased in *HuC* and *HuD* gene expression. Combined *Hu* siRNA clearly reduces all *Hu* genes expression.

The overall knockdown profile is summarised as percentages in a heatmap is displayed in Fig. 4.22.

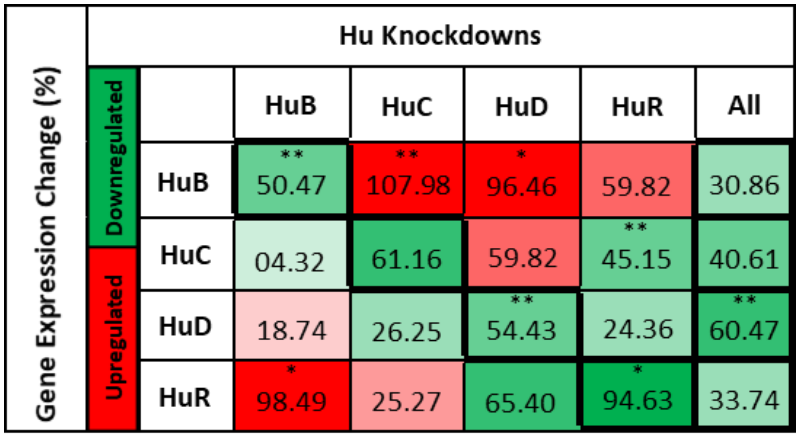

Figure 4.22: Heatmap displaying *Hu* gene expression change after Knockdown experiments in SK-N-AS Neuroblastoma cells. Colour intensity proportional to the amount. Statistical significance was calculated by a two-tailed t-test and is displayed by *P ≤ 0.05, **P ≤ 0.01, ***P ≤ 0.001. (n=3).

The heatmap displayed in Fig. 4.22 includes less statistically significant regulatory features. A model was developed to portray the significant regulation observed in a visual representation. Fig. 4.23 shows a model regulatory influences within the Hu family that exist in the SK-N-AS Neuroblastoma cell line.

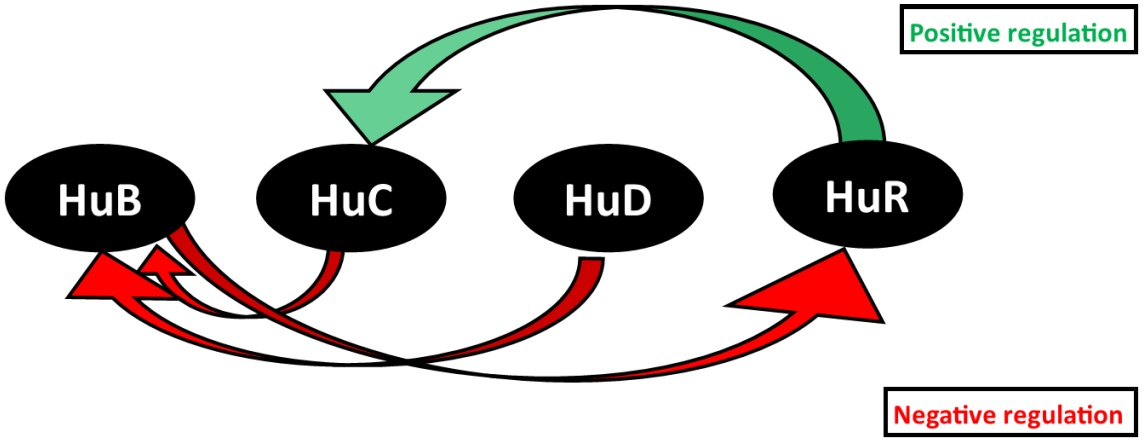

Figure 4.23: A model representing the statistically significant regulation of the Hu protein family in the Neuroblastoma cell like SK-N-AS. Colour intensity proportional to the change of gene expression compared to the control.

Based on levels of significance conducted by statistical two tailed t-test, decreases in *HuC* and *HuD* gene expression see an increase *HuB* expression. Additionally, a decreased expression of HuR significantly upregulated *HuC* expression.

Upon comparing both Neuroblastoma cell models of regulatory interactions, the only significant similarity between the two models is the decrease of *HuC* gene expression when *HuR* gene is knocked down. Since these two cell lines portray two initial different expression profiles of the Hu proteins, it is unfeasible to combine the two data sets but show that the observed regulatory effects of Hu proteins are possible.

4.5 Cellular morphology and invasion of normal astrocytes and Neuroblastoma cells

Human cancer is often diagnosed and classified through microscopy techniques through identification of cell origin and various cell attributes. Morphological characteristics of cells are often related to their functional abilities particularly those that are malignant (Idikio 2011).

4.5.1 Cellular morphological analysis

Often, cancer cells are defined by a large nucleus with prominent nucleoli, have little cytoplasm and are overall an irregular shape and size (Baba and Câtoi 2007). Microscopic analysis of Neuroblastoma and normal astrocytes is shown in Fig. 4.24. Cell images were obtained using an Eclipse II fluorescent inverted microscope and Microtec camera as described in Section 2.1.6.

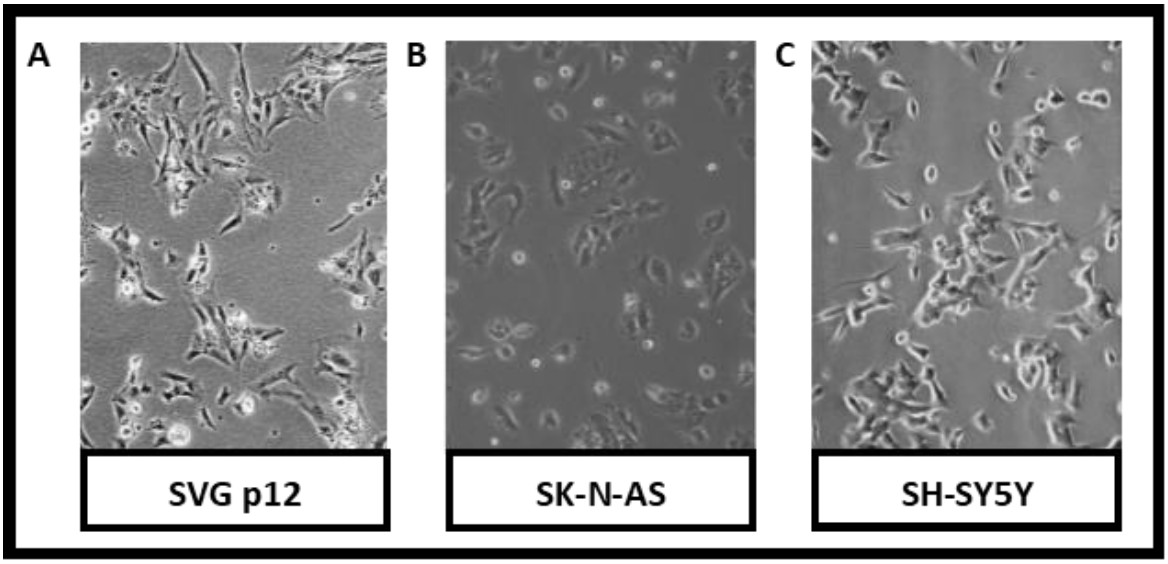

Figure 4.24: Microscopy images of each brain and Neuroblastoma cell line. Light microscopy at x20 objective. A) Normal astrocytes cell line, SVG p12. B) Neuroblastoma cell line, SK-N-AS. C) Neuroblastoma cell line, SH-SY5Y.

The Neuroblastoma cell lines grow as adherent monolayers and have an epithelial-like shape. There is a considerable degree of similarity in morphology of each Neuroblastoma cell line.

The normal astrocytes cell line SVG p12 typically grow in star-shaped cells called fibroblasts.

4.5.2 Cellular migrative potential

One hallmark of cancer cells is their ability to migrate and invade into distant tissues forming tumour metastases. To measure the invasiveness of the Neuroblastoma cells in culture, cell migration was calculated by the ability of the cells to invade into a 0.5% agarose gel matrix. It was captured through several microscopy imaging equipment. The images below were achieve using time-lapse photography captured by the CytoSMART™ camera as described in Sections 2.5 and 2.5.1.

First, the ability of the normal astrocytes to migrate into the gel was assessed and is shown in Fig. 4.25. The normal astrocyte cells SVG p12 did not migrate into the agarose gel matrix during the observed 42 hours as expected for a non-cancer cell line. The cells proliferate and grew in a line surrounding the agarose.

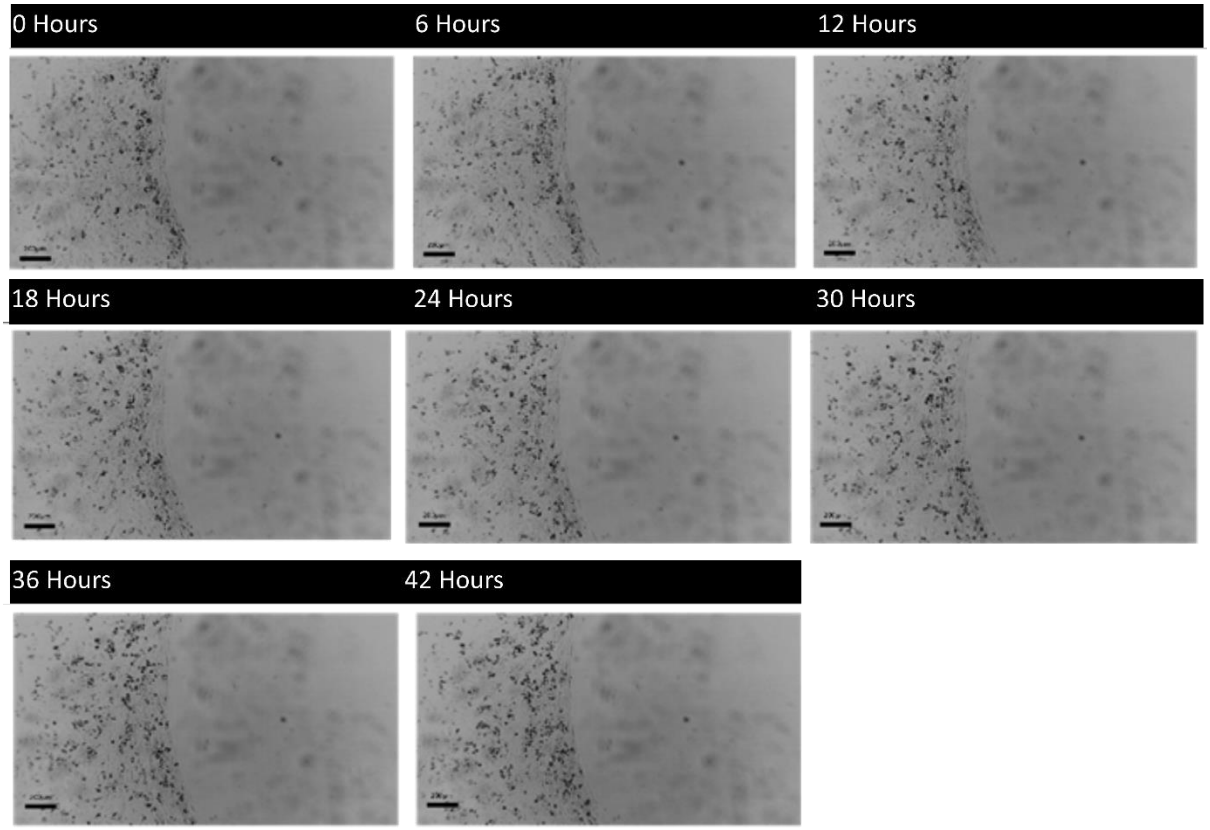

Figure 4.25: The migration of SVG p12, normal astrocyte cells into an agarose gel matrix. During the observed 42-hour period, no migration into the gel matrix was detected. Time-lapse photography of the cell migration can be viewed at: https://cytomate.com/access/Project_main/main.php?DiD=238&PiD=19644&ac1=92e93081fa6bd13ce510fd1cad4efcc8f3b9be40cac0df160fe49728dd028276&ac2=b8af21ea150c9f3367e00e143135c75d21d55c29158ae7a23a2f5c3e9a182ae6

The Neuroblastoma cells were then assessed for their ability to penetrate the gel matrix. In contrast to the normal astrocytes, both Neuroblastoma cell lines migrated into the agarose gel matrix as displayed in Fig. 4.26 and 4.27. A difference in migration rate over the observed 42-hour was seen.

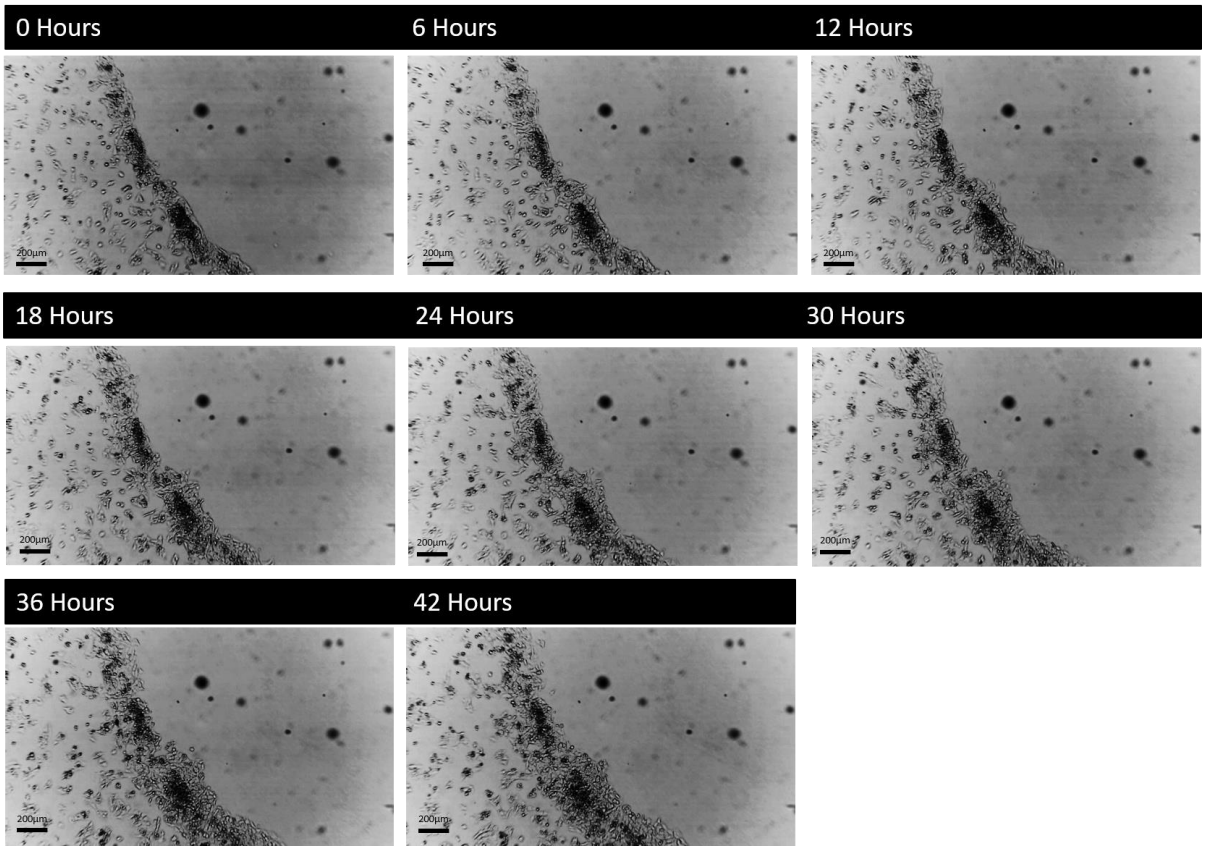

Figure 4.26: The migration of SK-N-AS Neuroblastoma cells into an agarose gel matrix. Over the observed 42-hour period, cells migrated into the gel matrix. Time-lapse photography of the cell migration can be viewed at: https://cytomate.com/access/Project_main/main.php?DiD=238&PiD=9849&ac1=cdca561ef977a7ffe181cc31181d7f20eee22891dc6da50db9aa7af006a53750&ac2=1ee64f16a15e4b0270a75d164393adc88fe312e8444ddf5363f6105a6aa7742a

The migration of SK-N-AS cells into the agarose gel matrix is shown in Fig. 4.26. SK-N-AS cells immediately started to migrate into the matrix (0 Hours). Over the 42-hour period, the cells migrated into the 31.37% of the gel displayed.

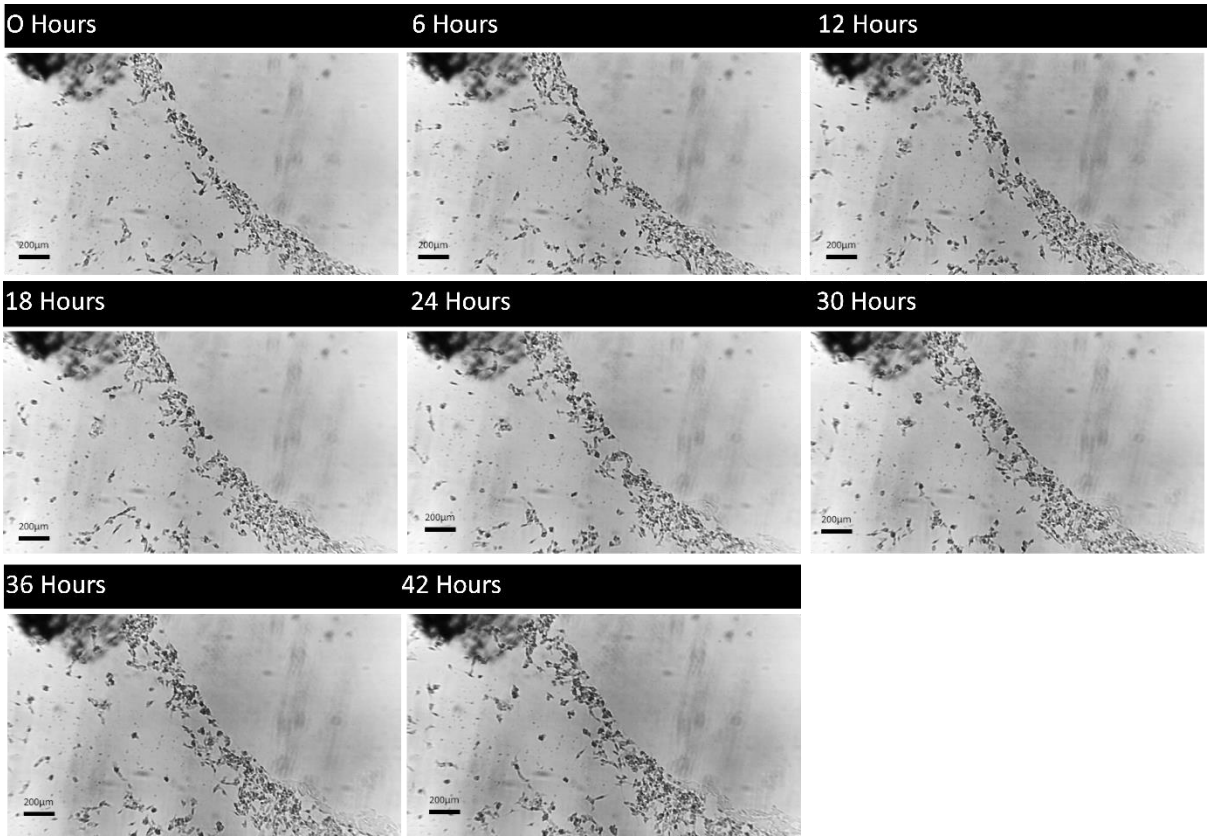

Figure 4.27: The migration of SH-SY5Y Neuroblastoma cells into an agarose gel matrix. Over the observed 42-hour period, cells migrated into the gel matrix. Time-lapse photography of the cell migration can be viewed at: https://cytomate.com/access/Project_main/main.php?DiD=238&PiD=19941&ac1=a952363d82989cf53da1a9c4440da1a2b9765a30b49c87cbe5fcbb84276f25af&ac2=e5ad51992f4567b12906250a4723a25827016e4a1c7cec36830141a4414a7d89

The migration of SH-SY5Y cells into the agarose gel matrix is shown in Fig. 4.27. The cells were seeded 24-hour post-transfection and once adhered to the flask, immediately began migrating into the gel matrix. Over the 42-hour period, the SH-SY5Y cells migrated into 18.92% of the displayed gel matrix.

The invasiveness of the Neuroblastoma cell lines SK-N-AS and SH-SY5Y and the normal astrocyte cells SVG p12 was compared and is shown in Fig. 4.28.

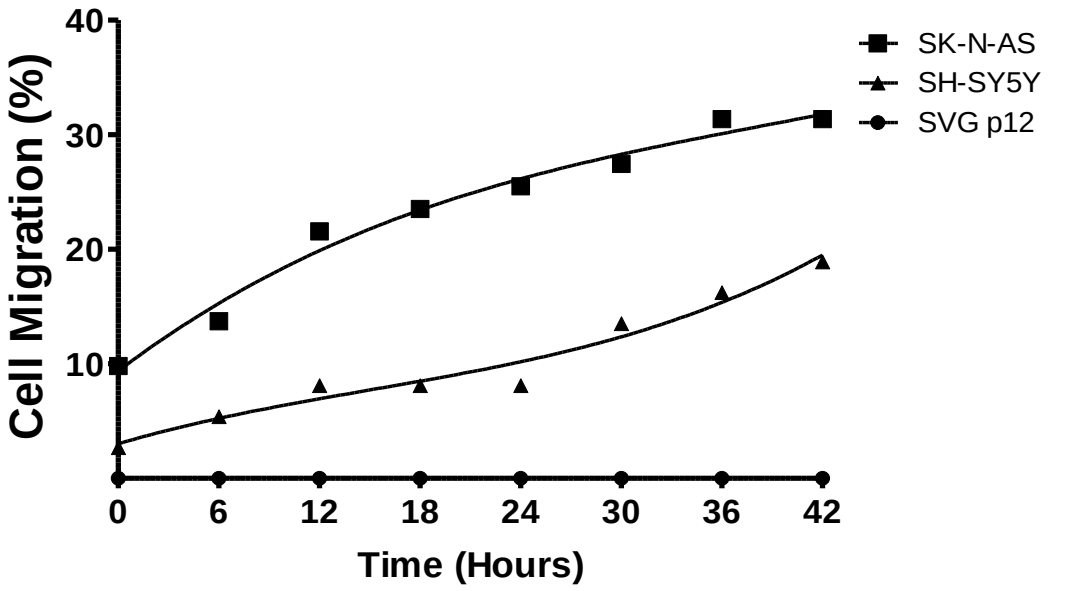

Figure 4.28: The migration of SK-N-AS and SH-SY5Y Neuroblastoma cells compared to the non-migration of SVG p12 astrocyte cells. Migration into the gel matrix was calculated by the percentage surface area invaded by the cells.

Migration of the normal astrocyte and Neuroblastoma cell lines over 42 hours is displayed in Fig. 4.28. SK-N-AS was the most migrative with a 12.45% increase in the migrative potential than the SH-SY5Y cells whilst normal astrocyte SVG p12 were shown to not penetrate the gel. In summary, the Neuroblastoma cell lines have a greater migrative potential than the normal astrocytes.

4.6 Cellular morphology, viability and migration following *Hu* knockdown in Neuroblastoma cells

Often cancer cells experience genomic alterations causing mutations that influence proliferation, cell motility and changes to cell morphology (Baba and Câtoi 2007). Cell

morphology can help determine the physiological state of the cells and can therefore be used to qualitatively assess to cell health.

4.6.1 Effect of *Hu* knockdowns in SH-SY5Y cells

To assess the effect of *Hu* gene expression on these features in Neuroblastoma, cells morphology was analysed following individual and combined *Hu* gene knockdowns. Cells were imaged to assess any changes to cell morphology through size and shape following *Hu* gene knockdowns. RT-qPCR of knockdown experiments confirmed a *Hu* gene knockdown at 48 hours, subsequently cell morphology was observed at this time point. Cell images were obtained using an Eclipse II fluorescent inverted microscope and Microtec camera as described in Section 2.1.6.

It is also important to mention, the images displayed in Figure 4.29 do not confer the confluency of the cell lines following *Hu* knockdowns. Other methods evaluate the proliferation rates described later in this section. Some cells had died, these were removed when the media was replaced prior to imaging.

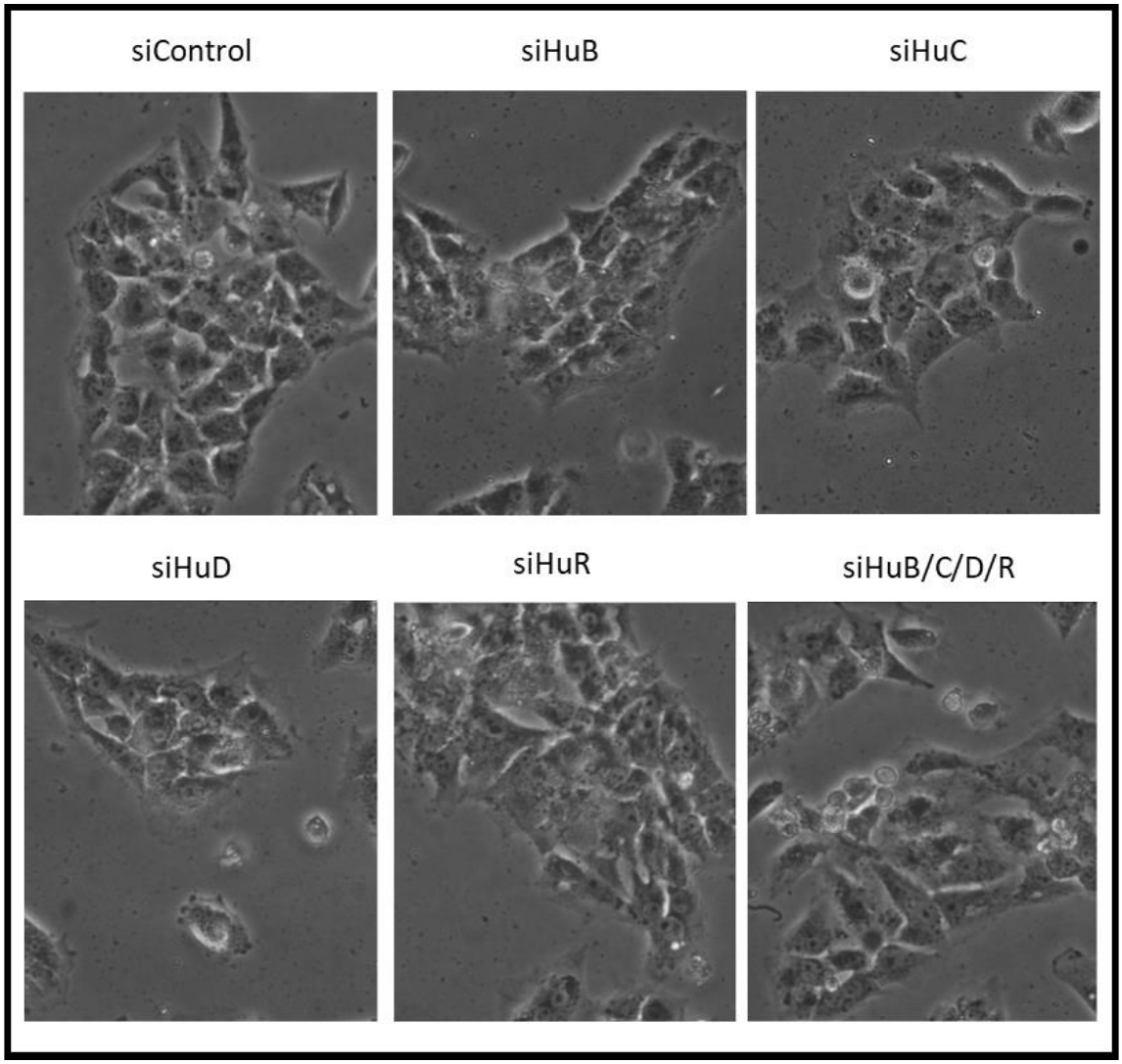

Figure 4.29: SH-SY5Y cell morphology 48-hours post-transfection with *Hu* siRNAs. SH-SY5Y cells with *Hu* genes knocked down in combination and individually. Light microscopy at 20x objective.

The morphology of SH-SY5Y has not been influenced by the individual or combined *Hu* gene knockdowns compared to the control non-target siRNA transfected cells.

The cell viability after *Hu* knockdowns both individually and in combination were assessed over 120 hours in SH-SY5Y cells using CellTiter 96® AQ_{ueous} One Solution assay (Section 2.6). Readings were taken at 24 hour intervals, 48 hours after transfection.

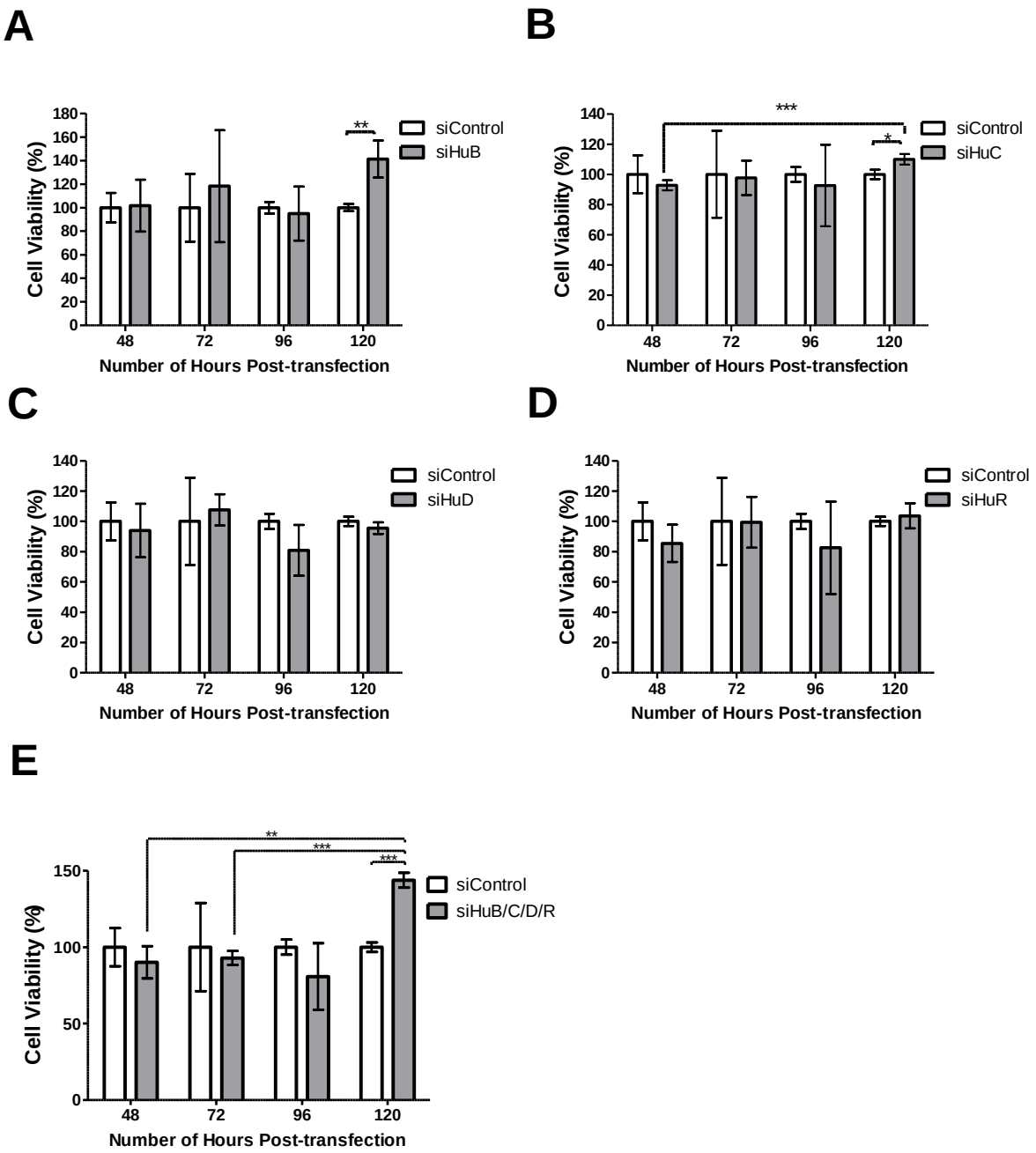

Figure 4.30: Cell viability of SH-SY5Y cells after knockdown experiments. Mean cell viability normalised to the control non-target siRNA treated cells. A) Effect of *HuB* knockdown. B) Effect of *HuC* knockdown. C) Effect of *HuD* knockdown. D) Effect of *HuR* knockdown. E) Effect of combined *Hu* knockdown. MTS absorbance was recorded at 490nm over a 120-hour period. Data are expressed as mean values ± SD. n=3. Statistical significance was calculated by a two-tailed t-test and is displayed by *P ≤ 0.05, **P ≤ 0.01, ***P ≤ 0.001. (n=3).

The SH-SY5Y cell viability profiles displayed in Fig. 4.30 showed that the highest variability of Hu knockdowns was at the 120-hour time point. At this time point, cell viability increased 43.72% following HuB knockdown, 9.92% following HuC knockdown and 41.23% in the combined *Hu* knockdown cells which were all significant. HuC showed a significant increase in viability when compared to the 48 hour sample whilst the combined Hu knockdown also showed a significant increase when compared to the 48 and 72 hours time points. HuD and HuR knockdown samples showed no significant change on viability between time points or when compared to the control.

Cell motility was measured before and after individual and combination *Hu* gene knockdowns with a scratch wound assay (Section 2.5.2). This assay measures the ability and speed of the cells to migrate into an artificially created cell-free gap until new cell-cell contacts are established. Cells were imaged every 24 hours.

The visual representation of SH-SY5Y cells migrating into a gap is shown in Fig. 4.31, Fig. 4.32 and Fig. 4.33. Whilst this method can show variable results, quantitative measurements for the 48-hour timepoint were recorded. Later timepoints although captured visually, show great variability due to changes in cell viability.

The control cells with a non-targeting siRNA (Fig. 4.31) showed an increase in motility following 24 hours where the cells became too confluent and started to detach at the wound edge.

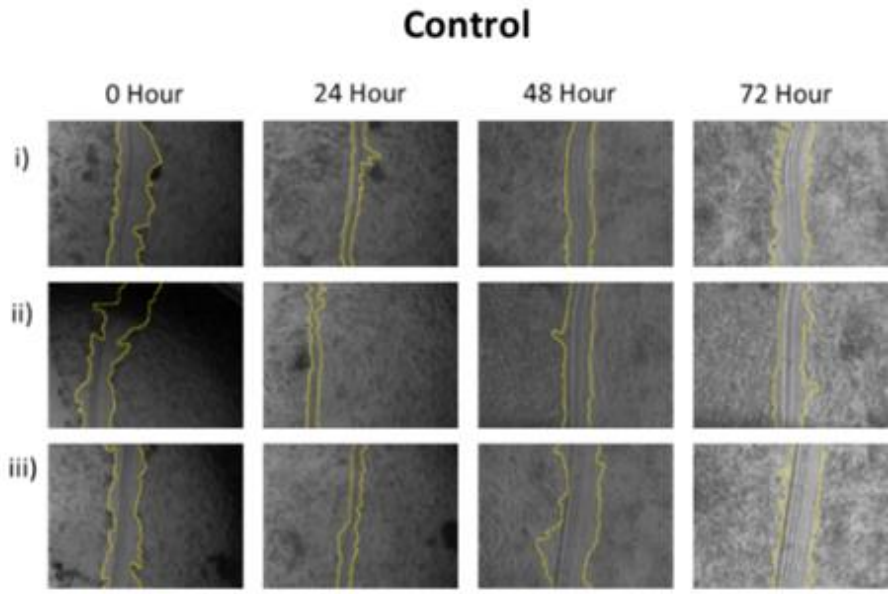

Figure 4.31: Scratch wound assays in control SH-SY5Y Neuroblastoma cells with non-targeting siRNA. Migration was assessed 48 hours post-transfection when cells were confluent. Images were taken for 72 hours. Wounds were generated after cell confluence following siRNA interference. Timepoints state the number of hours post-wound making. Yellow lines highlight the gap. Magnification x10.

Next, the effect of individual Hu gene knockdowns were observed (Fig. 4.32). Again a similar effect was observed in that an increase in motility following 24 hours resulted in the cells becoming too confluent and consequently start to detach at the wound edge. *HuC* knockdown resulted in detaching of cells following 48-hours so no images were obtained following that timepoint for that sample.

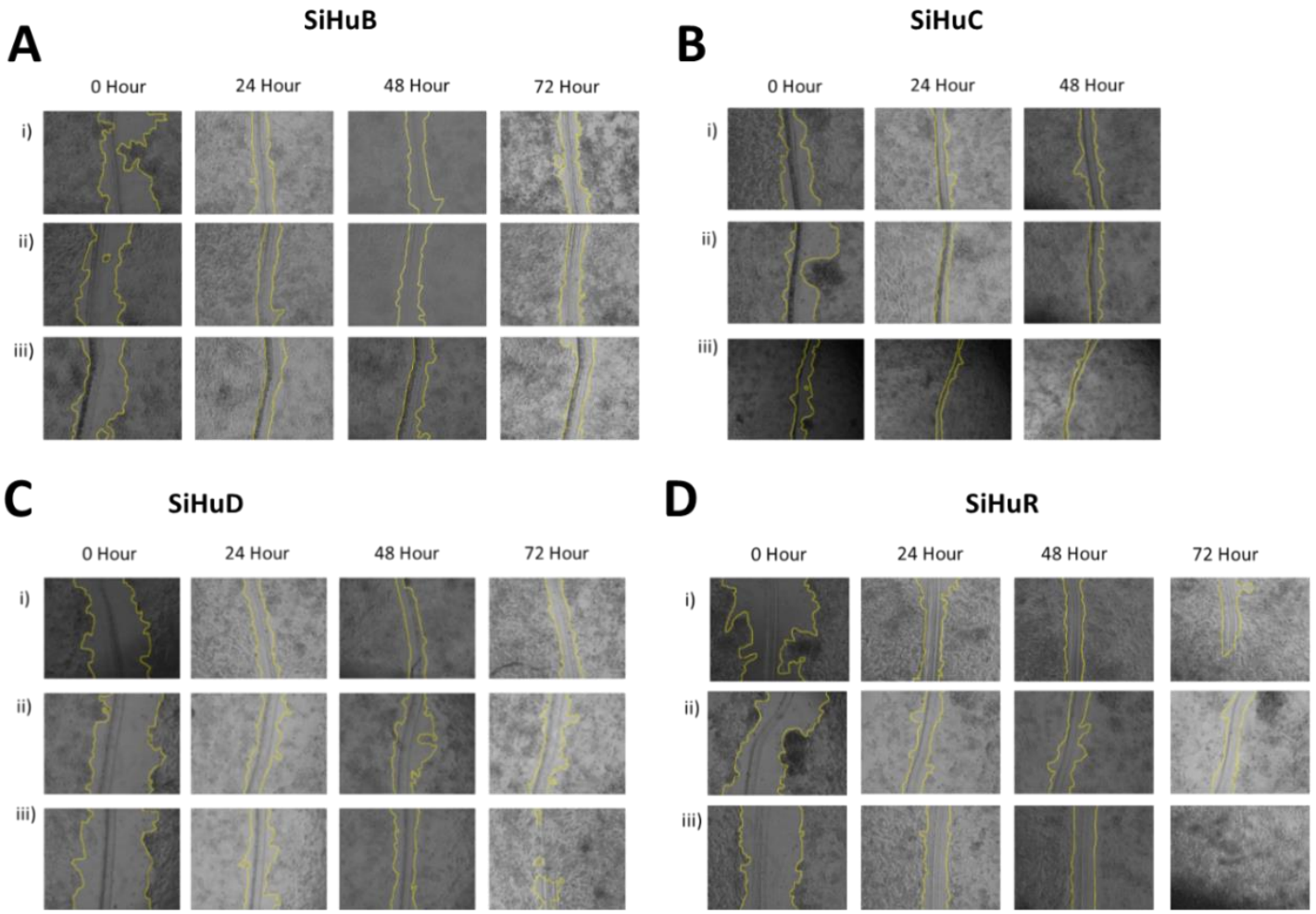

Figure 4.32: Scratch wound assays in SH-SY5Y Neuroblastoma cells following knockdown of *Hu* genes individually. Migration was assessed 48 hours post-transfection when cells were confluent. Images were taken for 72 hours. A) *HuB* knockdown B) *HuC* knockdown C) *HuD* knockdown D) *HuR* knockdown. Timepoints state the number of hours post-wound making. Yellow lines highlight the gap. Magnification x10.

The effect of a combined knockdown is shown in Figure 4.33.

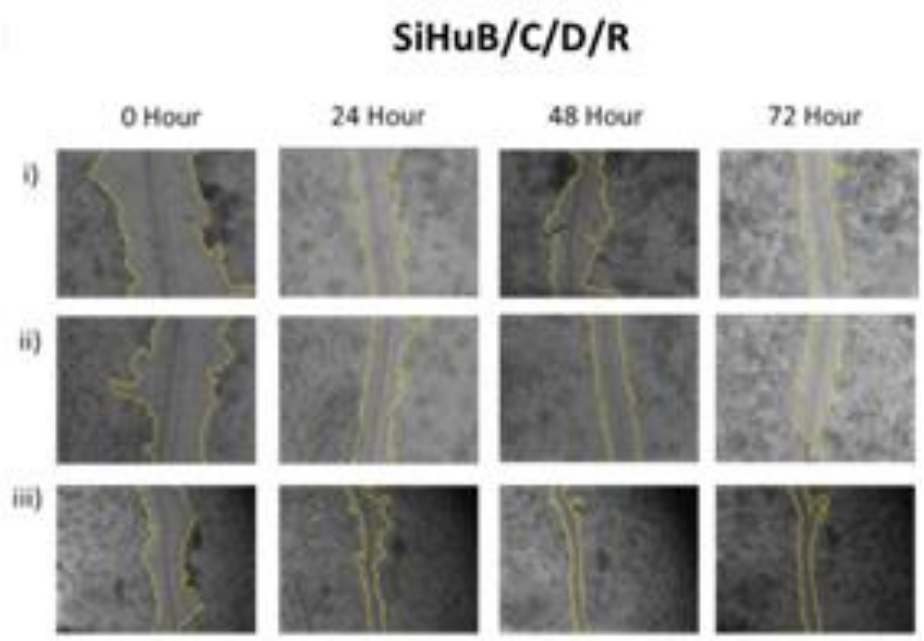

Figure 4.33: Scratch wound assays in SH-SY5Y Neuroblastoma cells following knockdown of *Hu* genes combined. Migration was assessed 48 hours post-transfection when cells were confluent. Images were taken for 72 hours. Wounds were generated after cell confluence following siRNA interference. Timepoints state the number of hours post-wound making. Yellow lines highlight the gap. Magnification x10.

Percentage migration into the cell-free gap was calculated for the 48 hour timepoint using ImageJ pixel analysis. Two-tailed t-test determined the statistical significance. This data is show in Fig. 4.33

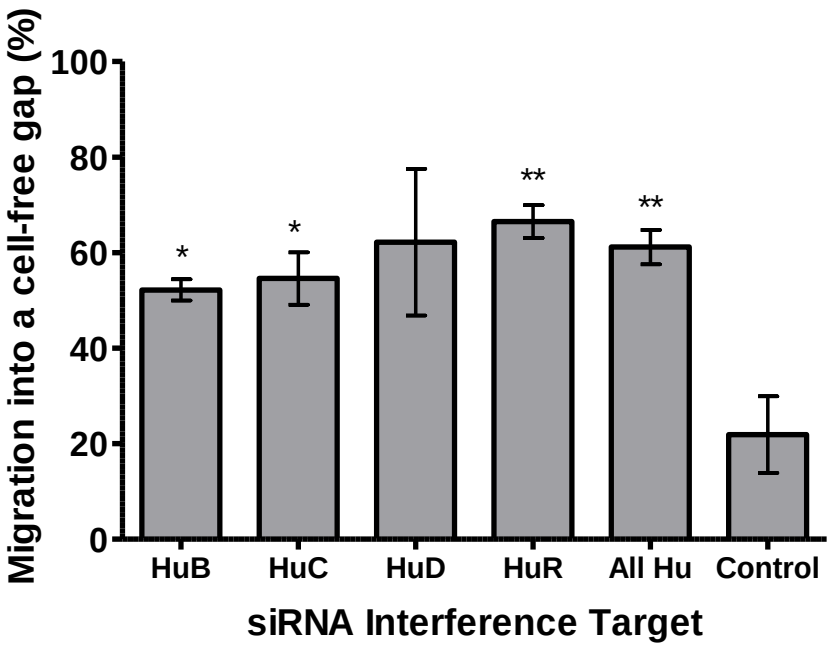

Figure 4.34: Cell migration of Neuroblastoma cells SH-SY5Y represented as the percentage of migration into the cell-free gap over 48 hours. The measure of cell motility was calculated in ImageJ through the measurement of pixels and conversion into a percentage to determine the rate of cell migration. Data showed the mean migration of cells into the cell-free gap over 48 hours. Error bars display ± SEM. Statistical significance was calculated by a two-tailed t-test and is displayed by *P ≤ 0.05, **P ≤ 0.01, ***P ≤ 0.001. (n=3).

Whilst defining the role of the Hu-family of RNA binding proteins in cell migration, it was observed that the most variation between individual and combined *Hu* gene knockdowns compared to the non-target control at the 48 hours timepoint. This is displayed in Fig. 4.33. All cells with either individual or combined *Hu* gene knockdowns had a greater directional migratory response in comparison to the controls.

Changes to the cellular properties observed following *Hu* gene knockdowns in the SH-SY5Y cell line are summarised in Fig. 4.35.

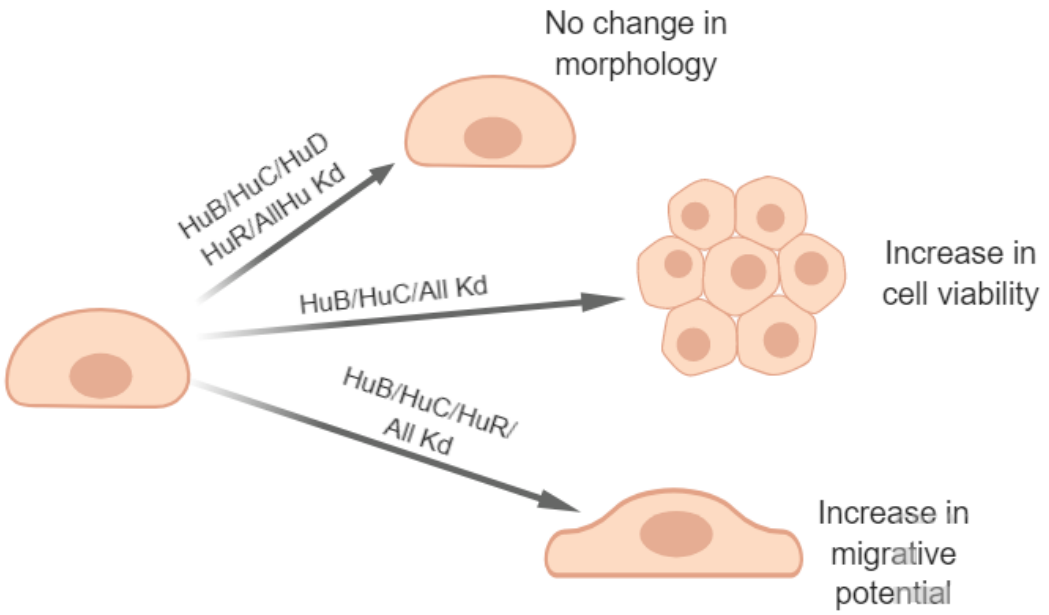

Figure 4.35: Changes in cellular properties following Individual and combined *Hu* gene family knockdown in the Neuroblastoma cell line SH-SY5Y.

Knockdown of individual *Hu* or combined *Hu* genes did not result in any morphological changes. However, an increase in viability could be seen following *HuB*, *HuC* and the combined knockdown of all four *Hu* genes. Additionally, a reduction of *HuB*, *HuC* and *HuR* individually and all *Hu* genes in combination revealed an increased migrative potential.

4.6.2 Effect of *Hu* knockdowns in SK-N-AS cells

Cells were imaged to assess any changes to cell morphology through size and shape following *Hu* gene knockdowns (Fig. 4.36). Images were obtained using an Eclipse II fluorescent inverted microscope and Microtec camera as described in Section 2.1.6.

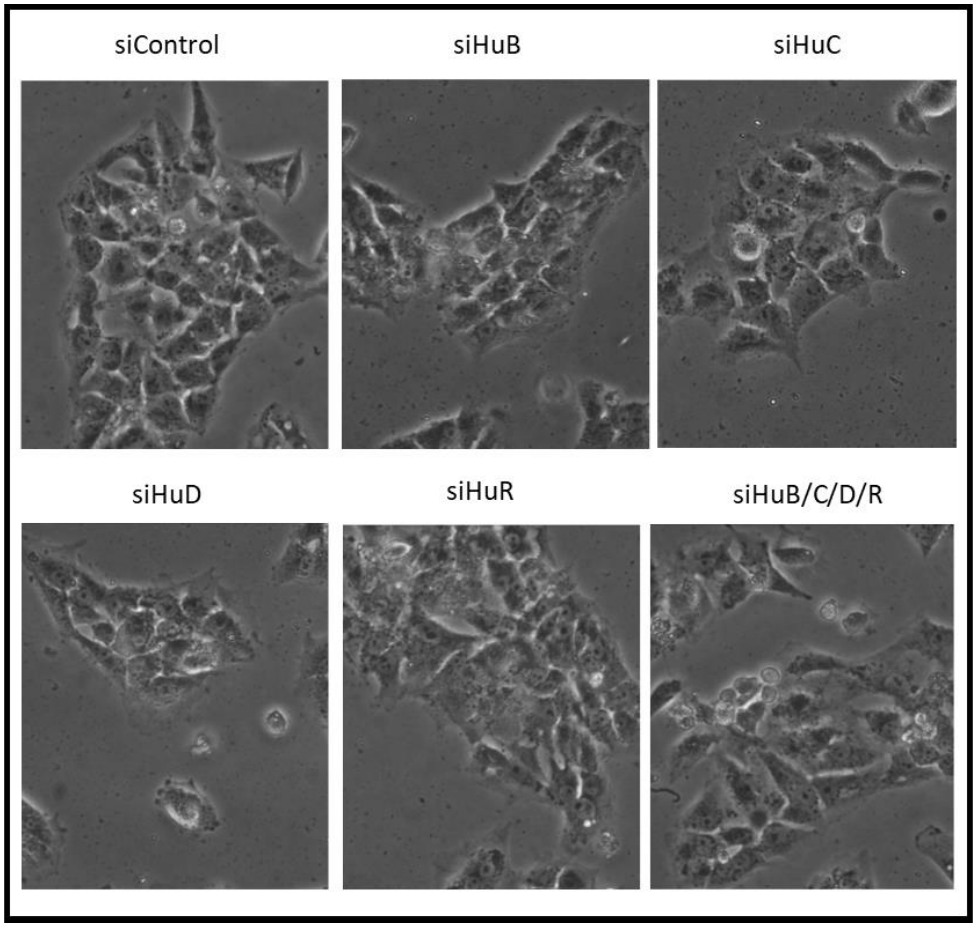

Figure 4.36: SK-N-AS cell morphology 48-hours post-treatment with siRNA. SK-N-AS cells with *Hu* genes knocked down in combination and individually. Light microscopy at 20x objective.

No morphological changes could be observed in SK-N-AS cells following knockdown of all Hu proteins individually and in combination in comparison to the control untreated cells.

The cell viability after *Hu* knockdowns both individually and in combination were assessed over 120 hours in SK-N-AS cells using CellTiter 96® AQ_{ueous} One Solution assay (Section 2.6). Readings were taken in 24 hour intervals, 48 hours after transfection.

The cell viability profile for SK-N-AS cells is displayed in Fig. 4.37.

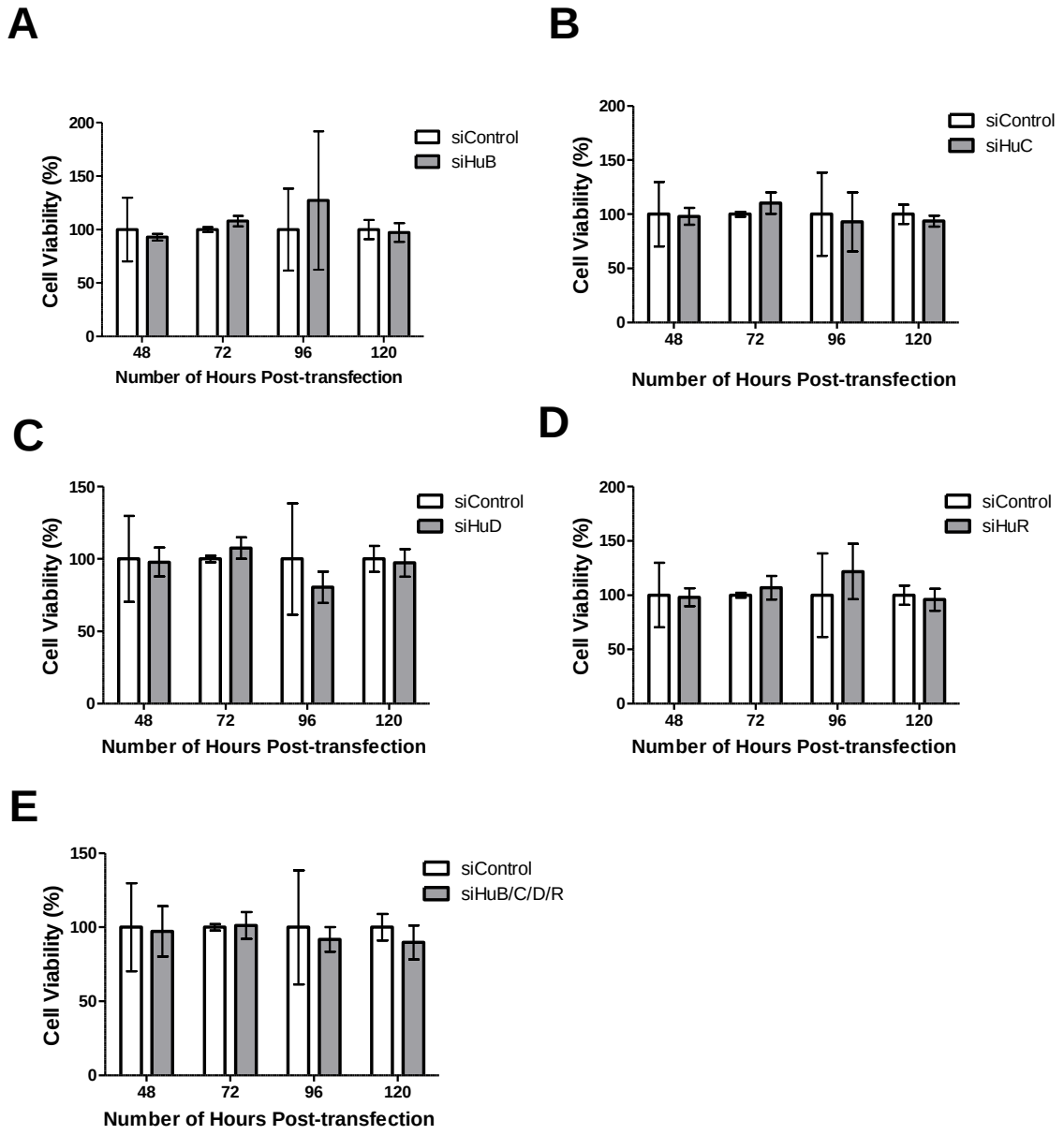

Figure 4.37: Cell viability of SK-N-AS cells after knockdown experiments. Cell viability normalised to the non-target control. A) Effect of *HuB* siRNA transfection. B) Effect of *HuC* siRNA transfection. C) Effect of *HuD* siRNA transfection. D) Effect of *HuR* siRNA transfection. E) Effect of combined *Hu* siRNA transfection. MTS absorbance was recorded at 570nm over a 120-hour period. Data are expressed as mean values ± SD of at least three separate determinations. No statistical significance was detected by a two-tailed t-test.

The cell viability of the control is set at 100%. At 96 hours where most variability is seen, viability increased 27.23% following *HuB* knockdown and 21.75% following *HuR* knockdown

although these values are not statistically significant. Cell viability reduced 7.08% following *HuC* knockdown,19.54% following *HuD* knockdown and 8.25% when all *Hu* genes were knocked down. Unfortunately, none of these values held significance.

To address if any of the *Hu* knockdowns influence cell motility, a scratch wound assay (Section 2.5.2) was performed and captured at 24 hour intervals starting 48 hours post-transfection. Images were captured using an Eclipse II fluorescent inverted microscope and Microtec camera as described in Section 2.1.6. The visual representation of SK-N-AS cells migrating are shown in Fig. 4.38, Fig. 4.39 and Fig. 4.40.

Whilst this method can show variable results, quantitative data for the 24-hour timepoint was recorded. Later timepoints although captured visually, show great variability due to changes in cell viability.

Damage induced by the wound to the cell layer showed a different pattern of disruption when comparing this cell line to the other Neuroblastoma cell line. This can be explained as a different effect to the extracellular matrix formed by all adherent cells in culture. Whilst wounds were induced using the same methods, SH-SY5Y cells formed a more uniform gap compared to the irregular disruption inflicted on the SK-N-AS cell monolayer. These cells still managed to migrate towards each other, filling in smaller areas but generally at a slower rate than the SH-SY5Y cells.

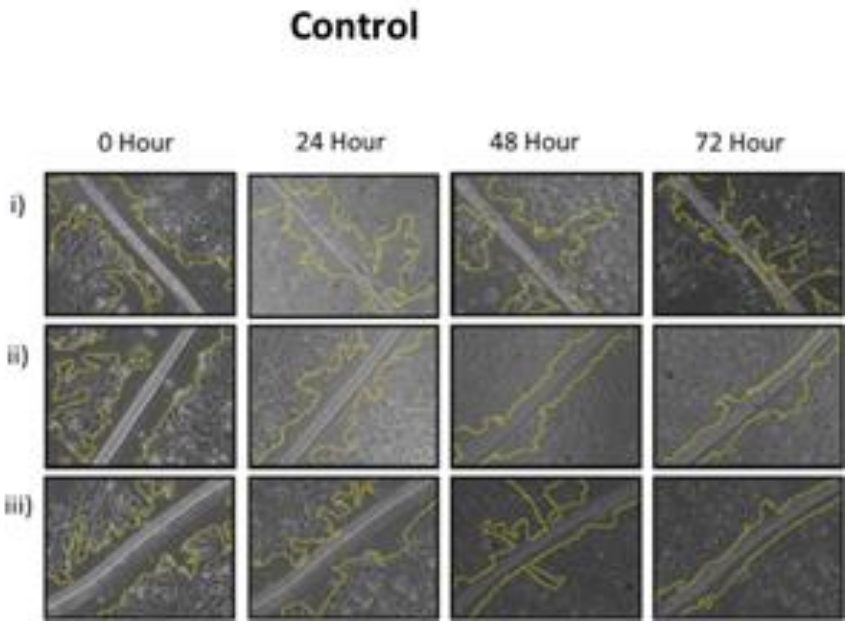

Figure 4.38: Scratch wound assays in control SK-N-AS Neuroblastoma cells with non-targeting siRNA. Migration was assessed 48 hours post-transfection when cells were confluent for 72 hours. Wounds were generated after cell confluence following siRNA interference. Timepoints state the number of hours post-wound making. Yellow lines highlight the gap. Magnification x10.

The effect of the individual Hu gene knockdowns are displayed in Figure 4.39.

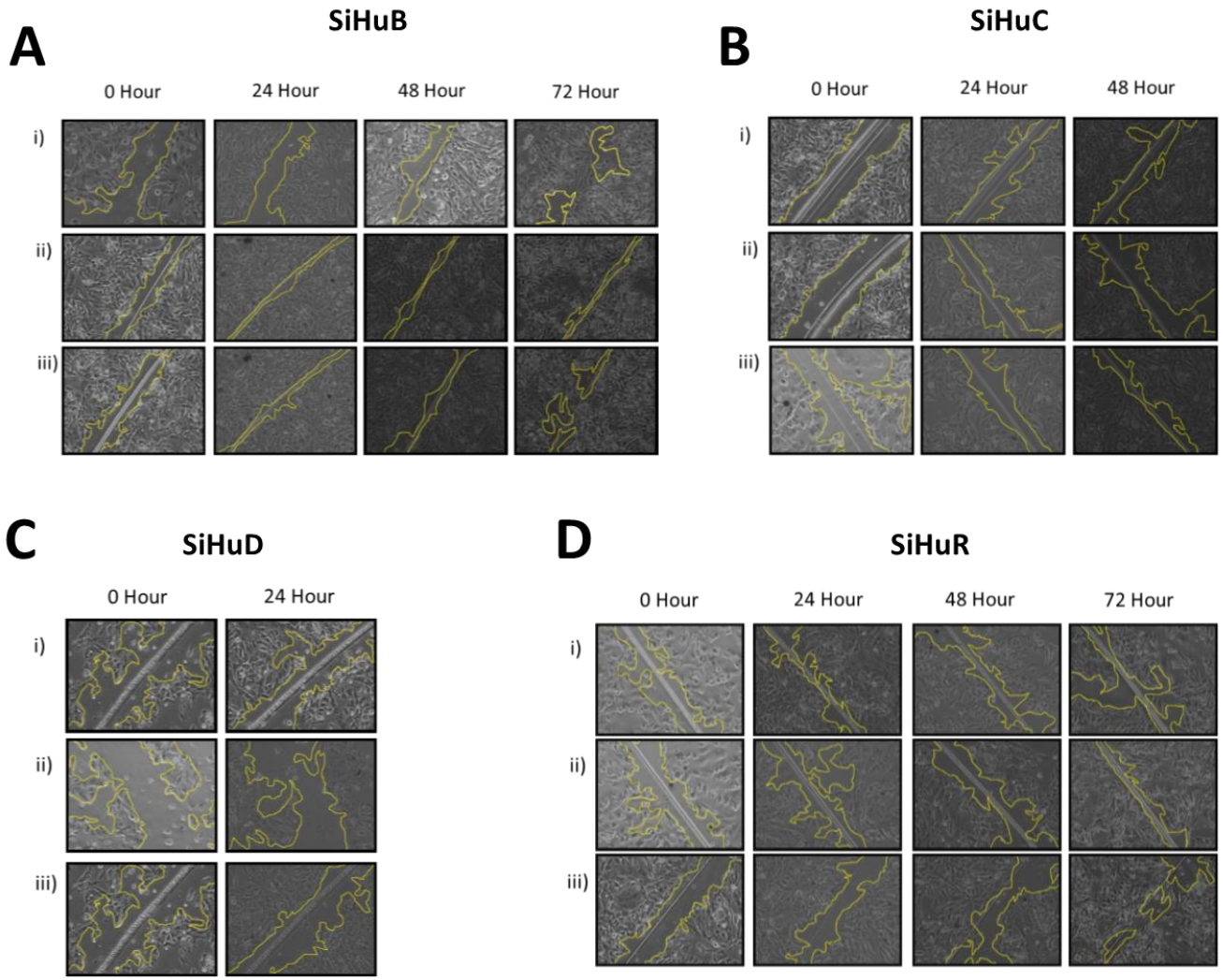

Figure 4.39: Scratch wound assays in SK-N-AS Neuroblastoma cells before and after knockdown of *Hu* genes individually. Migration was assessed 48 hours post-transfection when cells were confluent for 72 hours. A) *HuB* knockdown B) *HuC* knockdown C) *HuD* knockdown D) *HuR* knockdown. Timepoints state the number of hours post-wound making. Yellow lines highlight the gap. Magnification x10.

HuD knockdown resulted in detaching of cells following 24-hours so no images were obtained following that timepoint for that sample. The same occurred with *HuC* knockdown and combined *Hu* knockdowns after 72 hours. Interestingly, this correlates with viability data shown for this Neuroblastoma cell line SK-N-AS detailed in Fig. 4.37. Although not statistically significant, a decrease in viability is observed for these knockdowns at the 96-hours timepoint when compared to the non-target control.

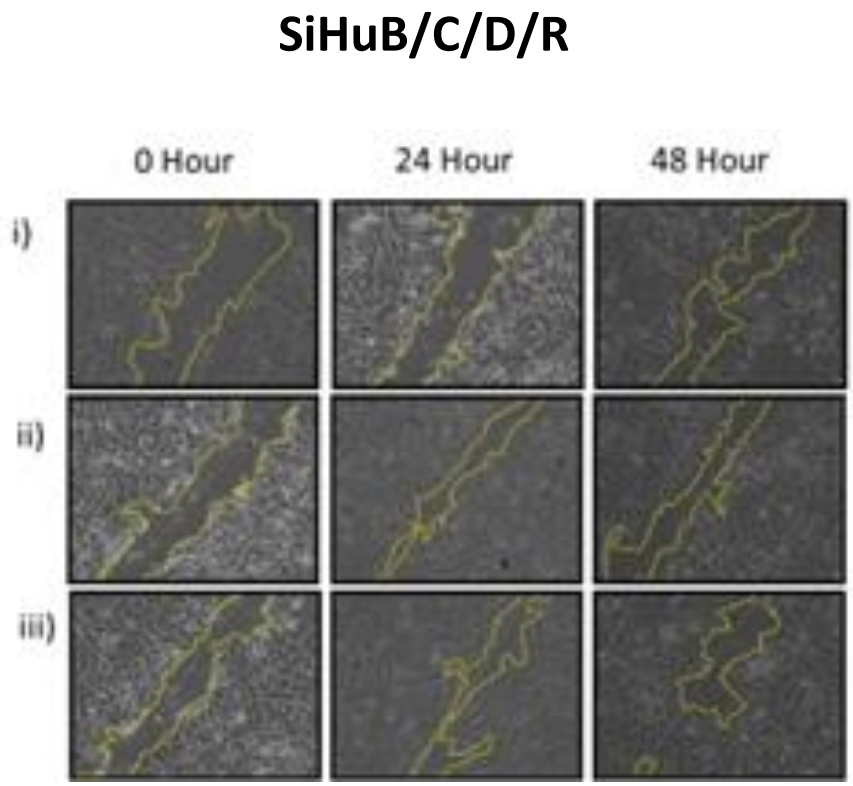

Figure 4.40: Scratch wound assays in SK-N-AS Neuroblastoma cells before and after knockdown of all *Hu* genes combined. Migration was assessed 48 hours post-transfection when cells were confluent for 72 hours. Wounds were generated after cell confluence following siRNA interference. Timepoints state the number of hours post-wound making. Yellow lines highlight the gap. Magnification x10.

Percentage migration into the cell-free gap was calculated for the 24 hour timepoint using ImageJ pixel analysis. Two-tailed t-test determined the statistical significance. This data is show in Fig. 4.41.

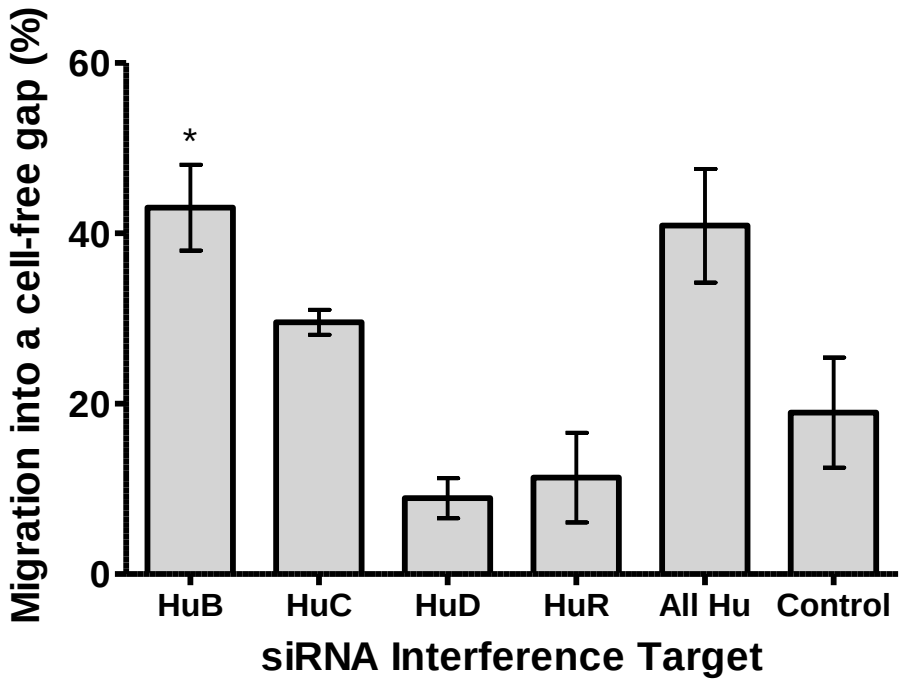

Figure 4.41: Cell migration of Neuroblastoma cells SK-N-AS represented as the percentage of migration into the cell-free gap over 24 hours. The measure of cell motility was calculated in ImageJ through the measurement of pixels and conversion into a percentage to determine the rate of cell migration. Data showed the mean migration of cells into the cell-free gap over 24 hours. Error bars display SEM. (n=3). Statistical significance was calculated by a two-tailed t-test and is displayed by *P ≤ 0.05, **P ≤ 0.01, ***P ≤ 0.001.

The cell migration profile displayed in Fig. 4.41 details a different migratory rate than the other Neuroblastoma cell line examined (Fig. 4.33). Whilst defining the role of the Hu-family of RNA binding proteins in cell migration in the SK-N-AS cell line, the most reliable data was at the 24-hour timepoint as cell growth was not affected during this time. At 24-hours, a significant 24.06% increase in the migratory rate of SK-N-AS cells was seen following *HuB*

knockdown. 10.62% increase following *HuC* knockdown and a 21.96% increase following combined Hu knockdown that were insignificant. *HuD* and *HuR* knockdowns showed a reduced migratory potential of 10.04% and 7.62% respectively both of which were also insignificant.

A summary of the overall effect of Hu interference in SK-N-AS cells is displayed in Figure 4.42. Knockdown of individual *Hu* or combined *Hu* genes in SK-N-AS cells did not result in any morphological changes. *HuB* knockdown increased the migrative potential of SK-N-AS cells.

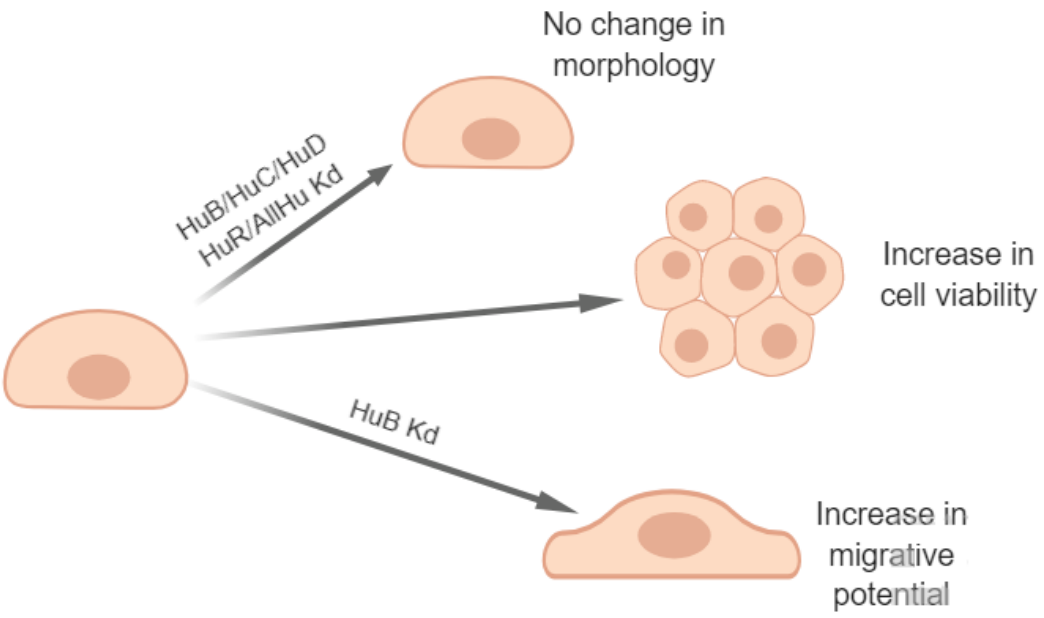

Figure 4.42: Changes in cellular properties following Individual and combined *Hu* gene family knockdown in the Neuroblastoma cell line SK-N-AS.

The two Neuroblastoma cell lines SH-SY5Y and SK-N-AS shared some similarities. There was no change in morphology following any *Hu* gene knockdowns. *HuB* gene knockdown resulted in a more migrative phenotype in both cell lines.

4.7 Effect of *Hu* knockdown on gene regulation and translational networks in Neuroblastoma

To assess the biological function of Hu proteins, the molecular targets of Hu proteins and the affect they have on those mRNA transcripts were determined through RT-qPCR before and after individual and combined Hu gene knockdowns. A collection of 91 pre-selected genes (Table 4.1) with appropriate controls were analysed before and after *Hu* gene knockdowns. The genes selected are thought to play a role in the development of Neuroepithelial neoplasms referenced by the National Library of Medicine database (NLM 2018). Gene targets are ranked based on frequency of gene expression changes in biomarker studies, popularity in overall medical research and popularity in current medical research (Biorad 2018).

The array of genes (Table 4.1) was screened to highlight target mRNAs influenced by the family of Hu RNA-binding proteins regulation to establish a role of their aberrant or overexpression in Neuroblastoma.

ABCB1	CCND1	CTNNB1	HIF1A	KIT	MMP9	RB1	TLR2	TBP
AKT1	CCND2	CXCL12	HLA-DRB1	KRAS	MYC	RRM2	TNF	GAPDH
APOE	CD44	CXCR4	HMOX1	MAP2K2	NFKB2	SERPINE1	TOP2A	HPRT1
ATM	CDK1	EGFR	IFNG	MAPK1	PCNA	SOD2	TYMS	
AURKA	CDK2	EGR1	IGF1	MAPK3	PIK3CA	SP1	UBB	
BCL2	CDKN1A	ERBB2	IGF1R	MDM2	PIK3R1	SPP1	UBC	
BDNF	CDKN2A	ESR1	IGFBP3	MKI67	PLAU	STAT3	VCAM1	
BIRC5	COL1A1	EZH2	IL10	MLH1	PRKCA	TCF7L2	VEGFA	
BRCA1	COL1A2	FN1	IL6	MMP1	PROM1	TERT	VIM	
CCNA2	CTBP2	GSK3B	ITGB1	MMP2	PTEN	TGFB1	WNT5A	
CCNB1	CTGF	GSTP1	KDR	MMP7	RAF1	TIMP1	ZWINT	

Table 4.1: Gene targets by the Neuroepithelial T1 PrimePCR™ Assay.

PrimePCR™ Disease state panels (Section 2.2.8) allow for an in-depth investigation of differentially expressed genes within Neuroblastoma. The targets on the panel are in line with the National Library of Medicine database (NLM 2018). Using cDNA from *Hu* gene knockdowns in the Neuroblastoma cell lines, SH-SY5Y and SK-N-AS, RT-qPCR of these panels facilitated initial screening of the genes. RT-qPCR data was analysed by the PrimePCR™ data analysis software provided by Bio-Rad.

4.7.1 Identification of mRNA target transcripts of *Hu* gene regulation in SH-SY5Y Neuroblastoma cells

The gene analysis of SH-SY5Y Neuroblastoma cells following *Hu* gene individual and combined knockdowns revealed a multitude of gene expression changes when compared to the non-target control. To identify the genes with the highest expression level changes, a set the threshold of 3 fold-cycle difference was applied.

siRNA Interference Target				
HuB	**HuC**	**HuD**	**HuR**	**Combined Hu**
IGFBP3	IGFBP3	IGFBP3	IGFBP3	IGFBP3
EGR1	EGR1	EGR1	EGR1	EGR1
			IL10	IL10
			ESR1	ESR1
BCL2			BCL2	
CCND2				CCDN2
	PROM1		FN1	COL1A1
			CXCL12	SERPIN
			MAPK3	
			IGFIK	
			SP1	
			NFKB2	
			VCAM1	

Table 4.2: Identification of targets for further gene analysis influenced by *Hu* gene knockdowns in Neuroblastoma cells SH-SY5Y. List of the 16 genes conforming to the criteria of a fold-change of at least 3. Highlighted genes are those consistent with two or more of the knockdown samples.

Of the 91 genes analysed shown in Table 4.2, there was 16 identified alterations consisting of both upregulated and downregulated expression of more than a 3.0 fold-change difference to the control non-targeting siRNA.

To further minimise the number of genes for analysis, targets expression that was affected by two or more *Hu* gene knockdowns were selected. Highlighted in blue in Table 4.2 are the six genes that conform to the criteria described above in the Neuroblastoma cell line SH-SY5Y.

Changes in *IGFBP3* and *EGR1* gene expression were consistent amongst all *Hu* gene knockdowns both individually and combined. *IL10* and *ESR1* gene expression was affected by HuR and combined Hu family knockdowns. *BCL2* expression changed upon *HuB* and *HuR* gene knockdowns whilst *CCND2* gene expression was affected by HuB and combined *Hu* family

knockdowns. A custom PrimePCR™ assay was designed to specifically target these genes to determine the extent of the *Hu* gene family in regulating these targets.

For each gene target, individual and combined *Hu* gene knockdown in SH-SY5Y cDNA was run with expression normalised to *β-Actin* and compared with the control non-target siRNA using the $2^{-\Delta\Delta Ct}$ method. Statistical significance was determined by a two-tailed t-test.

The relative fold-change in the transcript levels of B-cell lymphoma (*BCL2*) following knockdown of each *Hu* gene individually and in combination in the Neuroblastoma cell lines SH-SY5Y is displayed in Fig. 4.43. Gene expression was normalised to the non-target control.

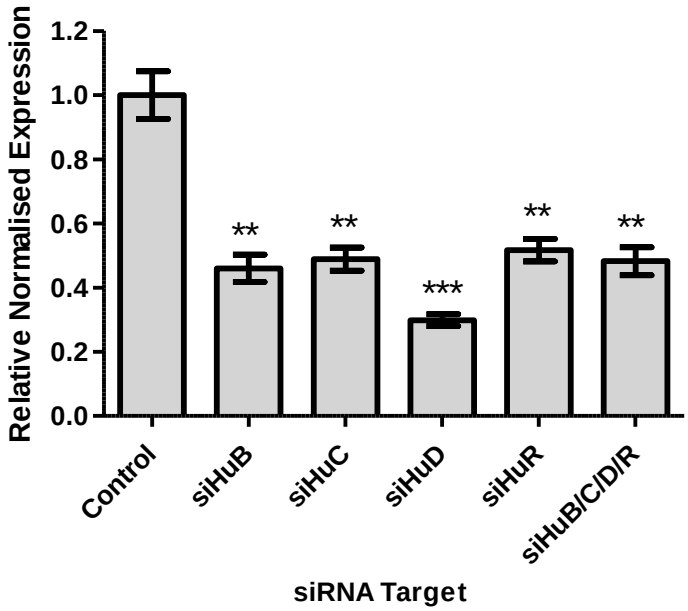

Figure 4.43: *BCL2* gene expression following individual and combined *Hu* gene family knockdowns in SH-SY5Y Neuroblastoma cells. *BCL2* gene expression was analysed by RT-qPCR in SH-SY5Y cells with siRNA interference of *HuB*, *HuC*, *HuD* and *HuR* both individually and in combination. The $2^{-\Delta\Delta Ct}$ results shown are an average of three replicates normalised to *β-Actin* and compared with the control non-target siRNA. Error bars display ± SEM. Statistical significance was calculated by a two-tailed t-test and is displayed by *P ≤ 0.05, **P ≤ 0.01, ***P ≤ 0.001. (n=3).

RT-qPCR revealed that there was statistically significant downregulation of *BCL2* gene expression in all knockdowns tested. An average decrease of 2.1-fold was observed for the siRNA interference of *HuB*, *HuC* and *HuR* and combination *Hu* gene when compared to the control. The highest knockdown was a 3.4-fold downregulation of *BCL2* mRNA level after knockdown of *HuD gene*.

Next, the expression of Cyclin D2 (*CCND2*) was analysed following *Hu* gene knockdowns (Fig. 4.44). Gene expression was normalised to *β-Actin* and compared with the control non-target siRNA.

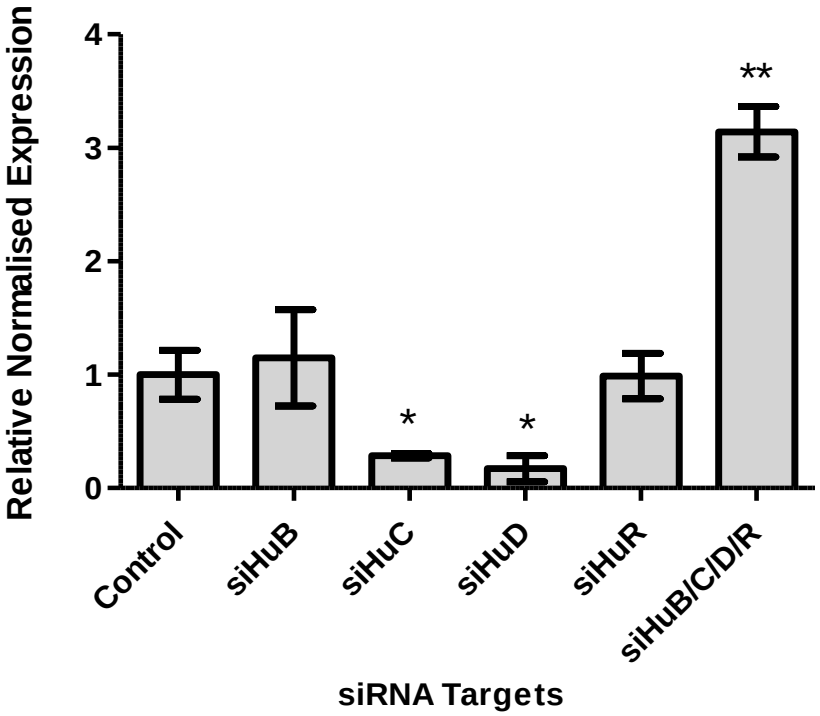

Figure 4.44: *CCND2* gene expression following individual and Hu family combined *Hu* gene knockdowns in SH-SY5Y Neuroblastoma cells. *CCND2* gene expression was analysed by RT-qPCR in SH-SY5Y cells with siRNA interference of *HuB*, *HuC*, *HuD* and *HuR* both individually and in combination. The $2^{-\Delta\Delta Ct}$ results shown are an average of three replicates normalised to *β-Actin* and compared with the control non-target siRNA. Error bars display ± SEM. Statistical significance was calculated by a two-tailed t-test and is displayed by *P ≤ 0.05, **P ≤ 0.01, ***P ≤ 0.001. (n=3).

The relative normalised expression of *CCND2* following siRNA interference of each *Hu* gene individually and in combination in the Neuroblastoma cell lines SH-SY5Y. RT-qPCR revealed a statistically significant downregulation of *CCND2* expression in *HuC* knockdown by 3.5-fold and in *HuD* knockdown, a downregulation of 5.8-fold. However, a statistically significant 2.1-fold increase of *CCND2* was observed after knockdown of all *Hu* genes in combination. *HuB* and *HuR* knockdown showed little change in *CCND2* gene expression.

Next, the expression of Early Growth Receptor 1 (*EGR1*) following siRNA interference of each *Hu* gene individually and in combination was analysed and is displayed in Fig 4.45.

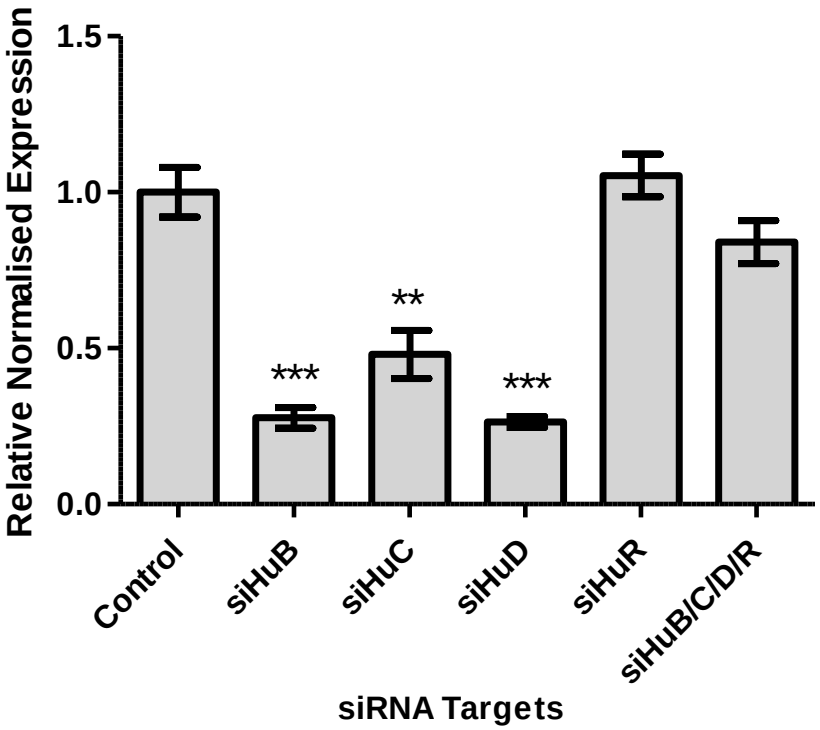

Figure 4.45: *EGR1* gene expression following *HuB*, *HuC* and *HuD*, *HuR* and combined *Hu* gene knockdowns in SH-SY5Y Neuroblastoma cells. *EGR1* gene expression was analysed by RT-qPCR in SH-SY5Y cells with siRNA interference of *HuB*, *HuC*, *HuD* and *HuR* both individually and in combination. The $2^{-\Delta\Delta Ct}$ results shown are an average of three replicates normalised to *β-Actin* and compared with the control non-target siRNA. Error bars display ± SEM. Statistical significance was calculated by a two-tailed t-test and is displayed by *P ≤ 0.05, **P ≤ 0.01, ***P ≤ 0.001. (n=3).

EGR1 gene expression was normalised to β-Actin and compared with the control non-target siRNA. *EGR1* expression levels were downregulated in SH-SY5Y cells with siRNA interference of *HuB*, *HuC* and *HuD* genes. After *HuB* knockdown, *EGR1* decreased by 3.7-fold, knockdown of *HuC* expression also resulted in a 2.1-fold down regulation and a *HuD* knockdown additionally showed a 3.8-fold decrease each of which was statistically significant. Little change was observed in *EGR1* gene expression following *HuR* and combined *Hu* family knockdowns.

Next, the expression of Estrogen Receptor 1 (*ESR1*) was analysed, the relative normalised gene expression is showed in Fig. 4.46.

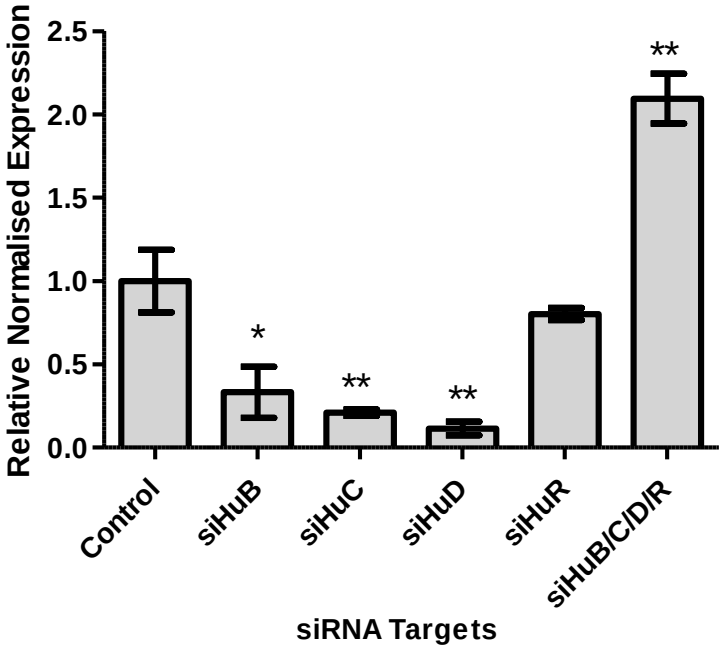

Figure 4.46: *ESR1* gene expression following individual and combined *Hu* gene family knockdowns in SH-SY5Y Neuroblastoma cells. *ESR1* gene expression was analysed by RT-qPCR in SH-SY5Y cells with siRNA interference of *HuB*, *HuC*, *HuD* and *HuR* both individually and in combination. The $2^{-\Delta\Delta Ct}$ results shown are an average of three replicates normalised to *β-Actin* and compared with the control non-target siRNA. Error bars display ± SEM. Statistical significance was calculated by a two-tailed t-test and is displayed by *P ≤ 0.05, **P ≤ 0.01, ***P ≤ 0.001. (n=3).

The relative normalised *ESR1* gene expression showed that after individual *Hu* gene knockdowns there was a decrease of *ESR1* expression when compared to the control. *ESR1* gene expression decreased following *HuB* knockdown by 3.0-fold, *HuC* knockdown by 4.8-fold and *HuD* knockdown by 8.7-fold, each were statistically significant. When the *Hu* genes were knocked down in combination, *ESR1* expression increased by 1.1-fold. No significant change was observed in *ESR1* expression upon *HuR* knockdown.

Next, the expression of Insulin-like growth factor-binding protein 3 (*IGFBP3*) was analysed following *Hu* gene knockdowns (Fig. 4.47).

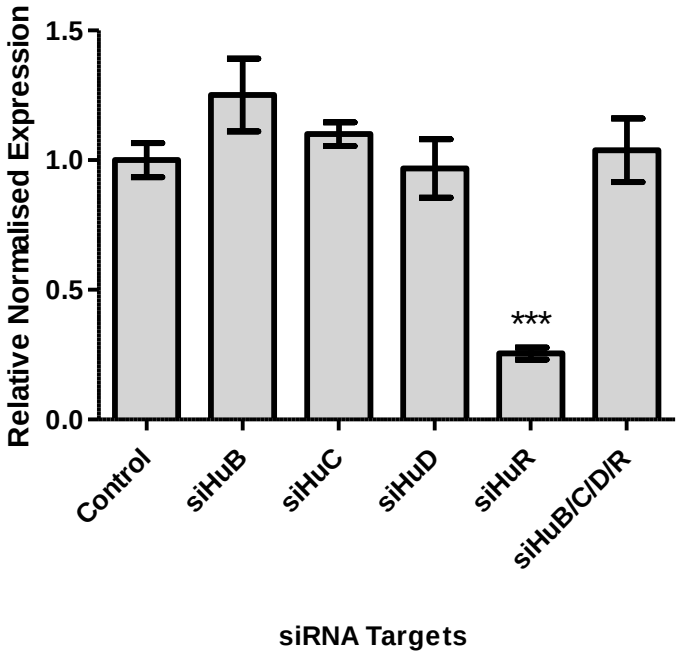

Figure 4.47: *IGFBP3* gene expression following individual and combined *Hu* gene family knockdowns in SH-SY5Y Neuroblastoma cells. *IGFBP3* gene expression was analysed by RT-qPCR in SH-SY5Y cells with siRNA interference of *HuB*, *HuC*, *HuD* and *HuR* both individually and in combination. The $2^{-\Delta\Delta Ct}$ results shown are an average of three replicates normalised to *β-Actin* and compared with the control non-target siRNA. Error bars display ± SEM. Statistical significance was calculated by a two-tailed t-test and is displayed by *P ≤ 0.05, **P ≤ 0.01, ***P ≤ 0.001. (n=3).

IGFBP3 gene expression was normalised to *β-Actin* and compared with the control non-target siRNA. RT-qPCR revealed a statistically significant downregulation of 3.9-fold in *IGFBP3* expression in *HuR* gene knockdown of SH-SY5Y cells. There was no significant difference in expression in all other knockdowns.

Next, the expression of Interleukin 10 (*IL10*) was analysed. The relative fold-change in the transcript levels of *IL10* expression following siRNA interference of each *Hu* gene individually and in combination in SH-SY5Y is displayed in Fig. 4.48. Gene expression was normalised to *β-Actin* and compared with the control non-target siRNA.

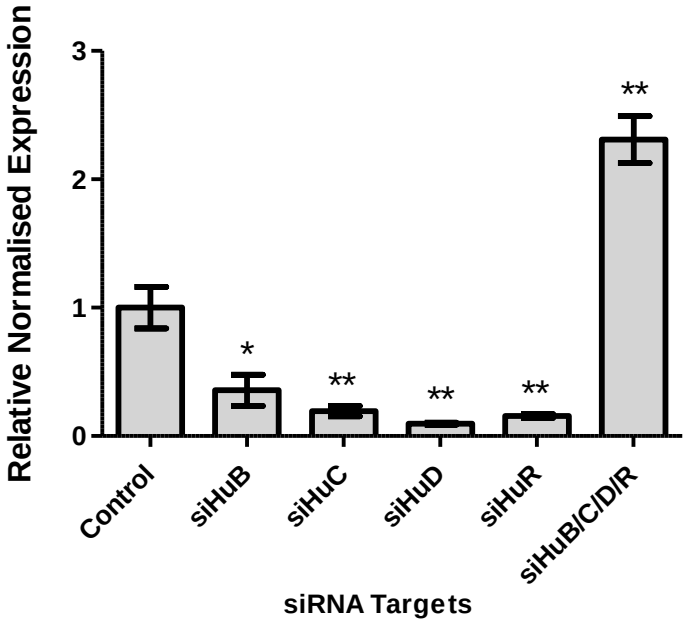

Figure 4.48: *IL10* gene expression following individual and combined *Hu* gene family knockdowns in SH-SY5Y Neuroblastoma cells. *IL10* gene expression was analysed by RT-qPCR in SH-SY5Y cells with siRNA interference of *HuB*, *HuC*, *HuD* and *HuR* both individually and in combination. The $2^{-\Delta\Delta Ct}$ results shown are an average of three replicates normalised to *β-Actin* and compared with the control non-target siRNA. Error bars display ± SEM. Statistical significance was calculated by a two-tailed t-test and is displayed by *P ≤ 0.05, **P ≤ 0.01, ***P ≤ 0.001. (n=3).

The relative normalised *IL10* gene expression, showed that after all individual *Hu* gene knockdowns, a decrease of *IL10* expression was observed when compared to the control. *HuB* siRNA interference decreased *IL10* expression by 2.8-fold, *HuC* siRNA interference showed a reduction of *IL10* expression by 5.1-fold, *HuD* siRNA interference resulted in a 10.4-fold decrease in *IL10* expression and *HuR* siRNA interference reduced it by 6.3-fold. When *Hu* genes were knocked down in combination, *IL10* expression increased by 1.3-fold. All changes to *IL10* gene regulation were statistically significant.

To summarise the expression of all the gene targets discussed above, a heat map was developed in Microsoft Excel using analysis from Biorad PrimePCR Analysis (Fig. 4.49).

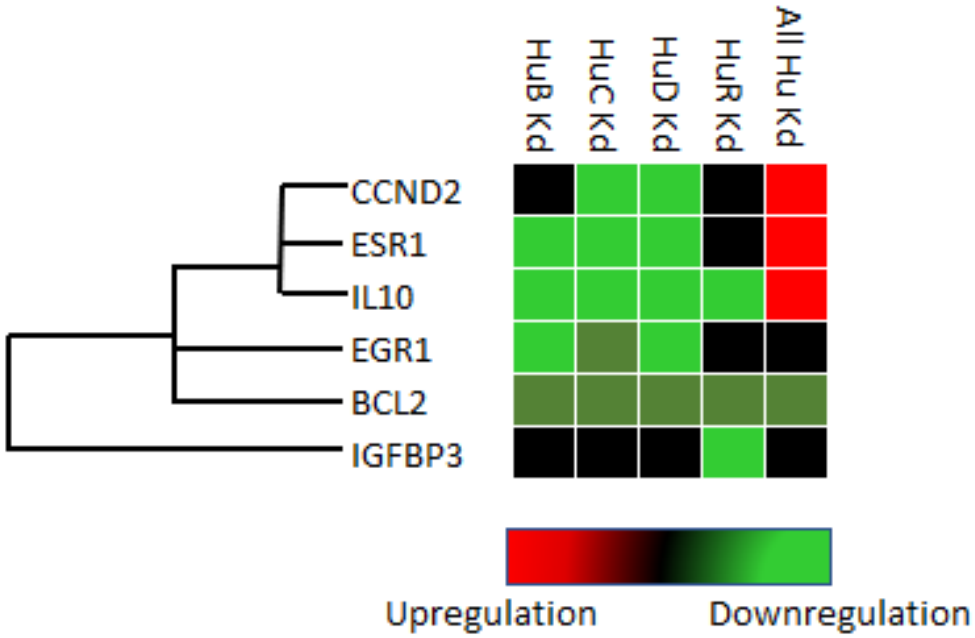

Figure 4.49: Heatmap of genes with differential expression in SH-SY5Y cells following *Hu* gene knockdowns individually and in combination. The relative gene expression data of multiple targets in each *Hu* gene knockdown individually and combined in SH-SY5Y. Targets are clustered according to their similarity in the gene expression pattern. (Up regulation; Red, Down regulation; Green, no change; Black, as shown by the key). The lighter the shade of colour, the greater the relative expression difference according to the magnitude of relative gene expression).

The heat map concludes that the most similarity was observed in the gene expression profiles of *CCND2*, *ESR1* and *IL10*. Knockdown of *HuC*, *HuD* and all *Hu* genes in combination for these profiles sees the same effect on the target genes expression. Of the *CCND2*, *ESR1*, *IL10* clustering, there was then a further 50% similarity to *EGR1* and *BCL2* with *HuB*, *HuD* and *HuC* knockdowns, which showed the same trend in the target gene expression. The least similarity was observed in the *IGFBP3* gene expression profile compared to the other target genes.

Interestingly, this heat map also highlights trends in the *Hu* knockdowns in the SH-SY5Y cells. Following *HuC* and *HuD* knockdown, five of the six gene targets expression decreased. *HuB* knockdown decreased its target gene expression in four of the genes. Also, all *Hu* genes knocked down in combination showed an increase in five of the target gene expression profiles including *CCND2*, *ESR1*, *IL10*, *EGR1*, and *IGFBP3*.

4.7.2 Identification of mRNA target transcripts of *Hu* gene regulation in SK-N-AS Neuroblastoma cells

Next, the targets displayed in Table 4.1 were screened by RT-qPCR following each *Hu* gene knockdown individually and in combination were in the second Neuroblastoma cell line, SK-N-AS. RT-qPCR data was analysed by the PrimePCR™ data analysis software provided by Bio-Rad.

The gene analysis of SK-N-AS Neuroblastoma cells following *Hu* gene individual and combined knockdowns revealed many gene expression changes when compared to the non-target control. Therefore, a threshold of 3.6 fold-cycle difference was set to maintain a more manageable number of genes to target for further analysis.

Of 91 genes named in Table 4.1, there were 35 genes that either became amplified, over-expressed or under-expressed and deleted by 3.6 fold-change difference in comparison to the control. These are summarised in Table 4.3.

siRNA Interference Target				
HuB	**HuC**	**HuD**	**HuR**	**Combined Hu**
MAPK3	MAPK3	MAPK3		
APOE	APOE	APOE		
FN1	FN1			
PRKCA	PRKCA			
CDK1	CDK1			
TOP2A	TOP2A			
CTGF	CTGF			
KRAS	KRAS			
GSTP1	GSTP1			
	EGR1	EGR1		
	MAP2K2	MAP2K2		
	TGFB1	TGFB1		
	BDNF	SERPINE1	UBC	PLAU
STAT3	GFB1	COL1A1	HLA-DRB1	
ATM	BCL2		PTEN	
RAF1	WNT5A			
VEGFA	IL10			
ITGB1	BRCA1			
MMP1	AURKA			
CCNB1				
PIK3CA				
COL1A2				

Table 4.3. Identification of targets for further gene analysis influenced by *Hu* gene knockdowns in Neuroblastoma cells SK-N-AS. The 35 genes conforming to the criteria of a fold-change of at least 3.6. Highlighted genes are those consistent with two or more of the knockdown samples.

To further minimise the number of genes for analysis, targets expression that was affected by two or more *Hu* gene knockdowns were selected. Highlighted in blue in Table 4.3 are the 12 genes that conform to the criteria described above in the Neuroblastoma cell line SK-N-AS.

MAPK3 and *APOE* gene expression changes were observed following *HuB*, *HuC* and *HuD* gene knockdowns. *FN1*, *PRKCA*, *CDK1*, *TOP2A*, *CTGF*, *KRAS* and *GSTP1* gene expression was affected by *HuB* and *HuC* knockdowns whilst, *EGR1*, *MAP2K2* and *TBFB1* expression was affected by *HuC* and *HuD* gene knockdowns. A custom PrimePCR™ assay was designed to specifically target these genes to determine the extent of the *Hu* gene family in regulating these targets.

For each gene target, individual and combined *Hu* gene knockdown in SH-SY5Y cDNA was run with expression normalised to *GAPDH* and compared with the control non-target siRNA using the $2^{-\Delta\Delta Ct}$ method. Statistical significance was determined by a two-tailed t-test.

First, the effect of single and combined *Hu* gene knockdown was assessed for the effects on Apolipoprotein E (*APOE*) expression. The relative fold-change in the transcript levels of APOE expression displayed in Fig. 4.50.

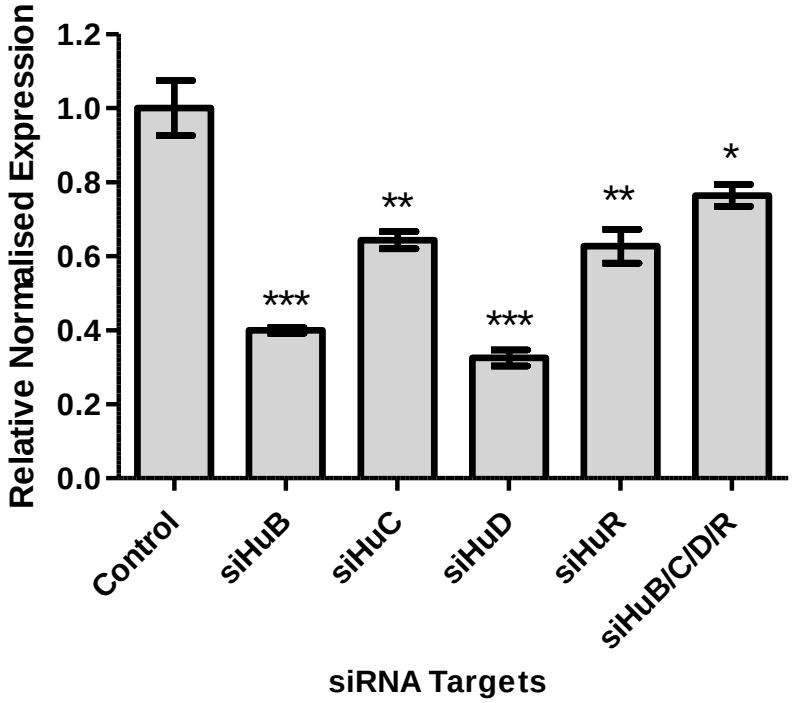

Figure 4.50: *APOE* gene expression following individual and combined *Hu* gene family knockdowns in SK-N-AS Neuroblastoma cells. *APOE* gene expression was analysed by RT-qPCR in SK-N-AS cells with siRNA interference of *HuB*, *HuC*, *HuD* and *HuR* both individually and in combination. The $2^{-\Delta\Delta Ct}$ results shown are an average of three replicates normalised to *GAPDH* and compared with the control non-target siRNA. Error bars display ± SEM. Statistical significance was calculated by a two-tailed t-test and is displayed by *P ≤ 0.05, **P ≤ 0.01, ***P ≤ 0.001. (n=3).

Apolipoprotein E expression decreased when all *Hu* genes were knocked down individually and combined in the SK-N-AS Neuroblastoma cell line. *APOE* expression decreased by 2.5-fold following *HuB* knockdown, 1.5-fold following *HuC* knockdown, 3.1-fold following *HuD* knockdown and 1.6-fold following *HuR* knockdown. Interestingly, the combined *Hu* family knockdown caused the lowest decrease expression in *APOE* by only 1.3-fold.

Next, the expression of Cyclin-dependent kinase 1 (*CDK1*) was analysed. The relative fold-change in the transcript levels of *CDK1* expression following siRNA interference of each *Hu*

gene individually and in combination in SK-N-AS is displayed in Fig 4.51. Gene expression was normalised to *GAPDH* and compared with the control non-target siRNA.

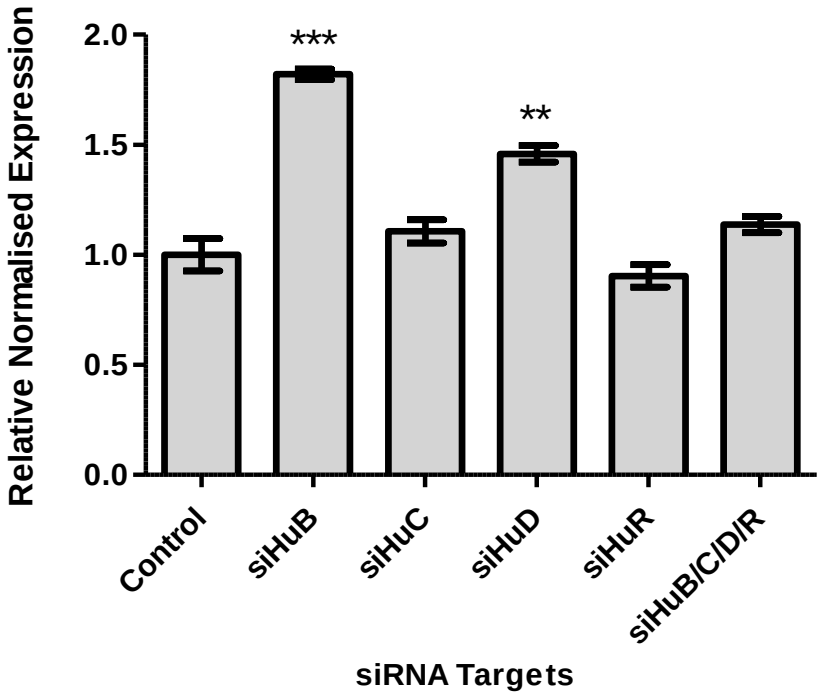

Figure 4.51: *CDK1* gene expression following individual and combined *Hu* gene family knockdowns in SK-N-AS Neuroblastoma cells. *CDK1* gene expression was analysed by RT-qPCR in SK-N-AS cells with siRNA interference of *HuB*, *HuC*, *HuD* and *HuR* both individually and in combination. The $2^{-\Delta\Delta Ct}$ results shown are an average of three replicates normalised to *GAPDH* and compared with the control non-target siRNA. Error bars display ± SEM. Statistical significance was calculated by a two-tailed t-test and is displayed by *P ≤ 0.05, **P ≤ 0.01, ***P ≤ 0.001. (n=3).

Kknockdown of *HuC* and *HuR* genes in SK-N-AS caused no significant change to Cyclin-dependent Kinase 1 (*CDK1*) gene expression. *HuB* siRNA interference induced an upregulation of *CDK1* expression by 0.8-fold, likewise *HuD* siRNA interference also increased *CDK1* expression by 0.5-fold. Combined *Hu* gene family knockdown resulted in a significant upregulation of *CDK1* by 0.1-fold.

Connective Tissue Growth Factor (*CTGF*) gene expression was analysed following siRNA interference of the *Hu* gene family in SK-N-AS cells (Fig 4.52). Gene expression was normalised to *GAPDH* and compared with the control non-target siRNA.

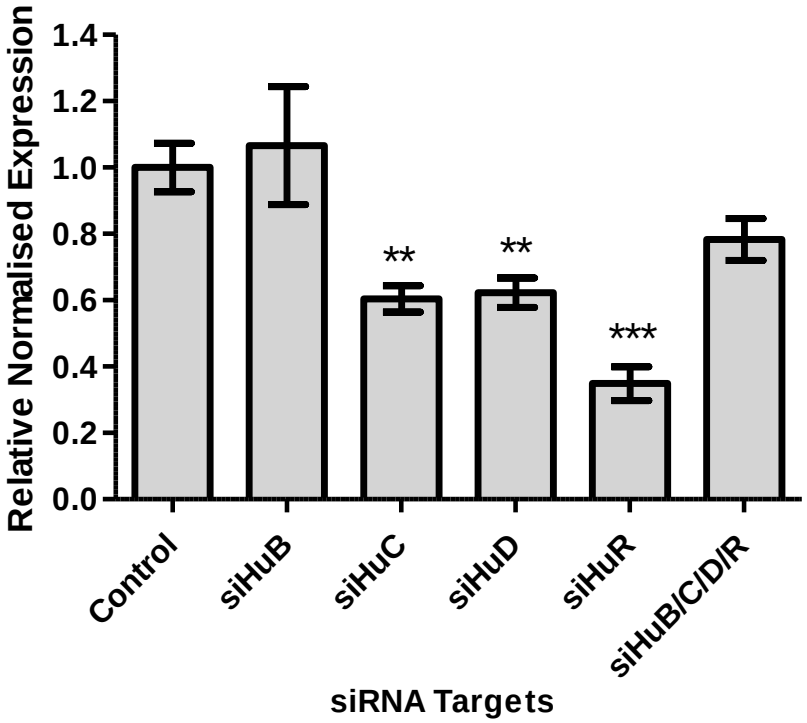

Figure 4.52: *CTGF* gene expression following *HuB*, *HuC*, *HuD* and *HuR* knockdowns and combined *Hu* gene family knockdowns in SK-N-AS Neuroblastoma cells. *CTGF* gene expression was analysed by RT-qPCR in SK-N-AS cells with siRNA interference of *HuB, HuC*, *HuD* and *HuR* individually and all *Hu* in combination. The $2^{-\Delta\Delta Ct}$ results shown are an average of three replicates normalised to *GAPDH* and compared with the control non-target siRNA. Error bars display ± SEM. Statistical significance was calculated by a two-tailed t-test and is displayed by *P ≤ 0.05, **P ≤ 0.01, ***P ≤ 0.001. (n=3).

Of the statistically significant data, *HuC*, *HuD* and *HuR* knockdowns all decreased *CTGF* gene expression by 1.7-fold, 1.6-fold and 2.9-fold respectively. HuB and Hu family combined gene knockdown did not show any statistical difference.

The next gene to be analysed is Early Growth Receptor 1 (*EGR1*) was analysed. The relative fold-change in the transcript levels of *EGR1* expression following siRNA interference of each *Hu* gene individually and combined in SK-N-AS cells is shown in Fig. 4.53. Gene expression was normalised to *GAPDH* and compared with the control non-target siRNA.

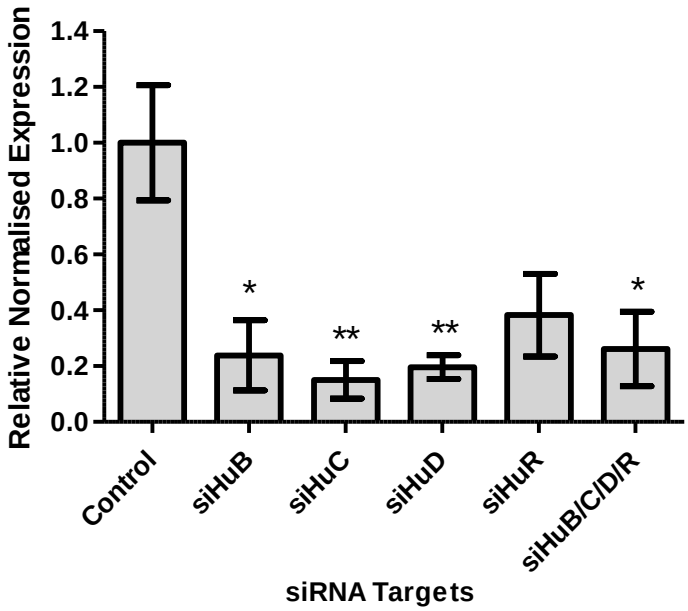

Figure 4.53: *EGR1* gene expression following individual and combined *Hu* gene family knockdowns in SK-N-AS Neuroblastoma cells. *EGR1* gene expression was analysed by RT-qPCR in SK-N-AS cells with siRNA interference of *HuB*, *HuC*, *HuD* and *HuR* both individually and in combination. The $2^{-\Delta\Delta Ct}$ results shown are an average of three replicates normalised to *GAPDH* and compared with the control non-target siRNA. Error bars display ± SEM. Statistical significance was calculated by a two-tailed t-test and is displayed by *P ≤ 0.05, **P ≤ 0.01, ***P ≤ 0.001. (n=3).

A reduction of *EGR1* gene expression was observed in all SK-N-AS cell samples varying with single or combined *Hu* gene knockdown. Of statistical significance was the reduction in *EGR1* expression by 6.6-fold following *HuC* knockdown down and 5.1-fold reduction following *HuD*

knockdown, whilst *Hu* genes knocked down in combination saw a reduction of *EGR1* expression by 3.8-fold.

Fibronectin 1 (*FN1*) gene expression was determined following siRNA interference of SK-N-AS cells (Fig 4.54). Gene expression was normalised to *GAPDH* and compared with the control non-target siRNA.

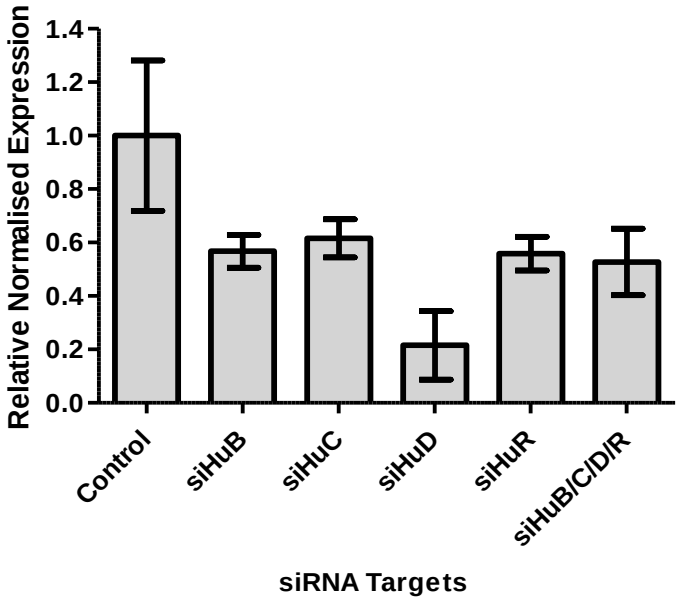

Figure 4.54: *FN1* gene expression following individual and combined *Hu* gene family knockdowns in SK-N-AS Neuroblastoma cells. *FN1* gene expression was analysed by RT-qPCR in SK-N-AS cells with siRNA interference of *HuB*, *HuC*, *HuD* and *HuR* both individually and in combination. The $2^{-\Delta\Delta Ct}$ results shown are an average of three replicates normalised to *GAPDH* and compared with the control non-target siRNA. Error bars display ± SEM. Statistical significance was calculated by a two-tailed t-test and is displayed by *P ≤ 0.05, **P ≤ 0.01, ***P ≤ 0.001. (n=3).

Fibronectin 1 gene expression decreased upon *Hu* gene knockdowns both individually and in combination in the Neuroblastoma cell line SK-N-AS. Whilst none were significant most likely

due to SEM in the control sample, all showed a reduction of at least 1.3-fold with *HuD* knockdown causing the greatest effect on *FN1* expression.

The effect of *Hu* gene siRNA interference on Glutathione S-Transferase Pi 1 (*GSTP1*) was determined in SK-N-AS cells and is shown in Fig. 4.55. Gene expression was normalised to *GAPDH* and compared with the control non-target siRNA.

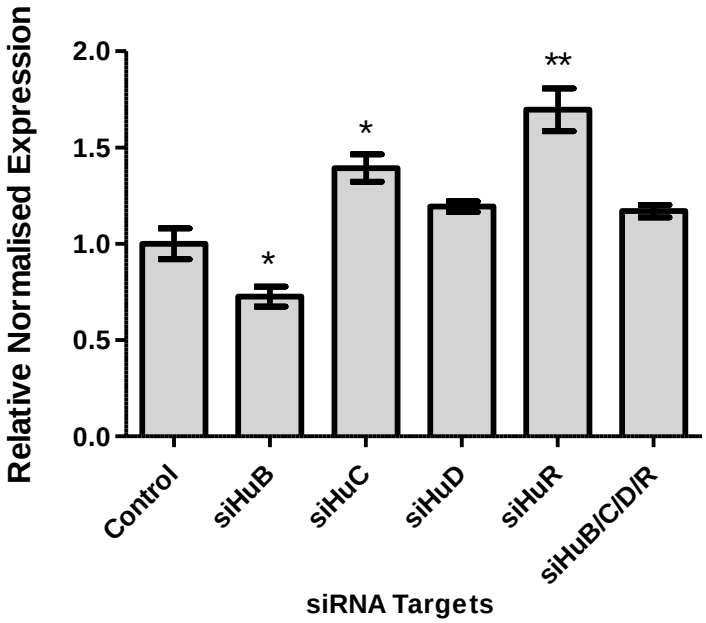

Figure 4.55: *GSTP1* gene expression following individual and combined *Hu* gene family knockdowns in SK-N-AS Neuroblastoma cells. *GSTP1* gene expression was analysed by RT-qPCR in SK-N-AS cells with siRNA interference of *HuB*, *HuC*, *HuD* and *HuR* both individually and in combination. The $2^{-\Delta\Delta Ct}$ results shown are an average of three replicates normalised to *GAPDH* and compared with the control non-target siRNA. Error bars display ± SEM. Statistical significance was calculated by a two-tailed t-test and is displayed by *P ≤ 0.05, **P ≤ 0.01, ***P ≤ 0.001. (n=3).

As seen in Fig. 4.55, a variable response was observed on Glutathione S-Transferase Pi 1 gene expression upon both individual and combination *Hu* gene knockdowns. *HuB* siRNA interference was the only knockdown to induce a decrease in *GSTP1* expression. In this

sample, *GSTP1* expression decreased by 1.4-fold. *HuC*, *HuD* and *HuR* siRNA interference saw an increased in *GSTP1* expression by 0.4-fold, 0.2-fold and 0.7-fold respectively. Additionally, when all *Hu* gene were knocked down in combination, an upregulation of 0.2-fold was observed in *GSTP1* gene expression.

The effect of *Hu* gene siRNA interference on Ki-ras2 Kirsten rat sarcoma viral oncogene homolog (*KRAS*) was determined in SK-N-AS cells and is shown in Fig. 4.56. Gene expression was normalised to *GAPDH* and compared with the control non-target siRNA.

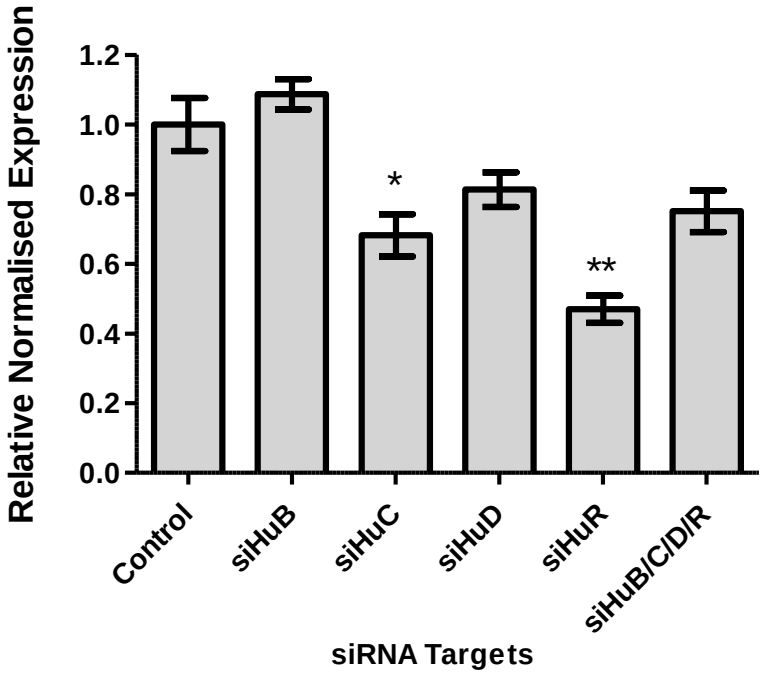

Figure 4.56: *KRAS* gene expression following individual and combined *Hu* gene family knockdowns in SK-N-AS Neuroblastoma cells. *KRAS* gene expression was analysed by RT-qPCR in SK-N-AS cells with siRNA interference of *HuB*, *HuC*, *HuD* and *HuR* both individually and in combination. The $2^{-\Delta\Delta Ct}$ results shown are an average of three replicates normalised to *GAPDH* and compared with the control non-target siRNA. Error bars display ± SEM. Statistical significance was calculated by a two-tailed t-test and is displayed by *P ≤ 0.05, **P ≤ 0.01, ***P ≤ 0.001. (n=3).

As seen in Fig. 4.56, a decrease in *KRAS* expression was observed for *HuC*, *HuD*, *HuR* and combined *Hu* gene knockdown. *KRAS* expression decreased significantly by 1.5-fold following *HuC* knockdown and 2.1-fold following *HuR* knockdown. *HuB*, *HuD* and combined *Hu* knockdown did not show any significant change to *KRAS* gene expression in the SK-N-AS cells.

Next, two members of the mitogen-activated kinase family were analysed, Mitogen-Activated Protein Kinase Kinase 2 (*MAP2K2* (Fig 4.57) and Mitogen-Activated Protein Kinase 3 *(MAPK3)* (Fig 4.58) for any change in gene expression following *Hu* gene knockdowns both individually and I combination. Gene expression was normalised to *GAPDH* and compared with the control non-target siRNA.

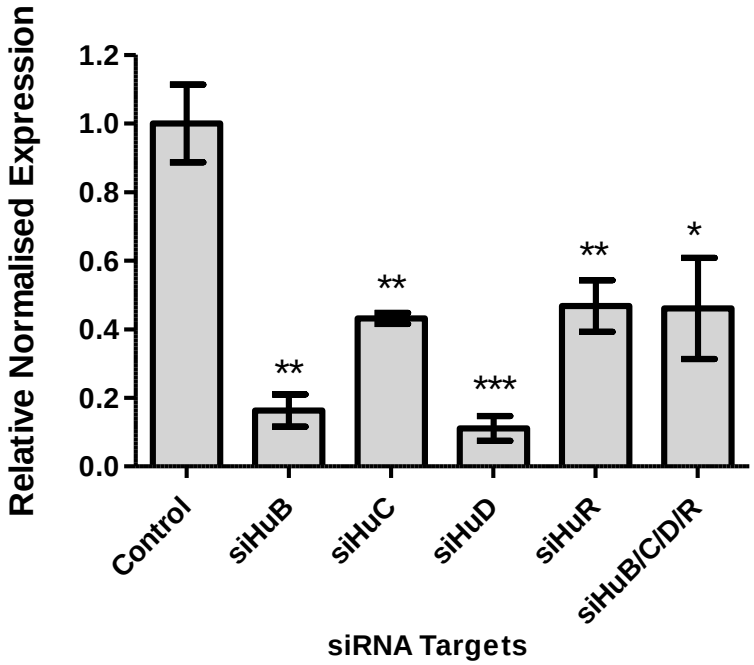

Figure 4.57: *MAP2K2* gene expression following individual and combined *Hu* gene family knockdowns in SK-N-AS Neuroblastoma cells. *MAP2K2* gene expression was analysed by RT-qPCR in SK-N-AS cells with siRNA interference of *HuB*, *HuC*, *HuD* and *HuR* both individually and in combination. The $2^{-\Delta\Delta Ct}$ results shown are an average of three replicates normalised to *GAPDH* and compared with the control non-target siRNA. Error bars display ± SEM. Statistical significance was calculated by a two-tailed t-test and is displayed by *P ≤ 0.05, **P ≤ 0.01, ***P ≤ 0.001. (n=3).

As seen in Fig. 4.57, the biggest reduction of Mitogen-Activated Protein Kinase Kinase 2 gene expression was observed in individual *HuB* and *HuD* knockdowns with a reduction of expression of 6.2-fold and 9.04-fold respectively. Upon *HuC* and *HuR* knockdown, *MAP2K2* expression decreased by 2.3-fold and 1.3-fold respectively. Combined *Hu* gene knockdown showed a reduction in *MAP2K2* expression of 2.2-fold.

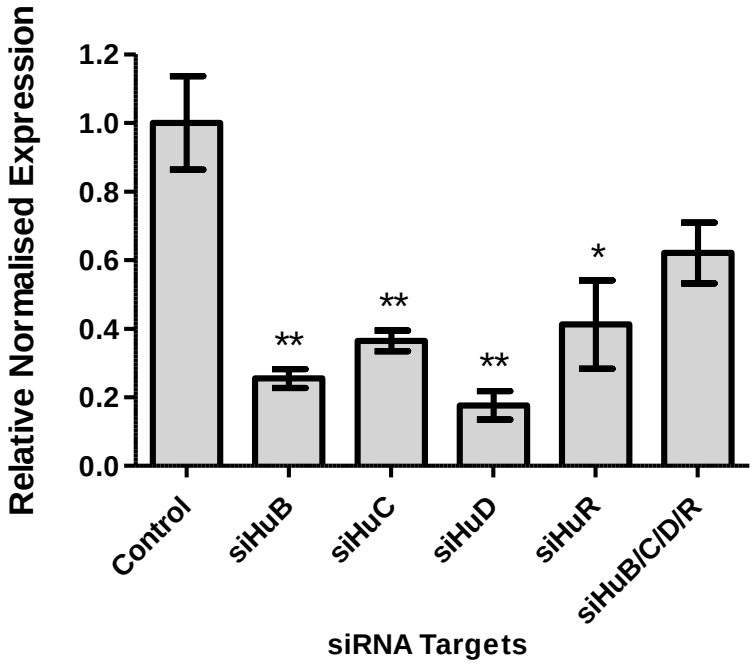

Figure 4.58: *MAPK3* gene expression following individual and combined *Hu* gene family knockdowns in SK-N-AS Neuroblastoma cells. *MAPK3* gene expression was analysed by RT-qPCR in SK-N-AS cells with siRNA interference of *HuB*, *HuC*, *HuD* and *HuR* both individually and in combination. The $2^{-\Delta\Delta Ct}$ results shown are an average of three replicates normalised to GAPDH and compared with the control non-target siRNA. Error bars display ± SEM. Statistical significance was calculated by a two-tailed t-test and is displayed by *P ≤ 0.05, **P ≤ 0.01, ***P ≤ 0.001. (n=3).

The expression profile of *MAPK3* gene expression following Hu individual and combined knockdowns. Like *MAP2K2*, the largest reduction in Mitogen-activated Protein Kinase 3 (*MAPK3*) gene expression was following *HuB* and *HuD* knockdown where expression

decreased by 3.6-fold and 5.7-fold respectively. *HuC* knockdown resulted in a 2.7-fold reduction in *MAPK3* expression whilst *HuR* knockdown showed a 2.4-fold decrease. Combined *Hu* gene knockdown showed the smallest effect on *MAPK3* expression although it still resulted in a 1.6-fold decrease.

An overall decreased of both kinases was observed upon single and combined *Hu* gene knockdowns in SK-N-AS cell line. Within this observation is a similar pattern for each sample whereby *HuB* and *HuD* knockdowns showed the most decrease in *MAP2K2* and *MAPK3* gene expression followed by *HuC*, *HuR* and combined *Hu* siRNA knockdowns in the SK-N-AS cell line.

Another member of the kinase family was analysed, Protein kinase C α (*PRKCA*). The relative fold-change in the transcript level expression following knockdowns of each *Hu* gene individually and combined shown in Fig 4.59. Gene expression was normalised to *GAPDH* and compared with the control non-target siRNA.

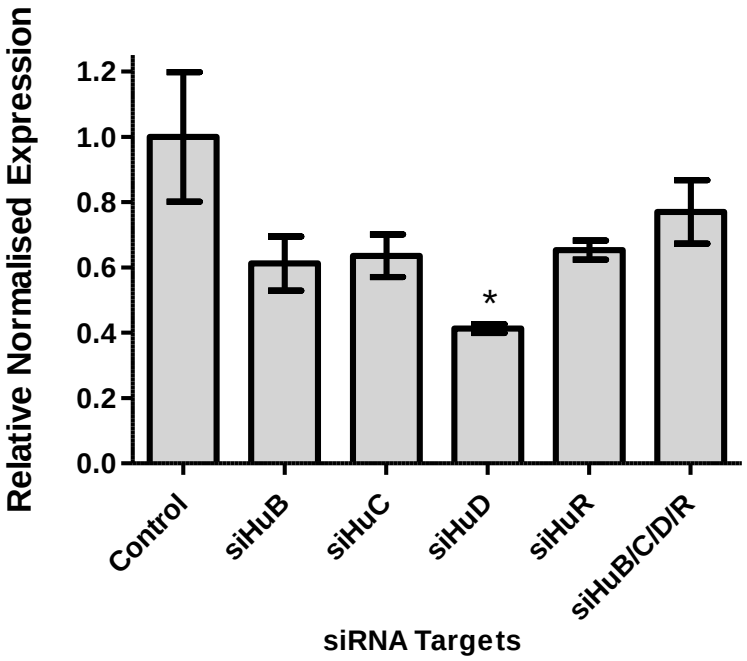

Figure 4.59: *PRKCA* gene expression following individual and combined *Hu* gene family knockdowns in SK-N-AS Neuroblastoma cells. *PRKCA* gene expression was analysed by RT-qPCR in SK-N-AS cells with siRNA interference of *HuB*, *HuC*, *HuD* and *HuR* both individually and in combination. The $2^{-\Delta\Delta Ct}$ results shown are an average of three replicates normalised to *GAPDH* and compared with the control non-target siRNA. Error bars display ± SEM. Statistical significance was calculated by a two-tailed t-test and is displayed by *P ≤ 0.05, **P ≤ 0.01, ***P ≤ 0.001. (n=3).

An overall reduction of Protein Kinase C Alpha gene expression upon *Hu* gene knockdowns. However, only *HuD* siRNA interference showed a significant effect of a 2.4-fold reduction in *PRKCA* gene reduction. Of the other *Hu* siRNA interference-induced SK-N-AS cells, an average 1.7-fold decrease in expression of *PRKCA* gene was observed.

The gene expression profile of Transforming growth factor beta 1 (*TGFB1*) (Fig 4.60) following *Hu* gene knockdowns was analysed. Gene expression was normalised to *GAPDH* and compared with the control non-target siRNA.

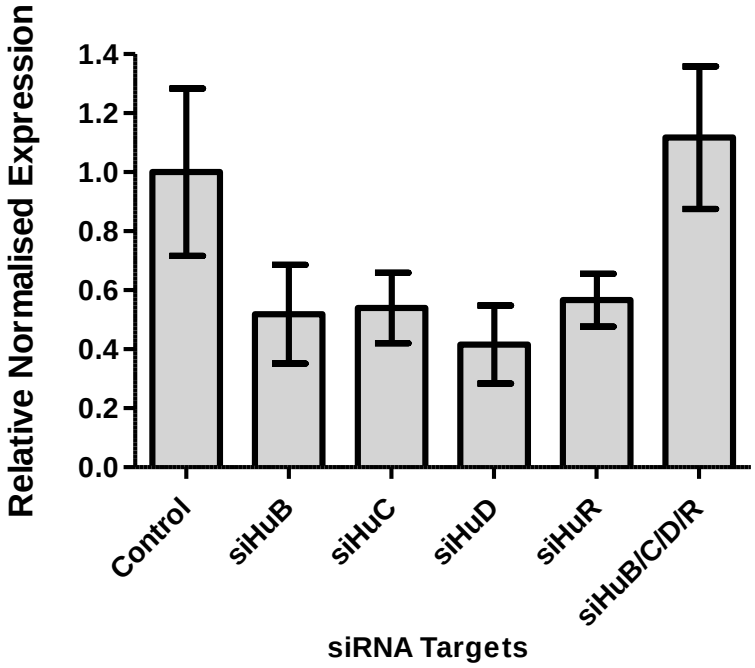

Figure 4.60: *TGFB1* gene expression following individual and combined *Hu* gene family knockdowns in SK-N-AS Neuroblastoma cells. *TGFB1* gene expression was analysed by RT-qPCR in SK-N-AS cells with siRNA interference of *HuB*, *HuC*, *HuD* and *HuR* and in combination. The $2^{-\Delta\Delta Ct}$ results shown are an average of three replicates normalised to *GAPDH* and compared with the control non-target siRNA. Error bars display ± SEM. Statistical significance was calculated by a two-tailed t-test and is displayed by *P ≤ 0.05, **P ≤ 0.01, ***P ≤ 0.001. (n=3).

There was no significant change in *TGFB1* gene expression following *Hu* gene knockdowns although a general observation showed a large decrease when all *Hu* genes were knocked down individually. If the *TGFB1* gene expression SEM would have been more accurate the results may well have represented a significant change.

DNA Topoisomerase II Alpha (*TOP2A*) gene expression was analysed following *Hu* gene knockdowns and is displayed in Figure 4.61. Gene expression was normalised to *GAPDH* and compared with the control non-target siRNA.

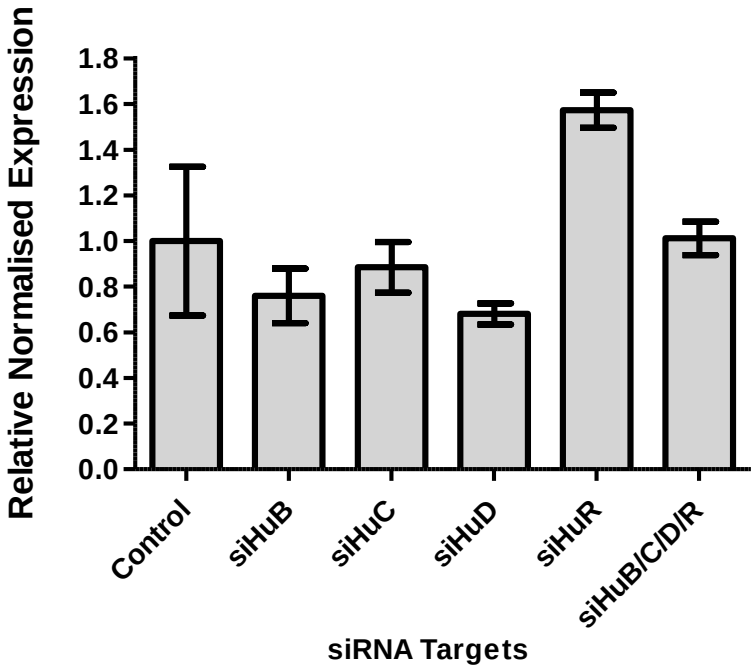

Figure 4.61: *TOP2A* gene expression following individual and combined *Hu* gene family knockdowns in SK-N-AS Neuroblastoma cells. *TOP2A* gene expression was analysed by RT-qPCR in SK-N-AS cells with siRNA interference of *HuB*, *HuC*, *HuD* and *HuR* and in combination. The $2^{-\Delta\Delta Ct}$ results shown are an average of three replicates normalised to *GAPDH* and compared with the control non-target siRNA. Error bars display ± SEM. Statistical significance was calculated by a two-tailed t-test and is displayed by *P ≤ 0.05, **P ≤ 0.01, ***P ≤ 0.001. (n=3).

As seen in Fig. 4.61, there was no significant change in expression of *TOP2A*. Variation was observed in the *TOP2A* gene expression up on *HuD* and *HuR* RNA interference but was not significant. *HuD* knockdown resulted in a decreased *TOP2A* expression by 1.5-fold. *HuR* interference showed an increased expression of *TOP2A* by 0.6-fold.

To summarise the expression of all the gene targets discussed above, a heat map was developed in Microsoft Excel using analysis from Biorad PrimePCR Analysis (Fig 4.62).

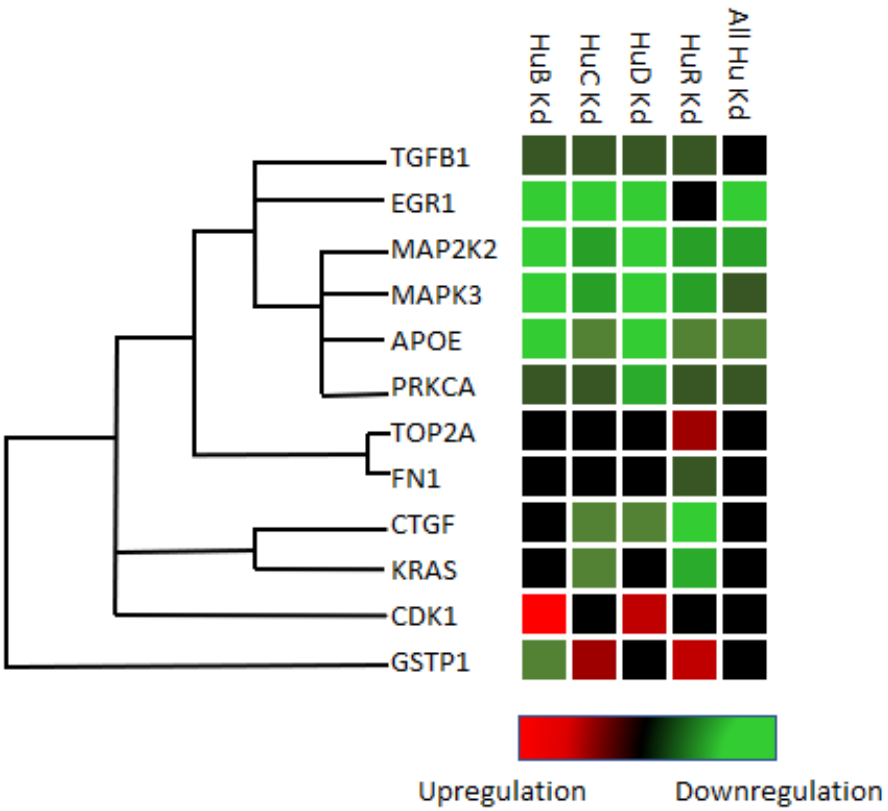

Figure 4.62: Heatmap of genes with differential expression in SK-N-AS cells following *Hu* gene knockdowns individually and in combination. The relative gene expression data of multiple target in each *Hu* gene knockdown in SK-N-AS. Targets are clustered according to their similarity in the gene expression pattern (Up regulation; Red, Down regulation; Green, no change; Black, as shown by the key). The lighter the shade of colour, the greater the relative expression difference according to the magnitude of relative gene expression).

The heatmap concludes the most similarity was observed between the gene expression profiles of the protein kinases *MAP2K2* and *MAPK3* along with *APOE* and *PRKCA*. Their expression profiles for each *Hu* knockdown in SK-N-AS was almost identical. Likewise, TOP2A and FN1 shared a high similarity. *EGR1* showed similar homology to *TGFB1.* These groups of targets shared about 30% similarity with *CTGF, KRAS* and *CDK1* in their expression profiles following *Hu* gene knockdowns. Importantly, *GSTP1* did not show any expression homology reflecting the greater divergence in the relationship to the other targets.

This heatmap clearly displays similarities within each *Hu* knockdown in that *HuB* and *HuD* knockdown resulted in a downregulation in 7 of the 12 genes analysed. *HuC* and *HuR* knockdown resulted in a downregulation in 8 of the 12 genes analysed.

4.7.3 Genes affected by *Hu* gene regulation in Neuroblastoma

To summarise the roles the genes targeting by Hu RNA-binding proteins have in cancer the pie chart displayed Fig. 4.63 was drawn.

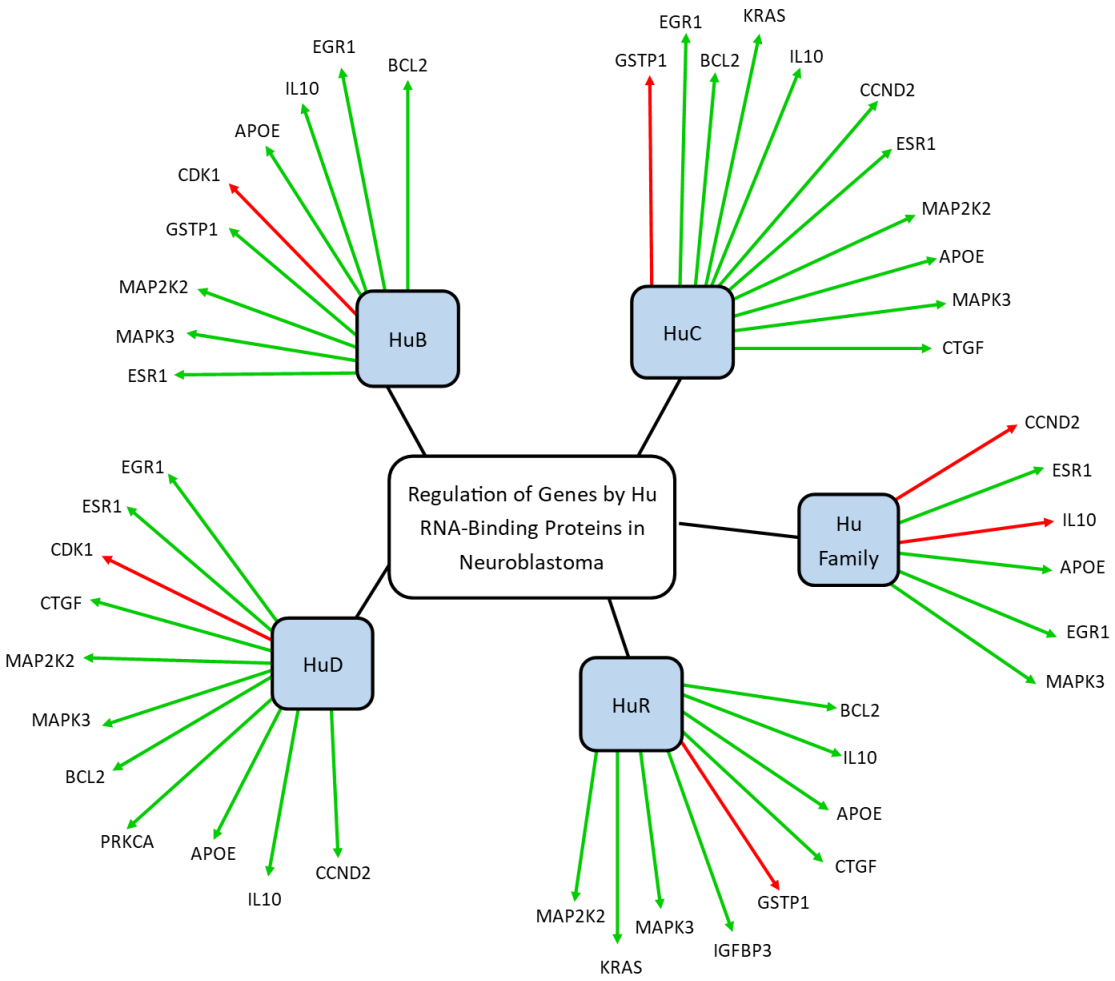

Figure 4.63 Map of *Hu* gene regulation targets identified through *Hu* gene knockdowns. The individual targets of each Hu protein individually and combined. Positive regulation is represented by a green arrow whilst negative regulation is shown by a red arrow.

The genes are separated into categories of the well-defined cancer hallmarks; Enhanced cell survival through self-sufficiency in growth signals, Enhanced cell proliferation through insensitivity to anti-growth signals evading apoptosis to produce limitless replication potential, Elevation of local angiogenesis, Evasion of immune response, Tissue invasion and metastasis and Reprogramming of energy metabolism.

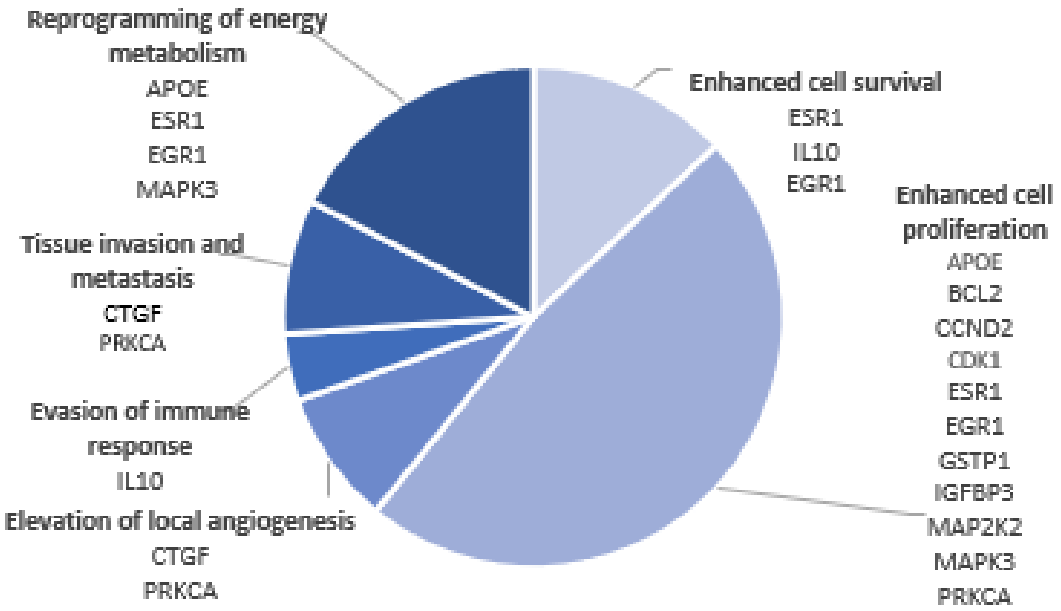

Figure 4.64: Categorisation of the statistically significant collective regulation of the Hu RNA-protein family in the Neuroblastoma cell like SH-SY5Y. mRNA targets of *Hu* gene regulation grouped by cancer hallmarks; Reprogramming of energy metabolism, tissue invasion and metastasis, evasion of the immune resonse, elevation of local angiongensis, enhanced cell survival and enhanced proliferation.

The pie chart displayed in Fig. 4.64 showed 49% of the genes collectively controlled by the Hu protein family are those involved in the enchanced cell survival group. 17% of the genes analysed were involved in the reprogramming of energy metablism, followed by 13% of the targets involved in enhanced cell survival. 9% of the genes were involved in tissue invasion

and metastasis and elevation of local angiogenesis. 4% of the gene targets were involved in evading the immune response.

4.8 Summary

There are several conclusions that can be drawn from the results present in this chapter. Gene expression data showed an upregulation of all neuronal *Hu* genes, *HuB*, *HuC*, *HuD* in the Neuroblastoma cells lines in comparison to the control astrocyte cell line. Upregulation of the ubiquitously expressed *HuR* was observed in one of the two Neuroblastoma cells SH-SY5Y. Secondly, regulatory influences amongst Hu proteins was proven. This level of regulatory influences was variable between the two Neuroblastoma cell lines SH-SY5Y and SK-N-AS. And finally, to identify targets that the Hu family of RNA-binding proteins control resulting in the development of cancer, following *Hu* gene individual and combined knockdowns, several mRNA transcripts were found to change their expression level identifying Hu's role at a genetic level. This confirms *Hu* genes participate in the regulation of these targets which is discussed in more detail below.

With an overall higher expression of the Hu family of RNA-binding proteins, SH-SY5Y Neuroblastoma cells showed an upregulation of all *Hu* genes whilst SK-N-AS showed upregulation of the neuronal Hu family members *HuB*, *HuC* and *HuD* only. Of the neuronal *Hu* members upregulated, the SH-SY5Y showed an overall higher expression in comparison to the other SK-N-AS cell line.

		Hu Protein											
Cell type	Cell line	HuB			HuC			HuD			HuR		
		PCR	WB	IF	PCR	WB	IF	PCR	WB	IF	PCR	WB	IF
Normal Astrocytes	SVGp12			B			B						B
Neuroblastoma	SK-N-AS			N			C			C			N
	SH-SY5Y			B			C			C			C

Table 4.4: Overall expression of HuB, HuC, HuD and HuR proteins in cell lines of normal astrocytes and Neuroblastoma cells. Each method of analysis including RT-qPCR (PCR), western blotting (WB) and immunofluorescent staining (IF) is shown. Green represents a positive result. Also shown is the localisation of the proteins determined through immune fluorescence cytoplasm is shown by C, the nucleus is represented by N, whilst B refers to both the cytoplasm and the nucleus.

Whilst gene expression analysis is important, equally as valuable is the translation of these genes into a functional protein product. Western blot analysis confirmed HuB and HuC proteins were expressed in all cell lines representative of normal astrocytes and Neuroblastoma, whilst HuD and HuR proteins were only detected in the Neuroblastoma cell lines.

The normal astrocytes cell line SVG p12 had the highest levels of HuB and HuC protein expression when normalised to the control GAPDH and compared to the Neuroblastoma cells. Based on the explanation of band sizes, HuB protein was detected as a monomer and dimer in the normal astrocytes and only as a dimer in the Neuroblastoma cells. Similarly, HuC protein was detected as a monomer and multimer in the normal astrocytes and only as a multimer in the Neuroblastoma cells. HuD protein was absent in normal astrocyte but present in the

Neuroblastoma cells. HuR protein detected by western blot at a low level in normal astrocytes when compared to the Neuroblastoma.

Studies of Hu protein localisation in astrocyte cells revealed HuB, HuC and HuR proteins were mainly localised in the nucleus of the cells with a lower presence in the cytoplasm. There was no detectable expression of HuD protein confirming western blot analysis.

In the Neuroblastoma cells, HuB protein was found predominantly localised to the nucleus although a faint staining revealed a low expression in the cytoplasm of the SK-N-AS cell line. HuC and HuD proteins were localised to the cytoplasm in both Neuroblastoma cell lines whilst HuR protein was found in the nucleus of the SK-N-AS cells and in the cytoplasm of SH-SY5Y cells.

Optimisation experiments for siRNA transfection efficiency showed DharmaFECT I most suitable for SH-SY5Y cells and JETprime for SK-N-AS cells. Knockdown efficiency was determined through RT-qPCR whilst protein knockdown was confirmed by western blotting. Higher efficiency was achieved when all *Hu* genes were knocked down together that could be explained by a regulatory mechanism within the *Hu* family.

Knockdown of *Hu* genes in Neuroblastoma cell lines, established a regulatory mechanism within the Hu family. The observed interplay between the different Hu proteins when individually or together knocked down resulted in two cell line-specific models displayed in Fig. 4.19 and Fig. 4.23. The described findings in Section 4.7, is in alignment with the known molecular heterogeneity within this disease. Of the since the only significant similarity within the two models is that following downregulation of HuC and HuR increases. However, the regulation observed by each Hu family members showed the extent of regulation that is

feasible. Three theories were proposed to explain the traits of regulatory influences observed; A compensatory effect where *Hu* gene family members become more expressed to compensate for each other's reduced expression. A regulatory mechanism in which Hu family members actively bind to *Hu* mRNA transcripts to regulate their expression during Hu reduced expression, a family member may also show decreased expression or become more expressed dependent on the effects of the *Hu's* RNA stabilisation effect on the transcript. Additionally, the changes observed could be due to off-target effects of *Hu* gene downregulation on certain pathways.

The assessed motility of the cell lines prior to knockdown experiments showed the two Neuroblastoma cell lines had a greater migrative potential than the normal astrocytes highlighting the Neuroblastoma cells have a more motile, invasive phenotype.

The knockdown of *Hu* genes individually and in combination showed no change to morphology in both Neuroblastoma cell lines. Significant changes were observed to cell viability only in the SH-SY5Y cell line. An increase in cell viability was observed following *HuB*, *HuC*, *HuR* and combined *Hu* knockdown in SH-SY5Y cells.

SH-SY5Y cells adopted a more migrative phenotype when *HuB*, *HuC* and *HuR* were knocked down individually and when *Hu* genes were knocked down in combination. SK-N-AS cells also saw an increase in migration following HuB knockdown.

Initial gene screening studies using pre-designed PrimePCR™ plates with genes thought to influence disease progression in Neuroepithelial cancers. Targets were identified for further analysis of gene expression change following individual and combined *Hu* siRNA interference. Due to the distinct variability in gene expression change of targets between the two

Neuroblastoma cell lines highlighted throughout these studies, the two cells lines were treated as individual models to identification of novel targets.

The influence of *Hu* gene regulation can be concluded as follows. Gene expression profiling of the 6 selected genes in SH-SY5Y Neuroblastoma cells revealed that individual and combined *Hu* gene knockdowns resulted in a reduction of *BCL2* gene expression. *CCND2* gene expression decreased following *HuC* and *HuD* individual knockdowns but increased following combined *Hu* gene knockdown. *EGR1* expression decreased following *HuB*, *HuC* and *HuD* individual gene knockdowns. *ESR1* expression decreased following individual *HuB*, *HuC* and *HuD* gene knockdowns and increased following combined *Hu* gene knockdown. The expression of *IGFBP3* was only affected during *HuR* knockdown, where its expression was reduced. Individual knockdowns of *Hu* gene observed a decrease in *IL10* gene expression. An increase in *IL10* gene expression was found following combined *Hu* gene knockdown. The heatmap for this data concluded that *HuC* and *HuD* have the largest effect on the expression of these chosen genes.

Of the 12 genes analysed in SK-N-AS cells, *APOE* and *MAP2K2* gene expression reduced following individual and combined *Hu* gene knockdowns. *CDK1* gene expression increased following *HuB* and *HuD* gene knockdowns. *CTGF* gene expression reduced following *HuC*, *HuD* and *HuR* gene knockdowns. *EGR1* gene expression decreased following *HuB*, *HuC* and *HuD* gene knockdowns, which is consistent with the SH-SY5Y cell lines. Combined *Hu* knockdown also resulted in an *EGR1* expression decrease. *GSTP1* expression decreased following *HuB* knockdown but increased following *HuC* and *HuR* gene knockdowns. *KRAS* gene expression decreased after *HuC* and *HuR* gene knockdowns. *MAPK3* gene expression decreased following all *Hu* individual gene knockdowns. *PRKCA* showed a reduced gene expression following *HuD*

gene knockdown. The overall heat map of this data revealed HuC and HuD followed closely by HuB as major players in the gene regulation of these targets.

The targets from both gene models were combined to show the extent of *Hu* gene regulation in Neuroblastoma. Their categorisation in cancer hallmarks concluded majority of the targets are involved in enhancing cell proliferation.

Importantly, highlighted consistently throughout these studies is the cellular and molecular variability typical of the heterogeneity in the Neuroblastoma cell lines used.

Chapter 5

Results

Part III: Expression of Hu proteins in Glioblastoma

Glioblastoma remains the most common and most malignant brain tumour, responsible for 2.5% of all cancer-related deaths (Hanif et al. 2017). HuR overexpression in Glioblastoma was initially reported by Nabors et al. (2001). Later, studies showed HuR localisation in Glioma cells influences its role within the cells and its function in developing the cancer. It was reported that HuR in Glioma is often present in the cytoplasm influencing a more malignant phenotype and therefore a poorer prognosis (Filippova et al. 2011).

Whilst some molecular targets of HuR in Glioblastoma have been identified e.g. *MSI1* (Vo et al. 2012), the extent of target transcripts of the ubiquitously expressed HuR and the neuronal Hu proteins, HuB, HuC and HuD are yet to be determined. These studies aim to identify the roles of these proteins in tumour initiation or development through their influence on molecular pathways.

This experiment focussed on building an expression profile of these Hu proteins in a Glioblastoma multiforme cell line and using a normal astrocyte cell line as a control. Knockdown studies of each Hu protein in the Glioblastoma multiforme cell lines were established to determine any specific effects on molecular pathways. The following cell lines were selected as suitable models to investigate Hu proteins in Glioblastoma; SVG p12 for normal astrocytes and U87-MG for Glioblastoma.

5.1 *Hu* gene expression in Glioblastoma and normal astrocytes

The gene expression level of all Hu proteins in Glioblastoma U87-MG cells and normal astrocytes SVG p12 were determined using quantitative RT-qPCR (described in Section 2.26). HuB (1), HuC (1), HuD (6), HuR (2) and β-Actin primer sequences are listed in Table 2.3 of Section 2.27. The fold-change of expression was analysed by comparing expression levels to the normal astrocyte cell line SVG p12. *β-Actin* was used as a housekeeping gene to normalise *Hu* expression. Statistical significance was calculated by a two-tailed t-test.

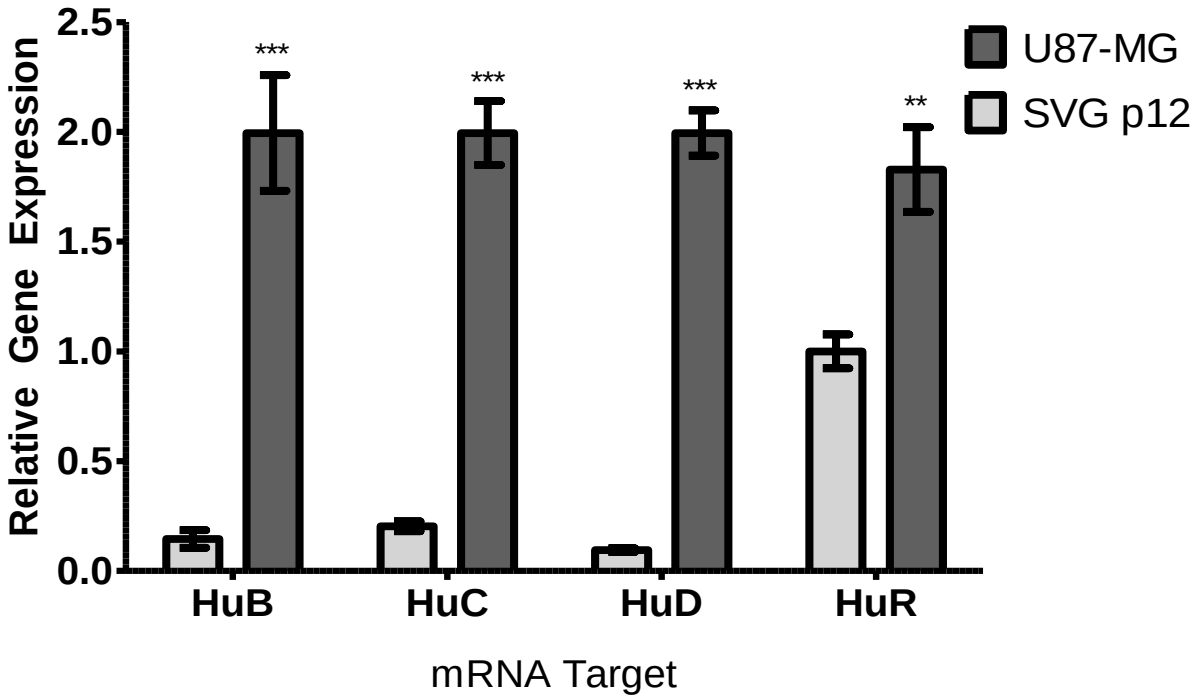

Figure 5.1: Gene expression of all the *Hu* protein family members Glioblastoma compared to normal astrocytes. *HuB*, *HuC*, *HuD* and *HuR* gene expression was analysed by RT-qPCR in Glioblastoma cells U87-MG and normal astrocytes SVG p12. The $2^{-\Delta\Delta Ct}$ results shown are an average of three replicates normalised to *β-Actin*. Error bars display ± SEM. Statistical significance was calculated by a two-tailed t-test and is displayed by *P ≤ 0.05, **P ≤ 0.01, ***P ≤ 0.001. (n=3).

The relative fold-change in the transcript levels of all *Hu* genes in the Glioblastoma cell line in comparison to the normal astrocyte cell line is displayed in Fig. 5.1. The normal astrocytes

expressed a low level of *HuB*, *HuC* and *HuD* gene, whilst *HuR* was expressed at higher levels. The data concludes all *Hu* genes were upregulated in the U87-MG Glioblastoma cell lines.

A 1.85 fold-increase of *HuB* gene expression was observed in U87-MG cells when compared to the SVG p12 normal astrocyte cell line. A similar expression increase was observed for *HuC* and for *HuD* by a 1.79 and 1.9 fold-change respectively. *HuR* gene expression showed a smaller 0.83 fold-increase in U87-MG cells compared to SVG p12 cells.

5.2 Hu protein expression and localisation in Glioblastoma and normal astrocytes

Gene expression studies at RNA level do not necessarily reflect the abundance of the protein product. Therefore, Western blot analysis (described in Section 2.3) was used to determine the protein expression in the Glioblastoma cell line, U87-MG and normal astrocyte cells, SVG p12. Astrocyte cells were also used as a control for Neuroblastoma studies in Chapter 4. Western blot analysis confirmed the presence of HuB and HuC proteins in the SVG p12 normal astrocyte cell line. Low expression of HuR was also observed with a distinct absence of HuD expression in the normal astrocytes.

The Hu protein family have been shown to shuttle between the nucleus and the cytoplasm (Doller et al. 2008b). Its subcellular location particularly in the cytoplasm has shown correlation with a poorer prognosis in Glioblastoma (Filippova et al. 2011). Therefore, immunofluorescence staining (Section 2.4.1) and fluorescent microscopy was used to determine the localisation of each Hu protein in Glioblastoma cells and astrocytes.

5.2.1 HuB protein expression

HuB protein expression was confirmed using western blotting (Section 2.3). Protein extracted from Glioblastoma cells and normal astrocytes were analysed for the presence of HuB protein with anti-HuB IgG. Anti-GAPDH IgG was used to detect GAPDH as a control protein.

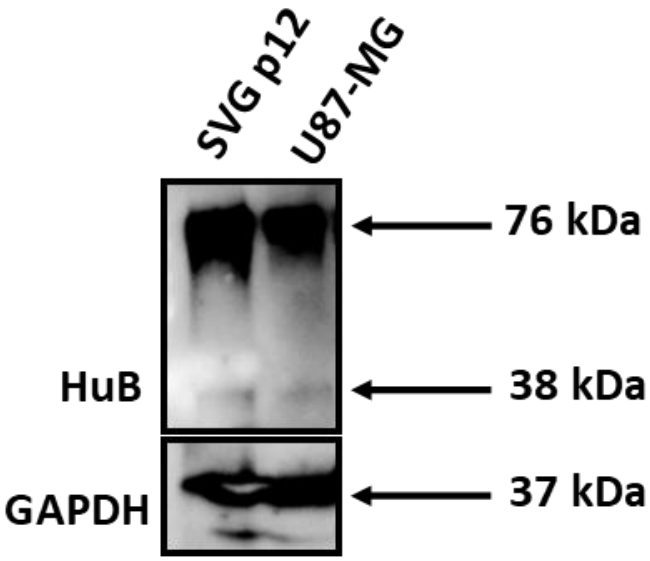

Figure 5.2: Representative western blot analysis of HuB protein with anti-HuB antibody. HuB and GAPDH protein expression in normal astrocytes SVG p12, and Glioblastoma cells U87-MG. GAPDH protein expression was used as a loading control. (n=3).

As shown in Fig. 4.2, HuB protein was detected in the normal astrocytes SVG p12 and Glioblastoma cells U87-MG. There is a faint band at 38kDa for each cell line and a higher migrating band at 76kDa which could be explained as a HuB dimer. A signal at 76kDa was also observed in Neuroblastoma cells (Fig. 4.2). GAPDH protein detection was used as a loading control and was detected at the expected size of 37kDa.

The signal intensity of GAPDH was comparable in both cells as well as for HuB. This differs from the gene expression profile displayed of HuB at RNA level (Fig. 5.1) where HuB protein was upregulated in the Glioblastoma cell line.

Subcellular localisation of HuB protein was determined for the Glioblastoma and normal astrocyte cell lines. Anti-HuB IgG was used with secondary Alexa green 488 FITC IgG. Cells were counterstained with DAPI nucleus stain.

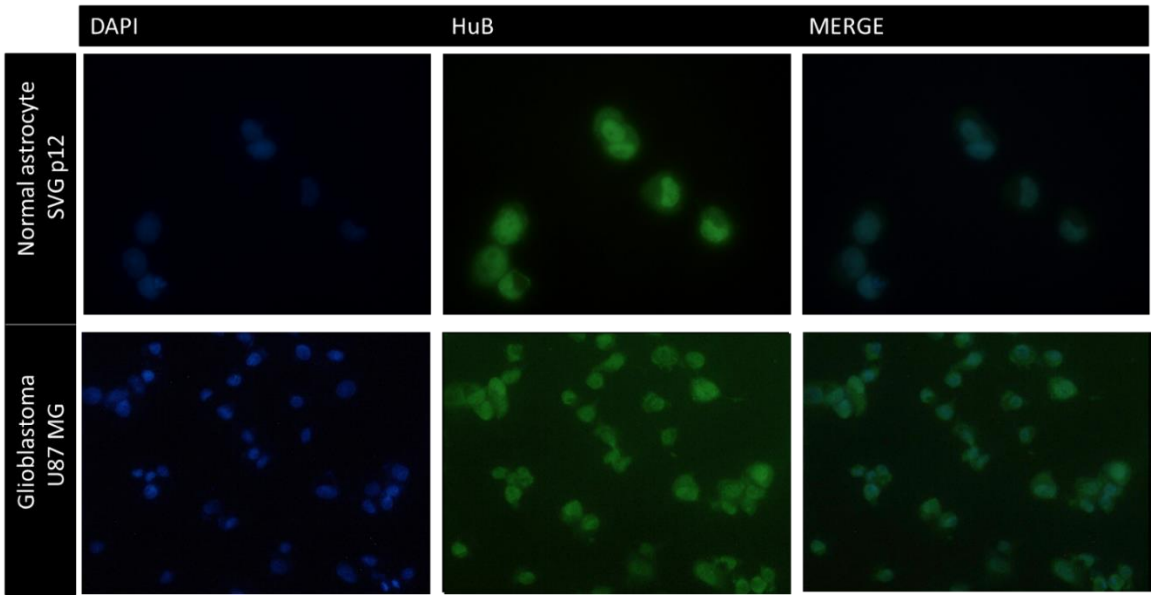

Figure 5.3: Example of the cellular localisation of HuB protein in normal astrocytes SVG p12 and Glioblastoma cells U87-MG. The left column displays staining of nuclei with DAPI (blue), the middle column is stained with anti-HuB (green) and the right column displays a merged picture of DAPI and anti-HuB staining. Magnification x20. (n=3).

As seen in Fig. 5.3, HuB expression was confirmed in both cell lines by anti-HuB immunofluorescent staining. This aligns with western blot analysis where HuB protein was also detected (Fig 5.2).

In normal astrocyte cells, SVG p12, HuB was expressed in both the nucleus and the cytoplasm which was shown by a stronger fluorescence co-localising with DAPI nucleus stain and a weaker signal in the surrounding cytoplasm. HuB was localised to the cytoplasm in Glioblastoma cells U87-MG.

5.2.2 HuC protein expression

HuC protein expression in U87 Glioblastoma cells and SVG p12 normal astrocytes was determined by western blot analysis (Section 2.3). The primary antibodies anti-HuC IgG and anti-GAPDH allowed for the detection of HuC and GAPDH proteins respectively and are displayed in Figure 5.4.

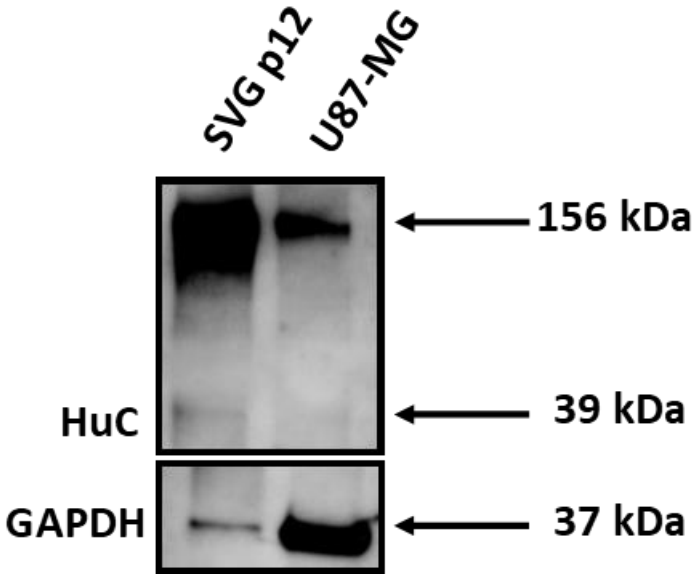

Figure 5.4: Example of western blot analysis of HuC protein with anti-HuC antibody. HuC and GAPDH protein expression in normal astrocytes SVG p12, and Glioblastoma cells U87-MG. GAPDH protein expression was used as a loading control. (n=3).

HuC was identified at its expected size of 37kDa in the SVG p12 cell line whilst a second stronger band was also detected at 156kDa in both cell lines which could be due to multimerisation of HuC. This higher molecular band was also found in Neuroblastoma Hu protein studies (Fig. 4.4).

GAPDH protein was detected at its expected size of 37kDa. HuC was expressed at a very high level in SVG p12 cells when compared to the weak GAPDH signal. HuB protein was comparable to the GAPDH loading control. This suggests a high HuC protein expression in SVG p12 cells in comparison to U87-MG cells. This differs from the gene expression data show in Fig 5.1, where *HuC* expression was higher at RNA level in U87-MG cells than in SVG p12 cells.

Immunofluorescent HuC protein labelling (Section 2.4.1) was performed to identify its' subcellular localisation. Anti-HuC IgG was used with the secondary Alexa green 488 FITC IgG. Cells were counterstained with DAPI nucleus stain for nuclear localisation. HuC immunostaining is shown in Figure 5.5.

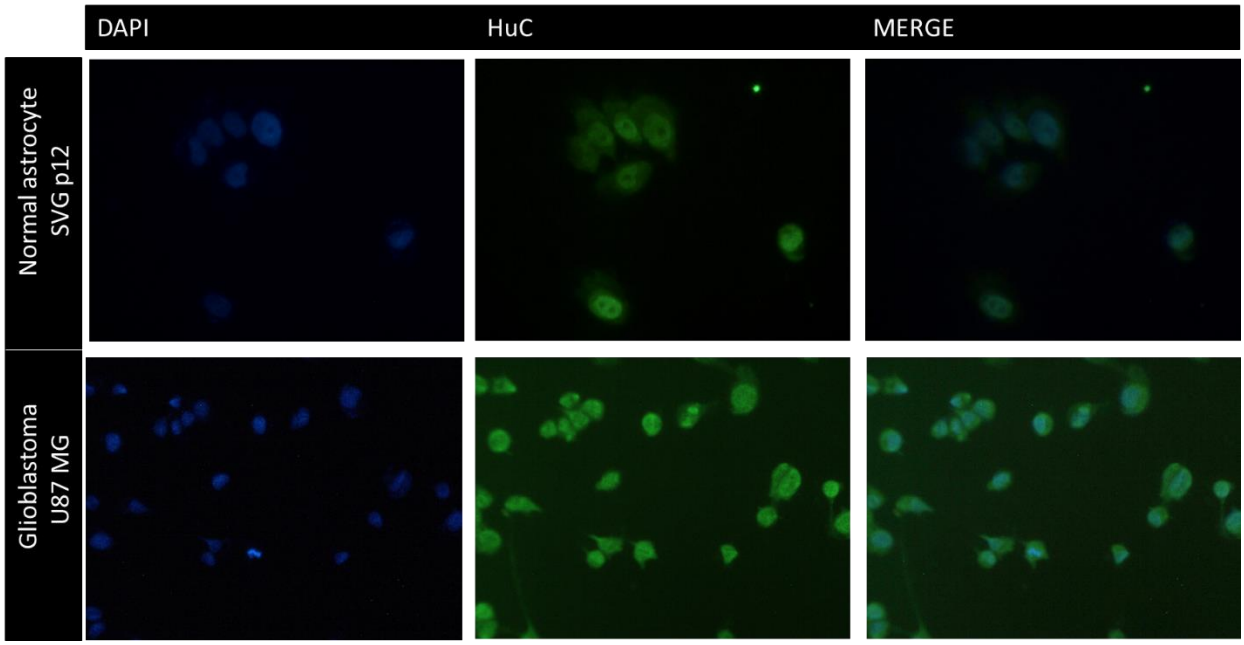

Figure 5.5: Representative cellular localisation of HuC protein in normal astrocytes SVG p12 and Glioblastoma cells U87-MG. The left column showed staining of nuclei with DAPI (blue), the middle column is stained with anti-HuC (green) and the right column displays a merged picture of DAPI and anti-HuC staining. Magnification x20. (n=3).

As seen in Fig. 5.5, HuC protein expression was observed in SVG p12 and U87-MG cell lines, confirming western blot data shown in Fig. 5.4. The strongest HuC protein fluorescence was observed in the cytoplasm of U87-MG cells. SVG p12 cells showed a strong signal for HuC protein in the nucleus with a weaker stain observed in the cytoplasm.

5.2.3 HuD protein expression

HuD protein was detected in only in U87 cells by western blot using HuD specific antibodies. HuD was absent in the control cell line. A comparable amount of GASPH protein used as loading control was observed in SVG and U87 Cells. Fig 5.6 showed HuD protein was detected at its expected molecular weight of 42kDa in Glioblastoma cells U87-MG.

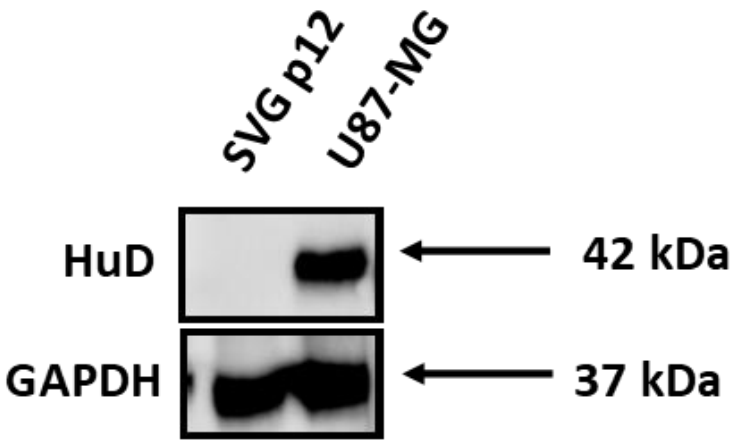

Figure 5.6: Example of western blot analysis of HuD protein with anti-HuD antibody. HuD and GAPDH protein expression in normal astrocytes SVG p12, and Glioblastoma cells U87-MG. GAPDH protein expression was used as a loading control. (n=3).

This correlates with *HuD* expression at an RNA-level shown in Fig. 5.1 where it was higher in U87-MG cells compared to the normal astrocytes SVG p12. Immunofluorescence staining using anti-HuD antibodies confirmed an absence of HuD in the normal astrocytes and a strong presence in the cytoplasm of Glioblastoma cells (Fig 5.7).

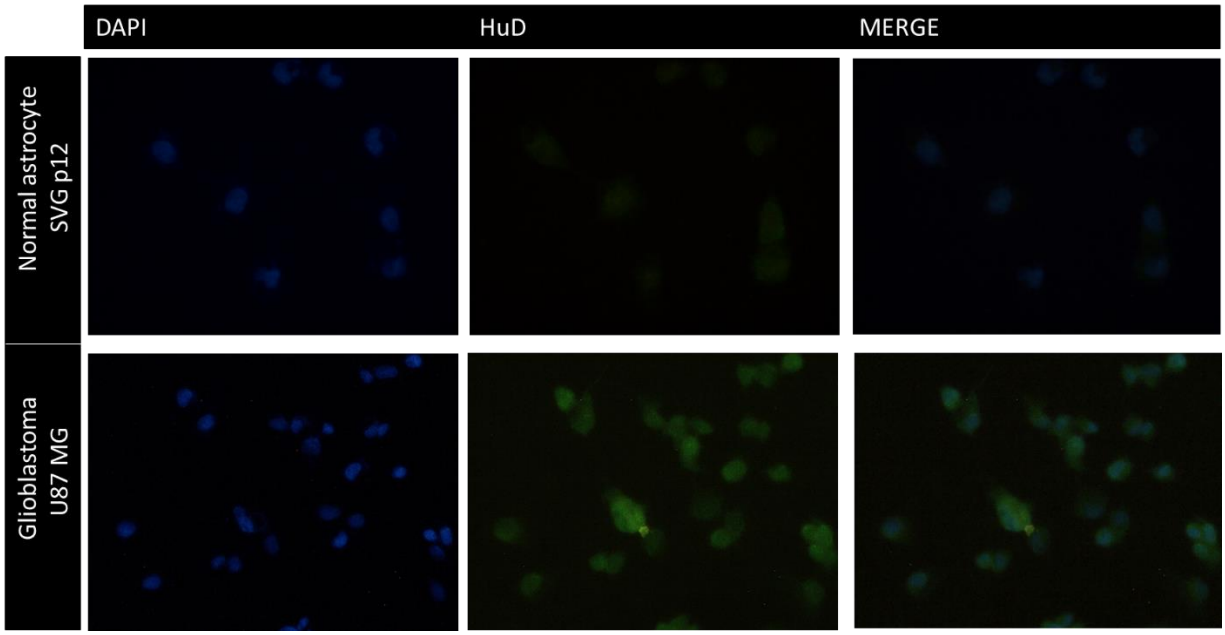

Figure 5.7: Representative cellular localisation of HuD protein in normal astrocytes SVG p12 and Glioblastoma cells U87-MG. The left column showed staining of nuclei with DAPI (blue), the middle column is stained with anti-HuD (green) and the right column displays a merged picture of DAPI and anti-HuD staining. Magnification x20. (n=3).

The immunofluorescence shown in Fig. 5.7 agrees with western blot data of HuD protein expression (Fig. 5.6) and *HuD* gene expression profile (Fig. 5.1) in the U87-MG cell line. HuD expression is confirmed in the cytoplasm only of the Glioblastoma cells.

5.2.4 HuR protein expression

HuR protein expression level and its cellular localisation was analysed in Glioblastoma U87-MG cells and normal astrocytes SVG p12. The primary antibodies anti-HuR IgG and loading control anti-GAPDH IgG were used for the detection of HuR and GAPDH proteins respectively.

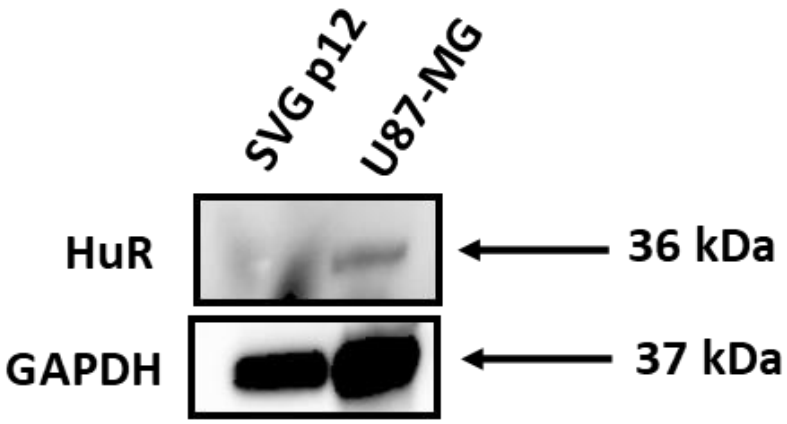

Figure 5.8: Example of a western blot analysis of HuR with anti-HuR antibody. HuR and GAPDH protein expression in U87-MG Glioblastoma cells and normal astrocytes SVG p12. GAPDH protein expression was used as a loading control. (n=3).

HuR protein was only detected in U87-MG cells at the expected size of 36kDa. GAPDH was detected at 37kDa in both cell lines. These results differ from the gene expression profile (Fig. 5.1), that showed HuR to be expressed in both cell lines. This suggests that the *HuR* gene to protein translation is low in the U87-MG Glioblastoma cells and could be explained by post-transcriptional modifications and post-translational regulatory events.

To identify HuR protein's subcellular location in these cells, immunofluorescence staining was performed (Section 2.4.1) (Fig. 5.9). Anti-HuR IgG was used with secondary Alexa 488 FITC IgG. Cells were counterstained with DAPI nucleus stain.

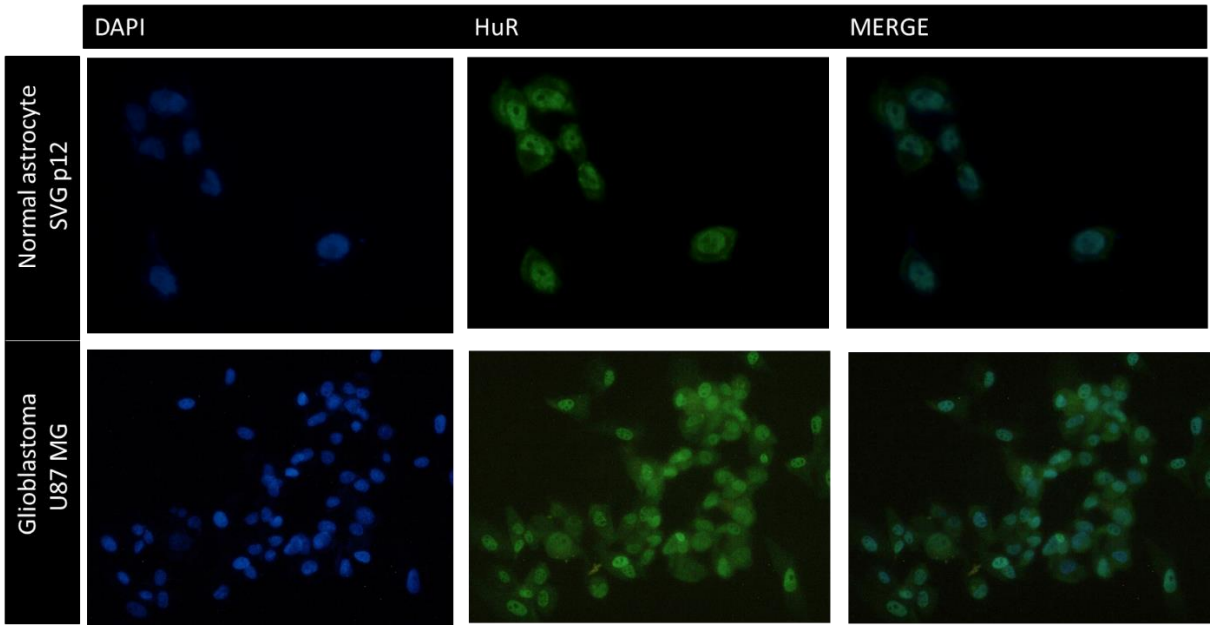

Figure 5.9: Representative cellular localisation of HuR protein in Glioblastoma U87-MG and normal astrocytes SVG p12. The left column showed staining of nuclei with DAPI (blue), the middle column with anti-HuR (green) and the right column displays a merged picture of DAPI and anti-HuR. Magnification x20. (n=3).

HuR protein expression was detected in normal astrocytes and Glioblastoma cells. The strongest staining in SVG p12 astrocyte cells co-localised with the DAPI stain and therefore showed HuR protein was predominantly in the nucleus with some weaker expression observed in the cytoplasm. HuR protein was also located in both the nucleus and cytoplasm in Glioblastoma cells U87-MG with the strongest staining observed in the nucleus of these cells.

HuR was not detected during western blot analysis however its presence during immunofluorescence studies confirms its protein expression. Therefore, it can be assumed that during western blot, HuR protein expression remained under the detection level.

5.3 Establishing *Hu* gene and protein knockdowns using siRNA interference in Glioblastoma cells

To determine the cellular and molecular role of the *Hu* family overexpression in Glioblastoma and its influence in the initiation and development of cancer, *Hu* gene knockdowns were established in the U87-MG cell line. U87-MG cells were tested for the most efficient transfection reagent, concentration of siRNA and time periods. Samples were collected and analysed. $2^{-\Delta\,\Delta CT}$ values were calculated normalised to *β-Actin*.

For each *Hu* gene in the U87-MG Glioblastoma cell line, a knockdown was established individually and in combination to knockdown the whole *Hu* family. Commercially available siRNAs were purchased to interfere with the genes *HuB*, *HuC*, *HuD*, *HuR*, *GAPDH* and a non-targeting siRNA. Each siRNA contained a pool of four interfering sequences (Table 2.4). In this specific cell-line, siRNAs were introduced with DharmaFECT I transfection reagent over 48 hours, for which the protocol is provided in Section 2.7.3.

RT-qPCR was performed to confirm *Hu* gene knockdowns. The cycling and reactions of RT-qPCR are described in Section 2.26. HuB (1), HuC (1), HuD (6), HuR (2) and β-Actin primer sequences are listed in Table 2.3 of Section 2.27. The fold-change of expression was analysed by comparing expression levels to the control non-targeting siRNA (Fig. 5.10). β-Actin was the housekeeping gene to which the data was normalised. Statistical significance was calculated by a two-tailed t-test.

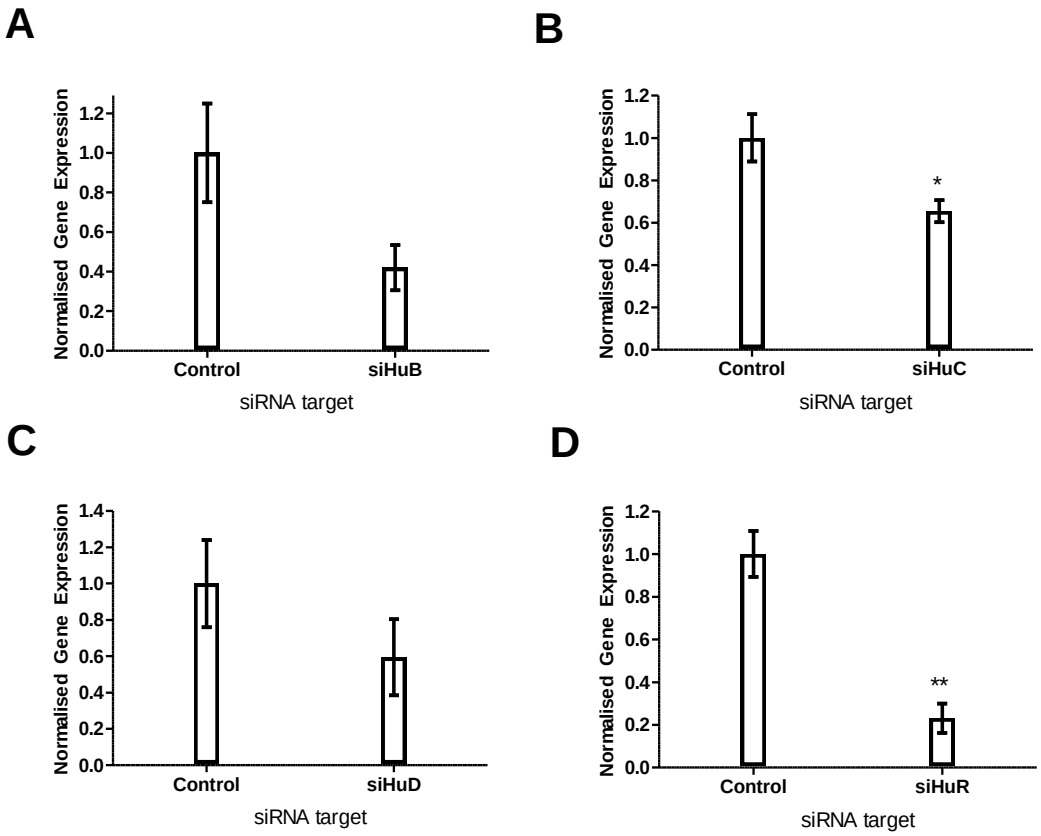

Figure 5.10: Knockdown efficiency of *Hu* genes after individual *Hu* siRNA interference in the Glioblastoma cell line U87-MG. *HuB* (A), *HuC* (B), *HuD* (C) and *HuR* (D) gene expression following *Hu* gene knockdowns was analysed by RT-qPCR in the Glioblastoma cell line, U87-MG. The $2^{-\Delta\Delta Ct}$ results shown are an average of three replicates normalised to *β-Actin* gene expression and compared with the control set at 1.00. Error bars display ± SEM. Statistical significance was calculated by a two-tailed t-test and is displayed by *P ≤ 0.05, **P ≤ 0.01, ***P ≤ 0.001. (n=3).

As seen in Fig. 5.10, in the Glioblastoma cell line, U87-MG, the knockdown efficiency was 2.4-fold for *HuB*, 1.5-fold for *HuC*, 1.7-fold for *HuD* and 4.3-fold for *HuR*. Whilst not as successful as Neuroblastoma studies, *HuC* and *HuR* knockdown were still statistically significant based on a two-tailed T-test.

Regulatory influences between the Hu protein family has previously been documented in research and observed in the previous chapter of this thesis. A combined *Hu* gene family knockdown was achieved and is shown in Fig. 5.11.

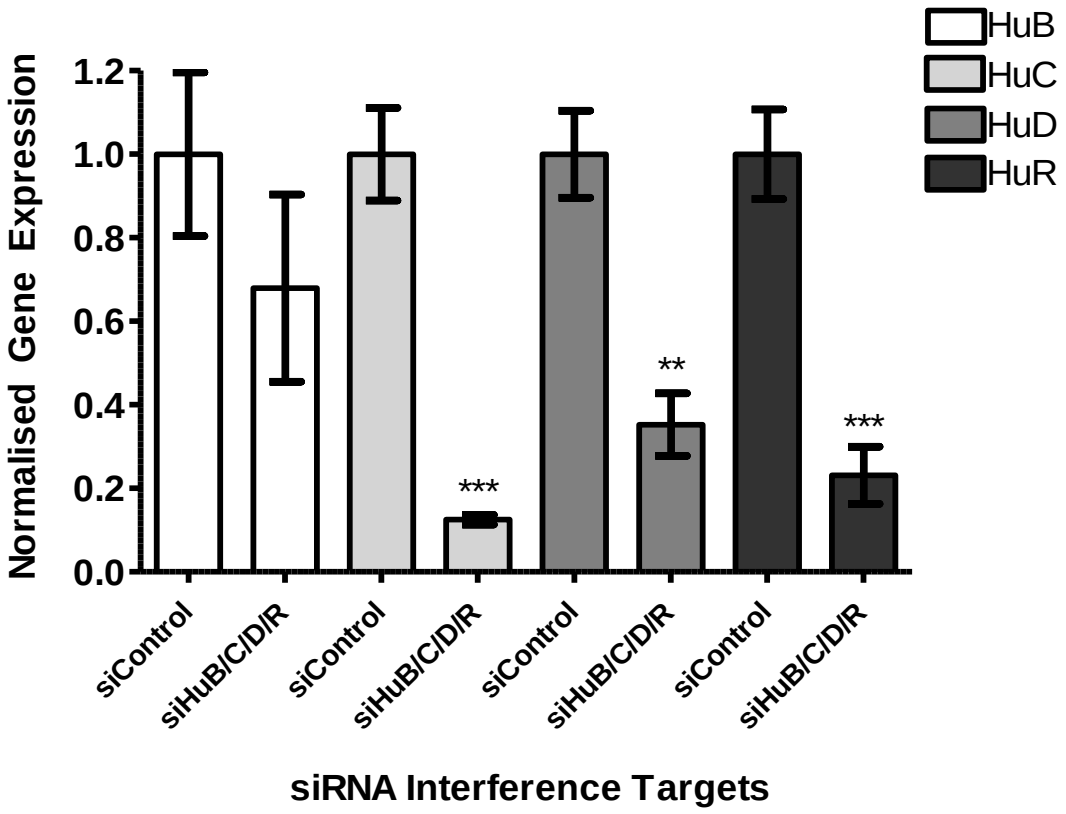

Figure 5.11: Combined siRNA interference of all *Hu* genes in the Glioblastoma cell line U87-MG. *HuB*, *HuC*, *HuD* and *HuR* gene expression following a full knockdown of each *Hu* gene in a single attempt in the U87-MG Glioblastoma cells. Samples were analysed by RT-qPCR. The $2^{-\Delta\Delta Ct}$ results shown are an average of three replicates normalised to *β-Actin* gene expression and compared with the control set at 1.00. Error bars display ± SEM. Statistical significance was calculated by a two-tailed t-test and is displayed by *P ≤ 0.05, **P ≤ 0.01, ***P ≤ 0.001. (n=3).

A combined knockdown of all four *HuB*, *HuC*, *HuD* and *HuR* genes was mostly successful. *HuC*, *HuD* and *HuR* knockdown increased overall. Unfortunately, *HuB* still proved challenging to knockdown in this cell line. The combined *Hu* family gene knockdown resulted in a decrease

of expression of 1.5-fold for *HuB*, 8-fold for *HuC*, 2.8-fold for *HuD* and 5.2-fold for *HuR*, of which the latter three were statistically significant as determined by a two-tailed t-test.

To confirm the *Hu* genes knockdowns' and the impact at protein-level, protein expression levels were analysed by western blot analysis 96-hour post-transfection (Section 2.3).

Each *Hu* gene knockdown both individually and in combination in Glioblastoma cells U87-MG was blotted and analysed for Hu protein. The primary antibodies anti-HuB, anti-HuC, anti-HuD, anti-HuR and anti-GAPDH were used. GAPDH was used as a control protein to normalise expression. The western blots are displayed in Figure 5.12.

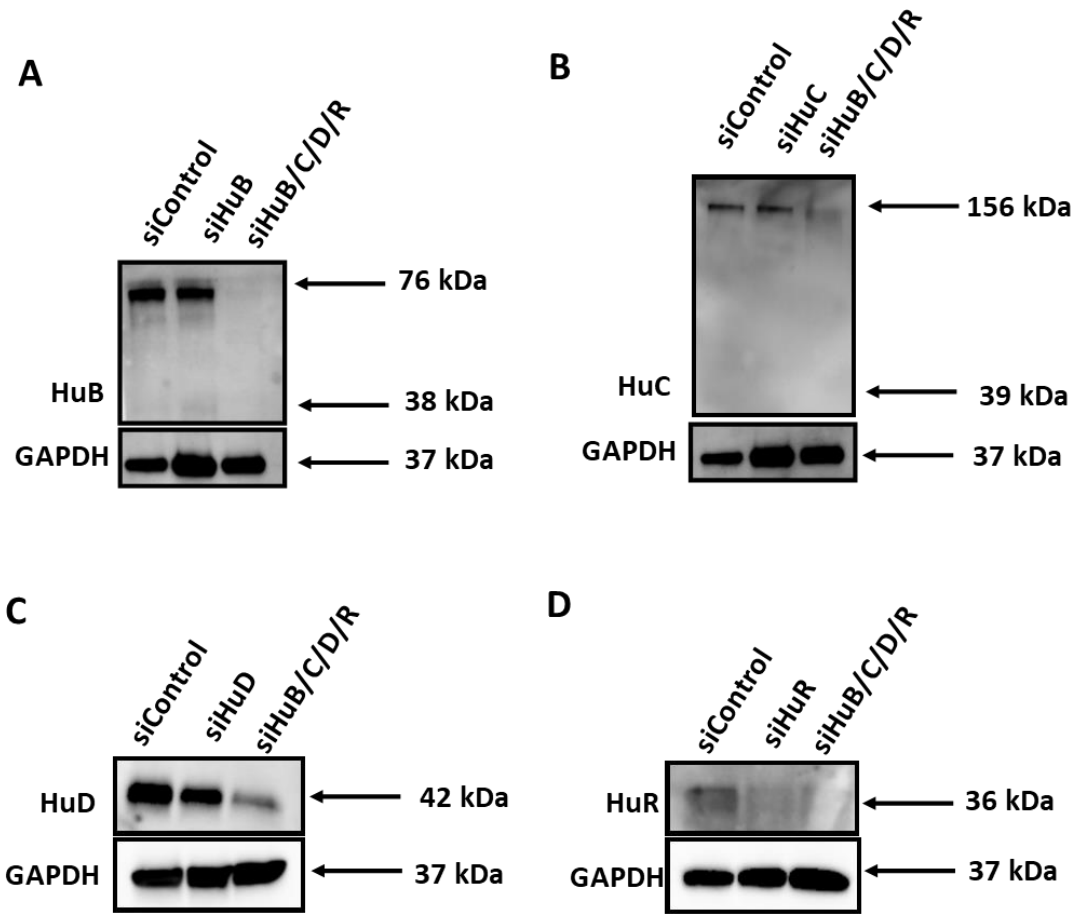

Figure 5.12: Hu protein expression during single and combined *Hu* knockdowns in U87-MG Glioblastoma cells. A) HuB protein reduction following single HuB and combined *Hu* family siRNA interference. B) HuC protein reduction following single HuC and combined *Hu* family siRNA interference. C) HuD protein partial reduction expression following single HuD and combined *Hu* family siRNA interference. D) HuR protein reduction following single HuR and combined *Hu* family siRNA interference. GAPDH protein expression was used as a loading control.

Western blot analysis shown in Fig. 5.12A displays the HuB protein was detected at 75 kDa, which is double of the expected size of 37kDa. This was earlier identified in Fig. 5.2. Due to the size of this band, it is most likely dimerisation of HuB. The *HuB* knockdown showed little reduction in HuB protein expressed. Following knockdown of all Hu family members in combination, HuB protein was absent. This trend was also observed for *HuC* (Fig. 5.12B) and

HuD (Fig. 5.12C) knockdowns. HuC protein was detected at 156kDa. This was previously documented in Fig 5.4 and was suspected to be HuC multimer. HuD was detected at its expected size of 42kDa. Shown in Fig. 5.12D, no HuR protein could be detected after the *HuR* siRNA knockdown.

The described difference in Hu individual and combined *Hu* gene knockdowns could be due to complex interplay between the *Hu* family members as previously shown in Neuroblastoma studies (Section 4.4). Observations concluded *Hu* gene family members can influence expression or translational efficiency by targeting their own or family members mRNA transcripts and regulating their expression. The next section (5.4) aims to study these regulatory influences.

5.4 Differential gene expression of Hu proteins following individual and combined *Hu* gene knockdowns in Glioblastoma

Due to differences in the gene expressions of single and combined knockdowns and the known ability of HuR to regulate its own expression, a gene expression profile was established to explore the possibility of a regulatory mechanism within the Hu family of RNA-binding proteins in Glioblastoma. The level of all individual *Hu* genes expression when individual *Hu* siRNA interference was performed was analysed and compared to the non-targeting control siRNA transfection.

RT-qPCR was performed to confirm *Hu* gene knockdowns and to determine any changes to the expression levels of other *Hu* genes. The cycling and reactions of RT-qPCR are described in Section 2.26. HuB (1), HuC (1), HuD (6), HuR (2) and β-Actin primer sequences are listed in Table 2.3 of Section 2.27. *β-Actin* was the housekeeping gene to which the data was

normalised and compared to the non-target control. Statistical significance was calculated by a two-tailed t-test.

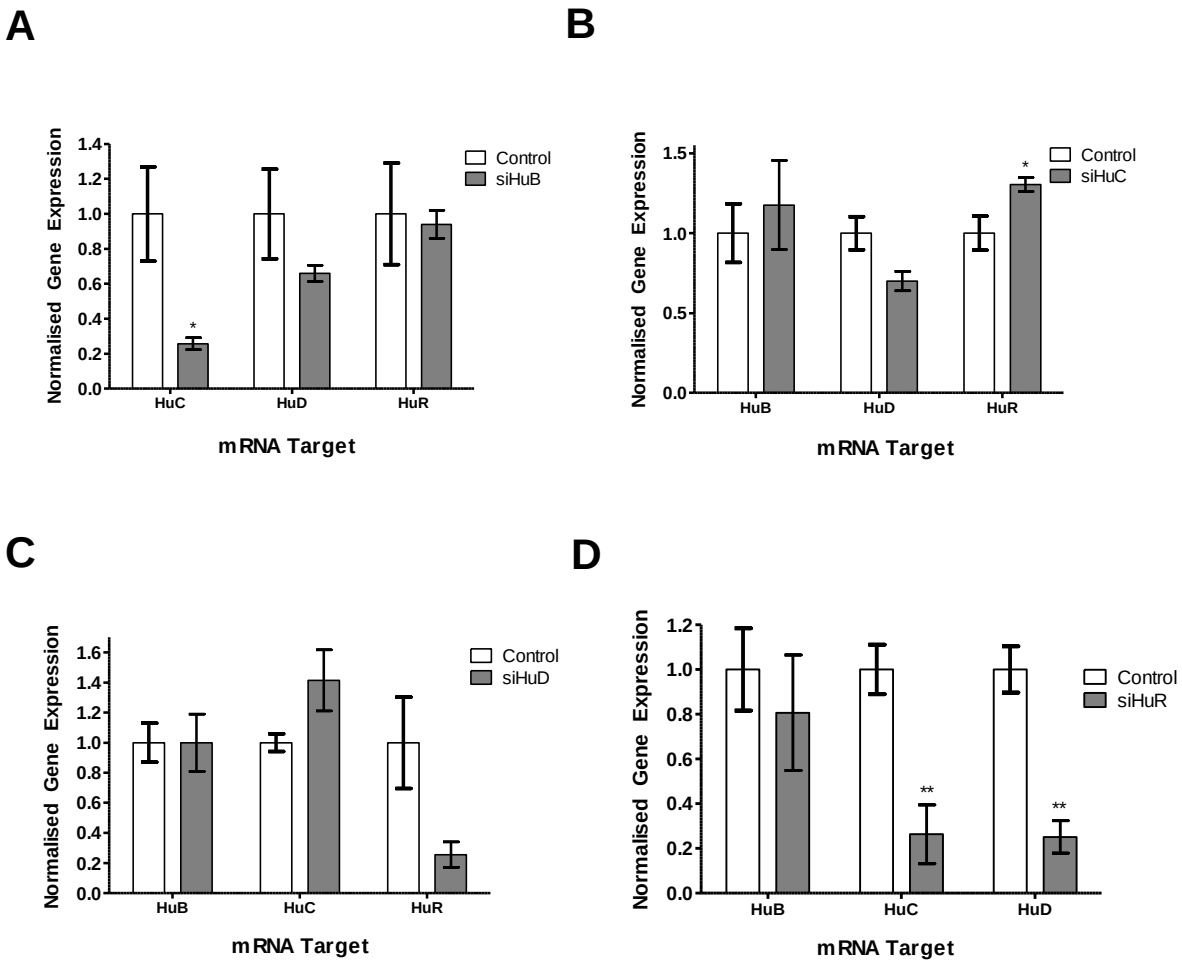

Figure 5.13: Influence of individual *Hu* gene knockdowns on other *Hu* gene family members expression levels in U87-MG, Glioblastoma cells. A) *HuB* Knockdown B) *HuC* Knockdown C) *HuD* Knockdown D) *HuR* Knockdown. The $2^{-2\text{-}\Delta\Delta Ct}$ results shown are an average of three replicates normalised to *β-Actin* gene expression and compared with the non-target control. Error bars display ± SEM. Statistical significance was calculated by a two-tailed t-test and is displayed by *P ≤ 0.05, **P ≤ 0.01, ***P ≤ 0.001. (n=3).

Here the initial *Hu* gene knockdown levels are those described previously in Fig. 5.10. Displayed in Fig. 5.13A, a 2.4-fold knockdown of *HuB* gene expression, resulted in a significant 3.9-fold reduction of *HuC* gene. No significant change was observed for *HuD* or *HuR*

expression. *HuC* siRNA interference is shown in Fig. 5.13B, a 1.5-fold knockdown of *HuC* showed a significant 0.3-fold increase in *HuR* expression. A 1.7-fold *HuD* siRNA knockdown (Fig 5.13C) did not significantly change the expression of the other genes. *HuR* siRNA knockdown (Fig. 5.13D) of 4.3-fold resulted in a significant decrease in *HuC* gene expression by 3.8-fold and *HuD* gene expression by 4.0-fold.

To better visualise the key expression changes after each *Hu* knockdown, the data from above displayed in Fig. 5.10, Fig. 5.11 and Fig. 5.13 is summarised in Fig. 5.14. The data is normalised to the same non-target controls of the siRNA interference transfection.

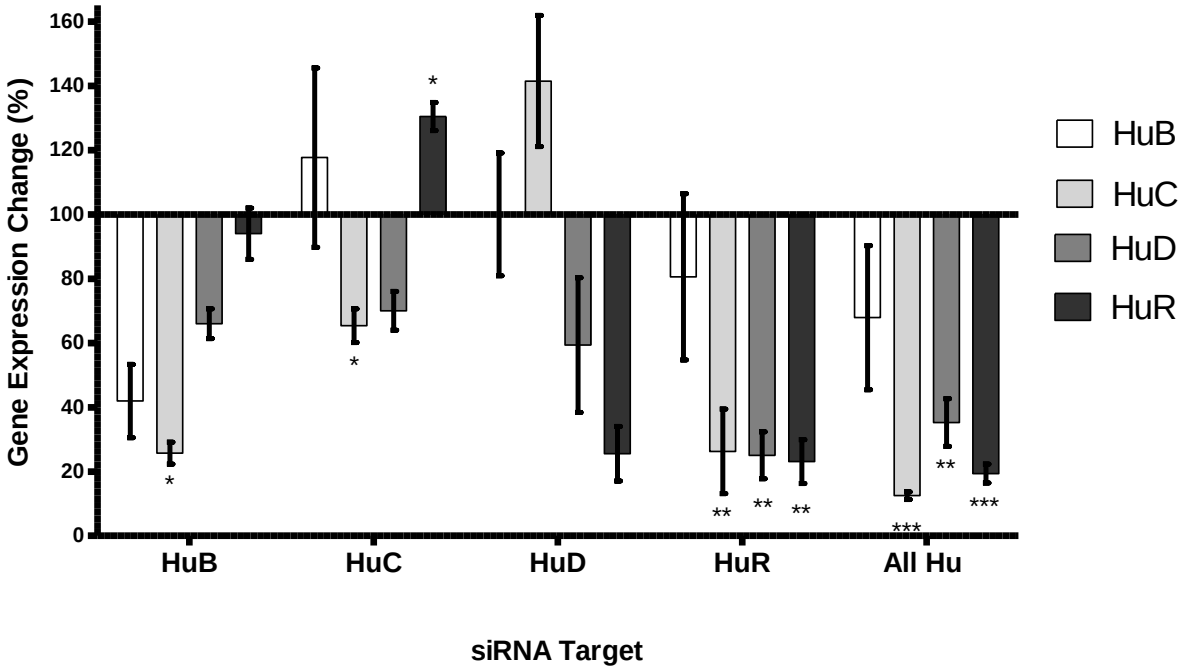

Figure 5.14: Complete profile of *Hu* gene expression in Glioblastoma cell line U87-MG, after knockdown of each individual Hu protein individually and combined. *HuB*, *HuC*, *HuD* and *HuR* expression following knockdown of each *Hu* gene both individually and in combination was analysed by RT-qPCR in U87-MG cells. The $2^{-\Delta\Delta Ct}$ results shown are an average of three replicates normalised to *β-Actin* gene expression and compared with the non-targeting control. Error bars display ± SEM. Statistical significance was calculated by a two-tailed t-test and is displayed by *P ≤ 0.05, **P ≤ 0.01, ***P ≤ 0.001. (n=3).

The effect of the combined knockdown on individual Hu expression is displayed in Fig. 5.14. *HuB* gene knockdown results in a *HuC* and *HuD* gene expression decrease, whilst there was little change to *HuR*. Upon *HuC* siRNA interference, *HuD* expression also decreased. However, *HuB* and *HuR* gene expression increased.

Following *HuD* siRNA interference, a decrease in *HuR* expression was observed along with increased *HuC* expression and no change in *HuB* expression. Upon *HuR* siRNA knockdown, there was a decrease in all other *Hu* genes. Fig. 5.14 also shows the knockdown all *Hu* gene in a single combined attempt. Since similarities are observed between *HuR* knockdown and combined *Hu* family knockdown, this could suggest HuR is the major player in the Hu family combined knockdown.

The overall knockdown profile is summarised as percentages in a heatmap and is displayed in Fig. 5.15.

Gene Expression Change (%)		Hu Knockdowns				
		HuB	HuC	HuD	HuR	All
Downregulated	HuB	58.05	17.67	0.00	1.41	32.10
	HuC	* 74.26	* 34.60	41.50	** 73.72	** 87.50
Upregulated	HuD	34.02	29.99	** 40.64	** 74.94	** 64.75
	HuR	6.01	* 30.45	74.47	** 76.88	** 80.62

Figure 5.15: Heatmap summarising *Hu* gene expression change after single and combined knockdown experiments in U87-MG Glioblastoma cells. Colour intensity proportional to the percentage change. Statistical significance was calculated by a two-tailed t-test and is displayed by *P ≤ 0.05, **P ≤ 0.01, ***P ≤ 0.001. (n=3).

In summary, a similar *Hu* gene expression profile is observed when all *Hu* genes are knocked down in combination and following individual *HuR* gene knockdown.

The differential expression changes in different Hu family members was previously described in Chapter 4 of the Neuroblastoma studies. In short, three possible explanations were described based around compensatory action, regulatory effects or consequences of off-target effects.

To conclude the differential expression, change within the Hu RNA-binding protein family, a model was drawn summarising how the regulation occurs and is shown in Figure 5.16.

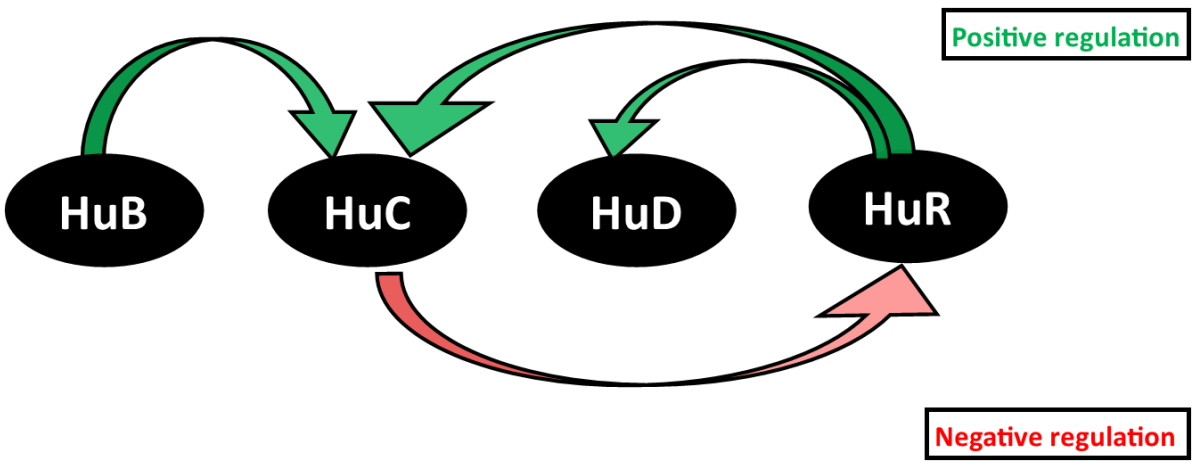

Figure 5.16: A model representing the regulation of the Hu protein family in the Glioblastoma cell-line U87-MG. Colour intensity proportional to the change in regulation.

The model summarises only statistically significant data determined by a two-tailed t-test. The model showed that following *HuR* knockdown, *HuD* and *HuC* gene expression also decreased as did *HuC* expression when *HuB* was knocked down. Following *HuC* knockdown, *HuR* gene expression increased.

Based on the three potential explanations that are described above for compensatory expression or regulatory influences within the Hu family, there are several conclusions that can be drawn in the U87-MG Glioblastoma cell model.

5.5 Cellular morphology of normal astrocytes and Glioblastoma cells

The morphology in which cells grow in the human body influences their function. In cancer, cells adopt a more invasive phenotype in which the cells are more robust and gain function. Glioblastoma are typically hard to treat due to the nature of their growth. These tumours are not considered a defined mass with clear borders, instead considered as diffuse Glioblastomas, they have finger-like projections called tendrils that extend into other parts of the brain (Armento 2017).

5.5.1 Cellular morphological analysis

Microscopic analysis of Glioblastoma and normal astrocytes is shown in Fig. 5.17. Cell images were obtained using an Eclipse II fluorescent inverted microscope and Microtec camera as described in Section 2.1.6.

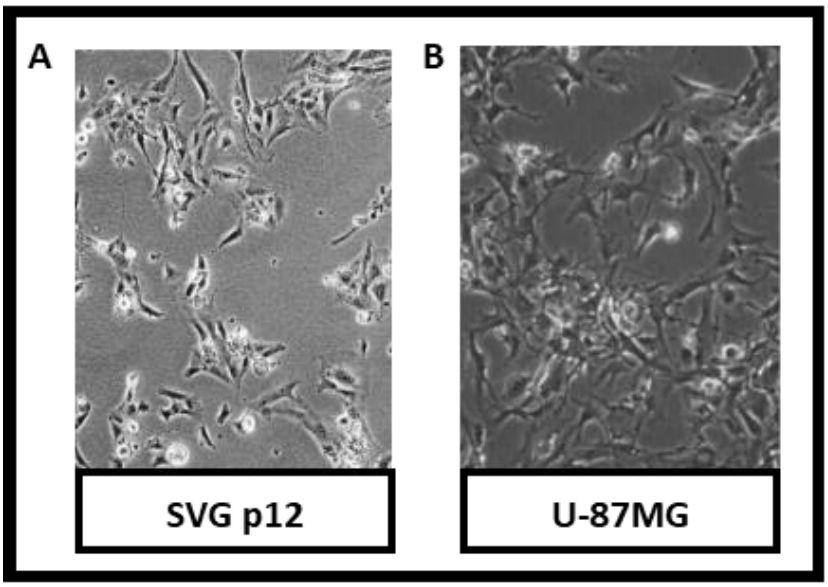

Figure 5.17: Microscopy images of the normal astrocytes and Neuroblastoma cell lines. Inverted light microscopy at x20 objective. A) Normal astrocytes cell line, SVG p12. B) Glioblastoma cell line, U87-MG.

Astrocytes form the supportive tissue of the brain. The normal astrocytes cell line SVG p12 was established from a foetus during the first trimester. These typically grow in star-shaped cells called fibroblasts. In culture, U87-MG Glioblastoma Multiforme cells grow with the same characteristic star-shape as SVG p12 astrocytes.

5.5.2 Cellular migrative potential

Cancer cells are known for their ability to migrate from the localised tumour and establish a secondary tumour also called a metastasises. A good measure of both cellular migration and invasion, which replicates the ability of a cancer cell to metastasise. Astrocyte and Glioblastoma cell migration was calculated by the ability of the cells to invade into a 0.5% agarose gel matrix. It was captured through several microscopy imaging equipment. The

images below were achieve using time-lapse photography captured by the CytoSMART™ camera as described in Sections 2.5 and 2.5.1.

First, the ability of the normal astrocytes to migrate into the gel was assessed and is shown in Fig. 5.18.

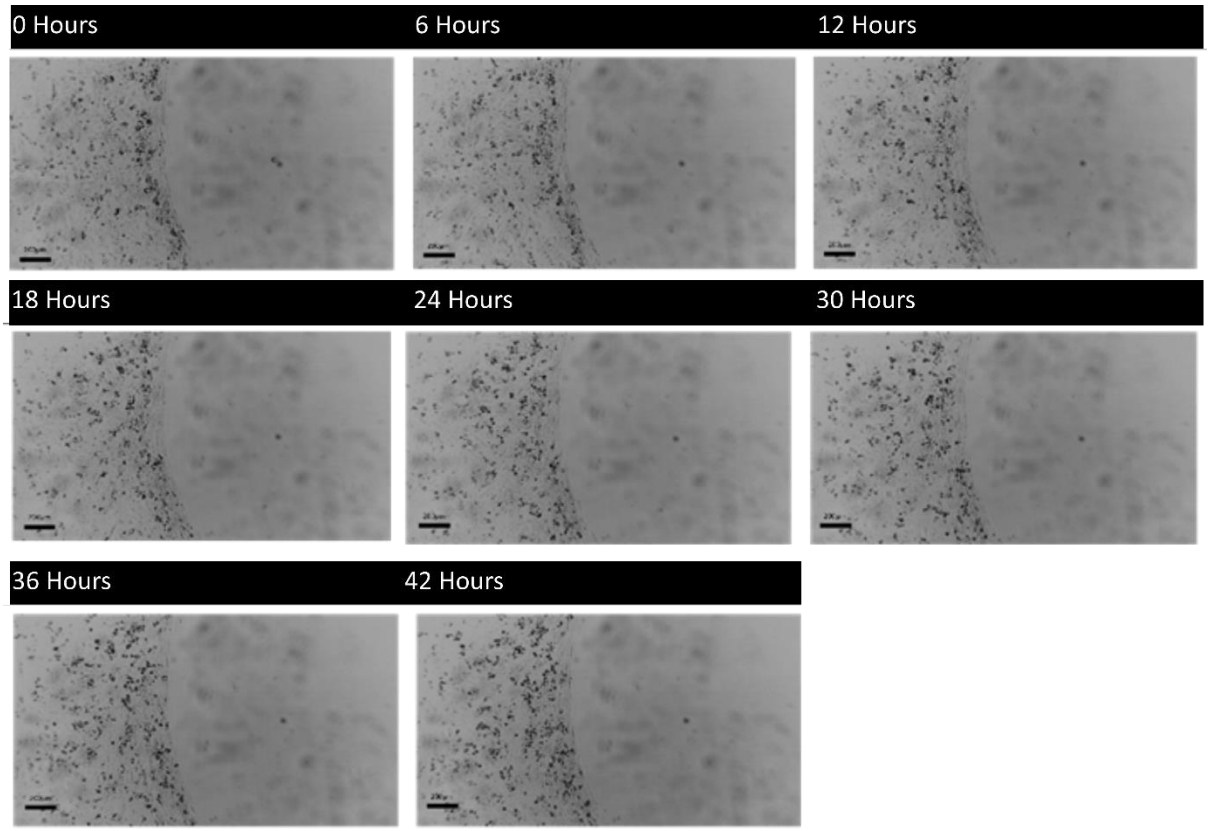

Figure 5.18: The migration of SVG p12, normal astrocyte cells into an agarose gel matrix. During the observed 42-hour period, no migration into the gel matrix was detected. (n=3). Time-lapse photography of the cell migration can be viewed at: https://cytomate.com/access/Project_main/main.php?DiD=238&PiD=19644&ac1=92e93081fa6bd13ce510fd1cad4efcc8f3b9be40cac0df160fe49728dd028276&ac2=b8af21ea150c9f3367e00e143135c75d21d55c29158ae7a23a2f5c3e9a182ae6

As previously observed in Section 4.5.2, the normal astrocytes, SVG p12 did not migrate into the agarose gel during the observed 42 hours and instead proliferated and grew in a line surrounding the agarose. This was expected for a non-cancer cell line.

The Glioblastoma U87-MG cells were then observed for their ability to migrate into an agarose gel matrix. The cells were seeded into a well and a period of 24 hours preceded to allow the cells to adhere for the migration was captured. Images were taken every 15 minutes for 42 hours.

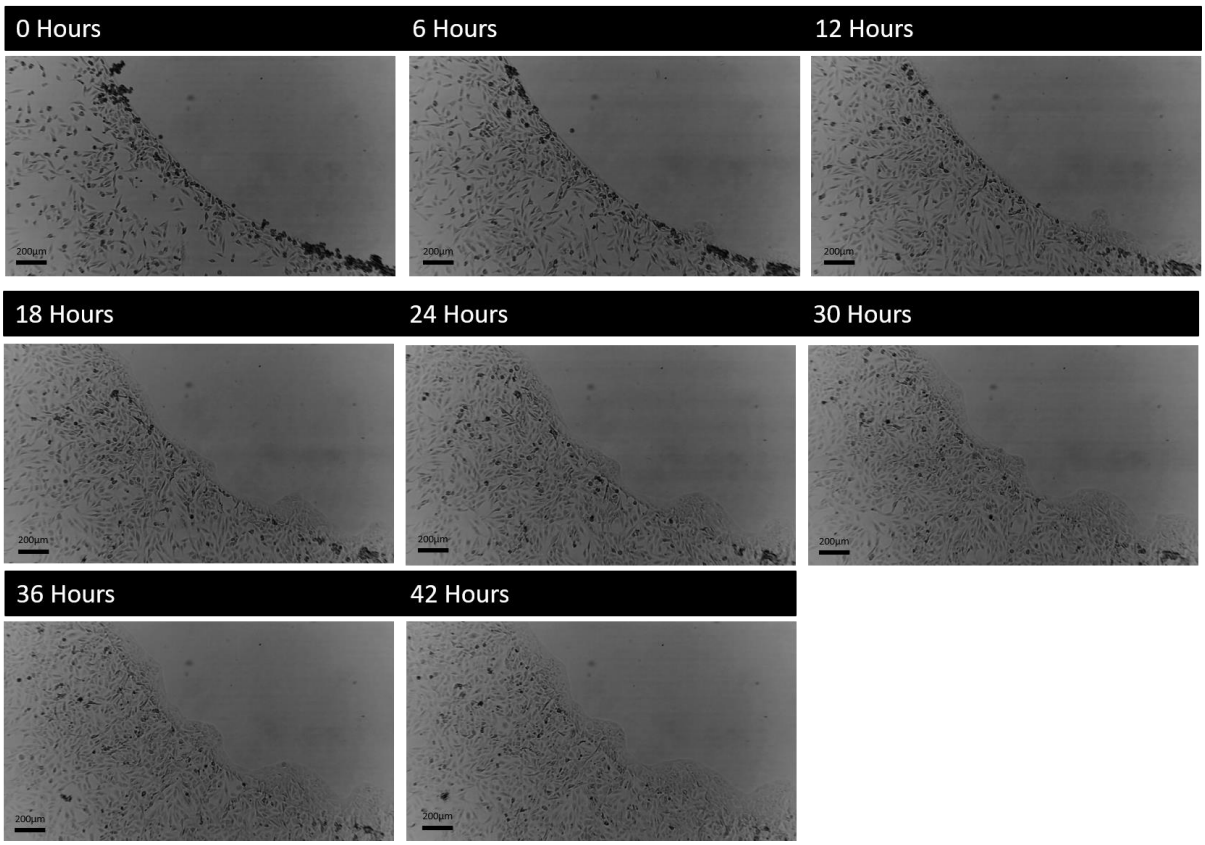

Figure 5.19: The migration of U87-MG Glioblastoma cells into an agarose gel matrix. Over the observed 42-hour period, cells migrated into the gel matrix. (n=3). Time-lapse photography of the cell migration can be viewed at: https://cytomate.com/access/Project_main/main.php?DiD=238&PiD=8247&ac1=12ca4d991e2c70becaec0c763bf609824808f4d35a3669db52b05566ede04374&ac2=dce32963547c525342b172a17bc4202c438aac32842dd495f2e45535aa7b1b68

The migration of U87-MG cells into the agarose gel matrix is shown in Fig. 5.19. U87-Mg cells started to migrate into the gel matrix at around 6-hours. A key hallmark of cancer is the ability of cells to invade and metastasis and this was portrayed by the U87-MG Glioblastoma cells penetrating the agarose gel matrix and proliferating.

The invasiveness of the Glioblastoma cell line U87-MG and the normal astrocyte cells SVG p12 was compared and is shown in Fig. 5.20.

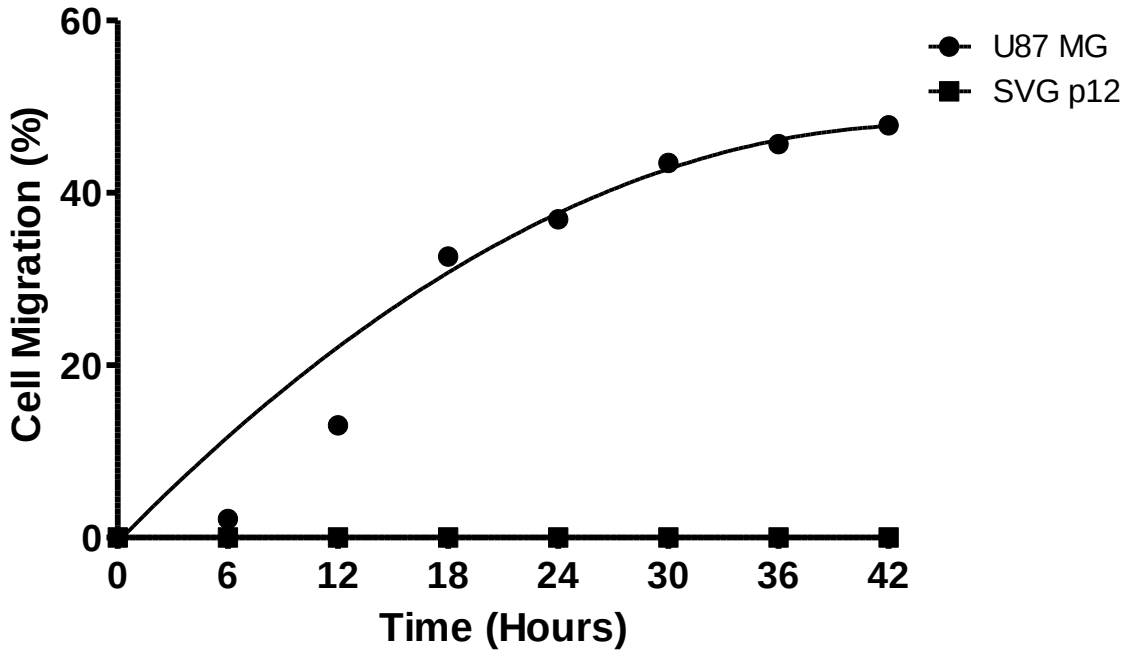

Figure 5.20: The migration of U87-MG Glioblastoma cells compared to the non-migration of SVG p12 astrocytes. Migration into the gel matrix was calculated by the percentage surface area invaded by the cells.

The U87-MG cells achieved a 47.82% invasion into the gel matrix over the 42-hour period observed through time-lapse photography. This finding highlights the greater migrative potential that Glioblastoma cells have compared to normal astrocytes.

5.6 Cellular morphology, viability and migration following Hu protein knockdown in Glioblastoma

As previously discussed in Section 4.6, cancer cells can contain many genomic mutations that contribute to changes in cellular phenotype that may manifest through cell proliferation, motility and morphology (Baba and Câtoi 2007).

To assess the effect of *Hu* gene expression on these features in Glioblastoma, cell morphology was analysed 48 hours following individual and combined *Hu* gene knockdowns. Cells were imaged to assess any changes to cell morphology through size and shape following *Hu* gene knockdowns. Images were obtained using an Eclipse II fluorescent inverted microscope and Microtec camera as described in Section 2.1.6.

As shown in Fig. 5.21, the morphology of U87-MG was not influenced by the individual or combined *Hu* gene knockdowns compared to the control non-target siRNA transfected cells.

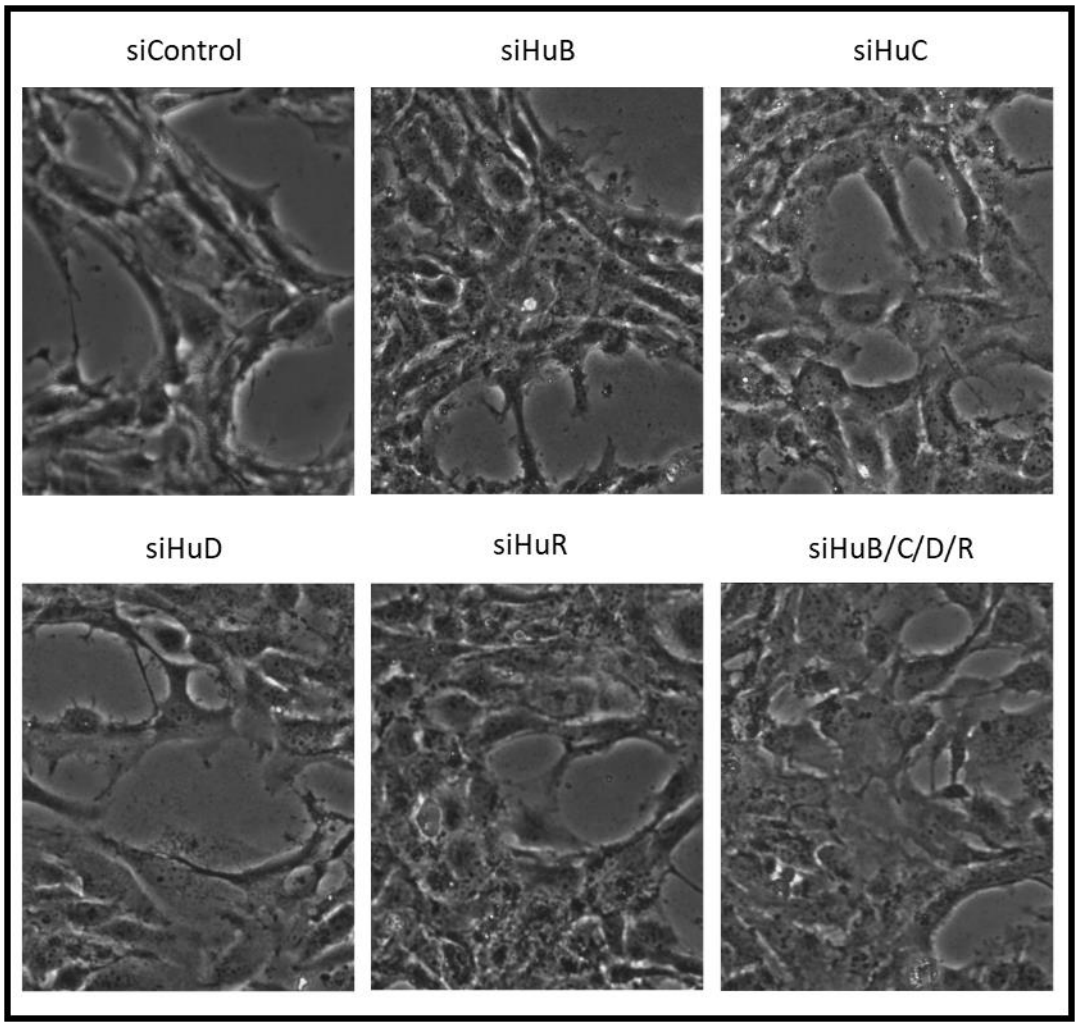

Figure 5.21: U87-MG cell morphology 48-hours post-transfection with *Hu* siRNAs. U87-MG cells with *Hu* genes knocked down in combination and individually. Light microscopy at 20x objective.

Some cells had died, these were removed when the media was replaced prior to imaging. It is also important to mention; these images do not confer the confluency of the cell lines following Hu knockdowns. Other methods to evaluate cell viability are described next in this section.

Cell viability of U87-MG cells with individual and combined *Hu* gene knockdowns was determined by CellTiter 96® AQ_{ueous} One Solution assay (Section 2.6). 48-hours post-transfection absorbance was recorded at 24-hour intervals over 120-hours. The absorbance

was then converted to a percentage and compared to the control non-targeting siRNA (Fig. 5.22).

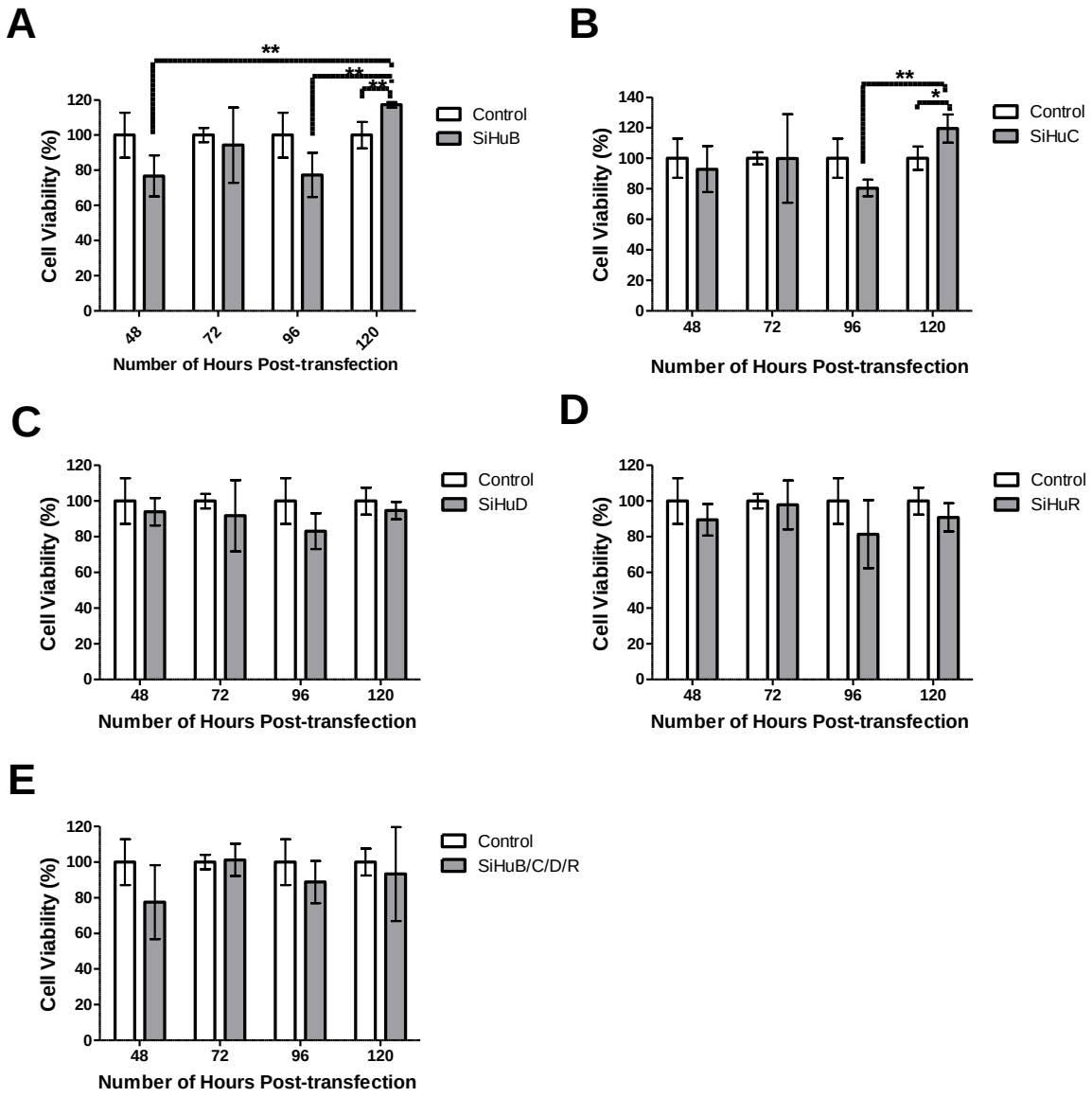

Figure 5.22: Cell viability of U87-MG cells after knockdown experiments. Mean cell viability normalised to the control non-target siRNA treated cells. A) Effect of *HuB* knockdown. B) Effect of *HuC* knockdown. C) Effect of *HuD* knockdown. D) Effect of *HuR* knockdown. E) Effect of combined *Hu* knockdown. MTS absorbance was recorded at 490nm over a 144-hour period. Data are expressed as mean values ± SD. n=3. Statistical significance was calculated by a two-tailed t-test and is displayed by *P ≤ 0.05, **P ≤ 0.01, ***P ≤ 0.001. (n=3).

Whilst defining the role of the Hu-family of RNA binding proteins, we observed that reduced expression of HuB and HuC resulted in an initial lower rate of cell viability compared to the control, however a conclusive increase at the 120-hour time point. At the 120-hour time point, U87-MG cells treated with HuB siRNA showed a reduction in cell viability in comparison to the control whilst *HuC* siRNA-treated cells showed an increase.

The knockdown of *HuD*, *HuR* and all *Hu* gene in combination, resulted in a decrease in cell overall viability in comparison to the non-target siRNA control. At 120 hours *HuD* knockdown resulted in a 5.38% decrease in cell viability compared to the control. Whilst *HuR* knockdown decreased cell viability by 9.11% and all *Hu* combined knockdown showed 6.70% decrease in cell viability.

Cell motility was measured before and after individual and combination *Hu* gene knockdowns with a scratch wound assay (Section 2.5.2). Migration images are shown in Fig. 5.23, Fig. 5.24 and Fig. 5.25. This assay measures the ability and speed of the cells to migrate into an artificially created cell-free gap until new cell-cell contacts are established. Cells were imaged over 48 hours.

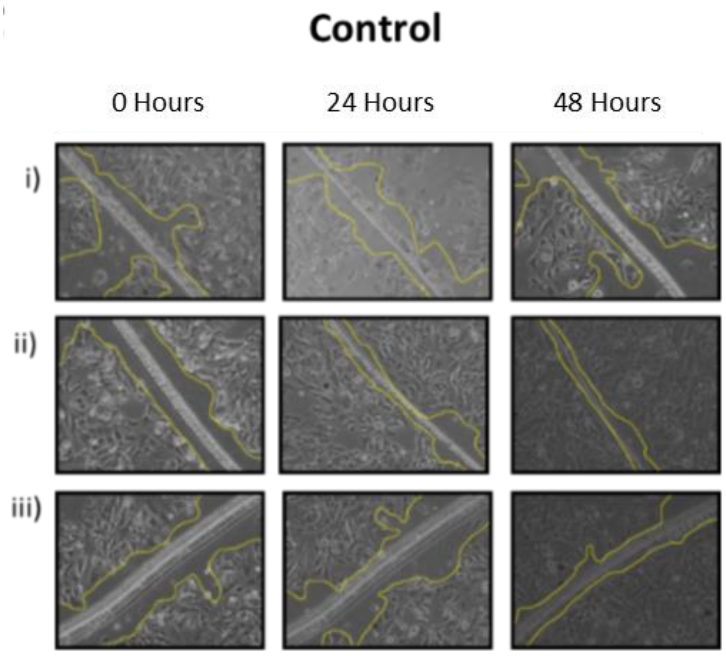

Figure 5.23: Scratch wound assays in control U87-MG Glioblastoma cells following interference with a non-targeting siRNA. Mobility was assessed 24 hours post-transfection when cells were confluent for 72 hours. Wounds were generated using a needle after cell confluence following siRNA interference. Timepoints state the number of hours post-wound making. Yellow lines highlight the gap. Magnification x10. (n=3).

The initial gap made by inducing a wound in the cell monolayer can be seen shrinking over the different time points.

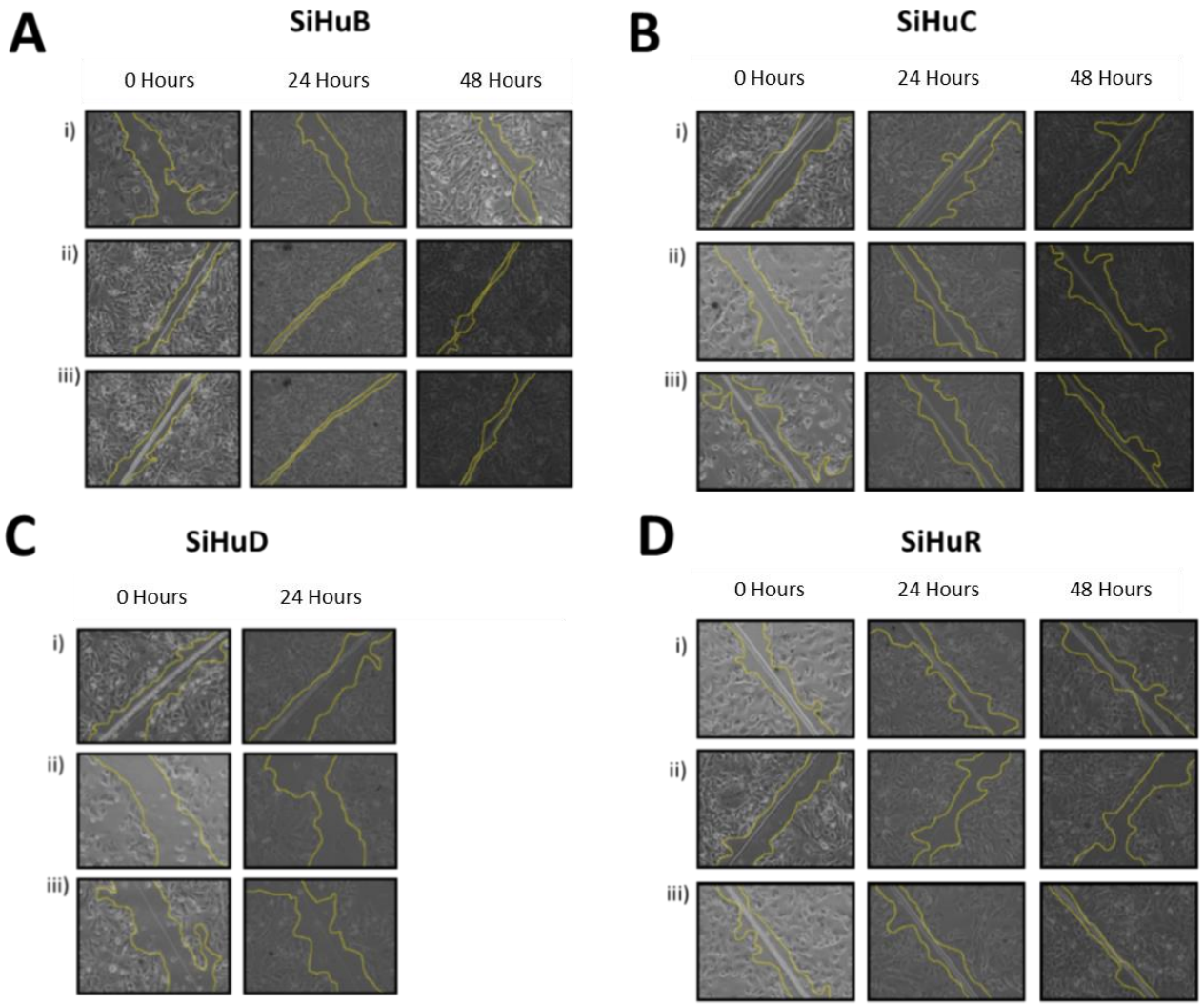

Figure 5.24: Scratch wound assays in U87-MG Glioblastoma cells following knockdown of *Hu* genes individually. Mobility was assessed 24 hours post-transfection when cells were confluent for 72 hours. A) *HuB* knockdown B) *HuC* knockdown C) *HuD* knockdown D) *HuR* knockdown. Timepoints state the number of hours post-wound making. Yellow lines highlight the gap. Magnification x10. (n=3).

The scratch wound assays following individual Hu gene knockdowns are displayed in Figure 5.24. An overall decrease in the wound can be seen over the timepoints. U87-MG cells with *HuD* knockdown detached from the flask following 24-hours so no images were taken at the 48-hour timepoint.

Next the effect of a combined Hu gene knockdown was determined and is displayed in Figure 5.25.

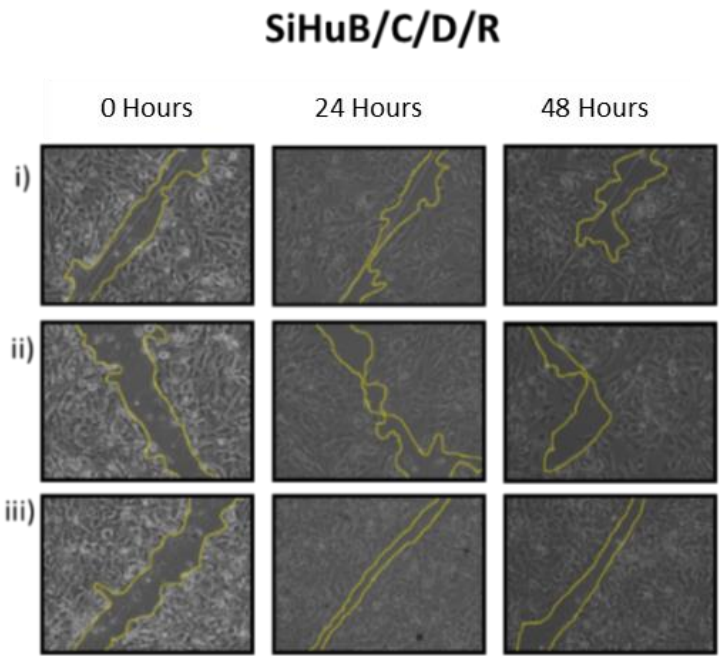

Figure 5.25: Scratch wound assays in U87-MG Glioblastoma cells following knockdown of *Hu* genes in combination. Mobility was assessed 24 hours post-transfection when cells were confluent for 72 hours. Wounds were generated after cell confluence following siRNA interference. Timepoints state the number of hours post-wound making. Yellow lines highlight the gap. Magnification x10. (n=3).

Percentage migration into the cell-free gap was calculated for the 24 hour timepoint using ImageJ pixel analysis. Two-tailed T-test determined the statistical significance. This data is show in Fig. 5.26

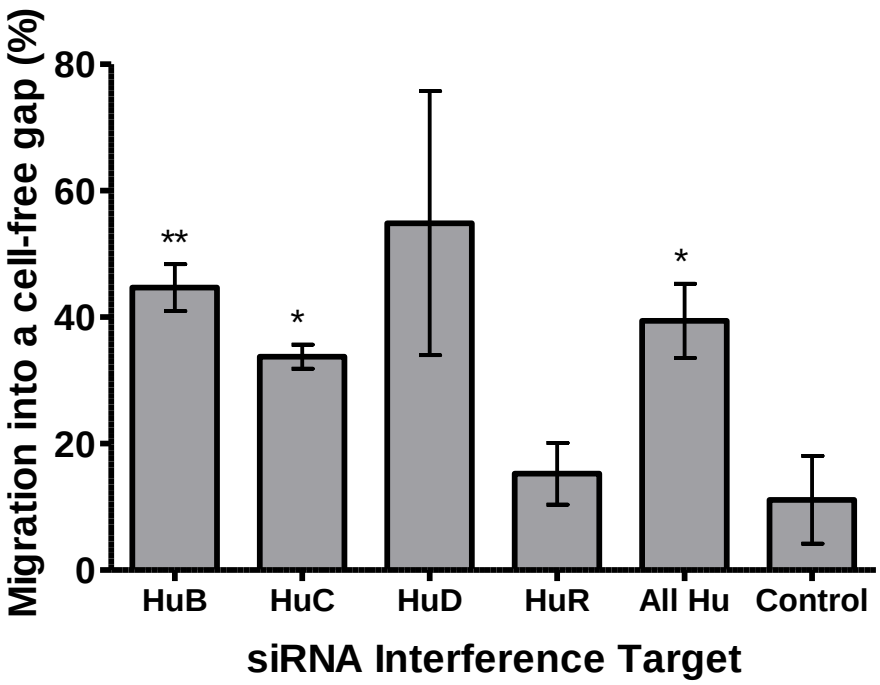

Figure 5.26: Cell migration of Glioblastoma cells U87-MG represented as the percentage of migration into the cell-free gap over 24 hours. The measure of cell motility was calculated in ImageJ through the measurement of pixels and conversion into a percentage to determine the rate of cell migration. Data showed the mean migration of cells into the cell-free gap over 24 hours. Error bars display ± SEM. Statistical significance was calculated by a two-tailed t-test and is displayed by *P ≤ 0.05, **P ≤ 0.01, ***P ≤ 0.001. (n=3).

The cell migration data in Fig. 5.25 displays that following *HuB*, *HuC* and combined *Hu* gene knockdowns, there was a significant increase in the cell migration in comparison to the non-target siRNA control. *HuB* knockdown resulted in a 33.58% increase, *HuC* knockdown showed a 22.76% increase whilst all *Hu* gene knocked down in combination resulted in a 28.30% increase in migrative potential.

A summary of changes to the cellular properties observed following *Hu* gene knockdowns in the U87-MG cell line, is displayed in Fig. 5.27.

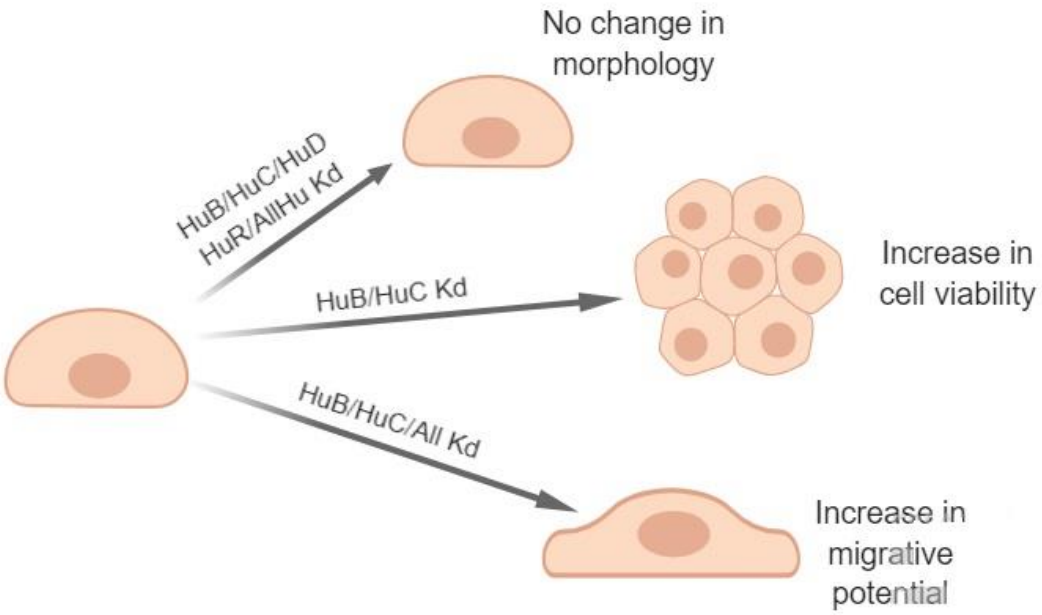

Figure 5.27: Changes in cellular properties following Individual and combined *Hu* gene family knockdown in the Glioblastoma cell line U87-MG.

No visible change in morphology was observed following any of the *Hu* gene knockdowns. *HuB* and *HuC* knockdowns both caused an increase in cell viability and migrative potential. All Hu knockdown also increased the U87-MG cells migrative potential.

5.7 Effect of *Hu* knockdown on gene regulation on translational networks in Glioblastoma

To identify gene networks the Hu RBPs are impacting in the development and progression of cancers, many genes known to influence Glioblastoma were analysed following knockdown of the Hu proteins. Ultimately, this will allow a better understanding of how *Hu* genes are functioning in the cancer and how they target translational pathways when they are aberrantly or overexpressed in Glioblastoma. Pre-designed PrimePCR™ assays with an array

of 91 primer sets in addition to controls targeting genes known to influence Glioblastoma were screened. This was to determine how Hu impacted networks and may influence fundamental cell processes.

U87-MG Glioblastoma cells were treated with siRNA and transfection reagents over a 48 hours period. RNA was then extracted, and reverse transcribed to cDNA. The knockdown was confirmed by real-time PCR before the samples were then run on PrimePCR™ assays. The pre-designed plate was run on RT-qPCR and analysed by the PrimePCR™ data analysis software provided by Bio-Rad.

AKT1	CD44	CXCR4	HRAS	MAPK3	PCNA	SERPINE1	TNF	TBP
APOE	CDK1	E2F1	IFNG	MDM2	PIK3CA	SOD2	TOP2A	GAPDH
ATM	CDK2	EGFR	IGF1	MKI67	PIK3R1	SP1	TYMS	HPRT1
AURKA	CDKN1A	ERBB2	IGFBP3	MLH1	PLAUR	SPP1	UBB	
BCL2	CDKN2A	ESR1	IL10	MMP1	PRKCA	STAT3	UBC	
BIRC5	COL1A1	EZH2	IL6	MMP2	PROM1	TCF7L2	VCAM1	
BRCA1	COL1A2	FN1	ITGB1	MMP7	PTEN	TERT	VEGFA	
CCNA2	CTBP2	GSK3B	KDR	MMP9	RAF1	TGFB1	VIM	
CCNB1	CTGF	GSTP1	KRAS	MYC	RB1	TIMP1	WNT5A	
CCNB2	CTNNB1	HIF1A	MAP2K2	NFKB2	RBM47	TIMP3	XPO5	
CCND1	CXCL12	HMOX1	MAPK1	NOTCH1	RRM2	TLR2	ZWINT	

Table 5.1: Gene targets by the Glioma T1 PrimePCR™ Assay.

Gene analysis of U87-MG Glioblastoma cells revealed many differential gene expression changes of other targets. To reduce the number of targets for further analysis, a threshold of 2.0 fold-cycle difference in gene expression was selected.

Of the 91 genes analysed shown in Table 5.1, there were 21 gene that conformed to this criterion and therefore had a differential gene expression consisting of either amplified, overexpressed, deleted or under expressed. These are shown in Table 5.2.

siRNA Interference Target				
HuB	**HuC**	**HuD**	**HuR**	**Combined Hu**
HMOX1	HMOX1	HMOX1	HMOX1	HMOX1
MMP9			MMP9	MMP9
NOTCH1	NOTCH1			NOTCH1
VCAM1	VCAM1		VCAM1	VCAM1
COL1A1			COL1A1	
	MMP1		MMP1	MMP1
			IGFBP3	IGFBP3
APOE	ITGB1	IGF1	FN1	PCNA
ERBB2	RAF1			
IL10	STAT3			
TERT	MLH1			
	PCNA			
	RB1			
	TCF7L2			
	TLR2			

Table 5.2: Identification of targets for further gene analysis influenced by *Hu* gene knockdowns in Neuroblastoma cells U87-MG. List of the 21 genes conforming to the criteria of a fold-change of at least 2. Highlighted genes are those consistent with two or more of the knockdown samples.

To limit the number of genes analysed in further studies and to identify the most important, genes whose expression was affected by two or more *Hu* gene knockdowns were selected. These are highlighted blue in Table 5.2. This lowered the gene selection to seven genes for the Glioblastoma cell line, U87-MG. A PrimePCR™ assay was designed to specifically target these genes to confirm their gene expression changes.

The relative fold-change in the transcript levels of alpha-1 type I collagen (*COL1A1*) following knockdown of each *Hu* gene individually and in combination in the Glioblastoma cell lines U87-MG is displayed in Fig. 5.28. Gene expression was normalised to the non-target control.

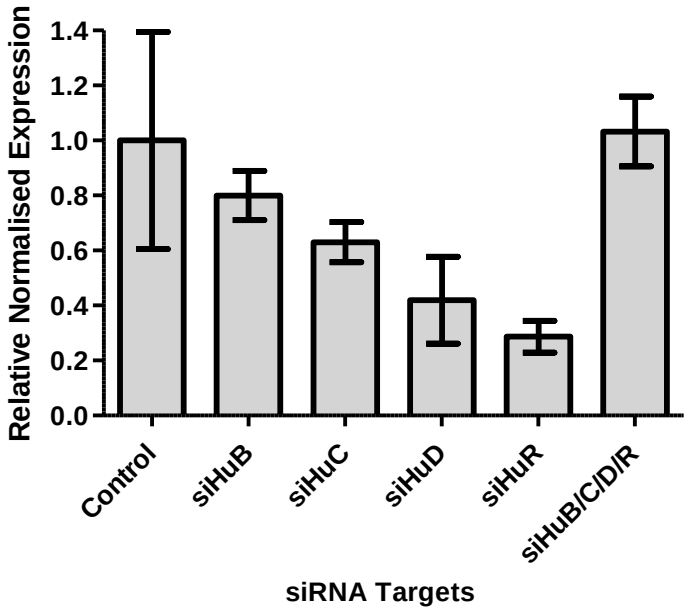

Figure 5.28: *COL1A1* gene expression following individual and combined *Hu* gene family knockdowns in U87-MG Glioblastoma cells. *COL1A1* gene expression was analysed by RT-qPCR in U87-MG cells with siRNA interference of *HuB*, *HuC*, *HuD* and *HuR* both individually and in combination. The $2^{-\Delta\Delta Ct}$ results shown are an average of three replicates normalised to *β-Actin* and compared with the control non-target siRNA. Error bars display ± SEM. Statistical significance was calculated by a two-tailed t-test and is displayed by *P ≤ 0.05, **P ≤ 0.01, ***P ≤ 0.001. (n=3).

The gene expression profile of *COL1A1* displays no statistical significance due to variation in the control. Although there was an overall general trend of decreased expression of *COL1A1* was observed when the *Hu* gene family were knocked down individually. A 1.3-fold decrease in expression was observed following *HuB* knockdown, a 1.6-fold decrease following *HuC* knockdown, a 2.4-fold decrease following *HuD* knockdown and a 3.5-fold decrease following

HuR knockdown. Little variation was seen when all *Hu* genes were knocked down in combination.

Next, the expression level of Heme Oxygenase 1 (*HMOX1*) was analysed for any alterations following Hu individual and combined gene knockdowns. This is displayed in Fig. 5.29.

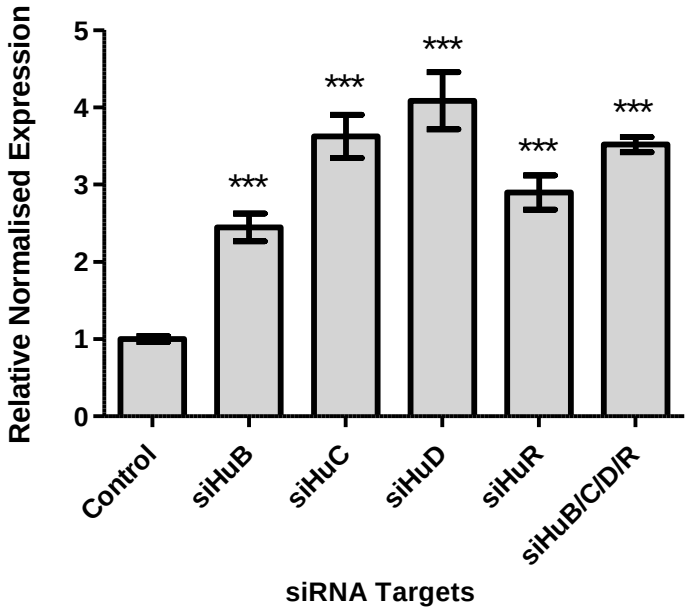

Figure 5.29: *HMOX1* gene expression following individual and combined *Hu* gene family knockdowns in U87-MG Glioblastoma cells. *HMOX1* gene expression was analysed by RT-qPCR in U87-MG cells with siRNA interference of *HuB*, *HuC*, *HuD* and *HuR* both individually and in combination. The $2^{-\Delta\Delta Ct}$ results shown are an average of three replicates normalised to *β-Actin* and compared with the control non-target siRNA. Error bars display ± SEM. Statistical significance was calculated by a two-tailed t-test and is displayed by *P ≤ 0.05, **P ≤ 0.01, ***P ≤ 0.001. (n=3).

The *HMOX1* gene expression profile displshowed an overall increased in *HMOX1* gene expression following *Hu* gene knockdowns. *HMOX1* gene expression increased by 1.4-fold following *HuB* knockdown, a 2.6-fold increase was observed following *HuC* knockdown, a 3.1-fold increase was observed following *HuD* knockdown and a 1.9-fold increase was observed

following *HuR* knockdown. Combined *Hu* gene knockdown resulted in a 2.5-fold increase in *HMOX1* gene expression. All upregulations observed were statistically significant following analysis by a two-tailed t-test.

Insulin-like growth factor-binding protein 3 (*IGFBP3*) gene expression was determined following individual and combined *Hu* gene knockdowns (Fig. 5.30).

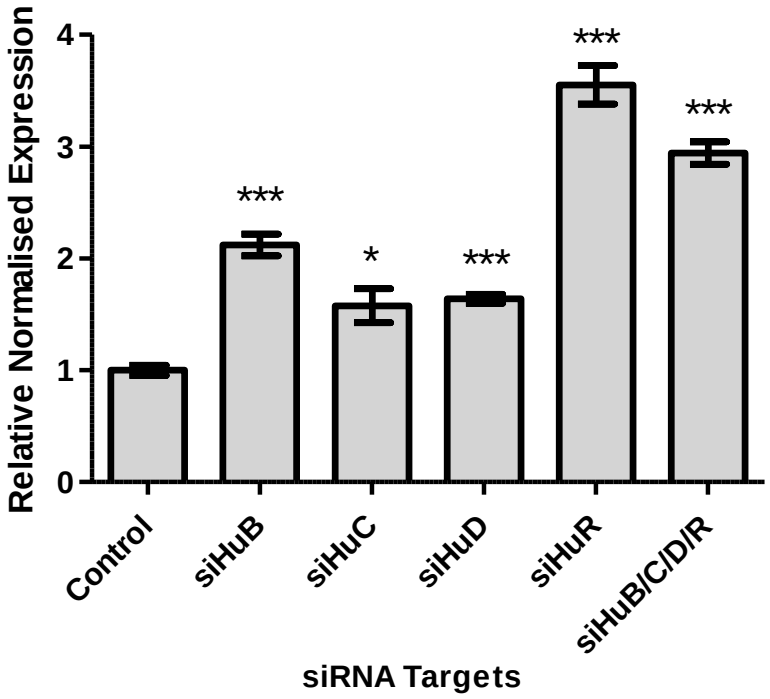

Figure 5.30: *IGFBP3* gene expression following individual and combined *Hu* gene family knockdowns in U87-MG Glioblastoma cells. *IGFBP3* gene expression was analysed by RT-qPCR in U87-MG cells with siRNA interference of *HuB*, *HuC*, *HuD* and *HuR* both individually and in combination. The $2^{-\Delta\Delta Ct}$ results shown are an average of three replicates normalised to *β-Actin* and compared with the control non-target siRNA. Error bars display ± SEM. Statistical significance was calculated by a two-tailed t-test and is displayed by *P ≤ 0.05, **P ≤ 0.01, ***P ≤ 0.001. (n=3).

Insulin-like growth factor-binding protein 3 (IGFBP3) gene expression showed an overall increase following *Hu* gene knockdowns. *IGFBP3* gene expression increased by 1.1-fold

following *HuB* knockdown, 0.6-fold following *HuC* knockdown, 0.6-fold following *HuD* knockdown and 2.6-fold following *HuR* knockdown. Combined *Hu* gene knockdown resulted in an increase of 1.9-fold in *IGFBP3* gene expression. All expression changes were statistically significant.

Matrix metallopeptidase 1 (*MMP1*) gene expression following *Hu* gene individual and combined knockdowns was then profiled and is shown in Figure 5.31.

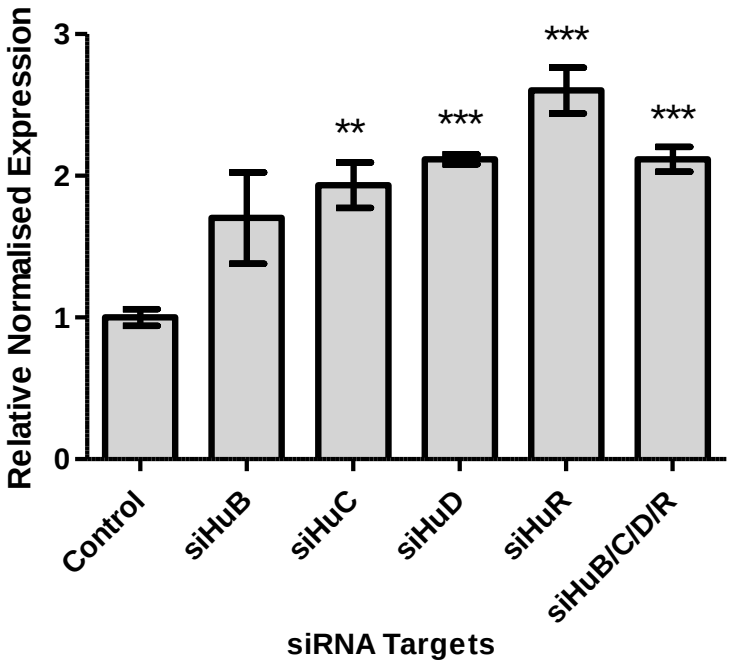

Figure 5.31: *MMP1* gene expression following individual and combined *Hu* gene family knockdowns in U87-MG Glioblastoma cells. *MMP1* gene expression was analysed by RT-qPCR in U87-MG cells with siRNA interference of *HuB*, *HuC*, *HuD* and *HuR* both individually and in combination. The $2^{-\Delta\Delta Ct}$ results shown are an average of three replicates normalised to *β-Actin* and compared with the control non-target siRNA. Error bars display ± SEM. Statistical significance was calculated by a two-tailed t-test and is displayed by *P ≤ 0.05, **P ≤ 0.01, ***P ≤ 0.001. (n=3).

Following all *Hu* gene knockdowns both individually and in combination, *MMP1* expression increased. Following HuB knockdown, *MMP1* expression increased by 0.7-fold, 0.9-fold following HuC knockdown, 1.1-fold following *HuD* knockdown and 1.6-fold following *HuR* knockdown, of which the latter three are significant. Combined *Hu* gene knockdowns saw an increase in *MMP1* gene expression by 1.1-fold that was also significant.

A further member of the Matrix metallopeptidases was analysed Matrix metallopeptidase 9 (*MMP9*) and is displayed in Figure 5.32.

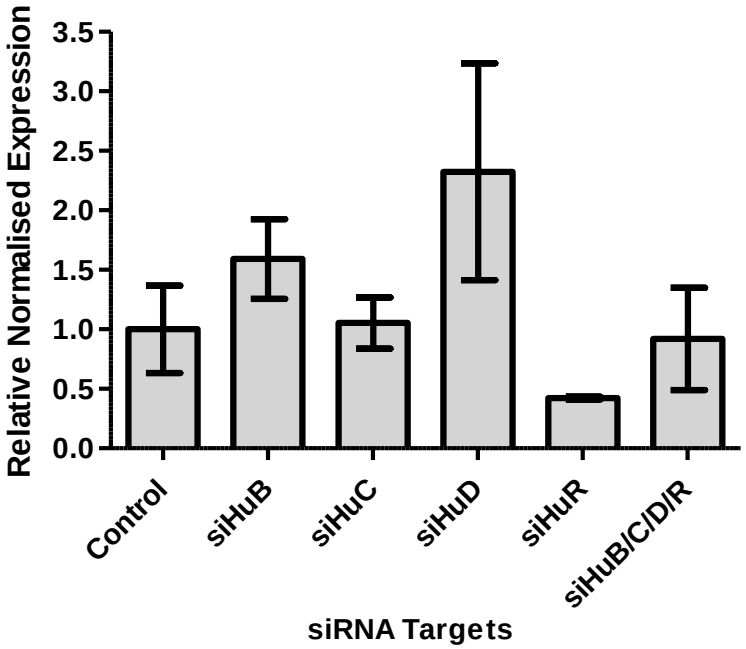

Figure 5.32: *MMP9* gene expression following individual and combined *Hu* gene family knockdowns in U87-MG Glioblastoma cells. *MMP9* gene expression was analysed by RT-qPCR in U87-MG cells with siRNA interference of *HuB*, *HuC*, *HuD* and *HuR* both individually and in combination. The $2^{-\Delta\Delta Ct}$ results shown are an average of three replicates normalised to *β-Actin* and compared with the control non-target siRNA. Error bars display ± SEM. Statistical significance was calculated by a two-tailed t-test and is displayed by *P ≤ 0.05, **P ≤ 0.01, ***P ≤ 0.001. (n=3).

The gene expression profile of *MMP9* displays no statistical significance due to variation within samples. No obvious trend is observed, however a 1.3-fold increase in *MMP9* gene expression was observed following *HuD* gene knockdown and a 2.4-fold decrease following *HuR* knockdown.

The expression profile of Notch homolog 1 (*NOTCH1*) was analysed following *Hu* gene individual and combined gene knockdowns (Fig. 5.33).

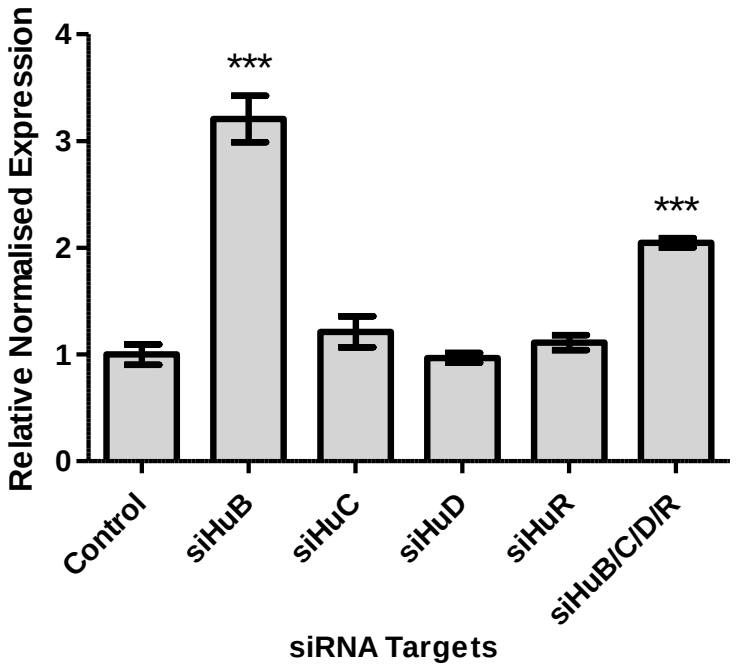

Figure 5.33: *NOTCH1* gene expression following individual and combined *Hu* gene family knockdowns in U87-MG Glioblastoma cells. *NOTCH1* gene expression was analysed by RT-qPCR in U87-MG cells with siRNA interference of *HuB*, *HuC*, *HuD* and *HuR* both individually and in combination. The $2^{-\Delta\Delta Ct}$ results shown are an average of three replicates normalised to *β-Actin* and compared with the control non-target siRNA. Error bars display ± SEM. Statistical significance was calculated by a two-tailed t-test and is displayed by *P ≤ 0.05, **P ≤ 0.01, ***P ≤ 0.001. (n=3).

NOTCH1 gene expression showed little change following *HuC*, *HuD* and *HuR* gene knockdowns. However, upon *HuB* knockdown, an increase of 2.2-fold was observed and a 1.0-fold increase following combined *Hu* gene knockdowns of which both were statistically significant.

The vascular cell adhesion molecule 1 (*VCAM1*) gene expression profile was established following individual and combined *Hu* gene knockdowns (Fig. 5.34).

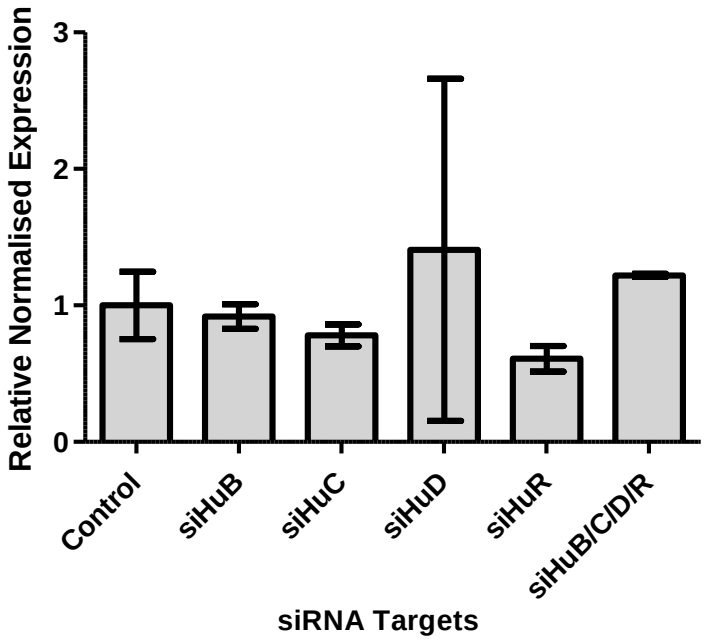

Figure 5.34: *VCAM1* gene expression following individual and combined *Hu* gene family knockdowns in U87-MG Glioblastoma cells. *VCAM1* gene expression was analysed by RT-qPCR in U87-MG cells with siRNA interference of *HuB*, *HuC*, HuD and HuR both individually and in combination. The $2^{-\Delta\Delta Ct}$ results shown are an average of three replicates normalised to *β-Actin* and compared with the control non-target siRNA. Error bars display ± SEM. Statistical significance was calculated by a two-tailed t-test and is displayed by *P ≤ 0.05, **P ≤ 0.01, ***P ≤ 0.001. (n=3).

The *VCAM1* gene expression profile showed no statistical significance. There were very little differences observed in the gene expression. The most distinct changes observed, was an upregulation of *VCAM1* gene expression following HuD knockdown which can be discredited due to its large SEM. The second largest difference is the 1.6-fold decrease in *VCAM1* expression following *HuR* gene knockdown.

To summarise the expression of all the gene targets discussed above, a heat map was developed in Microsoft Excel using analysis from Biorad PrimePCR Analysis (Fig 5.35).

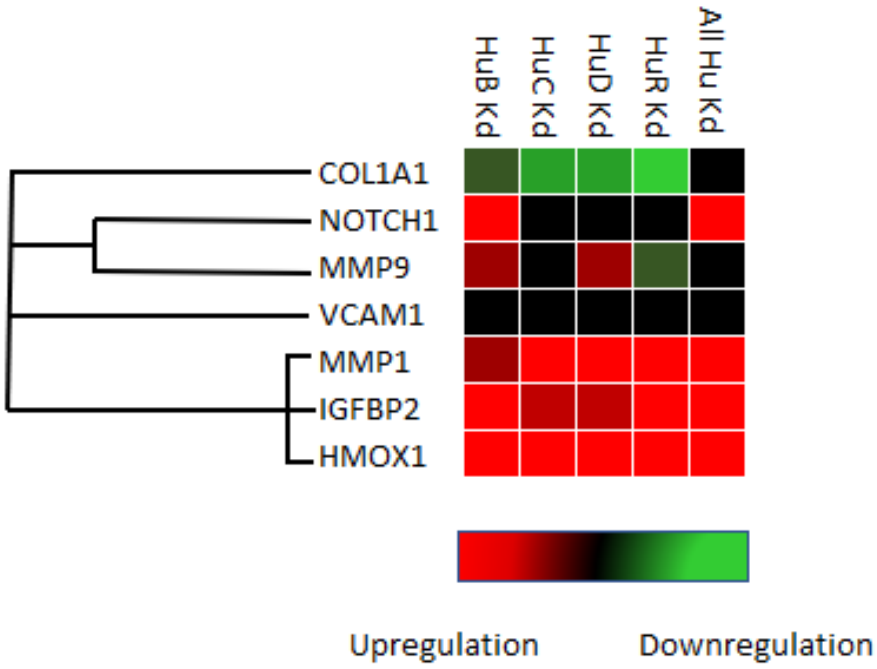

Figure 5.35: Heatmap of genes with differential expression in U87-MG cells following *Hu* gene knockdowns individually and in combination. The relative gene expression data of multiple targets in each *Hu* gene knockdown in U87-MG. Targets are clustered according to their similarity in the gene expression pattern. (Up regulation; Red, Down regulation; Green, no change; Black. The lighter the shade of colour, the greater the relative expression difference according to the magnitude of relative gene expression).

The heat map displayed Fig. 5.35, concludes that the most similar expression profiles were that of *MMP1, HMOX1* and *IGFBP3*. *VCAM1* and *COL1A1* displayed no similarity to the other genes. *MMP9* and *NOTCH* shared small similarities within their expression profiles.

The heatmap also highlighted trends between the Hu knockdowns. Following combined *Hu* gene knockdowns, 4 of the 7 genes were upregulated including *NOTCH1*, *MMP1*, *IGFBP3* and *HMOX1*. *HuB* knockdown showed 5 of the 7 genes were downregulated which included *NOTCH1*, *MMP9*, *MMP1*, *HMOX1* and *IGFBP3*.

The array of genes affected by Hu RNA-binding proteins in Neuroblastoma are summarised in Fig. 5.36.

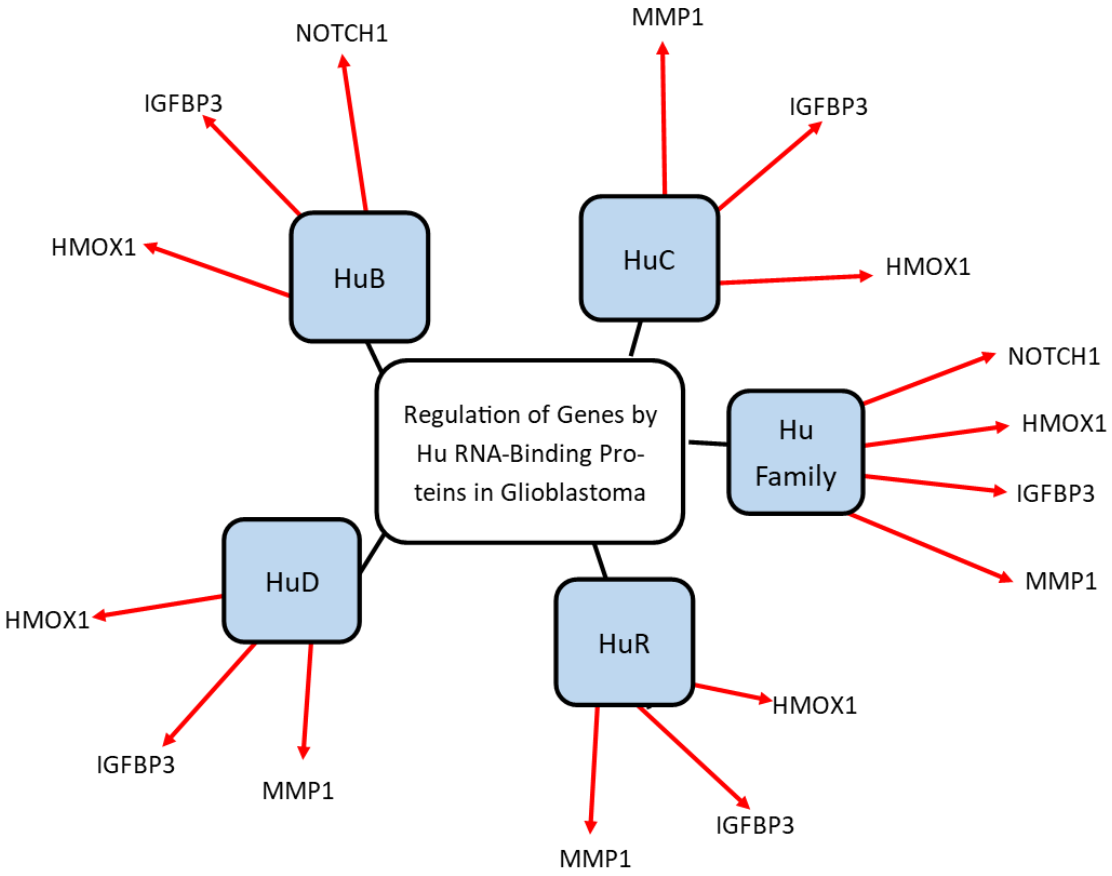

Figure 5.36 Map of *Hu* gene regulation targets identified through *Hu* gene knockdowns in U87-MG cells. The individual targets of each Hu protein individually and combined. Negative regulation is shown by a red arrow.

All the statistically significant regulation of genes following *Hu* gene individual and combined knockdowns are displayed in Fig. 5.36. Interestingly, all the genes were upregulated following the *Hu* gene knockdowns, showing that *Hu* genes play a role in negatively regulating their expression in that upon a downregulation of *Hu* gene expression, the regulatory control is lost, and their gene targets expression increases.

Additionally, all the genes named in Fig. 5.35, play a role in cell proliferation or metastasis or both.

5.8 Summary

The investigations into the Hu RNA-binding protein family and its role in Glioblastoma is shown in this chapter. The expression of each Hu gene and protein is summarised in Table 5.4.

		Hu Protein											
Cell type	Cell line	HuB			HuC			HuD			HuR		
		PCR	WB	IF	PCR	WB	IF	PCR	WB	IF	PCR	WB	IF
Normal Astrocytes	SVGp12			B			B						B
Glioblastoma	U87-MG			C			C			C			N

Table 5.3: Overall expression of HuB, HuC, HuD and HuR proteins in cell lines of normal astrocytes and Glioblastoma cells. Each method of analysis including RT-qPCR (PCR), western blotting (WB) and immunofluorescent staining (IF) is shown. Green represents a positive result. Also shown is the localisation of the proteins determined through immune fluorescence cytoplasm is shown by C, the nucleus is represented by N, whilst B refers to both the cytoplasm and the nucleus.

Gene expression data showed an upregulation of *HuB*, *HuC*, *HuD* and *HuR* gene expression in the U87-MG Glioblastoma cell line when compared to the normal astrocytes SVG p12. Western blot analysis confirmed all Hu proteins were also present in the Glioblastoma cell line. HuD and HuR proteins were absent in the normal astrocytes. However, HuR protein was later confirmed present through immunofluorescent staining.

Hu localisation studies revealed HuB, HuC and HuR proteins were localised to the nucleus with fainter expression present in the cytoplasm whilst HuD protein was confirmed absent. In U87-

MG Glioblastoma cells, the neuronal Hu proteins were present in the cytoplasm whilst HuR protein was predominantly localised in the nucleus with weaker expression in the cytoplasm.

A knockdown of each *Hu* gene individually and in combination was established in the Glioblastoma U87-MG cells (Fig. 5.10). Knockdown efficiency was determined through RT-qPCR. Protein knockdowns were confirmed by western blotting (Fig. 5.12). As previously shown, HuB protein was detected at twice its expected size and HuC protein was detected at four times its expected size. HuB, HuC and HuD protein expression decreased following individual knockdowns and was completely absent in the combined knockdown for HuB and HuC proteins. HuD's protein expression decreased following combined *Hu* gene knockdowns but was not as large as the other Hu proteins. *HuR* was knocked down at a protein level following individual and combined *Hu* gene knockdowns.

A higher knockdown efficiency was observed when all *Hu* genes were knocked down in combination compared to individual knockdowns except for *HuB* observed in Fig. 5.10 and Fig. 5.11. Since this was observed, gene studies were performed to identify any changes to *Hu* gene family members upon individual *Hu* gene knockdowns.

From these findings, it became apparent there was a level of regulatory control occurring within the *Hu* gene family that lead to the production of the model displayed in Fig. 5.16. From this model, it can be concluded that upon *HuC* knockdown, *HuR* gene expression increased showing HuC protein negatively regulates *HuR* gene expression. *HuB* knockdown resulted in a downregulation of *HuC* gene as did *HuR* knockdown on *HuD* and *HuC* gene expression. This indicates HuB positively regulates *HuC* gene expression and HuR positively regulates *HuC* and *HuD* gene expression. Three proposed theories are discussed for these regulatory influences and are discussed in Section 5.4.

Initial studies of the naïve cells migrative potential, U87-MG cells were able migrate into an agarose cell matrix whereas SVG p12 cells weren't showing Glioblastoma cells have a more migrative phenotype than normal astrocytes.

Following knockdown studies, no change in cellular morphology was observed, however changes in viability and migration potential were observed. Over 120 hours, *HuB* and *HuC* knockdown in U87-MG cells caused a significant increase in cell viability when compared to the control. The cells migrative potential increased following *HuB*, *HuC* and combined *Hu* gene knockdowns.

To identify genes that the Hu-RNA binding protein family target, a pre-designed PrimePCR™ arrays containing genes thought to be involved in Gliomas determined through the National Library of Medicine. Whilst lots of genes expression level changed following individual and *Hu* gene knockdown, a criterion was set to minimise the number of targets for further study. Genes with a gene expression change of 2.0 fold-change cycles and consistent amongst 2 or more of the Hu knockdowns reduced the targets to seven genes. The genes studied were *HMOX1*, *MMP9*, *NOTCH1*, *VCAM1*, *COL1A1*, *MMP1* and *IGFBP3*.

In-depth gene studies on the targets described above revealed a significant upregulation in *NOTCH1*, *IGFBP3* and *HMOX1*, following *HuB* gene knockdown. Upregulation was also observed in *MMP1*, *IGFBP3* and *HMOX1* following *HuC*, *HuD* and *HuR* individual knockdowns. *NOTCH1*, *HMOX1*, *IGFBP3* and *MMP1* gene expression increased following *Hu* family combined knockdown. This is suggestive of a negative regulatory effect of the *Hu* family on those genes. Each of these genes has an effect of cell proliferation or metastasis in cancer development.

Chapter 6

Discussion

Part I: Expression of Hu proteins in Small cell lung cancer, Non-small cell lung cancer and normal bronchial epithelium

Worldwide, lung cancer is considered one of the leading causes of cancer-related death (Matsumoto et al. 2012). Lung cancers are divided into two categories, Small cell lung cancer (SCLC) and Non-small cell lung cancer (NSCLC). SCLC represents 15-20% of all lung cancers in the western world (Lampaki et al. 2016).

Since 1970, there have been over 40 clinical trials conducted on SCLC patients with no significant improvement. The treatment remains unchanged consisting of combinational chemotherapeutic drugs of etoposide and cisplatin or etoposide and carboplatin (Sundstrom et al. 2002, Okamoto et al. 2007).

SCLC is diagnosed at a late stage resulting in a poor prognosis (Matsumoto et al. 2012). Current research into lung cancers stems the idea of identifying a set of new novel antibody markers. Targeting the biology and behaviour of the cancer will allow earlier diagnosis and could be used for a national screening program. Additionally, identifying more specific targets will aid the development of treatments to improve overall the survival rate.

In many cancers including Small cell lung cancer, neuronal Hu proteins are ectopically expressed in tissues or HuR is found overexpressed and this is thought to have a detrimental effect on the cells contributing to the disease. Their role in cancer development is mainly thought to be related to their role in stabilising mRNA transcripts where oncogenes are

stabilised and tumour suppressor genes are destabilised (King 1997, López de Silanes et al. 2003, Hostetter et al. 2008).

Ectopic Hu expression was originally discovered due to investigations into the cause of paraneoplastic disorders in patients with SCLC. These patients show a higher titre of autoantibodies against Hu proteins (Trier et al 2012).

Therefore, Hu proteins could be potential markers for the early detection of SCLC. This would impact the diagnosis and treatment of SCLC since treatment of early stage SCLC has a better prognosis.

6.1 The family of Hu RNA-binding proteins and their presence in lung cancers

To investigate the Hu RNA-binding proteins expression levels in lung cancers, cell lines representative of the normal bronchial epithelial tissue, Non-small cell lung cancer and Small cell lung cancer, were examined.

HuR is the most studied gene in the *Hu* family and its overexpression in cancers is well documented and related to a more aggressive cancer. As expected, *HuR* mRNA was expressed in all tested cell lines as HuR protein is expressed ubiquitously. There was a significant overexpression of *HuR* in two of the SCLC cell lines and one of the NSCLC lines when compared to the normal bronchial epithelial cells supporting the idea that *HuR* is functionally upregulated in cancers (Abdelmohsen and Gorospe 2010). This has previously been documented in SCLC (Onganer et al. 2005) and NSCLC (Wang et al. 2009).

The two suspension Small cell lung cancer cell lines, NCI-H69 and NCI-H345 showed *HuB*, *HuC* and *HuD* ectopic gene expression, whilst the third semi-adherent cell line, CorL88 displayed *HuC* and *HuD* gene expression. The absence of the neuronal *Hu* family members in the control normal bronchial epithelial cells and NSCLC cells suggests that the expression of these genes could influence SCLC development. Interestingly, lung cancer cell lines NCI-H69 and NCI-H345 represent a more severe form of SCLC with a considerably poorer prognosis.

The ectopic expression of the neuronal Hu proteins in SCLC supports existing knowledge that HuB, HuC and HuD can be ectopically expressed in SCLC tumours but not in Non-small cell lung cancers (Manley et al. 1995). Correlation exists between SCLC patients, a high titre of HuB and HuD protein antibodies and the development of paraneoplastic disorders. In these disorders, the expression of neuronal Hu proteins by the SCLC tumour provokes an autoimmune response against both the tumour and nervous tissue resulting in neurological disorders (Trier et al 2012). The oncogenic properties of Hu proteins and how they become expressed and respectively overexpressed in some tumours is unknown, although it is suggested somatic mutations may play a key role (D'Alessandro et al 2010).

RBPs contribution to SCLC carcinogenesis can be explained by their ability to bind to mRNA transcripts of oncogenes or tumour suppressor genes affecting their stability and consequently influencing oncogenic signalling pathways (Wang et al. 2015).

Hu proteins bind directly to AU-rich sequences found in the introns and 3′ untranslated regions of many short-lived mRNAs. They can target a large range of transcripts involved in cancer development including those responsible for proliferation, invasion and metastasis, angiogenesis and immunomodulation. This allows aberrant and over-expressed RBPs to provide a regulatory function specific to the cancer needs (Wurth 2012).

Genome-wide studies of *Hu* expression revealed major differences between mRNA transcript presence and protein expression. It also revealed that protein expression vary in different conditions such as during development, environmental stress and during disease (Re et al. 2016). Therefore, protein expression studies using western blot were performed for each Hu protein detection.

Western blotting interestingly revealed strong HuB protein expression in CorL88, NCI-H345 and NCI-H69 SCLC cell lines as well as faint staining in the NSCLC cell lines, NCI-H322 and NCI-H358. The mRNA expression of *HuB* was almost undetectable in NSCLC cells when compared to the normal bronchial epithelial cell, analysed by the ΔΔCT method. Low *HuB* expression at RNA level and high protein expression detected through western blot suggests a high translation rate.

HuC and HuD protein expression was only detected in NCI-H345 and NCI-H69 SCLC cell lines despite the third SCLC cell line CorL88 also showed a *HuC* and *HuD* at RNA level. This could be explained by mRNA instability or a low translational rate of *HuC* and *HuD* in the CorL88 SCLC cells.

In summary, ectopic expression of the neuronal Hu proteins, HuB, HuC and HuD proteins was observed in Small cell lung cancer. An upregulation of HuR was observed in all NSCLC and SCLC cells.

Whilst the results have currently demonstrated the aberrant and over expression of the Hu RNA-binding protein family that is definite at both gene expression and protein level in SCLC, the subcellular localisation of the Hu proteins within cells is as important to the pathogenicity of the cancer.

HuB, HuC and HuD protein expression is in the cytoplasm of neurons whist HuR protein is predominantly expressed in the nucleus (Gao and Keene 1996, Kasashima et al. 1999, Good 1995).

HuR's cytoplasmic overexpression is associated with a clinically poorer cancer phenotype. As previously discussed in Section 1.10, HuR cytoplasmic localisation in Oesophageal tumours is associated with lymph node metastasis, high-grade malignancy and poor survival rates (Zhang et al. 2014). Large tumours in Breast cancer are usually p53 positive, oestrogen and progesterone receptor negative, and show upregulated cytoplasmic HuR (Heinonen et al. 2007, Calaluce et al. 2010). Chemically induced mice lung tumours expressed elevated levels of cytoplasmic HuR (Blaxall et al. 2000). In NSCLC specifically, cytoplasmic HuR induced angiogenesis and lymph-angiogenesis through the upregulation of VEGF-C (Wang et al. 2011).

Whilst HuR protein could not be detected by western blot in the normal bronchial epithelial cells, a clear localisation to the nucleus could be shown by immunofluorescence. Furthermore, HuR protein was also localised to the nucleus in both NSCLC cells lines. This was consistent with HuR's expected subcellular localisation. HuR's nuclear role is in regulating the export of bound mRNAs to the cytoplasm protecting them from decay (Brennan and Steitz 2001). HuR protein expression in nucleus of NSCLC cells correlates to a more treatable cancer diagnosis.

In NCI-H345 and NCI-H69 SCLC cells specifically, all Hu proteins expression was confirmed by western blot and immunofluorescence. This shows the ectopic expression detected at RNA level leads to a protein product that can be identified by specific Hu antigens. Anti-Hu fluorescence staining revealed the Hu family of proteins resided in the nucleus of the NCI-H69 cell line, whilst all Hu proteins were detected in the cytoplasm in the NCI-H345 cell line. This

data highlights the variability of SCLC and the differential localisation of Hu proteins can be explained by the different cell types that been found in SCLC cancer samples. Contrary to their normal localisation in neurons, HuB, HuC and HuD protein in NCI-H69 and HuR in NCI-H345 were alternatively localised, a feature conserved to SCLC cells.

There is little known about how the subcellular localisation of neuronal Hu proteins affects the cancerous phenotype. However, research into the posttranscriptional gene regulatory role of Hu proteins and their ability to influence mRNA transcript stability provides a possible explanation of how these cells contribute to disease (Zaharieva et al. 2015b). In the nucleus, Hu proteins control polyadenylation and splicing. Whilst in the cytoplasm, Hu proteins regulate mRNA stability by binding to AU-rich elements (AREs) of many short-lived mRNAs (Kim and Gorospe 2008, Zhu et al. 2007).

The presence of HuR in the cytoplasm of NCI-N345 SCLC cells is indicative of nucleo-cytoplasmic shuttling, a process that is discussed in Section 1.7.3. In the cytoplasm, HuR mediates mRNA stabilisation through its ability to interact directly with an mRNA transcript by binding to AREs in their 3'UTR enabling translation into a protein (Abdelmohsen and Gorospe 2010). Hu proteins target an array of RNA transcripts coding for transcription factors, cytokines, growth factors and proto-oncogenes (Wang et al. 2015). Many of HuR's targets are oncogenes therefore promoting stabilisation and translation of mRNA transcripts in SCLC will aid cancer initiation and progression.

Whilst *HuC* gene expresison was observed in CorL88 SCLC cells, HuC protein could not be detected by western blot or immunofluorescence staining suggesting the expressed RNA detected by RT-qPCR is inactive and therefore not translated into a protein. CorL88 cells showed weak staining of HuD in the cytoplasm whilst HuR was observed in the nucleus

corresponding to their normal localisation described in the literature (Gao and Keene 1996, Kasashima et al. 1999, Good 1995). HuD was previously undetected by western blot in CorL88 cells, yet fluorescence staining showed a weak signal of HuD protein in the cytoplasm, its natural residing location.

6.2 Cellular properties of normal lung and lung cancer cells

Cell culture observations revealed similar morphology within each cell subtypes of SCLC, NSCLC and the normal bronchial epithelial cells separately. SCLC has impressive morphological features during in-vitro studies and this could be related to its pathogenicity. These cells are small and round with small nucleus to cytoplasm ratio. They grow in clusters regardless of whether they are in suspension or attach to the vessel in which they are cultured (Brambilla et al. 2001).

All three SCLC cell lines grew in clusters. NCI-H345 and NCI-H69 of the SCLC cell lines grew in suspension while the third CorL88 is a semi adherent cell line. Interestingly, the semi adherent CorL88 cell line differed in its Hu protein expression at RNA and protein level compared to the other two SCLC cells lines and gives rise to further studies of Hu derived targets that influence anchorage dependence.

The two NSCLC cell lines and the normal bronchial epithelial cells shared a similar morphology with adherent properties. This allowed studies of motility.

These cells were tested for their ability to migrate into a gel matrix. Interestingly, one of the NSCLC cell lines, NCI-H358 was able to migrate into the gel matrix showing a more motile cell phenotype. This could represent the ability of the cells to metastasize into distant organs

forming secondary tumours. This finding highlights a difference in migrative potential within the NSCLC tumours but also concludes that it is possible for some NSCLC tumour to have a metastatic phenotype.

In this study, the ectopic expression of the neuronal *Hu* genes *HuB*, *HuC* and *HuD* in SCLC were identified with an overexpression of *HuR* in both SCLC and NSCLC. Current diagnosis of SCLC relies heavily on the morphology in which the lung tumour cells present. This along with the developmental stage of the disease determines the course of treatment the patient is offered. A large degree of variability between *Hu* gene and protein expression was observed as well as differential cellular localisation even within the SCLC cells with similar morphology. This highlights the importance of the development of new diagnostic methods particularly focussed on molecular subtyping of cancers since the morphology is not sufficient.

6.3 Concluding Remarks

The proposition of using *Hu* gene and protein expression to develop a grading system could be beneficial to current diagnosis methods, however further studies would be required to support this theory. Initially, the aberrant expression of these proteins in the cells should be determined due to its significance but then also the sub-cellular expression of these proteins is indicative of their role within the cells which is essentially the most important factor.

The expression and prognostic value of the neuronal *Hu* genes and proteins could initially be used an indicator of SCLC through detection of anti-Hu antibodies in the blood as previously described by D'Alessandro et al. (2008), or in very early lung tumour tissue. It was established that aberrant *HuB*, *HuC*, *HuD* and overexpression of *HuR* in SCLC may influence the progress of the cancers through their natural role as RNA-binding proteins. By regulating splicing

patterns and the stability of mRNA transcripts, the ectopic Hu proteins along with natural-occurring lung-specific RNA-binding proteins, increase the number of transcripts expressed overall in the tumour due to their individual target transcripts, expanding the number of genes transcribed. The extra Hu protein action gives rise to a genetically-rich enhanced cell type influencing the cancers development and progression. The extent of Hu profiling can be used as a prognosis method in that the more of the *Hu* genes actively working the more enhanced the cancer cells are and likely to be a more aggressive phenotype.

The subcellular Hu localisation in the SCLC cells could serve as method to better predict prognosis. This also gives rise to Hu proteins as therapeutic targets regardless of their role since by targeting cells only containing the aberrantly expressed proteins, the tumour tissue, and the evidence that a triple depletion of neuronal *Hu* genes in mice was lethal (Akamatsu et al. 2005).

The ability to transfect SCLC-cell lines proved extremely difficult, this is thought to be due to their growth in suspension. Therefore, considering this reason and previous research on this cancer and Hu proteins, it was decided to focus our future studies on Glioblastoma and Neuroblastoma. If studies into SCLC were continued, CRISPR technology would have been used to knockout the *Hu* genes in these cell lines.

Due to the inability to knockdown the *Hu* genes it was impossible to determine if using Hu proteins as targets to knockdown genetically within SCLC cells would impact the tumours growth. If this was the case, immunotherapeutic testing and therapeutic drugs could be applied to several different malignancies of solid tumours where Hu proteins are indicated not just SCLC and NSCLC.

Chapter 7

Discussion

Part II: Expression of Hu proteins in Neuroblastoma

Neuroblastoma is an embryonal tumour of the peripheral sympathetic nervous system. It represents 15% of all childhood cancer deaths and has an average 5-year survival rate of less than 50% (Maris et al. 2007, Ehrlich et al. 2014). The molecular heterogeneity and phenotypic diversity of Neuroblastoma is responsible for a wide range of clinical presentations and varying response to treatments. The severity of this disease drives the need to yield actionable therapeutic targets for this highly fatal cancer (Louis and Shohet 2015).

Hu proteins and their corresponding antibodies have been found in Neuroblastoma. Ball and King (1997) found that in primary NB tissue, samples that expressed the highest *Hel-N1* (*HuB*) or *HuD* levels were *MYCN* unamplified tumours. *HuB* and *HuD* upregulated gene expression in this cancer provides an excellent model for Hu protein analysis.

Whilst Hu activity is reported in many cancers and thought to have oncogenic properties, unfortunately, the mechanisms that modulate its ectopic and overexpression in tumours is largely unknown. It is suggested somatic mutations may play a key role (D'Alessandro et al 2010). *HuR* specifically is localised in chromosome 19p13.2 and this particular locus has been associated many translocations and oncogenic advances in human tumours (Ma and Furneaux 1997).

7.1 The family of Hu RNA-binding proteins and their presence in Neuroblastoma

The *Hu* gene expression profiling in Neuroblastoma focused on three cell lines; normal astrocytes, SVG p12, as a control and two Neuroblastoma cell lines, SH-SY5Y and SK-N-AS. Using relative fold change expression analysis ($2^{-\Delta\Delta Ct}$) and *ß-Actin* as an internalised standard, the expression levels of each Hu gene was analysed. The RT-qPCR data of the two Neuroblastoma cell lines was normalised to the control cell line, SVGp12 normal astrocytes cell line which by itself had the lowest gene expression of *HuB*, *HuC*, *HuD* and *HuR*.

Hu gene analysis revealed an upregulation of the neuronal *Hu* genes in both Neuroblastoma cell lines compared to the control astrocyte cell line. These genes are known to be differentially expressed at various stages of embryonic neuronal development. *HuB* expression occurs very early in development whilst *HuC* and *HuD* expression appear later in embryonic development (Marusich et al. 1994, Yano et al. 2016). Since Neuroblastoma is an embryonal-derived tumour, an upregulated expression of all the neuronal *Hu* genes in tumours, may induce a gain-in-function where a new molecular function or a new pattern of gene expression is observed.

The ubiquitously expressed *HuR* was significantly upregulated in SH-SY5Y Neuroblastoma cells. *HuR* gene expression levels are often elevated in cancer cells and are reduced in senescent and quiescent cells (Dai et al. 2012). This upregulated expression of *HuR* suggests an additional role in this cell line compared to the second Neuroblastoma cell line, SK-N-AS and the control normal astrocyte cell line.

A comparison of the two Neuroblastoma cell lines showed an overall higher gene expression of all Hu proteins in SH-SY5Y cells than the second Neuroblastoma cell line SK-N-AS when compared to the control astrocytes.

This variation of *Hu* gene expression in these two cell lines aligns with the described variation of *HuB* and *HuD* expression at a densitometric levels in samples of Neuroblastoma tissue as determined through RNase protection assay (Ball and King 1997).

The observed gene expression profile of Hu proteins does not necessarily mean that the same levels of expression is detected at protein level. Additionally, a proteins intracellular localisation determines it functional effect (Zaharieva et al. 2015b). Previously studies have shown that Hu proteins can redistribute between the nucleus and cytoplasm. The neuronal Hu members HuB, HuC, HuD are mainly located in the cytoplasm with a small amount of protein detected in the nucleus (Gao and Keene 1996, Antic and Keene 1998). Hu proteins subcellular localisation can be quite variable depending on the cell type. A more cytoplasmic-defined localisation is observed in many tumour cells (Antic and Keene 1997).

It is well established that in the nucleus, Hu proteins regulate processes such as alternative splicing and polyadenylation and are also involved in the export of bound mRNAs to the cytoplasm protecting them from decay (Brennan and Steitz 2001, Zhu et al. 2007, Izquierdo 2008). In the cytoplasm, they continue to act on these mRNA transcripts by binding directly and upregulating a transcripts potential (Brennan and Steitz 2001).

HuB was expressed at RNA level in all cell lines as confirmed by RT-qPCR gene analysis. Protein expression levels did not correlate with transcript mRNA levels detected by the gene analysis. Normal astrocytes showed the least *HuB* gene expression at an almost undetectable level when compared to the Neuroblastoma cells following $2^{-\Delta\Delta Ct}$ gene quantification. However, at a protein level, HuB showed a four times higher expression compared to GAPDH expression suggesting a high translational rate for HuB in normal astrocytes, SVGp12. This could be

explained by the embryonic origin of this cell line when HuB is expressed during neuronal development as mentioned above.

In addition to the expected Hu signal at 38kDa, a band at 76kDa was detected which could be a HuB dimer. This is rather a usual occurrence following the denaturation of proteins before the Western blot but offers an explanation. The presence of HuB could be confirmed by immunofluorescence and a localisation in both the cytoplasm and nucleus was found.

The nuclear localisation of HuB in normal astrocytes is inconsistent with the regular localisation of HuB protein. The presence neuronal Hu family proteins in the cytoplasm and the nucleus of the normal astrocytes is not surprising since they share similarities with neurons in that both reside in cortical areas, contribute to the maintenance of the central nervous system and allow metabolic interplay between astrocytes and neurons. In neurons, Hu proteins can appear to be distributed equally in both the nucleus and cytoplasm (Antic and Keene 1997). As a post-transcriptional gene regulator, HuC protein can act to influence splicing patterns and mRNA export when it is localised in the nucleus.

The SK-N-AS Neuroblastoma cells showed equal expression of HuB to GAPDH expression as determined through band intensity. Compared to SH-SY5Y cells, SK-N-AS cells have a higher protein expression which is consistent with the gene expression data. In SH-SY5Y cells, HuB proteins shows less than half of the control GAPDH protein expression.

In SK-N-AS and SH-SY5Y Neuroblastoma cells, only the higher band at 76 kDa could be detected which could be a result of HuB protein dimerisation. HuB was localised mainly in the nucleus, with a weaker signal in the cytoplasm in these cells. HuB protein is normally restricted to the cytoplasm in undifferentiated neurons where it co-localises with ribosomes controlling mRNA metabolism and neuronal differentiation (Gao and Keene 1996). The

presence of neuronal Hu proteins in the nucleus is not unusual as it is well documented that Hu proteins can translocate from the cytoplasm to the nucleus playing crucial roles in posttranscriptional gene regulation (Doller et al. 2008b).

HuB nuclear localisation in the Neuroblastoma cell line SK-N-AS, could be explained by its upregulated gene expression and high protein level whereby it is proactively transported to the nucleus in a ratio-dependent mechanism. As previously described, in the nucleus, HuB can regulate alternative splicing of mRNA transcripts and can assist in the export of mRNA transcripts to the cytoplasm protecting them from decay (Zhu et al. 2007, Ince-Dunn et al. 2012, Brennan and Steitz 2001).

One feature of cancer cells is a high proliferation rate. In the cytoplasm, HuB protein can bind and regulate the stability and translation of many mRNA transcripts involved in proliferation. This increases the molecular advantage of a cell (Brennan and Steitz 2001).

HuC protein was found to be highly expressed in the normal astrocytes, SVG p12. In this cell line, it was detected as a monomer at the expected size of 39kDa and around four times the expected size of HuC protein, suggesting HuC experiences multimerisation. HuC protein was predominantly localised in the nucleus of the SVG p12 astrocytes, although a lower a level of HuC protein was also observed in the cytoplasm.

The nuclear localisation of HuC in normal astrocytes is inconsistent with the regular localisation of HuC protein and is thought to be due to similar effects described about HuB where there is an increased demand for mRNA regulation in the nucleus.

Similar to the effects seen in the embryonic cell line, the stresses upon a cancer cell may result in HuC being recruited to the nucleus. In the nucleus, it can regulate the splice patterns of mRNA transcripts and assist in their translocation to the cytoplasm for additional processing.

In both Neuroblastoma cell lines, only the higher molecular band four times the size of the expected 39kDa was detected by Western blotting. This is potentially significant of HuC protein multimerisation. HuC was expressed equally and about half of the GADPH control protein expression. At RNA expression level in SH-SY5Y cells showed a HuC higher expression level than SK-N-AS cells highlighting again that RNA expression levels do not necessarily reflect on the abundance at protein level.

HuC protein expression and localisation was also confirmed by immunofluorescence studies. HuC was localised in both the cytoplasm and the nucleus in the normal astrocytes and SH-SY5Y, Neuroblastoma cells. In SK-N-AS cells, HuC protein was expressed in the cytoplasm only. HuC protein is reportedly expressed in the cytoplasm of differentiated neurons (Okano and Darnell 1997).

The larger protein moieties detected in normal astrocytes and Neuroblastoma cells could be explained by a dimerization or multimerisation of HuB and HuC, respectively. It is known that Hu monomers can bind to each other or themselves at the third RRM and hinge region of Hu RNA-binding proteins structure displayed in Fig. 1.6. (Fialcowitz-White et al. 2007, Kasashima et al. 2002).

Dimerisation and multimerisation of the neuronal proteins is thought to contribute to their ability to form large ribonucleoprotein (RNP) complexes. These form from protein-protein interactions that then bind RNA (Kasashima et al. 2002). RNP complexes then bind with the translational apparatus of the cell, upregulating transcript stability and translation (Antic and Keene 1998).

Protein analysis revealed HuD was absent in normal astrocytes but present in the Neuroblastoma cells. HuD protein expression in the SH-SY5Y cells was comparable to the GAPDH control. In SK-N-AS cells, HuD protein was expressed about 20% of the control band

intensity. Overall, a higher HuD protein expression was observed in the SH-SY5Y cells that correlates with gene expression levels.

The absence of HuD protein in normal astrocytes was confirmed by immunofluorescent staining. In SK-N-AS and SH-SY5Y cells, HuD protein was found in the cytoplasm only which aligns with the described localisation of HuD in neuronal development (Kasashima et al. 1999).

Ball and King (1997) reported that upregulation of *HuB* and *HuD* gene expression correlated with unamplified *MYCN* levels in primary Neuroblastoma tissue. A upregulation of *HuB* and *HuD* was found in both Neuroblastoma cell lines, SH-SY5Y and SK-N-AS and their known status of *NMYC*-non-amplified cells (Peirce and Findley 2015, Veas-Perez de Tudela et al. 2010).

Western blot analysis showed a very low expression of HuR in the normal astrocytes cell line SVG p12. A low abundance of HuR was confirmed by immunofluorescence with a predominant localisation to the nucleus.

A slightly increased expression of HuR compared to GADPH was seen in both Neuroblastoma cell lines. The protein expression level aligns with the *HuR* RNA expression level which showed a upregulation in both Neuroblastoma cell lines, but not statistically significant in SK-N-AS cells.

HuR protein was localised in the nucleus of the SK-N-AS cells and in the cytoplasm of SH-SY5Y cells. In neurons, HuR protein expression is predominantly seen in the nucleus of normal cells, but upon cellular signals HuR shuttles between the nucleus and the cytoplasm (Good 1995, Fan and Steitz 1998).

RNA-binding proteins localisation often determines the extent of transcript stability, translation rate and degradation (Zhu 2009). The cytoplasmic localisation of HuR protein in

SH-SY5Y cells could be linked to its overexpression. Often when an upregulation of HuR protein in the nucleus occurs, the cells actively translocate HuR protein to the cytoplasm (Doller et al. 2008b). In the cytoplasm, HuR protein can participate in roles such as regulating mRNA translation, stability and degradation.

HuR is the most extensively researched Hu protein in cancer related studies; it's upregulation and cytoplasmic localisation has been linked to a severe phenotype of cancer resulting in a poor prognosis (Table 1.2).

7.2 Regulatory interactions of Hu RNA-binding proteins in Neuroblastoma

Members of the Hu family can bind their own mRNA and mRNA of other family members and influence their expression (Bolognani et al. 2009, Mansfield and Keene 2012). Hu proteins bind mRNA sequences containing a distant AU-rich elements and once bound stabilise the target transcripts (Pullmann et al. 2007, Al-Ahmadi et al. 2009).

HuR protein specifically auto-regulates its' own expression through a negative feedback loop maintaining HuR homeostasis in proliferating cells. This occurs in response to cellular stress by promoting alternative polyadenylation site usage. HuR protein residing in the nucleus contains a GU-rich element overlapping with the HuR major polyadenylation signal. Following upregulation of HuR protein, the expression of the long 2.4kb isoform of *HuR* containing an AU-rich element is destabilised, reducing its protein level. This maintains a steady expression of HuR in the cell (Dai et al. 2012).

To understand the regulatory interactions of Hu RNA-binding proteins, a single and combined knockout of the *Hu* genes was established in SH-SY5Y and SK-N-AS Neuroblastoma cells using siRNA interference.

Observations in Neuroblastoma cells but particularly in the SH-SY5Y cell line, where a high overall expression of *Hu* genes was observed, were suggestive of a regulatory mechanism occurring between Hu family members an overall more efficient knockdown of Hu gene expression was achieved in a combined knockdown compared to the individual knockdowns. This was later confirmed by western blot where the most efficient knockdown of each individual Hu protein was through the combined *Hu* siRNA knockdown.

In the single knockdowns of *HuR* and *HuD*, all the other Hu family members mRNA levels also reduced. In the combined knockdown, an increased efficiency was seen for the neuronal *Hu* genes, *HuB*, *HuC* and *HuD*. *HuR* gene expression following combined *Hu* gene knockdown correlated a combined effect of the individual knockdowns of *HuD* and *HuR*. *HuR* mRNA levels decreased by 27% following *HuD* knockdown, 81% following *HuR* knockdown and 70% following combined *Hu* family knockdown. Overall, it can be concluded that HuD and HuR the main players in regulating other Hu proteins expression.

Hu family proteins are highly conserved not just within their sequence but in their roles as posttranscriptional regulators. *ELAV* is the Drosophila homolog of the human *Hu* genes. Zaharieva et al. (2015) found that Drosophila family members can regulate each other's target transcripts. *ELAV*-related Sex-lethal regulated *ELAV* targets. They also described a dosage-compensation relationship between Sex-lethal and RBP9 proteins.

It appears familial Hu proteins are possibly able to functionally counteract the depletion of another. The work described in this thesis found regulatory mechanisms within the Hu family network. This led to the development of a hypothetical model of Hu protein interactions for each of the Neuroblastoma cell lines.

The hypothetical model describes the potential interactions and regulatory interplays as follows. Firstly, an auto-regulation of Hu protein family members where they can target their own transcripts and regulate their expression in a feedback loop. Secondly, the regulation could be due to a functional compensation, during which other *Hu* genes become upregulated for the decreased expression of other *Hu* family members after the knockdown. And finally, the observed effects could due to an off-target effect of *Hu* gene regulation, whereby a mRNA transcript affected by the *Hu* genes regulation triggers a feedback loop, affecting the expression of a different *Hu* gene family member. Since, miRNAs and other RBPs have also shown to influence Hu protein expression, it's important to consider potential other upstream or downstream regulators of the Hu family proteins, which itself highlights the need to identify other signalling pathways important for Hu regulatory function (Al-ahmadi et al. 2013).

In the SH-SY5Y cell line, HuB is potentially a negative regulator of *HuC* and *HuD* gene expression. This could be explained that HuB bind to AREs of *HuC* and *HuD* mRNA transcripts which leads to a regular expression of their mRNA in the cells. Therefore, when *HuB* is downregulated, consequently the expression of *HuC* and *HuD* would increase. Alternatively, *HuC* and *HuD* genes may compensate for the decreased expression of *HuB* gene by upregulating their own expression. There is also the possibility that *HuB* knockdown results in off targets effects subsequently upregulating *HuC* and *HuD* gene expression through downstream activators. This could be HuB acts of a different target transcript that also affect *HuC* and *HuD* gene regulation and the described effects could be due to the effect on that different transcript initially.

When *HuC* gene expression was reduced, a significant increase of *HuR* gene expression was observed. This could be explained by HuC protein actively controlling the transcription of *HuR* mRNA or that the increase in *HuR* gene expression compensates for *HuC* gene activities.

HuD seems to positively regulate the gene expression of the other neuronal *Hu* genes, *HuB* and *HuC*. Whilst HuR upregulated the gene expression of all the other *Hu* genes in this Neuroblastoma cell model. When *HuD* or *HuR* gene expression was decreased, the other *Hu* genes expression were also reduced. This is most likely due to HuD and HuR proteins binding directly to the mRNA transcripts of the other *Hu* genes and stabilising their expression or it could be due to off target effects where a different mRNA affected by *HuD* or *HuR* knockdown influences the other neuronal Hu proteins. HuC protein was also found to be a positive regulator of *HuB* gene expression, since *HuB* gene expression decreased when *HuC* gene was knocked down. This can be explained by the same possible interpretation as described for HuD regulation of *HuB* and *HuC*. In the SK-N-AS cell line, the following explanations are based on three hypothesised regulatory interactions that were previously discussed in Section 4.4.1. HuC and HuD are negative regulators of *HuB* expression. The regulatory influences of HuC and HuD proteins on *HuB* gene expression may be explained by direct binding of HuC or HuD proteins to the mRNA transcripts of *HuB* gene and stabilising its expression. Therefore, upon *HuC* and *HuD* siRNA knockdown, *HuB* mRNA transcript is no longer under this regulatory control and its expression increases. It is also possible that HuB compensates for the reduced gene expression of *HuC* and *HuD*. This level of regulation can be explained by the same interpretations discussed for HuC's regulation of *HuR*.

HuR knockdown appears as a positive regulator of *HuC* expression as a decrease in *HuC* expression occurs. This can be explained by the fact that HuR binds directly to *HuC's* mRNA

transcript and stabilises its expression. Therefore, when *HuR* expression is reduced, *HuC's* transcript becomes unstable. Additionally, this could be caused by off target effects of *HuR's* downregulation. HuC and HuR are located on the same chromosome, 19p13.2 where HuC is centromeric to HuR (Van Tine et al. 1998).

Correlation between nuclear HuR and its ability to auto-regulate its own transcript was documented by Dai et al. (2012). HuR autoregulates its expression by promoting alternative polyadenylation site usage through a negative feedback loop. This often leads to a large amount of cytoplasmic HuR as it's the nuclear HuR that induces this action. In the Neuroblastoma cell line SH-SY5Y, overexpression of *HuR* gene showed a predominant protein presence in the cytoplasm contributing to this theory.

These regulatory interactions observed of HuR may apply to other Hu proteins since their sequences and function is highly conserved. This may also explain the inability to achieve higher than a 50% knockdown of *HuB* gene in SK-N-AS cells.

The observed higher molecular weight of HuB and HuC in western blots that could be a result of a dimerisation or multimerisation respectively, has been shown to allow Hu proteins to upregulate their own mRNA transcripts and further bind with additional Hu proteins at the third RRM and hinge region as previously described (Fialcowitz-White et al. 2007, Kasashima et al. 2002).

In Neuroblastoma, HuB and HuC proteins were revealed as major players in only the negative regulation of other *Hu* genes. In SK-N-AS cells, HuB protein was a negative regulator of *HuR* gene expression. This was shown by *HuB* gene knockdown and a resulting increase in *HuR* gene expression. Also, HuC protein negatively regulated *HuB* gene expression. In SH-SY5Y cells, HuB protein was a negative regulator of *HuC* and *HuD* gene expression, since following

HuB knockdown, *HuC* and *HuD* gene expression increased significantly. Additionally, HuC protein was a negative regulator of *HuR* gene expression.

Of the two cell regulatory models, the only similarity is that HuC is a negative regulator of *HuR* gene expression. However, if these models were combined, HuB and HuR protein can regulate each other's expression, as can HuB and HuD, HuC and HuR.

This presented study on gene expression and the regulatory network of Hu proteins highlights the compensatory effects of which is important to be considered for gene therapies. Further study would require complete knockouts of the *Hu* genes that could be achieved by CRISPR. Also, miRNA analysis would help understand the extended regulation of *Hu* genes.

7.3 Hu proteins and their influence on Neuroblastoma cell phenotype

The knockdown studies of single and combined *Hu* genes were assessed for their effect on cellular properties. No clear changes of the cell morphology were observed following individual or combined *Hu* gene knockdowns.

MTS studies revealed *HuB*, *HuC* and combined *Hu* gene knockdowns increased cell viability in SH-SY5Y cells but not in SK-N-AS cells. This suggests that in the cell, HuB and HuC proteins can act in manner to maintain a steady rate of cell viability and without this control, a possible upregulation in cell viability could occur. This would suggest HuB and HuC proteins have tumour suppressor properties. This may be occurring through direct regulation of transcripts involved in cell viability or through regulating transcripts whose downstream targets affecting cell viability. In Glioblastoma, HuB protein has previously been described as a tumour suppressor (Tarter 2013).

Cell migration, invasion and chemotaxis are typically involved in diverse processes from embryonic development and differentiation to angiogenesis, immune response, wound healing and cancer cell metastasis (Khabar 2017).

Cell mobility and cell invasiveness was measured through cell migration into an agarose gel matrix. When compared, SK-N-AS cells had an overall more invasive phenotype than SH-SY5Y cells before any knockdown experiments. In a wound healing assay, *HuB* gene knockdown increased the migrative potential of both Neuroblastoma cell lines, as did individual *HuC* and *HuR* knockdown and combined *Hu* gene knockdown in the SH-SY5Y cell lines. Differences observed between the cell lines may be related to the higher overall expression of *Hu* genes in SH-SY5Y cells compared to the SK-N-AS cells. Interestingly, *HuB* gene expression was highest in the SK-N-AS cells which was the only effective gene knockdown in producing cellular effects.

The increased motility after *Hu* gene knockdowns suggests that *Hu* gene play a role in the relative migration rate of these cells. The described effects of HuB, HuC and HuR inducing a more migrative phenotype, suggests that the *Hu* genes role in the cell, is to maintain a relative rate of migration.

7.4 Gene targets regulated by Hu proteins in Neuroblastoma

The influence of *Hu* gene expression on potential mRNA targets was analysed. Gene amplifications of *Hu* genes and consequential increases in their protein expression are likely to impact translational networks and change fundamental cellular processes. Hu proteins can modulate the stability of ARE-containing mRNAs *in vitro* positively as well as negatively (Brennan and Steitz 2001).

A commercially available array consisting of 91 mRNA targets described in the National Library of Medicine database and thought to contribute to the development Neuroepithelial disorders was used. Gene expression levels were analysed following single and combined Hu gene knockdowns in both Neuroblastoma cell lines SH-SY5Y and SK-N-AS. In each Neuroblastoma cell line, a unique alteration in target gene expression was observed.

Considering each cell line as an individual model and to reduce the number of target genes for analysis, several parameters were set. A 3.0 cycle fold-change difference in gene expression compared to the control non-targeting siRNA expression was selected for the SH-SY5Y samples following individual and combined gene knockdowns when compared to the non-targeting knockdown control. A fold-change of 3.6 cycles was selected for SK-N-AS Neuroblastoma cells. An additional selection for the genes were ones that were consistent in two or more of the knockdowns observed within each cell line. For the SH-SY5Y cell line, 6 genes were identified to meet these criteria and 12 genes for the cell line SK-N-AS.

A knockdown of *Hu* genes individually and combined in SH-SY5Y cells revealed that B-cell lymphoma (*BCL2*) mRNA transcript levels were affected, showing a lower expression. This shows that in the Neuroblastoma cell model SH-SY5Y, Hu proteins regulate the expression of *BCL2* transcript probably by stabilising its mRNA. Ishimaru et al. (2009) identified HuR as a component of Bcl-2 messenger ribonucleoprotein (mRNP) complexes in in HL60 Leukaemia cells and A431 Carcinoma cells. *BCL2* mRNA contains AU-rich elements in the 3'-untranslated region to which Hu proteins can bind to and regulate (Schiavone et al. 2000). A schematic diagram showing how Hu protein can bind and regulate mRNA transcripts is demonstrated in Fig. 1.6.

Bcl-2 is an anti-apoptotic protein and mediator of cell survival and cell death, by regulating caspase-dependent and caspase-independent cell death pathways (Nunez and Clarke, M. F. 1994). Bcl-2 is known to affect the progression of diseases such as cancer, autoimmune diseases and neurological conditions such as stroke and neurodegenerative diseases (Hughes et al. 2006, Akhtar et al. 2004, Kirkin et al. 2004). The potential influence of *Hu* genes in neurodegenerative disorders and its ability to regulate *BCL2* transcript has previously been discussed in Section 1.8.

Cyclin D2 (*CCND2*) gene was shown to be regulated by HuC and HuD proteins in SH-SY5Y cells. Following knockdown of these *Hu* genes, *CCND2* expression also decreased suggesting HuC and HuD positively regulate the stability of *CCND2* mRNA transcript promoting its' expression. Cyclins are involved in controlling the cell cycle progression for which their expression is tightly regulated (Johnson and Walker 1999). HuR protein was documented in Colorectal carcinoma cells, RKO, to regulate cell division and checkpoint responses by stabilising the transcripts of key cell cycles regulators, namely cyclin A and cyclin B1 (Wang et al. 2000) Therefore, it is not surprisingly that HuC and HuD show this effect on *CCND2*.

Following a combined *Hu* gene knockdown, a large upregulation of *CCND2* was observed. This is unusual but can be described by genetic compensation. This is a widespread phenomenon, where the reduced or loss of expression of one gene is compensated by another with a similar function and expression pattern. There are multiple RBPs in the human genome that co-regulate mRNA targets. Keene (2007) described a model in which mRNAs encoding for proteins with similar functions are co-ordinately regulated as post-transcriptional RNA operons or regulons, through a ribonucleoprotein-driven mechanism

(Keene 2007). This co-regulation of mRNA transcripts has also been described for the Drosophila Hu homolog, *ELAV*, and its family members (Zaharieva et al. 2015b)

The decrease of Hu protein expression could induce the expression of other RNA binding proteins to compensate for Hu's cell vital functions in posttranscriptional gene regulation of target RNAs, here acting on Cyclin D2 expression (El-Brolosy and Stainier 2017). HuR protein and the eukaryotic translation initiation factor 4E (*eIF4E*) are RNA regulons sharing targets that regulate survival and proliferation-related genes such as c-myc, cyclin D1 and *VEGF* (Wurth 2012, Topisirovic et al. 2009).

Importantly, this shows how targeting HuB or HuC protein individually could be beneficial in the reducing *CCND2* expression whilst a knockdown of all Hu proteins seems to have the contrary effect. The influence of Hu proteins on target RNAs in Neuroblastoma that are involved in cell proliferation, and the compensatory aspects when Hu proteins are downregulated, highlight the underlying molecular complexity of the disease and a concept that must be considered for therapeutic approaches.

Early Growth Receptor 1 (*EGR1*) gene encodes a transcription factor required for programmed cell death or apoptosis in both normal and tumour cells (Adamson and Mercola 2002). Here it was shown that following *HuB*, *HuC* and *HuD* gene knockdowns in SH-SY5Y cells, *EGR1* gene expression also decreased. This shows that the neuronal Hu proteins act as positive regulators of *EGR1* mRNA expression. The same effect on *EGR1* was also observed in the second Neuroblastoma cell line, SK-N-AS. In this cell line, the combined *Hu* gene knockdown also significantly decreased *EGR1* gene expression. In addition, in SK-N-AS cells, the combined knockdown of all Hu proteins showed a significant decrease of *EGR1* expression while in SH-SY5Y cells, only a moderate decrease was observed.

These findings suggest that in Neuroblastoma cells, the neuronal *Hu* genes actively regulate *EGR1* gene expression either directly or indirectly and consequently stimulating tumour growth (Adamson and Mercola 2002). In Prostate cancer, *EGR1* is overexpressed. *EGR1* was linked to several target genes including cyclin D2 (Virolle et al. 2003).

As mentioned in SH-SY5Y cell line, the combined *Hu* gene knockdown did not reduce the *EGR1* expression much, therefore *EGR1* could upregulate *CCND2* expression. However, in SK-N-AS cell, the expression of *CCND2* was not selected as a target following the criteria described above, therefore this interpretation cannot proved.

Neuroblastomas are often defined by a poor outcome if an amplified state of proto-oncogene *MYCN* is found (Cohn et al. 2009). *MYCN* is a member of the MYC family of transcription factors regulating cellular processes including survival, proliferation, and differentiation (Westermark et al. 2011). Lovén et al. (2010) shows an array of *MYCN*-induced miRNAs including the micro RNAs, miR-18a and miR-19a, that target and repress Estrogen Receptor 1 (*ESR1*) gene expression. *ESR1* encodes the protein estrogen receptor α. *ESR1* expression in Neuroblastoma tumours has been shown to induce a favourable disease outcome.

Individual knockdowns of *HuB*, *HuC* and *HuD* genes showed their proteins are positive regulators of *ESR1* gene expression, as when *HuB*, *HuC* and *HuD* gene expression decreases, *ESR1* also does. In the SH-SY5Y cells, HuB, HuC and HuD proteins must be acting on the *ESR1* gene transcript to maintain a steady regulation, potentially demonstrating a tumour suppressor role. SH-SY5Y cells do not show *MYCN* amplification and no interference with *ESR1* regulation by MYCN must be considered. However, it has been shown that *MYCN* becomes upregulated in SH-SY5Y cells when treated with nutlin-3 and doxorubicin, due to cellular stress (Peirce and Findley 2015). Upon knockdown of the Hu family in combination, *ESR1* gene

expression increased, suggesting that a downregulation of the *Hu* family could be a potential target for gene therapy leading to higher *ESR1* gene expression. Lovén et al. (2010) showed higher ESR1 expression induced growth arrest and neuronal differentiation in Neuroblastoma cells.

Insulin-Like Growth Factors play a crucial role in the regulation of cell proliferation, differentiation, apoptosis and transformation (Clemmons and Jones 1995). Insulin-like growth factor-binding protein 3 (*IGFBP3*) was shown to be positively regulated by HuR RNA-binding protein. This was shown in mouse embryonic stem cells where a knockdown of HuR decreased *IGFBP3* expression. It showed *IGFBP3* contains a HuR binding motif in its 3'-UTR that upon HuR binding, increased stability of the transcript (Wang et al. 2014). This suggests HuR as a novel target to reduce *IGFBP3* since a HuR knockdown resulted in a decrease in IGFBP3 expression in the SH-SY5Y cells.

The anti-inflammatory cytokine Interleukin-10 (*IL10*) has previously been reported to regulate the expression of HuR (Prasanna et al. 2009). To maintain normal physiology, IL10 balances anti-inflammatory regulatory T-cells and proinflammatory IL17-expressing T-cells. Mice deficient in *IL10* have increased inflammatory responses often causing cancer, demonstrating a tumour suppressive effect of *IL10* (Oft 2014). The data presented shows that after the individual knockdown of *Hu* genes in SH-SY5Y, *IL10* expression was decreased. Therefore, Hu genes may post-transcriptionally regulate *IL10* expression or *IL10* expression may decrease because of down-stream effects following *Hu* gene depletion. A combined knockdown of all *Hu* genes leads to a significant increase in *IL10* expression. This is most certainly an off-target effect, where different genes compensate for *Hu* gene expression decrease.

It could be hypothesised that a combined *Hu* family knockdown may provide a good therapeutic target since there is a large increase in *IL10* expression, that would induce an anti-tumour effect. Overexpression of a synthetic *IL10* has shown to induce anti-tumour immunity (Oft 2014). However, this must be confirmed by further experiments looking at the interaction of Hu proteins on multiple levels.

An upregulation of Apolipoprotein E (*APOE*) is commonly associated with the Alzheimer's disease pathology (Diedrich et al. 1991). Likewise, *Hu* genes have been implicated in Alzheimer's pathology and regulation of genes implicated in A*β*PP processing (Amadio et al. 2010).

ApoE proteins function in lipid metabolism and neuronal homeostasis (Huang, Yadong and Mahley 2014). There are three variants isoforms of ApoE proteins of which the ApoE3 variant has previously been identified in SH-SY5Y Neuroblastoma cells (Dupont-Wallois et al. 1997). In Neuroblastoma, ApoE has also been shown to affect cell viability when oxidised by a phospholipid (Hoy et al. 2000).

In Ovarian cancer, ApoE was shown to be a tumour-associated marker required for increased proliferation and cell survival. Knockdown experiments in ovarian cells, OVCAR3, resulted in cell-cycle arrest and apoptosis (Chen et al. 2005).

In the presented study, *APOE* gene expression was downregulated following all individual and combined *Hu* gene knockdowns in SK-N-AS cells. This highlights that the *APOE* gene is targeted directly or indirectly by the *Hu* gene family maintaining its regulation in these cells. Further experiments would be required to prove that the knockdown of Hu protein results in a decrease of APOE inducing cell death in a *vivo* model.

As previously mentioned, Neuroblastoma has a poor prognosis if proto-oncogene *MYCN* is amplified (Cohn et al. 2009). A study in Neuroblastoma cells showed that cells treated with

CDK1 inhibitors showed a reduced expression of *MYCN* and survivin expression. They concluded CDK1 inhibition induced cell cycle arrest and apoptosis through interruption of the miR-34a–*MYCN*–survivin pathway (Chen et al. 2013).

A knockdown of *HuB* and *HuD* genes individually in SH-SY5Y cells, resulted in an increased *CDK1* gene expression. This shows HuB and HuD proteins have a repressive regulatory effect on *CDK1*, either through direct or indirect effect on the *CDK1* gene transcript.

Studies into Connective Tissue Growth Factor (*CTGF*) expression in breast carcinoma revealed *CTGF* contains five HuR binding motifs and is therefore regulated by HuR protein (Heinonen et al. 2011). The data presented in this study confirms HuR protein as a regulator of *CTGF* in SK-N-AS cells. The downregulation of *HuR* lead to a decreased *CTFG* expression. *CTGF* expression was also downregulated when *HuC* and *HuD* genes were knocked down individually. This potentially shows that these Hu proteins also regulate *CTGF*. These results suggest that in the SK-N-AS Neuroblastoma cells, Hu proteins modulate *CTGF* mRNA levels during post-transcriptional events ensuring its expression is maintained. CTGF is a matrix-associated protein and its functions in cancer is related to angiogenesis and tumour growth and even cancer cell migration and invasion (Chu et al. 2008). This highlights the potential oncogenic effects of HuR, HuC and HuD in relation to the CTGF transcript in these cells.

High expression levels of Glutathione S-Transferase Pi 1 (*GSTP1*) mRNA that encodes a detoxifying enzyme expression have been associated with decreased survival in Neuroblastoma patients. Further investigation revealed N-Myc as a transcriptional regulator of *GSTP1*. N-Myc also regulates the expression of several ATP-binding cassette (ABC) transporters, further increasing the level of regulatory control in drug metabolism. This could explain the high multi-drug resistance observed in Neuroblastoma (Fletcher et al. 2012). SK-

N-AS cells are typically *MYCN*-non-amplified cells, although *MYCN* expression can be induced through treatment induced cellular stress as previously described (Prochazka et al. 2013).

GSTP1 gene expression was reduced following *HuB* gene knockdown. This shows that HuB protein is a positive regulator of *GSTP1* expression. In contrast, HuC and HuR proteins were revealed as negative regulator of *GSTP1* gene expression since their knockdown resulted in increased *GSTP1* expression levels. This is suggestive of a tumour-suppressor function to maintain low/moderate *GSTP1* expression in the SK-N-AS Neuroblastoma cells. These observed differences in the effect of single Hu proteins on the expression of certain genes highlights molecular heterogeneity of this type of cancer and the difficulty of establishing an effective treatment.

Transforming growth factor beta (*TGF-β1*) mRNA has previously been reported in Neuroblastoma and normally plays a role in the homeostasis of proliferation and differentiation (Lolascon et al. 2000). TGF-β normally functions in cell growth inhibition, however it is documented that several cancers develop resistance to TGF-β (Polyak 1996). *TGF-β1* mRNA levels decreased in SK-N-AS cells following all *Hu* gene individual and combined knockdowns. Although this downregulation was not significant, it forms an intricate part in the Neuroblastoma network. The observed regulation suggests that Hu proteins upregulate *TGF-β1* expression in the SK-N-AS cells.

TGF -β1 binds to one of three cell surface receptors namely TGF-βR1, TGF-βR2. and TGF-βR3. Lolascon et al. (2000) reports TGF-βR3 is extensively reduced in the later stages of Neuroblastoma development.

Protein kinase C α (*PKCα*), belongs to a family of proteins that emit signals inducing lipid hydrolysis. These signals stimulate other factors such as G protein-coupled receptors and tyrosine kinase receptors, which lead to activation of pathways ultimately activating protein

kinase C (Newton 1995). In Breast cancer, Protein kinase C α induces a more migrative phenotype of breast cancer cells through FOXC2-mediated repression of p120-catenin (Pham et al. 2017).

Following *HuD* gene knockdown in SK-N-AS cells, *PKCα* was also reduced suggesting a positive regulation of HuD protein on *PKCα* mRNA transcript. In these cells, HuD protein would maintain the expression of *PKCα*, which may have the same effect as in Breast cancer cells, inducing a more migrative phenotype.

Ki-ras2 Kirsten rat sarcoma viral oncogene homolog (*KRAS*) forms part of a group of GTP-binding proteins called the RAS family that are characterised by a catalytic G domain (Wennerberg et al. 2005). K-Ras protein is involved in signalling pathways intracellularly, transporting signals from the cell surface to the nucleus. Their signalling cascade is initiated by molecules like TGF-β1 binding to cell surface receptors. Overall K-Ras can modulate normal cellular functions such as cell differentiation, growth, chemotaxis, migration and apoptosis through activation of downstream targets such as cytoplasmic kinases. In cancer, K-Ras can therefore influence transformation, angiogenesis, invasion and metastasis (Zuber et al. 2000).

A screening of relapsed Neuroblastomas revealed 29 somatic mutations of which eighteen were forecast to initiate the RAS-MAPK signalling pathway. 61% of activating mutations in the RAS-MAPK pathway were detected in Neuroblastoma cell lines. KRAS particularly has shown to have a activating somatic mutation in Neuroblastoma (Eleveld et al. 2015).

In SK-N-AS cells, *HuC* and *HuR* individual gene knockdowns resulted in a decrease in *KRAS* gene expression, suggestive of a positive regulatory effect of HuC and HuR proteins on *KRAS* mRNA. This is most likely due to an indirect effect, since there is no evidence to suggest *KRAS*

mRNA contains an AU-rich element in its 3'UTR region for Hu proteins to bind directly to. Only 10% of all mRNA transcripts are thought to contain AREs in their 3'UTR (Halees et al. 2008).

Mitogen-activated protein (*MAP*) kinases are downstream effectors in the RAS-MAPK signalling pathway. They aid in the relaying extracellular signals to implement intracellular responses. The combined effects of MAPKs function to modulate cell growth, cell differentiation and cell death (Schaeffer and Weber 1999).

Mitogen-activated protein kinase 2 (*MAP2K2*) gene expression was reduced following individual and combined *Hu* gene knockdowns in SK-N-AS Neuroblastoma cells. Mitogen-activated protein kinase 3 (*MAPK3*) serves downstream of MAP2K2 and showed a significant decrease in expression following all individual *Hu* gene knockdowns. A decrease also occurred following combined *Hu* gene knockdown but was not statistically significant. *MAPK* mRNA are not reported to have ARE in their 3' untranslated regions therefore concluding Hu gene regulation occurs due to an indirect effect. This is most likely an upstream regulator of *MAPK*.

7.5 Concluding remarks

Hu gene analysis revealed its upregulated expression in all Neuroblastoma cells lines when compared to the control normal astrocytes. Hu protein was observed in its natural location except for HuD in SH-SY5Y cell where it is located in the nucleus. This was most interesting since this cell line showed the most Hu protein expression overall. Whilst this aberrant localisation of HuD protein is usually associated with a poorer diagnosis, *HuD* knockdowns did not reveal any *in vitro* cell phenotypic gain of migration or viability.

The HuB protein dimerisation and HuC protein multimerisation described in Section 7.1, are thought to increase the binding potential of their proteins in binding to themselves and other proteins. Further correlating this theory was that HuB and HuC proteins were seen to be major

players in the expression of mRNA targets discussed in Section 7.4. *HuB* knockdown influenced changes in RNA levels of four of the six transcripts analysed. Whilst *HuC* knockdown influenced the expression of five of the six transcripts. Additionally, *HuB* knockdown induced a more migrative phenotype in both Neuroblastoma cell lines whilst in the SH-SY5Y cell line, *HuB* knockdown also saw an increase in cell viability. Also observed in the SH-SY5Y cells was a more migrative phenotype following *HuC* and *HuR* knockdowns and greater viability following *HuC* knockdown. Further highlighting HuB and HuC as large influencers in the cellular phenotype.

The regulatory interactions described in both Neuroblastoma cell lines showed that through either direct effect on each other or off-target effects of *Hu* gene regulation, the regulation loops back to affect the expression of a different member of the Hu RNA-binding protein family. Despite either mechanism, a high level of regulation is observed if the two models were combined. This highlights the need for genome wide studies when considering targets for personalised targeted therapies, especially where genes are as highly conserved as the Hu family of RNA-binding proteins are.

Gene expression studies identified targets of *Hu* genes at RNA level. Of these genes, *Hu* generally displayed a positive regulatory effect on their transcripts upregulating their expression or a negative regulatory effect maintaining a steady expression in the cell through direct binding of the mRNA transcript or in-directly through cascade effects. Either way this revealed *Hu* genes collectively as major players in regulating the transcripts of *BCL2*, *EGR1*, *IL10*, *APOE*, *CDK1*, *GSTP1*, *MAP2K2*, *MAPK3*, *ESR1*, *CTGF*, *PRKCA*, *KRAS IGFBP3* and *CCND2* in the Neuroblastoma cell models. Following generalised classification of the function of these genes, it was found the targets contribute to a pathogenic phenotype of many cancer hallmarks including energy metabolism, cell survival and proliferation, invasion and

metastasis, immune response and angiogenesis. HuB and HuC were on numerous occasions found to be potentially acting in a tumour suppressive function. However, overall, the regulation of these transcripts contributed to an oncogenic phenotype.

Interestingly, some of these targets fall into the RAS-MAPK signalling pathway adding a potential new dimension to how Hu proteins modulate gene expression.

Chapter 8

Discussion

Part III: Expression of Hu proteins in Glioblastoma

Glioblastoma multiforme is an astrocytoma that is challenging to treat because of their proliferative and metastatic ability (Ware et al. 2003). With a two-year survival rate for adults aged 46-64 of just 7.7% and 2.1% for patients over 65, this highlights the aggressiveness of the disease and the need for further research (Bolognani et al. 2012).

HuR is known to be over-expressed in human gliomas (Bolognani et al. 2012). Its expression is often seen localised to the cytoplasm where it's thought to bind and upregulate cancer-related mRNA targets such as *TNF-α*, *VEGF* and *IL-8*. Stabilisation of these oncogenes promotes a higher grade tumour and poorer prognosis (Nabors et al. 2003).

Reports highlighting the significance of HuR expression in Glioblastoma were established in 2001, where the tumours were reported to overexpress HuR in the nucleus of the cells by Nabors et al. (2001). HuB has previously been reported to have tumour suppressor properties in Glioblastomas (Tarter 2013).

8.1 The family of Hu RNA-binding protein and their presence in Glioblastoma

The *Hu* gene expression profiling in Neuroblastoma focused on two cell lines; normal astrocytes, SVG p12, as a control and the Glioblastoma cell line, U87-MG. Using relative fold change express when analysed ($2^{-\Delta\Delta Ct}$) and *ß-Actin* as an internalised standard, the expression levels of each *Hu* gene was analysed. The RT-qPCR data of the Glioblastoma cell line was

normalised to the control cell line, SVGp12 normal astrocytes cell line which by itself had the lowest gene expression of *HuB*, *HuC*, *HuD* and *HuR*. The upregulated expression of the *Hu* genes in the Glioblastoma cells suggests an additional role in this cell line compared to the normal astrocytes.

HuB gene expression was detected in the cell lines for normal astrocytes and Glioblastoma, however a significant upregulation of *HuB* expression was observed in the U87-MG Glioblastoma cells. This observation was also seen in the expression profiles of *HuC*, *HuD* and *HuR* gene expression.

Despite the upregulation of *HuB* at RNA level in U87-MG cells, HuB protein detection through western blotting revealed an almost equal expression of HuB protein in the normal astrocytes and Glioblastoma cells.

HuB protein was detected at its expected size of 38kDa and an additional band at 76kDa that could be a dimer. The higher molecular weight band could be indicative of a HuB dimer and had a stronger signal then the monomer. The higher molecular weight band in HuB protein analysis was also detected in protein analysis of Neuroblastoma cell lines SH-SY5Y and SK-N-AS (Section 7.1).

The presence of HuB was confirmed by immunofluorescence. HuB localisation was determined as both the nucleus and cytoplasm in normal astrocytes, but only in the cytoplasm of the Glioblastoma cells. HuB protein resides in the cytoplasm of undifferentiated neurons where it co-localises to the ribosomes controlling mRNA metabolism and neuronal differentiation (Gao and Keene 1996). Whilst the cytoplasm is the normal location for HuB, an upregulation of cytoplasmic Hu expression is often seen in tumour cells (Antic and Keene 1997), consistent with the localisation described here.

HuC protein showed a much higher expression in the normal astrocytes than in U87-MG cells. HuC was detected at the expected size of 39kDa and around four times the expected size at 156kDa, that could represent a multimer of HuC protein. This was also detected previously in Neuroblastoma studies (Section 7.1). Both the monomer and suggested multimer were detected in the SVG p12 astrocyte cell line, however only the multimer was found in U87-Mg Glioblastoma cells.

Like HuB, HuC protein was localised to both the nucleus and cytoplasm in normal astrocytes but only in the cytoplasm of the Glioblastoma cells, which is described as the normal localisation in differentiated neurons (Okano and Darnell 1997).

The subcellular distribution of Hu proteins is reported to vary amongst tumour cell lines, whereby expression of Hu proteins is mostly seen in the cytoplasm. However, in neurons from the hippocampus and neocortex, Hu proteins can be equally distributed in both cellular compartments (Antic and Keene 1997). The equal distribution between the cytoplasm and the nucleus is seen for HuC and HuD proteins in normal astrocytes. The nuclear presence of neuronal Hu proteins, observed in the normal astrocytes is known due to their involvement in functional regulatory processes such as alternative splicing, polyadenylation and mRNA decay.

The larger protein moieties detected in normal astrocytes and Glioblastoma cells are consistent with homo-dimerisation and homo-multimerisation of HuB and HuC proteins, respectively. This was also found in the Neuroblastoma cell lines SH-SY5Y and SK-N-AS (Section 7.1). Multimerisation as described above is a structural feature that ensures specificity for RNA target recognition (Soller and White, Kalpana 2004).

Western blot and immunostaining revealed an absence of HuD protein in normal astrocytes, despite a low expression at mRNA level. HuD protein expression in U87-MG cells revealed a similar expression level to that of GAPDH protein and immunofluorescence showed HuD protein was localised to the cytoplasm.

HuR protein expression was not detected in SVG p12 astrocytes and showed only a weak protein expression in U87-MG Glioblastoma cells, despite a high RNA expression level seen with qPCR. HuR protein expression was confirmed Immunofluorescence in both cell lines and is mostly located in the nucleus with a weaker signal in the cytoplasm. A nuclear location of HuR has been described for many cell types (Hinman and Lou 2008). HuR protein has a nuclear-cytoplasmic shuttling sequence (HNS) in the hinge region of the protein which allows it to translocate between the two cellular compartments (Fan and Steitz 1998). The cytoplasmic localisation of HuR is often correlated to a more aggressive cancer phenotype. The localisation of HuR is related to its subcellular function. In the nucleus Hu proteins regulate processes such as alternative splicing and preparing mRNA for export in the cytoplasm whilst in the cytoplasm, they regulate transcript stability and mRNA decay. HuR overexpression and its localisation in the cytoplasm has been described in Glioblastoma. In the cytoplasm it stabilises factors such as VEGF, BCL-2 and IL8. When HuR was silenced, cells showed a decrease in anchorage-independent growth and cell proliferation (Filippova et al. 2017). A summary of known mRNA targets stabilised by Hu proteins are listed in Table 1.1.

8.2 Regulatory interactions of Hu RNA-binding proteins in Glioblastoma

Regulatory interactions between different Hu proteins have been described for Neuroblastoma in Section 7.2. The influence of individual and combined *Hu* knockdowns on the expression of the other Hu protein members was analysed in U87-MG cells as well.

A more efficient knockdown of *Hu* gene expression was achieved in the combined approach in U87-MG cells compared to individual knockdowns for the *Hu* genes *HuC*, *HuD* and *HuR*. *HuB* knockdown decreased in efficiency following combined *Hu* gene knockdowns compared to the single Hu gene knockdown.

Western blot analysis confirmed a more efficient knock down was also seen at protein level in the combined *Hu* siRNA transfection.

Details of the knockdown data and the influences of gene expression between the different Hu proteins is summarised in a hypothetical model (Fig. 5.16) of interaction for U87-MG Glioblastoma cells. As previously described for Neuroblastoma cell lines, there are three potential explanations to interpret the up or down regulation of different Hu proteins after an individual or combined *Hu* gene knockdowns. Firstly as a result of an individual knockdown other Hu protein family members become more expressed to compensate for the reduced expression of a different Hu family member (Zaharieva et al. 2015b). A second interpretation is a regulatory effect, whereby Hu family members target each other's transcripts stabilising and controlling their expression. A third interpretation is that the observed effects could due to a feedback loop of other Hu protein targets that then affect the regulation of different *Hu* genes.

Overall, RNA and protein expression showed that there is a statistically significant change in gene expression following a *HuB* knockdown resulting in a decreased expression of *HuC*. A *HuD* siRNA knockdown did not significantly change the expression of the other *Hu* genes. When HuR was knocked down a significant decrease in HuC and HuD mRNA levels was observed.

HuR is potentially a positive regulator of *HuC* and *HuD* mRNA transcripts since following *HuR* knockdown a significant decrease in *HuC* and *HuD* mRNA was also observed. Therefore, upon HuR depletion, the control is no longer there so HuC and HuD expression also decreases. Alternatively, different HuR targets that influence the expression of HuC and HuD are less expressed after HuR knockdown which the leads to a down regulation of *HuC* and *HuD* gene expression as well.

HuB was also found to be a positive regulator of *HuC*, since a knockdown of *HuB* lead to a decreased expression of *HuC*. This can be explained by the same mechanism described above. The decrease of HuB can either directly or indirectly by other HuB targets, influence the expression level of *HuC* mRNA.

HuC itself negatively regulates *HuR* expression leading to an increase in *HuR* mRNA expression following *HuC* knockdown. Utilising its role as an RNA-binding protein enables HuC proteins to regulate *HuR* mRNA transcripts by binding directly to ARE in its 3'-UTR regions, destabilising the transcript. Alternatively, *HuR* gene may compensate for the decreased expression of HuC by upregulating its own expression. There is also a possibility that *HuC* knockdown results in off-target effects subsequently upregulating *HuR* expression.

The regulatory effects of HuB and HuC may be linked to the HuB protein dimerisation and HuC protein multimerisation in the Glioblastoma cells (Kasashima et al. 2002). These actions allow Hu proteins to upregulate mRNA transcripts and further bind with additional Hu proteins through the action of forming ribonucleoprotein complexes (Kasashima et al. 2002, Hinman et al. 2013).

Whilst further clarification is required to fully understand the interaction between different Hu proteins, a first insight into the complex regulatory network of Hu proteins is described above. The interplay and compensatory of the Hu family members could potentially apply to other highly conserved RBP members and may need to be considered in targeted therapy approaches.

8.3 Hu proteins and their influence on Glioblastoma cell phenotype

To understand the contribution of Hu proteins on cellular properties, cell viability, morphology and migrative potential were assessed after the described individual or combined *Hu* gene knockdowns. There were no clear changes to the U87-MG cell morphology following individual or combined *Hu* gene knockdowns.

MTS assays showed that *HuB* and *HuC* individual gene knockdowns significantly increased the U87-MG cell viability compared to the control non-targeting siRNA cells. This suggests that in U87-MG cells, HuB and HuC proteins are potentially functioning to maintain a steady rate of cell viability. Without the regulatory control of HuB and HuC proteins in the cells, a possible upregulation in cell viability could occur. This would indicate a tumour suppressive effect of *HuB* and *HuC* knockdown on cell viability and is consistent with effects observed in Neuroblastoma (Section 7.3). This tumour suppressive function of HuB particularly, is documented in Glioblastoma studies (Tarter 2013). An interpretation of this regulation is that

HuB and HuC proteins modulate cell viability by binding to an array of mRNA transcripts, that can directly or indirectly affect cell survival and cell death pathways.

The general cell mobility and invasiveness was measured through a cell migration into an agarose gel matrix. When compared to the normal astrocyte cells, SVGp12, the U87-MG cells had a more invasive phenotype. This is typical of Glioblastoma cells and present issues during treatment since surgery to remove the tumour sees a high re-occurrence rate since the tumour cells have already invaded normal brain tissue (Demuth and Berens 2004).

In a wound healing assay of U87-MG cells, individual *HuB* and *HuC* gene knockdowns along with a combined *Hu* gene knockdown generated an increased directional migratory cell response. The increased motility following *HuB* and *HuC* gene knockdowns suggests that Hu proteins play a role to maintain a relative migratory rate. This is possibly through influencing the stability of mRNA transcripts that function directly or indirectly lead into cell migratory pathways. The described findings may support genetic studies or give rise to networks in which Hu proteins influence. It is also suggestive of HuB and HuC proteins functioning with tumour suppressor properties also observed in the cell viability assays in this cell line.

8.4 Gene targets regulated by Hu RNA-binding proteins

It is well established that Hu proteins function as post-transcriptional gene regulators (Hinman and Lou 2008). To gain a better understanding of the molecular role and function of Hu proteins in Glioblastoma, an array of 91 genes were screened following individual and combined *Hu* gene knockdowns. The genes are documented in the National Library of Medicine database as key players in the development of Glioblastoma tumours.

Several parameters were set to identify key target genes of Hu protein regulation. A minimum of a 2.0 cycle fold-change difference from the control non-targeting siRNA was required. An

additional criterion was set that the expression changes must be consistent between two or more of the *Hu* gene knockdowns. This identified seven genes for further analysis.

HMOX1, a cell-surface marker was seen upregulated by 54% glioma tissue compared to normal brain tissue. Following cell injury or stress, Glioblastoma cell lines showed an increased expression of HMOX1 by 81% and the protein was located in the cytoplasm. High HMOX1 expression is associated with a decreased survival time. HMOX1 protein was also shown to regulate Glioblastoma cell proliferation (Gandini et al. 2014). An additional study found HMOX1 expression in pseudopalisading cells that reside in the hypoxic region of Glioblastoma tumour. Increased HMOX1 expression correlates with increased invasion in Glioblastoma tumours (Ghosh et al. 2016).

In U87-MG cells, a knockdown of *Hu* genes individually and combined revealed Heme Oxygenase 1 (*HMOX1*) mRNA transcript was affected by *Hu* genes showing an increase in its expression. This defines *Hu* genes as negative regulators of *HOMX1* expression, however this is likely through indirect effects since the *HMOX1* transcript does not contain an AU-rich sequence in its 3' prime UTR.

Insulin-like growth factor-binding protein 3 (*IGFBP3*) was previously identified to be affected by HuR protein regulation in the Neuroblastoma studies (Section 7.4). In Glioblastoma cells, it was shown that following all *Hu* gene knockdowns both individually and combined, *IGFBP3* expression increased. This probably through Hu proteins binding to a Hu binding motif in the 3'-UTR of *IGFBP3* mRNA transcript. This increased expression was observed at the highest level following both *HuR* individual knockdown and the *Hu* family combined knockdown. It is important to consider the effect seen in the combined knockdown is potentially only caused by the observed effect on *IGFBP3* by the *HuR* knockdown.

The observed regulation suggests that in the U87-MG cells, the *Hu* genes are regulating the *IGFBP3* expression in a negative manner to maintain a steady level in the cells. Without Hu proteins control and more specifically Hu's regulatory control, an upregulation in *IGFBP3* gene expression.

Since IGFBP3 regulates cell proliferation, differentiation, apoptosis and transformation (Clemmons and Jones 1995), maintaining a steady expression level of IGFBP3 in the cells ensuring it is not upregulated is suggestive of a tumour suppressor effect. On the contrary, HuR in Neuroblastoma SH-SY5Y cells was shown to have a positive regulatory effect inducing a potential oncogenic effect and further highlighting variability with Hu gene regulation (Section 7.4).

One of the most important hallmarks of malignant gliomas is their invasive behaviour (Demuth and Berens 2004). Matrix metallopeptidases exhibit proteolytic activity towards extracellular matrix molecules, which induce a more invasive motile phenotype in cells (Fillmore et al. 2001). Matrix metallopeptidase 1 (*MMP1*) and Matrix metallopeptidase (*MMP9*) gene expression was analysed following individual and combined *Hu* gene knockdowns. *MMP1* expression increased significantly following *HuC*, *HuD*, *HuR* individual gene knockdowns and a combined *Hu* gene knockdown in U87-MG cells.

Whilst the profile of *MMP9* expression showed no statistically significant changes due to variation in the control, it could still be observed that *HuB* and *HuD* gene knockdowns increase *MMP9* expression. In contrast, *HuR* gene knockdown decreased *MMP9* expression. *MMP9* specifically has been shown to have an AU-rich element in its 3'-UTR to which HuR is known to bind providing protection against degradation (Akool et al. 2003). These studies confirm findings by Akool et al. (2003), that HuR binds to *MMP9*. This is also consistent with downregulation of *MMP1* and *MMP9* expression following *HuR* knockdown and confirms HuR

is acting on their mRNA transcripts to maintain their expression in the cell in a positive manner. Since MMP expression is correlated with a more motile phenotype, it explains the increased invasive phenotype of Glioblastoma cells when compared to normal astrocytes.

The observed differences in the effect of single Hu proteins on the expression of a single gene, and the fact that HuD protein can have both positive and negative effects on *MMP* expression highlights the heterogeneity of Glioblastoma and provides and explanation in the difficulty of creating an effective treatment.

Interestingly, the Ras-dependent MAPK/ERK signalling pathway, that it is consitently highlighted in these Hu gene target studies, maintains increased *MMP9* levels in immortalised keratinocytes through cooperation with α3β1 integrin that stabilises the *MMP9* transcript (Iyer 2005).

The Notch signalling pathway is involved in cellular processes such as stem cell proliferation and maintenance (Stockhausen et al. 2010). It was established that *NOTCH1* is expressed in 71% of Glioblastoma tumours (Han et al. 2017). Furthermore, knockdown of *NOTCH1* mRNA in Glioblastoma cells, both *in vitro* and *in vivo* induced apoptosis. It was found that Notch binds with NF-κB (*p65*), that plays a key role in the proliferation of Glioblastoma cells (Hai et al. 2018).

Individual *HuB* knockdown and combined *Hu* gene knockdown showed that *NOTCH1* expression increased. There was no change in *NOTCH1* expression following the other *Hu* genes individual knockdowns, HuB protein could be major player in the combined knockdown, and *HuB's* reduced expression results in an increase in *NOTCH1* expression. The observed upregulated expression of *NOTCH1* mRNA is suggestive of HuB's role to maintain a steady state of NOTCH1 protein abundance in the U87-MG cells. Without HuBs regulatory

control, *NOTCH1* expression would be even higher in the cells which is indicative of tumour suppressor role of HuB on the *NOTCH1* transcript.

The gene expression profile of alpha-1 type I collagen (*COL1A1*) and Vascular cell adhesion protein 1 (*VCAM1*) did not produce any statistically significant data due to large unfortunate variation in the control. There was an observable progressive decrease in expression in *COL1A1* from *HuB* to *HuC* to *HuD* to *HuR* knockdown, suggesting there may be a regulatory mechanism of HuR on *COL1A1*, but this would need repeating to clarify.

8.5 Concluding remarks

Gene analysis showed an upregulated expression of all *Hu* genes in the U87-MG Glioblastoma cells when compared to the control normal astrocytes. Neuronal Hu proteins showed their normal cytoplasmic localisation. HuR protein was found in both the cytoplasm and the nucleus. HuR is normally localised in the nucleus and a cytoplasmic HuR localisation has been associated with a more aggressive cancer and poor survival rate. This is thought to be due to HuR's ability to stabilise transcripts encoding for oncogenes and transcripts involved in cancer progression. On a cellular level, *in vitro* studies did not show any changes in the viability or migration of U87-MG cells after the *HuR* knockdown.

The HuB protein dimerisation and HuC protein multimerisation are thought to contribute to a greater binding potential of the Hu proteins (Kasashima et al. 2002). HuB and HuC were shown to influence the same number of targets as were HuD and HuR. Interesting, on the initial gene array *HuB* and *HuC* Knockdown did affect more target genes but this would need further analysis to confirm this observation. In the Glioblastoma cells, HuB and HuC were revealed as major players in modulating cell viability and motility determined by MTS and

wound healing assay, respectively. When *HuB* and *HuC* were knocked down, an increase in the viability and migration was observed suggesting their targets on a molecular level may influence cell anchorage and adhesion pathways as well as cell survival and cell death pathways.

From the collected data, a regulatory Hu network was hypothesised within the Glioblastoma U87-MG cells. The described regulations correspond to similar interaction found in the Neuroblastoma cell lines. The main findings of the regulatory mechanisms are that HuB is a positively regulator of *HuC* and HuR positively regulates *HuC* and *HuD* mRNA transcripts. Whilst HuC is a negative regulator of *HuR*, this shows the complex compensatory interactions of this highly conserved protein family members which has to be considered in target specific therapies.

Gene expression studies in the U87-MG Glioblastoma cell line identified targets of *Hu* genes at RNA level. Mainly a negative regulatory effect was observed that maintained a steady expression of target transcripts. The transcripts regulated by Hu proteins were *NOTCH1*, *HMOX1*, *IGFBP3*, *MMP1*. A knockdown of all Hu proteins resulted in an increase in *HMOX1* expression. Maintaining a low *HMOX1* expression in cells is associated with an increased survival rate suggesting a tumour suppressive effect of Hu proteins (Gandini et al. 2014). The same effect was observed for *IGFBP3* mRNA levels which increased after *Hu* knockdowns. Since *IGFBP3* is responsible for cell proliferation and differentiation, a coordinated regulation prevents cells from uncontrolled growth (Clemmons and Jones 1995).

Also, *MMP1* expression was negatively controlled by Hu proteins and after *Hu* knockdown an increase in expression was observed. *HuB* knockdown resulted in an increase in *NOTCH1* mRNA again showing the negative regulatory control of the Hu proteins on this set of targets.

The negative control of this set of target genes by Hu proteins suggest a role for Hu proteins as tumour suppressors. To elucidate the role of Hu proteins in tumorigenesis of Glioblastoma a genome wide expression analysis to look at the influence of Hu proteins on cancer related targets would be needed.

Chapter 9

Conclusions and future work

Part IV: Overall effect of Hu proteins in cancers

In this thesis, it has been shown that Hu proteins show varied expression profiles between Non-small cell lung cancer, Small cell lung cancer, Neuroblastoma and Glioblastoma. Knockdown studies in Neuroblastoma and Glioblastoma cell lines allowed an insight in the role of these proteins at a cellular level but also on a molecular level. Regulatory interactions were observed with the Hu family of RNA-binding proteins. And finally, an abundance of gene targets were identified to which *Hu* genes had a positive or negatively regulatory effect on.

9.1 Influence of Hu proteins on cellular properties in cancer

An increased cell motility could be observed after a *HuB* knockdown in both Neuroblastoma and Glioblastoma cell lines, SH-SY5Y, SK-N-AS and U87-MG. This suggests that in these cells, HuB is acting on transcripts to maintain a moderate level of migration control that results in a high mobility of these cell after HuB knockdown. These findings supports research presented by Tarter (2013) where HuB is described as a potential tumour suppressor. Their study found that HuB controls the expression of genes involved in cell adhesion and motility and that a loss of HuB expression increases the degree of stemness in glioma cells.

HuB and *HuC* gene knockdowns increased cell viability in SH-SY5Y Neuroblastoma cells and U87-MG Glioblastoma. If HuB and HuC protein expression is downregulated, cell viability increases again highlighting a potential tumour suppressor mechanism of these two Hu

proteins. None of the *Hu* gene knockdowns resulted in a cell morphology change in the Neuroblastoma and Glioblastoma cell models used.

9.2 Regulatory interactions of Hu proteins in cancer

Assessing the effect of regulatory influences of different Hu family proteins on each other's gene expression in Neuroblastoma and Glioblastoma showed some similarities. HuR was found to positively regulate the expression of *HuC* in all cell models.

In the SH-SY5Y Neuroblastoma cell line and U87-MG Glioblastoma cell line, additional similarities in the gene expression of other Hu proteins regulation were observed. HuR positively regulated *HuD* and *HuC* negatively regulated *HuR*. The HuR and HuC interactions reveal they can both regulate each other's proteins levels ensuring an abundance of each protein in the cells. A summary of the Hu protein regulation in regard to the gene expression of other family members in in Neuroblastoma and Glioblastoma is displayed in Fig. 9.1.

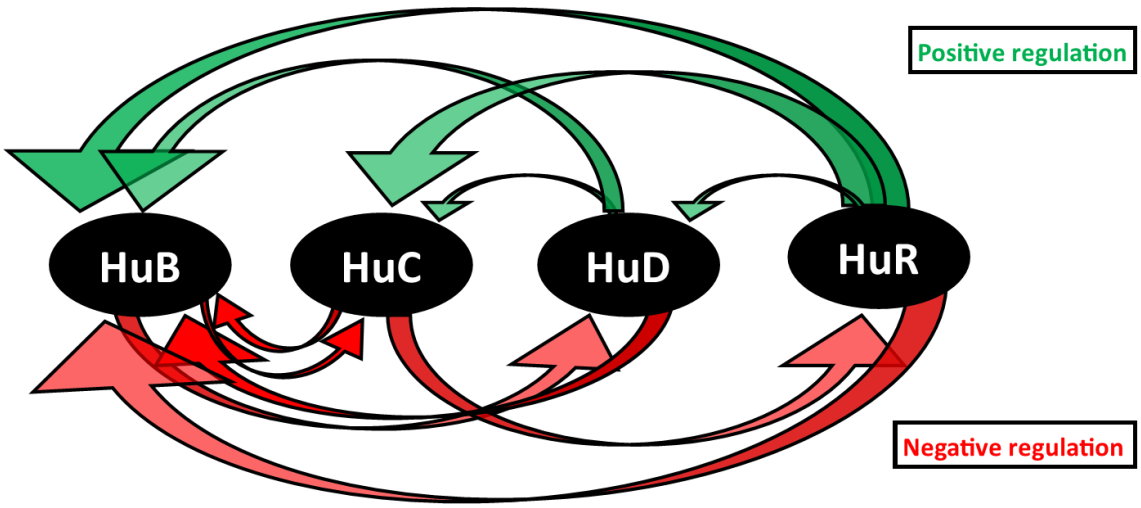

Figure 9.1: Hypothesised regulatory interactions achieved by the Hu family of RNA-binding proteins in Neuroblastoma and Glioblastoma cell models. Overlay of the regulatory pattern observed in Neuroblastoma and Glioblastoma cell lines.

9.3 Gene targets regulated by Hu proteins

Hu proteins have been shown to regulate the expression of an array of different mRNA transcripts. When analysed, some of the Hu proteins showed oncogenic as well as tumour suppressive effects depending on the knocked down Hu protein. Analysis of effected target genes after *Hu* gene knockdowns showed that many of the target genes are members of the MAPK signalling pathway. Some targets were upstream regulators of the pathways and others were downstream effectors. In addition, some of the other targets have been closely linked to the MAPK signalling pathway.

The evolutionary conserved family of mitogen-activated protein kinases (MAPKs) includes extracellular signal-regulated kinase (ERK), p38 isoforms, and c-Jun N-terminal kinase (JNK) (Schaeffer and Weber 1999, Chakraborti et al. 2003). The MAPK pathways are activated by diverse extracellular and intracellular stimuli controls fundamental cellular processes such as growth, proliferation, differentiation, migration and apoptosis through a series of phosphorylation events (Dhillon et al. 2007). Interestingly, deregulation of the MAPK signalling pathway has been implicated in many neurodegenerative diseases including Alzheimer's disease and Parkinson's disease (Kim and Choi 2010). These disorders are also linked to the paraneoplastic Hu syndrome.

Doller et al. (2008) previously identified a link between Hu proteins and MAPK showing that cytoplasmic shuttling of HuR is potentially regulated by MAPK and its downstream kinases MK2, AMPK PKC family. AMPK phosphorylates and acetylates importin-a1, a nuclear transportation protein resulting in nuclear accumulation of HuR (Kim et al 2008). This nuclear HuR is then transported to the cytoplasm in a ratio-driven exchange. They concluded MAP

kinases increase cytoplasmic HuR and therefore may participate in stabilisation or translation or both of TNFa, IL6, IL8, COX-2 GMCSF, uPa and UPAR (Doller et al 2008).

Summarised in Fig. 9.2. is an extended version of the MAPK signalling pathway showing the interactions between signalling pathway components from the cell surface to gene transcription. Hu proteins seem to influence the regulation of different targets of the network however the underlying mechanism and the interplay of these targets must be determined. In relapsed Neuroblastomas, eighteen somatic mutations were identified that initiated the RAS-MAPK signalling pathway (Eleveld et al. 2015).

Further gene profiling would be required to confirm the influence of Hu proteins on other MAPK signalling pathways targets and if the knockdown would influence upstream or downstream target of the pathway.

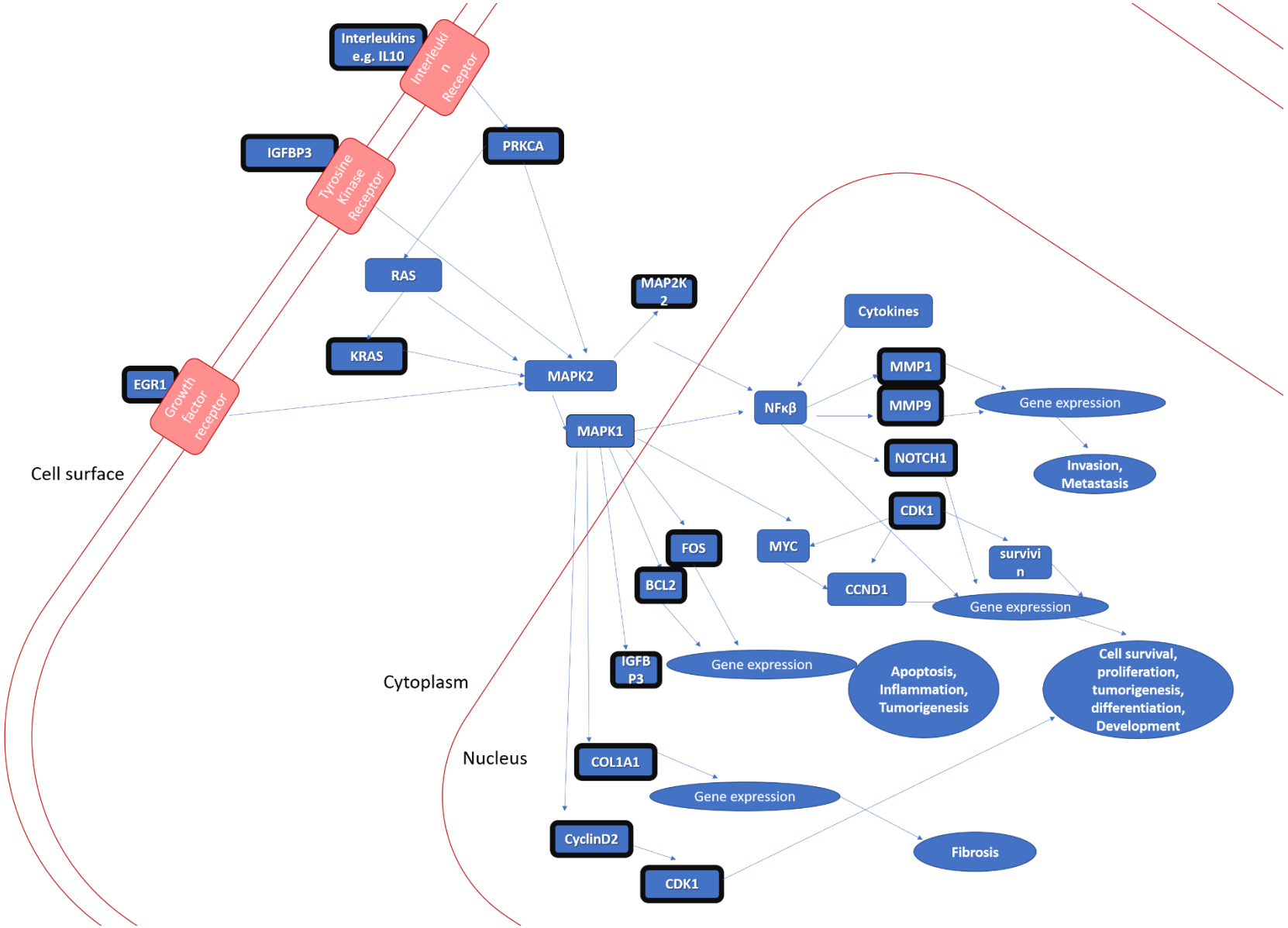

Figure 9.2: Extended MAPK signalling pathway. MAPK signalling pathway with genes highlighted in black that are affected by Hu gene regulation.

9.4 Therapeutic intervention: Hu proteins as potential targets in screening, diagnosis, monitoring and treatment of cancers

The identification of RBPs, mRNA targets and underlying molecular mechanism can give rise to new targets for cancer therapy and a need for the development of RNA-based therapeutics to treat human diseases (Wurth 2012, Cooper. et al. 2009).

The aberrant expression of Hu protein observed in SCLC, Neuroblastoma and Glioblastoma could define Hu expression as biomarker in diagnosing cancer.

Pagliarini et al. (2015) concluded future treatments for cancer will include screening individual patients for specific splicing-alterations and developing anti-cancer treatments in response to these findings. Personalised, targeted treatments based on the molecular genetics of tumours provides the key to future treatment (Dietel and Sers 2006).

In this thesis, an individual pattern of *Hu* gene targets was established and have been implicated in the pathogenicity of cancers. Within the Hu family, differential Hu protein members showed an upregulation of targets whilst others downregulated the same target depending on the transcripts role but also highlighting the different regulatory effect Hu proteins can have on mRNA transcripts' for example, HuR and HuB seemed to show both oncogenic and tumour suppressive regulation within on cell line. This results in HuB and HuC showing both oncogenic and tumour suppressive phenotypes within one cell line. A more in depth study of individual *Hu* genes and their effects would therefore be required before conclusively understanding the role of Hu proteins in Small cell lung cancer, Neuroblastoma and Glioblastoma.

RBPs were considered relatively 'undruggable' targets due to their structure and deficiency in well-defined binding pockets (Wu et al. 2015). Treatment with systemic immunotoxin

therapy in patients with solid tumours has been unsuccessful due to poor penetration into the tumour (Ehrlich et al. 2014). However, the development of RNA interference (RNAi) to silence any gene gives rise to a new approach of therapeutic intervention. Current research stems the idea of developing methods to deliver siRNAs to the site of action in cells of target tissues (Kanasty et al. 2013). A recent strategy suggested by Jimbo et al. (2015), uses lipidoid nanoparticles to deliver siRNA to target tumour sites. Other mechanisms to target RNA in cells include the use of antisense oligonucleotides, antisense snRNA and RNA interference (Cooper et al. 2009).

9.5 Future Research

siRNA used in this thesis for knocking down the expression of target genes isn't as efficient as 'Clustered regularly interspaced in between short palindromic repeats' (CRISPR). This technology allows editing of the genome with great specificity, precision and efficiency.

The inability to knockdown Hu proteins in lung cancer using siRNA interference proved a huge limitation therefore further experiment could be performed using CRISPR. It is a natural defence mechanism found in many of bacteria. This new method would allow a complete knockout of the *Hu* genes, guaranteeing to reveal the extent of its effects.

This CRISPR technology would enable 100% knockouts in all the studies rather than a knockdown that leaves some functioning gene. Since, the Hu proteins can also auto-regulate themselves and a small amount of remaining protein can be sufficient to influence its own expression and target other mRNAs for regulation. This technology along with RNA-seq and ribosomal profiling can allow a more in-depth quantifiable level of mRNA and protein levels following knockout experiments.

As advances in medical science move towards personalised targeted treatments, core signalling pathways will need to be established to ensure these treatments will be 100% effective. Here, genetic compensation was observed following knockdown of the Hu gene in combination that could have adverse effect in a targeted therapy. Additionally, miRNA analysis could help understand the extended regulation of *Hu* genes.

References

Abdelmohsen, K and Gorospe, M (2010) 'Posttranscriptional Regulation of Cancer Traits by HuR'. in *Wiley Interdisciplinary Reviews: RNA*. vol. 1 (2). 214–229

Abdelmohsen, K, Hutchison, E.R., Lee, E.K., Kuwano, Y., Kim, M.M., Masuda, K., Srikantan, S., Subaran, S.S., Marasa, B.S., Mattson, M.P., and Gorospe, Myriam (2010) 'MiR-375 Inhibits Differentiation of Neurites by Lowering HuD Levels.' *Molecular and cellular biology* 30 (17), 4197–4210

Abdelmohsen, K, Pullmann, R., Lal, A., Kim, H.H., Galban, S., Yang, X, Blethrow, J.D., Walker, M., Shubert, J., Gillespie, D.A., Furneaux, Henry, and Gorospe, Myriam (2007) 'Phosphorylation of HuR by Chk2 Regulates SIRT1 Expression'. *Molecular Cell* 25 (4), 543–557

Abdelmohsen, K, Srikantan, S., Kuwano, Y., and Gorospe, M (2008) 'MiR-519 Reduces Cell Proliferation by Lowering RNA-Binding Protein HuR Levels'. *Proceedings of the National Academy of Sciences* [online] 105 (51), 20297–20302.

Adamson, E.D. and Mercola, D. (2002) 'Egr1 Transcription Factor: Multiple Roles in Prostate Tumor Cell Growth and Survival'. in *Tumor Biology*.

Agami, R. (2010) 'MicroRNAs, RNA Binding Proteins and Cancer'. *European Journal of Clinical Investigation* 40 (4), 370–374

Akamatsu, W., Fujihara, H., Mitsuhashi, T., Yano, M., Shibata, S., Hayakawa, Y., Okano, Hirotaka James, Sakakibara, S.-I., Takano, H., Takano, T., Takahashi, T., Noda, T., and Okano, H. (2005) 'The RNA-Binding Protein HuD Regulates Neuronal Cell Identity and Maturation.' *Proceedings of the National Academy of Sciences of the United States of America* [online] 102 (12), 4625–30.

Akhtar, R.S., Ness, J.M., and Roth, K.A. (2004) 'Bcl-2 Family Regulation of Neuronal Development and Neurodegeneration'. *Biochimica et Biophysica Acta (BBA) - Molecular Cell Research* [online] 1644 (2), 189–203.

Akool, E.S., Kleinert, H., Hamada, F.M.A., Abdelwahab, M.H., Förstermann, U., Pfeilschifter, J., and Eberhardt, W. (2003) 'Nitric Oxide Increases the Decay of Matrix Metalloproteinase 9 MRNA by Inhibiting the Expression of MRNA-Stabilizing Factor HuR.' *Molecular and cellular biology*

Al-Ahmadi, W., Al-Ghamdi, M., Al-Haj, L., Al-Saif, M., and Khabar, K. S A (2009) 'Alternative Polyadenylation Variants of the RNA Binding Protein, HuR: Abundance, Role of AU-Rich Elements and Auto-Regulation'. *Nucleic Acids Research* 37 (11), 3612–3624

Al-ahmadi, W., Al-ghamdi, M., Al-souhibani, N., and Khabar, Khalid S A (2013) *MiR-29a Inhibition Normalizes HuR over-Expression and Aberrant AU-Rich MRNA Stability in Invasive Cancer*.

Alifieris, C. and Trafalis, D.T. (2015) 'Glioblastoma Multiforme: Pathogenesis and Treatment.' *Pharmacology & therapeutics* 152, 63–82

Alt, J.R., Cleveland, J.L., Hannink, M., and Diehl, J.A. (2000) 'Phosphorylation-Dependent Regulation of Cyclin D1 Nuclear Export and Cyclin D1-Dependent Cellular Transformation'. *Genes and Development* 14 (24), 3102–3114

Amadio, M., Bucolo, C., Leggio, G.M., Drago, F., Govoni, S., and Pascale, A. (2010) 'The PKC/HuR/VEGF Pathway in Diabetic Retinopathy'. *Biochemical Pharmacology* 80 (8), 1230–

1237

Anderson, N.E., Cunningham, J.M., and Posner, J B (1987) 'Autoimmune Pathogenesis of Paraneoplastic Neurological Syndromes.' *Critical reviews in neurobiology* [online] 3 (3), 245–99.

Doller, A., Huwiler, A., Muller, H.H.R. and Pfeilschifter W.E. (2007) 'Protein Kinase C -Dependent Phosphorylation of the MRNA-Stabilizing Factor HuR: Implications for Posttranscriptional Regulation of Cyclooxygenase-2'. *Molecular biology of the cell* 18 (December), 986–994

Antic, D. and Keene, J D (1997) 'Embryonic Lethal Abnormal Visual RNA-Binding Proteins Involved in Growth, Differentiation, and Posttranscriptional Gene Expression.' *American journal of human genetics* [online] 61 (2), 273–278.

Antic, D. and Keene, J D (1998) 'Messenger Ribonucleoprotein Complexes Containing Human ELAV Proteins: Interactions with Cytoskeleton and Translational Apparatus.' *Journal of cell science* 111 (Pt 2, 183–197

Aranda-Abreu, G.E., Behar, L, Chung, S, Furneaux, H, and Ginzburg, I (1999) 'Embryonic Lethal Abnormal Vision-like RNA-Binding Proteins Regulate Neurite Outgrowth and Tau Expression in PC12 Cells.' *The Journal of neuroscience : the official journal of the Society for Neuroscience* 19 (16), 6907–6917

Armento, A, Ehlers J, Schötterl S and Naumann U (2017) 'Molecular Mechanisms of Glioma Cell Motility'. in *Glioblastoma*. Bisbane: Codon Publications

Aronov, S., Aranda, G., Behar, Leah, and Ginzburg, Irith (2002) 'Visualization of Translated Tau Protein in the Axons of Neuronal P19 Cells and Characterization of Tau RNP Granules.' *Journal of cell science* 115, 3817–3827

Atasoy, U, Watson, J., Patel, D., and Keene, J D (1998) 'ELAV Protein HuA (HuR) Can Redistribute between Nucleus and Cytoplasm and Is Upregulated during Serum Stimulation and T Cell Activation.' *Journal of cell science* 111 (Pt 2, 3145–3156

ATCC (2016a) *BEAS-2B (ATCC® CRL-9609™)* [online] available from <https://www.lgcstandards-atcc.org/Products/All/CRL-9609.aspx?geo_country=gb>

ATCC (2016b) *NCI-H345 [H345] (ATCC HTB-180)* [online] available from <https://www.lgcstandards-atcc.org/Products/All/HTB-180.aspx?geo_country=gb>

ATCC (2016c) *NCI-H358 [H-358, H358] (ATCC® CRL-5807™)* [online] available from <https://www.lgcstandards-atcc.org/Products/All/CRL-5807.aspx?geo_country=gb>

ATCC (2016d) *NCI-H69 [H69] (ATCC® HTB-119™)* [online] available from <https://www.lgcstandards-atcc.org/Products/All/HTB-119.aspx?geo_country=gb>

ATCC (2016e) *SH-SY5Y (ATCC® CRL-2266™)* [online] available from <https://www.lgcstandards-atcc.org/Products/All/CRL-2266.aspx?geo_country=gb>

ATCC (2016f) *SK-N-AS (ATCC® CRL-2137™)* [online] available from <https://www.lgcstandards-atcc.org/products/all/CRL-2137.aspx?geo_country=gb>

ATCC (2016g) *SVG P12 (ATCC® CRL-8621™)* [online] available from <https://www.lgcstandards-atcc.org/products/all/CRL-8621.aspx?geo_country=gb>

ATCC (2016h) *U-87 MG (ATCC® HTB-14™)* [online] available from <https://www.lgcstandards-atcc.org/products/all/HTB-14.aspx?geo_country=gb>

Baba, A. and Câtoi, C. (2007) 'Tumour Cell Morphology'. in *Comparative Oncology*. Bucharest: The Publishing House of the Romanian Academy

Ball, N.S. and King, P. H. (1997) 'Neuron-Specific Hel-N1 and HuD as Novel Molecular Markers of Neuroblastoma: A Correlation of HuD Messenger RNA Levels with Favorable Prognostic Features'. *Clinical Cancer Research* 3 (10), 1859–1865

Beckel-Mitchener, A.C., Miera, A., Keller, R., and Perrone-Bizzozero, N.I. (2002) 'Poly(A) Tail Length-Dependent Stabilization of GAP-43 MRNA by the RNA-Binding Protein HuD'. *Journal of Biological Chemistry* 277 (31), 27996–28002

Bernards, A. (1995) 'Neurofibromatosis Type 1 and Ras-Mediated Signaling: Filling in the GAPs'. *Biochimica et Biophysica Acta (BBA) - Reviews on Cancer* [online] 1242 (1), 43–59.

Betticher, D.C., Thatcher, N., Altermatt, H.J., Hoban, P., Ryder, W.D., and Heighway, J. (1995) 'Alternate Splicing Produces a Novel Cyclin D1 Transcript'. *Oncogene* [online] 11 (5), 1005–1011.

Biorad (2018) *PrimePCR Pathways* [online] available from <http://www.bio-rad.com/en-uk/prime-pcr-assays/pathway/primepcr-pathways> [24 September 2018]

Bissell, M.J. and Labarge, M.A. (2005) 'Context, Tissue Plasticity, and Cancer: Are Tumor Stem Cells Also Regulated by the Microenvironment?' in *Cancer Cell*. vol. 7 (1). 17–23

Boise, L.H., González-García, M., Postema, C.E., Ding, L., Lindsten, T., Turka, L.A., Mao, X., Nuñez, G., and Thompson, C.B. (1993) 'Bcl-x, a Bcl-2-Related Gene That Functions as a Dominant Regulator of Apoptotic Cell Death'. *Cell* [online] 74 (4), 597–608

Bolognani, F., Contente-Cuomo, T., and Perrone-Bizzozero, N.I. (2009) 'Novel Recognition Motifs and Biological Functions of the RNA-Binding Protein HuD Revealed by Genome-Wide Identification of Its Targets'. *Nucleic Acids Research* 38 (1), 117–130

Bolognani, F., Gallani, A.I., Sokol, L., Baskin, D.S., and Meisner-Kober, N. (2012) 'MRNA Stability Alterations Mediated by HuR Are Necessary to Sustain the Fast Growth of Glioma Cells'. *Journal of Neuro-Oncology* 106 (3), 531–542

Brambilla, E, Travis, W D, Colby, T. V, Corrin, B., and Shimosato, Y. (2001) 'The New World Health Organization Classification of Lung Tumours.' *The European respiratory journal* [online] 18 (6), 1059–1068.

Brennan, C M and Steitz, J a (2001) 'HuR and MRNA Stability.' *Cellular and molecular life sciences : CMLS* 58 (2), 266–277

Bronicki, L. and Jasmin, B. (2013) 'Emerging Complexity of the HuD/ELAVl4 Gene; Implications for Neuronal Development, Function, and Dysfunction'. *Rna* [online] 1019–1037.

Bronicki, L.M., Belanger, G., and Jasmin, B. J. (2012) 'Characterization of Multiple Exon 1 Variants in Mammalian HuD MRNA and Neuron-Specific Transcriptional Control via Neurogenin 2'. *Journal of Neuroscience* 32 (33), 11164–11175

Buckanovich, R.J. and Darnell, R B (1997) 'The Neuronal RNA Binding Protein Nova-1 Recognizes Specific RNA Targets in Vitro and in Vivo.' *Molecular and cellular biology*

Burd, C.J., Petre, C.E., Morey, L.M., Wang, Ying, Revelo, M.P., Haiman, C.A., Lu, S., Fenoglio-Preiser, C.M., Li, Jiwen, Knudsen, E.S., Wong, J., and Knudsen, K.E. (2006) 'Cyclin D1b Variant Influences

Prostate Cancer Growth through Aberrant Androgen Receptor Regulation.' *Proceedings of the National Academy of Sciences of the United States of America* [online] 103 (7), 2190–5.

Busà, R., Paronetto, M.P., Farini, D., Pierantozzi, E., Botti, F., Angelini, D.F., Attisani, F., Vespasiani, G., and Sette, C (2007) 'The RNA-Binding Protein Sam68 Contributes to Proliferation and Survival of Human Prostate Cancer Cells.' *Oncogene* 26 (30), 4372–4382

Calaluce, R., Gubin, M.M., Davis, J.W., Magee, J.D., Chen, Jing, Kuwano, Y., Gorospe, Myriam, and Atasoy, Ulus (2010) 'The RNA Binding Protein HuR Differentially Regulates Unique Subsets of MRNAs in Estrogen Receptor Negative and Estrogen Receptor Positive Breast Cancer.' *BMC cancer* [online] 10, 126.

Campos-Melo, D., Droppelmann, C. a., Volkening, K., and Strong, M.J. (2014) 'RNA-Binding Proteins as Molecular Links between Cancer and Neurodegeneration'. *Biogerontology* [online] 15 (6), 587–610.

Caput, D., Beutler, B., Hartog, K., Thayer, R., Brown-Shimer, S., and Cerami, A. (1986) 'Identification of a Common Nucleotide Sequence in the 3'-Untranslated Region of MRNA Molecules Specifying Inflammatory Mediators.' *Proceedings of the National Academy of Sciences of the United States of America* 83 (6), 1670–1674

Chakraborti, S., Mandal, M., Das, S., Mandal, A., and Chakraborti, T. (2003) 'Regulation of Matrix Metalloproteinases. An Overview'. in *Molecular and Cellular Biochemistry*.

Chelly, J. and Mandel, J.-L. (2001) 'Monogenic Causes of X-Linked Mental Retardation'. *Nat Rev Genet* [online] 2 (9), 669–680.

Chen, Jian, McKay, R.M., and Parada, L.F. (2012) 'Malignant Glioma: Lessons from Genomics, Mouse Models, and Stem Cells.' *Cell* 149 (1), 36–47

Chen, Y.-C., Pohl, G., Wang, T.-L., Morin, P.J., Risberg, B., Kristensen, G.B., Yu, A., Davidson, B., and Shih, I.-M. (2005) 'Apolipoprotein E Is Required for Cell Proliferation and Survival in Ovarian Cancer.' *Cancer research* 65 (1), 331–337

Chen, Yun, Tsai, Y.-H., and Tseng, S.-H. (2013) 'Inhibition of Cyclin-Dependent Kinase 1-Induced Cell Death in Neuroblastoma Cells through the MicroRNA-34a-MYCN-Survivin Pathway'. *Surgery* [online] 153 (1), 4–16.

Chen, Yuntao, Tian, D., Ku, L., Osterhout, D.J., and Feng, Y. (2007) 'The Selective RNA-Binding Protein Quaking I (QKI) Is Necessary and Sufficient for Promoting Oligodendroglia Differentiation.' *The Journal of biological chemistry* 282 (32), 23553–23560

Chmara, M., Wozniak, A., Ochman, K., Kobierska, G., Dziadziuszko, R., Sosinska-Mielcarek, K., Jassem, E., Skokowski, J., Jassem, J., and Limon, J. (2004) 'Loss of Heterozygosity at Chromosomes 3p and 17p in Primary Non-Small Cell Lung Cancer.' *Anticancer research* 24 (6), 4259–4263

Cho, N.H., Kang, S., Hong, S., An, H.J., Choi, Y.H., Jeong, G.B., and Choi, H.K. (2006) 'Elevation of Cyclin B1, Active Cdc2, and HuR in Cervical Neoplasia with Human Papillomavirus Type 18 Infection.' *Cancer letters* [online] 232 (2), 170–8.

Chu, C.-Y., Chang, C.-C., Prakash, E., and Kuo, M.-L. (2008) 'Connective Tissue Growth Factor (CTGF) and Cancer Progression.' *Journal of biomedical science* 15 (6), 675–685

Chung, Sangmi, Jiang, L., Cheng, Simon, and Furneaux, Henry (1996) 'Purification and Properties of HuD, a Neuronal RNA-Binding Protein'. *Journal of Biological Chemistry* 271 (19), 11518–11524

Clark, M.J., Homer, N., O'Connor, B.D., Chen, Zugen, Eskin, A., Lee, H., Merriman, B., and Nelson, S.F. (2010) 'U87MG Decoded: The Genomic Sequence of a Cytogenetically Aberrant Human Cancer Cell Line'. *PLoS Genetics* 6 (1)

Clemmons, D.R. and Jones, J.I. (1995) 'Insulin-Like Growth Factors and Their Binding Proteins: Biological Actions*'. *Endocrine Reviews* [online] 16 (1), 3–34.

Cohn, S.L., Pearson, A.D.J., London, W.B., Monclair, T., Ambros, P.F., Brodeur, G.M., Faldum, A., Hero, B., Iehara, T., Machin, D., Mosseri, V., Simon, T., Garaventa, A., Castel, V., and Matthay, K.K. (2009) 'The International Neuroblastoma Risk Group (INRG) Classification System: An INRG Task Force Report'. *Journal of Clinical Oncology* 27 (2), 289–297

Cook, R.F., Miller, Y.E., and Bunn, P.A. (1993) 'Small Cell Lung Cancer: Etiology, Biology, Clinical Features, Staging, and Treatment'. *Current Problems in Cancer* [online] 17 (2), 73–141.

Cooper, T.A., Wan, L., and Dreyfuss, G. (2009) 'RNA and Disease'. in *Cell*. vol. 136 (4). 777–793

Coulon, A., Flahaut, M., Mühlethaler-Mottet, A., Meier, R., Liberman, J., Balmas-Bourloud, K., Nardou, K., Yan, P., Tercier, S., Joseph, J.-M., Sommer, L., and Gross, N. (2011) 'Functional Sphere Profiling Reveals the Complexity of Neuroblastoma Tumor-Initiating Cell Model'. *Neoplasia (New York, N.Y.)* [online] 13 (10), 991–1004.

Croce, C.M. (2008) 'Oncogenes and Cancer. Supplementary Appendix'. *The New England journal of medicine* [online] 358 (5), 502–11.

D'Alessandro, V., Muscarella, L.A., Copetti, M., Zelante, L., Carella, M., and Vendemiale, G. (2008) 'Molecular Detection of Neuron-Specific ELAV-like-Positive Cells in the Peripheral Blood of Patients with Small-Cell Lung Cancer'. *Cellular oncology : the official journal of the International Society for Cellular Oncology* [online] 30 (4), 291–297.

D'Alessandro, V., Muscarella, L.A., la Torre, A., Bisceglia, M., Parrella, P., Scaramuzzi, G., Storlazzi, C.T., Trombetta, D., Kok, K., De Cata, A., Sperandeo, M., Zelante, L., Carella, M., and Vendemiale, G. (2010) 'Molecular Analysis of the HuD Gene in Neuroendocrine Lung Cancers'. *Lung Cancer* 67 (1), 69–75

Dai, W., Zhang, G., and Makeyev, E. V. (2012) 'RNA-Binding Protein HuR Autoregulates Its Expression by Promoting Alternative Polyadenylation Site Usage'. *Nucleic Acids Research* 40 (2), 787–800

Dalmau, J, Graus, F., Cheung, N.K., Rosenblum, M.K., Ho, a, Cañete, a, Delattre, J.Y., Thompson, S.J., and Posner, J B (1995) 'Major Histocompatibility Proteins, Anti-Hu Antibodies, and Paraneoplastic Encephalomyelitis in Neuroblastoma and Small Cell Lung Cancer.' *Cancer* [online] 75 (1), 99–109.

Dalmau, Josep and Furneaux, HM (1992) 'The Expression of the Hu (Paraneoplastic Encephalomyelitis/Sensory Neuronopathy) Antigen in Human Normal and Tumor Tissues.' *The American journal …* [online] 141 (4), 881–886.

Dalmau, Josep and Rosenfeld, M.R. (2008) 'Paraneoplastic Syndromes of the CNS'. in *Lancet Neurology*. vol. 7 (4). 327–340

Danilin, S., Sourbier, C., Thomas, L., Rothhut, S., Lindner, V., Helwig, J.-J., Jacqmin, D., Lang, H., and Massfelder, T. (2009) 'Von Hippel-Lindau Tumor Suppressor Gene-Dependent MRNA Stabilization of the Survival Factor Parathyroid Hormone-Related Protein in Human Renal Cell Carcinoma by the RNA-Binding Protein HuR.' *Carcinogenesis* 30 (3), 387–96.

Darnell, R. B. and DeAngelis, L.M. (1993) 'Regression of Small-Cell Lung Carcinoma in Patients with Paraneoplastic Neuronal Antibodies'. *The Lancet* 341 (8836), 21–22

Darnell, R B (1996) 'Onconeural Antigens and the Paraneoplastic Neurologic Disorders: At the Intersection of Cancer, Immunity, and the Brain.' *Proceedings of the National Academy of Sciences of the United States of America* 93 (10), 4529–4536

Darnell, Robert B (2010) 'RNA Regulation in Neurologic Disease and Cancer.' *Cancer research and treatment : official journal of Korean Cancer Association* 42 (3), 125–129

Datta, K., Mondal, S., Sinha, S., Li, Jinping, Wang, E., Knebelmann, B., Karumanchi, S.A., and Mukhopadhyay, D. (2005) 'Role of Elongin-Binding Domain of von Hippel Lindau Gene Product on HuR-Mediated VPF/VEGF MRNA Stability in Renal Cell Carcinoma.' *Oncogene* [online] 24 (53), 7850–8.

David, C.J. and Manley, J.L. (2010) 'Alternative Pre-MRNA Splicing Regulation in Cancer: Pathways and Programs Unhinged'. in *Genes and Development*. vol. 24 (21). 2343–2364

DeLuca, I., Blachère, N.E., Santomasso, B., and Darnell, Robert B (2009) 'Tolerance to the Neuron-Specific Paraneoplastic HuD Antigen.' *PloS one* [online] 4 (6).

Demuth, T. and Berens, M.E. (2004) 'Molecular Mechanisms of Glioma Cell Migration and Invasion.' *Journal of neuro-oncology* 70 (2), 217–228

Denkert, C., Weichert, W., Pest, S., Koch, I., Licht, D., Köbel, M., Reles, A., Sehouli, J., Dietel, M., and Hauptmann, S. (2004) 'Overexpression of the Embryonic-Lethal Abnormal Vision-like Protein HuR in Ovarian Carcinoma Is a Prognostic Factor and Is Associated with Increased Cyclooxygenase 2 Expression'. *Cancer Research* 64 (1), 189–195

Denli, A.M., Tops, B.B.J., Plasterk, R.H. a, Ketting, R.F., and Hannon, G.J. (2004) 'Processing of Primary MicroRNAs by the Microprocessor Complex.' *Nature* [online] 432 (7014), 231–5.

Derti, A., Garrett-Engele, P., Macisaac, K.D., Stevens, R.C., Sriram, S., Chen, Ronghua, Rohl, C.A., Johnson, J.M., and Babak, T. (2012) 'A Quantitative Atlas of Polyadenylation in Five Mammals.' *Genome research* 22 (6), 1173–1183

Deschênes-Furry, J., Mousavi, K., Bolognani, F., Neve, R.L., Parks, R.J., Perrone-bizzozero, N.I., and Jasmin, Bernard J (2007) *The RNA-Binding Protein HuD Binds Acetylcholinesterase MRNA in Neurons and Regulates Its Expression after Axotomy*. 27 (3), 665–675

Dhillon, A.S., Hagan, S., Rath, O., and Kolch, W. (2007) 'MAP Kinase Signalling Pathways in Cancer'. *Oncogene* 26, 3279.

Diedrich, J.F., Minnigan, H., Carp, R.I., Whitaker, J.N., Race, R., Frey, W., and Haase, A.T. (1991) 'Neuropathological Changes in Scrapie and Alzheimer's Disease Are Associated with Increased Expression of Apolipoprotein E and Cathepsin D in Astrocytes'. *J.Virol.*

Dietel, M. and Sers, C. (2006) 'Personalized Medicine and Development of Targeted Therapies: The Upcoming Challenge for Diagnostic Molecular Pathology. A Review'. in *Virchows Archiv*. vol. 448 (6). 744–755

Doller, A., Akool, E.-S., Huwiler, A., Müller, R., Radeke, H.H., Pfeilschifter, J., and Eberhardt, W. (2008a) 'Posttranslational Modification of the AU-Rich Element Binding Protein HuR by Protein Kinase Cdelta Elicits Angiotensin II-Induced Stabilization and Nuclear Export of Cyclooxygenase 2 MRNA.' *Molecular and cellular biology* [online] 28 (8), 2608–25.

Doller, A., Pfeilschifter, J., and Eberhardt, W. (2008b) 'Signalling Pathways Regulating Nucleo-Cytoplasmic Shuttling of the MRNA-Binding Protein HuR'. in *Cellular Signalling*. vol. 20 (12). 2165–2173

Doller, A., Schlepckow, K., Schwalbe, H., Pfeilschifter, J., and Eberhardt, W. (2010) 'Tandem Phosphorylation of Serines 221 and 318 by Protein Kinase Cdelta Coordinates MRNA Binding and Nucleocytoplasmic Shuttling of HuR.' *Molecular and cellular biology* 30 (6), 1397–1410

Doller, A., Schulz, S., Pfeilschifter, J., and Eberhardt, W. (2013) 'RNA-Dependent Association with Myosin IIA Promotes F-Actin-Guided Trafficking of the ELAV-like Protein HuR to Polysomes.' *Nucleic acids research* [online] 41 (19), 9152–67.

Dong, R., Lu, J.G., Wang, Q., He, X.L., Chu, Y.K., and Ma, Q.J. (2007) 'Stabilization of Snail by HuR in the Process of Hydrogen Peroxide Induced Cell Migration'. *Biochemical and Biophysical Research Communications* 356 (1), 318–321

Dong, R., Yang, G.-D., Luo, N.-A., and Qu, Y.-Q. (2014) 'HuR: A Promising Therapeutic Target for Angiogenesis.' *Gland Surgery* [online] 3 (3), 203–6.

Dormoy-Raclet, V., Ménard, I., Clair, E., Kurban, G., Mazroui, R., Di Marco, S., von Roretz, C., Pause, A., and Gallouzi, I.-E. (2007) 'The RNA-Binding Protein HuR Promotes Cell Migration and Cell Invasion by Stabilizing the Beta-Actin MRNA in a U-Rich-Element-Dependent Manner.' *Molecular and cellular biology* 27 (15), 5365–5380

Doxakis, E. (2014) 'RNA Binding Proteins: A Common Denominator of Neuronal Function and Dysfunction'. *Neuroscience Bulletin* 30 (4), 610–626

Driver, J.A. (2012) 'Understanding the Link between Cancer and Neurodegeneration'. in *Journal of Geriatric Oncology*. vol. 3 (1). 58–67

Dupont-Wallois, L., Soulié, C., Sergeant, N., Wavrant-de Wrieze, N., Chartier-Harlin, M.-C., Delacourte, A., and Caillet-Boudin, M.-L. (1997) 'ApoE Synthesis in Human Neuroblastoma Cells'. *Neurobiology of Disease* [online] 4 (5), 356–364.

Eberhardt, W., Badawi, A., Biyanee, A., and Pfeilschifter, J. (2016) 'Cytoskeleton-Dependent Transport as a Potential Target for Interfering with Post-Transcriptional HuR MRNA Regulons'. *Frontiers in Pharmacology* 7 (August), 1–7

Ehrlich, D., Wang, Bo, Lu, W., Dowling, P., and Yuan, R. (2014) 'Intratumoral Anti-HuD Immunotoxin Therapy for Small Cell Lung Cancer and Neuroblastoma'. *Journal of Hematology & Oncology* [online] 7 (1), 1–8.

El-Brolosy, M.A. and Stainier, D.Y.R. (2017) 'Genetic Compensation: A Phenomenon in Search of Mechanisms'. *PLoS genetics* 13 (7),

Eleveld, T.F., Oldridge, D.A., Bernard, V., Koster, J., Colmet Daage, L., Diskin, S.J., Schild, L., Bentahar, N.B., Bellini, A., Chicard, M., Lapouble, E., Combaret, V., Legoix-Né, P., Michon, J., Pugh, T.J., Hart, L.S., Rader, J., Attiyeh, E.F., Wei, J.S., Zhang, S., Naranjo, A., Gastier-Foster, J.M., Hogarty, M.D., Asgharzadeh, S., Smith, M.A., Guidry Auvil, J.M., Watkins, T.B.K., Zwijnenburg, D.A., Ebus, M.E., van Sluis, P., Hakkert, A., van Wezel, E., van der Schoot, C.E., Westerhout, E.M., Schulte, J.H., Tytgat, G.A., Dolman, M.E.M., Janoueix-Lerosey, I., Gerhard, D.S., Caron, H.N., Delattre, O., Khan, J., Versteeg, R., Schleiermacher, G., Molenaar, J.J., and Maris, J.M. (2015) 'Relapsed Neuroblastomas Show Frequent RAS-MAPK Pathway Mutations'. *Nature genetics* 47 (8), 864–871.

Ellor, S. V, Pagano-Young, T.A., and Avgeropoulos, N.G. (2014) 'Glioblastoma: Background, Standard Treatment Paradigms, and Supportive Care Considerations.' *The Journal of law, medicine & ethics : a journal of the American Society of Law, Medicine & Ethics* 42 (2), 171–182

Erson-Bensan, A.E. (2016) 'Alternative Polyadenylation and RNA-Binding Proteins.' *Journal of molecular endocrinology* 57 (2), F29-34

Fan, X.C. and Steitz, J.A. (1998) 'HNS, a Nuclear-Cytoplasmic Shuttling Sequence in HuR (Nuclear Localization RNA Degradation and Nuclear Export)'. *Biochemistry* 95, 15293–15298

Faustino, N.A., Cooper, T. a, and Andre, N. (2003) 'Pre-MRNA Splicing and Human Disease.' *Genes & Development* 17 (4), 419–437.

Ferguson, S. and Lesniak, M.S. (2005) 'Percival Bailey and the Classification of Brain Tumors'. *Neurosurgical Focus*

Fialcowitz-White, E.J., Brewer, B.Y., Ballin, J.D., Willis, C.D., Toth, E.A., and Wilson, G.M. (2007) 'Specific Protein Domains Mediate Cooperative Assembly of HuR Oligomers on AU-Rich MRNA-Destabilizing Sequences'. *Journal of Biological Chemistry* 282 (29), 20948–20959

Fidler, I.J. (2003) 'The Pathogenesis of Cancer Metastasis: The "seed and Soil" Hypothesis Revisited'. in *Nature Reviews Cancer*.

Filippova, N., Yang, Xiuhua, Ananthan, S., Sorochinsky, A., Hackney, J.R., Gentry, Z., Bae, S., King, P., and Nabors, L.B. (2017) 'Hu Antigen R (HuR) Multimerization Contributes to Glioma Disease Progression'. *Journal of Biological Chemistry* 292 (41)

Filippova, N., Yang, Xiuhua, King, P., and Nabors, L.B. (2012) 'Phosphoregulation of the RNA-Binding Protein Hu Antigen R (HuR) by Cdk5 Affects Centrosome Function'. *Journal of Biological Chemistry* 287 (38), 32277–32287

Filippova, N., Yang, Xiuhua, Wang, Yimin, Gillespie, G.Y., Langford, C., King, Peter H, Wheeler, C., and Nabors, L.B. (2011) 'The RNA-Binding Protein HuR Promotes Glioma Growth and Treatment Resistance.' *Molecular cancer research : MCR* 9 (5), 648–659

Fillmore, H.L., VanMeter, T.E., and Broaddus, W.C. (2001) 'Membrane-Type Matrix Metalloproteinases (MT-MMPs): Expression and Function during Glioma Invasion.' *Journal of neuro-oncology* 53 (2), 187–202

Fisher, P.G., Wechsler, D.S., and Singer, H.S. (1994) 'Anti-Hu Antibody in a Neuroblastoma-Associated Paraneoplastic Syndrome.' *Pediatric neurology* 10 (4), 309–312

Fletcher, J.I., Gherardi, S., Murray, J., Burkhart, C.A., Russell, A., Valli, E., Smith, J., Oberthuer, A., Ashton, L.J., London, W.B., Marshall, G.M., Norris, M.D., Perini, G., and Haber, M. (2012) 'N-Myc Regulates Expression of the Detoxifying Enzyme Glutathione Transferase GSTP1, a Marker of Poor Outcome in Neuroblastoma.' *Cancer research* 72 (4), 845–853

Fredericks, A.M., Cygan, K.J., Brown, B. a, Fairbrother, W.G., and Biology, C. (2015) *RNA-Binding Proteins: Splicing Factors and Disease*. 893–909

Gabay, M., Li, Yulin, and Felsher, D.W. (2014) 'MYC Activation Is a Hallmark of Cancer Initiation and Maintenance'. *Cold Spring Harbor perspectives in medicine* 4 (6)

Gallouzi, I.E., Brennan, Christopher M, Stenberg, M.G., Swanson, M.S., Eversole, A., Maizels, N., and Steitz, Joan a (2000) 'HuR Binding to Cytoplasmic MRNA Is Perturbed by Heat Shock.'

Proceedings of the National Academy of Sciences of the United States of America 97 (7), 3073–8.

Gandini, N.A., Fermento, M.E., Salomon, D.G., Obiol, D.J., Andres, N.C., Zenklusen, J.C., Arevalo, J., Blasco, J., Lopez Romero, A., Facchinetti, M.M., and Curino, A.C. (2014) 'Heme Oxygenase-1 Expression in Human Gliomas and Its Correlation with Poor Prognosis in Patients with Astrocytoma.' *Tumour biology : the journal of the International Society for Oncodevelopmental Biology and Medicine* 35 (3), 2803–2815

Gao, F.B., Carson, C.C., Levine, T., and Keene, J D (1994) 'Selection of a Subset of MRNAs from Combinatorial 3' Untranslated Region Libraries Using Neuronal RNA-Binding Protein Hel-N1.' *Proceedings of the National Academy of Sciences of the United States of America* 91 (23), 11207–11211

Gao, F.B. and Keene, J D (1996) 'Hel-N1/Hel-N2 Proteins Are Bound to Poly(A)+ MRNA in Granular RNP Structures and Are Implicated in Neuronal Differentiation.' *Journal of cell science* 109 (Pt 3, 579–589

Gerstberger, S., Hafner, M., and Tuschl, Thomas (2014) 'A Census of Human RNA-Binding Proteins'. *Nature Reviews Genetics* 15 (12), 829–845.

Ghosh, D., Ulasov, I. V, Chen, LiPing, Harkins, L.E., Wallenborg, K., Hothi, P., Rostad, S., Hood, L., and Cobbs, C.S. (2016) 'TGFbeta-Responsive HMOX1 Expression Is Associated with Stemness and Invasion in Glioblastoma Multiforme.' *Stem cells (Dayton, Ohio)* 34 (9), 2276–2289

Ghosh, M., Aguila, H.L., Michaud, J., Ai, Y., Wu, M., Hemmes, A., Ristimaki, A., Guo, C., Furneaux, Henry, and Hla, T. (2009) 'Essential Role of the RNA-Binding Protein HuR in Progenitor Cell Survival in Mice'. *J. Clin. Invest.* 119 (12), 3530–3543

Ghosh, Shubhendu and Jacobson, A. (2010) 'RNA Decay Modulates Gene Expression and Controls Its Fidelity'. *Wiley interdisciplinary reviews. RNA* 1 (3), 351–361.

Ghosh, Sriparna, Sullivan, C.A.W., Zerkowski, M.P., Molinaro, A.M., Rimm, D.L., Camp, R.L., and Chung, G.G. (2008) 'High Levels of Vascular Endothelial Growth Factor and Its Receptors (VEGFR-1, VEGFR-2, Neuropilin-1) Are Associated with Worse Outcome in Breast Cancer'. *Human Pathology* 39 (12), 1835–1843.

Giles, K.M., Daly, J.M., Beveridge, D.J., Thomson, A.M., Voon, D.C., Furneaux, Henry M., Jazayeri, J.A., and Leedman, P.J. (2003) 'The 3'-Untranslated Region of P21WAF1mRNA Is a Composite Cis-Acting Sequence Bound by RNA-Binding Proteins from Breast Cancer Cells, Including HuR and Poly(C)-Binding Protein'. *Journal of Biological Chemistry* 278 (5), 2937–2946

De Giorgio, R., Bovara, M., Barbara, G., Canossa, M., Sarnelli, G., De Ponti, F., Stanghellini, V., Tonini, M., Cappello, S., Pagnotta, E., Nobile-Orazio, E., and Corinaldesi, R. (2003) 'Anti-HuD-Induced Neuronal Apoptosis Underlying Paraneoplastic Gut Dysmotility'. *Gastroenterology* 125 (1), 70–79

Glazer, R.I., Vo, Dat T, and Penalva, Luiz O F (2012) 'Musashi1: An RBP with Versatile Functions in Normal and Cancer Stem Cells.' *Frontiers in bioscience (Landmark edition)* 17, 54–64

Glisovic, T., Bachorik, J.L., Yong, J., and Dreyfuss, G. (2008) 'RNA-Binding Proteins and Post-Transcriptional Gene Regulation.' *FEBS letters* 582 (14), 1977–86.

Glisson, B. and Byers, L. (2015) *Pathobiology and Staging of Small Cell Carcinoma of the Lung* available from <http://www.uptodate.com.ezproxy.is.ed.ac.uk/contents/pathobiology-and-

staging-of-small-cell-carcinoma-of-the-lung?source=search_result&search=small+cell+lung+cancer&selectedTitle=1~150>

Goldstraw, P., Ball, D., Jett, J.R., Le Chevalier, T., Lim, E., Nicholson, A.G., and Shepherd, F.A. (2011) 'Non-Small-Cell Lung Cancer'. *The Lancet* 378 (9804), 1727–1740.

Good, P.J. (1995) 'A Conserved Family of Elav-like Genes in Vertebrates.' *Proceedings of the National Academy of Sciences of the United States of America* 92 (10), 4557–4561

Goossens, S., Vandamme, N., Van Vlierberghe, P., and Berx, G. (2017) 'EMT Transcription Factors in Cancer Development Re-Evaluated: Beyond EMT and MET'. *Biochimica et Biophysica Acta (BBA) - Reviews on Cancer* 1868 (2), 584–591.

Graus, F., Dalmou, J., Reñé, R., Tora, M., Malats, N., Verschuuren, J.J., Cardenal, F., Viñolas, N., Garcia del Muro, J., Vadell, C., Mason, W P, Rosell, R, Posner, J B, and Real, F.X. (1997) 'Anti-Hu Antibodies in Patients with Small-Cell Lung Cancer: Association with Complete Response to Therapy and Improved Survival.' *Journal of clinical oncology : official journal of the American Society of Clinical Oncology* 15 (8), 2866–2872

Guo, X. and Hartley, R.S. (2006) 'HuR Contributes to Cyclin E1 Deregulation in MCF-7 Breast Cancer Cells'. *Cancer Research* 66 (16), 7948–7956

Ha, M. and Kim, V.N. (2014) 'Regulation of MicroRNA Biogenesis.' *Nature reviews. Molecular cell biology* 15 (8), 509–524.

Hai, L., Zhang, Chen, Li, T., Zhou, X., Liu, B., Li, S., Zhu, M., Lin, Y., Yu, S., Zhang, K., Ren, B., Ming, H., Huang, Yubao, Chen, Lei, Zhao, P., Zhou, H., Jiang, T., and Yang, Xuejun (2018) 'Notch1 Is a Prognostic Factor That Is Distinctly Activated in the Classical and Proneural Subtype of Glioblastoma and That Promotes Glioma Cell Survival via the NF-KB(P65) Pathway'. *Cell Death & Disease* 9 (2), 158.

Halees, A.S., El-badrawi, R., and Khabar, K. S A (2008) 'ARED Organism: Expansion of ARED Reveals AU-Rich Element Cluster Variations between Human and Mouse'. *Nucleic Acids Research*

Halees, A.S., Hitti, E., Al-Saif, M., Mahmoud, L., Vlasova-St Louis, I. a, Beisang, D.J., Bohjanen, P.R., and Khabar, K. (2011) 'Global Assessment of GU-Rich Regulatory Content and Function in the Human Transcriptome.' *RNA biology* 8 (4), 681–91.

Hammond, S.M. (2015) 'An Overview of MicroRNAs'. *Advanced drug delivery reviews* 87, 3–14.

Han, J., Knops, Judith F, Longshore, J.W., and King, Peter H (1996) 'Localization OfHuman Elav-like Neuronal Protein 1(Hel-N1) on Chromosome 9p21 by Chromosome Microdissection Polymerase Chain Reaction and Fluorescencein SituHybridization'. *Genomics* 36 (1), 189–191.

Han, N., Hu, G., Shi, L., Long, G., Yang, L., Xi, Q., Guo, Q., Wang, Jianhua, Dong, Z., and Zhang, M. (2017) 'Notch1 Ablation Radiosensitizes Glioblastoma Cells.' *Oncotarget* 8 (50), 88059–88068

Hanahan, D. and Weinberg, R.A. (2011) 'Hallmarks of Cancer: The next Generation'. in *Cell*. vol. 144 (5). 646–674

Hanif, F., Muzaffar, K., Perveen, K., Malhi, S.M., and Simjee, S.U. (2017) 'Glioblastoma Multiforme: A Review of Its Epidemiology and Pathogenesis through Clinical Presentation and Treatment'. *Asian Pacific journal of cancer prevention : APJCP* 18 (1), 3–9.

Hansford, L.M., McKee, Amy E., Zhang, L., George, R.E., Ted Gerstle, J., Thorner, P.S., Smith, K.M.,

Thomas Look, A., Yeger, H., Miller, F.D., Irwin, M.S., Thiele, C.J., and Kaplan, D.R. (2007) 'Neuroblastoma Cells Isolated from Bone Marrow Metastases Contain a Naturally Enriched Tumor-Initiating Cell'. *Cancer Research* 67 (23), 11234–11243

Harmsma, M., Schutte, B., and Ramaekers, F.C.S. (2013) 'Serum Markers in Small Cell Lung Cancer: Opportunities for Improvement.' *Biochimica et biophysica acta* 1836 (2), 255–72.

Hata, A.N., Engelman, J.A., and Faber, A.C. (2015) 'The BCL2 Family: Key Mediators of the Apoptotic Response to Targeted Anticancer Therapeutics'. *Cancer discovery* 5 (5), 475–487.

Hay, E.D. and Zuk, A. (1995) 'Transformations between Epithelium and Mesenchyme: Normal, Pathological, and Experimentally Induced'. *American Journal of Kidney Diseases*

Heinonen, M., Fagerholm, R., Aaltonen, K., Kilpivaara, O., Aittomäki, K., Blomqvist, C., Heikkilä, P., Haglund, C., Nevanlinna, H., and Ristimäki, A. (2007) 'Prognostic Role of HuR in Hereditary Breast Cancer.' *Clinical cancer research : an official journal of the American Association for Cancer Research* 13 (23), 6959–6963

Heinonen, M., Hemmes, A., Salmenkivi, K., Abdelmohsen, Kotb, Vilen, S.-T., Laakso, M., Leidenius, M., Salo, T., Hautaniemi, S., Gorospe, Myriam, Heikkila, P., Haglund, C., and Ristimaki, A. (2011) 'Role of RNA Binding Protein HuR in Ductal Carcinoma in Situ of the Breast.' *The Journal of pathology* 224 (4), 529–539

Hinman, M. N. and Lou, H. (2008) 'Diverse Molecular Functions of Hu Proteins'. in *Cellular and Molecular Life Sciences*. vol. 65 (20). 3168–3181

Hinman, Melissa N, Zhou, H.-L., Sharma, A., and Lou, Hua (2013) 'All Three RNA Recognition Motifs and the Hinge Region of HuC Play Distinct Roles in the Regulation of Alternative Splicing'. *Nucleic Acids Research* 41 (9), 5049–5061.

Ho, L.H., Taylor, R., Dorstyn, Loretta, Cakouros, D., Bouillet, Philippe, and Kumar, Sharad (2009) 'A Tumor Suppressor Function for Caspase-2.' *Proceedings of the National Academy of Sciences of the United States of America* 106 (13), 5336–5341

Hostetter, C., Licata, L.A., Witkiewicz, A., Costantino, C.L., Yeo, C.J., Brody, J.R., and Keen, J.C. (2008) 'Cytoplasmic Accumulation of the RNA Binding Protein HuR Is Central to Tamoxifen Resistance in Estrogen Receptor Positive Breast Cancer Cells'. *Cancer Biology and Therapy* 7 (9), 1496–1506

Hoy, A., Leininger-Muller, B., Jolivalt, C., and Siest, G. (2000) 'Effect of Apolipoprotein E on Cell Viability in a Human Neuroblastoma Cell Line: Influence of Oxidation and Lipid-Association.' *Neuroscience letters* 285 (3), 173–176

Huang, Yadong and Mahley, R.W. (2014) 'Apolipoprotein E: Structure and Function in Lipid Metabolism, Neurobiology, and Alzheimer's Diseases'. *Neurobiology of disease* 72 Pt A, 3–12.

Hughes, P., Bouillet, P, and Strasser, A. (2006) 'Role of Bim and Other Bcl-2 Family Members in Autoimmune and Degenerative Diseases'. in *Current Directions in Autoimmunity* vol. 9. 74–94.

Hutvágner, G., McLachlan, J., Pasquinelli, A.E., Bálint, E., Tuschl, T, and Zamore, P.D. (2001) 'A Cellular Function for the RNA-Interference Enzyme Dicer in the Maturation of the Let-7 Small Temporal RNA.' *Science (New York, N.Y.)* 293 (5531), 834–838.

Hyeon, H.K., Abdelmohsen, Kotb, Lal, A., Pullmann, R., Yang, Xiaoling, Galban, S., Srikantan, S., Martindale, Jennifer L., Blethrow, J., Shokat, K.M., and Gorospe, Myriam (2008) 'Nuclear HuR

Accumulation through Phosphorylation by Cdk1'. *Genes and Development* 22 (13), 1804–1815

Idikio, H.A. (2011) 'Human Cancer Classification: A Systems Biology-Based Model Integrating Morphology, Cancer Stem Cells, Proteomics, and Genomics'. in *Journal of Cancer*.

Ince-Dunn, G., Okano, Hirotaka J., Jensen, K.B., Park, W.Y., Zhong, R., Ule, J., Mele, A., Fak, J.J., Yang, C.W., Zhang, Chaolin, Yoo, J., Herre, M., Okano, H., Noebels, J.L., and Darnell, Robert B. (2012) 'Neuronal Elav-like (Hu) Proteins Regulate RNA Splicing and Abundance to Control Glutamate Levels and Neuronal Excitability'. *Neuron* 75 (6), 1067–1079

Inman, M. V., Levy, S., Mock, B.A., and Owens, G.C. (1998) 'Gene Organization and Chromosome Location of the Neural-Specific RNA Binding Protein Elavl4'. *Gene* 208 (2), 139–145

Iolascon, A., Giordani, L., Borriello, A., Carbone, R., Izzo, A., Tonini, G P, Gambini, C., and Della Ragione, F. (2000) 'Reduced Expression of Transforming Growth Factor-Beta Receptor Type III in High Stage Neuroblastomas'. *British journal of cancer* 82 (6), 1171–1176.

Ishimaru, D., Ramalingam, S., Sengupta, T.K., Bandyopadhyay, S., Dellis, S., Tholanikunnel, B.G., Fernandes, D.J., and Spicer, E.K. (2009) 'Regulation of Bcl-2 Expression by HuR in HL60 Leukemia Cells and A431 Carcinoma Cells.' *Molecular cancer research : MCR* 7 (8), 1354–1366

Iwanaga, N., Kamachi, M., Aratake, K., Izumi, Y., Ida, H., Tanaka, F., Tamai, M., Arima, K., Nakamura, Hideki, Origuchi, T., Kawakami, A., and Eguchi, K. (2005) 'Regulation of Alternative Splicing of Caspase-2 through an Intracellular Signaling Pathway in Response to pro-Apoptotic Stimuli'. *Journal of Laboratory and Clinical Medicine* 145 (2), 105–110.

Iyer, V. (2005) ' 3 1 Integrin Regulates MMP-9 MRNA Stability in Immortalized Keratinocytes: A Novel Mechanism of Integrin-Mediated MMP Gene Expression'. *Journal of Cell Science*

Izquierdo, J.M. (2008) 'Hu Antigen R (HuR) Functions as an Alternative Pre-MRNA Splicing Regulator of Fas Apoptosis-Promoting Receptor on Exon Definition.' *The Journal of biological chemistry* 283 (27), 19077–19084

Jain, R.G., Andrews, L.G., McGowan, K.M., Pekala, P.H., and Keene, J D (1997) 'Ectopic Expression of Hel-N1, an RNA-Binding Protein, Increases Glucose Transporter (GLUT1) Expression in 3T3-L1 Adipocytes.' *Molecular and cellular biology* 17, 954–962

Jeyaraj, S., Dakhlallah, D., Mill, S.R., and Lee, B.S. (2005) 'HuR Stabilizes Vacuolar H+-Translocating ATPase MRNA during Cellular Energy Depletion'. *Journal of Biological Chemistry* 280 (45), 37957–37964

Jimbo, M., Blanco, F.F., Huang, Yu-hung, Telonis, A.G., Screnci, B.A., Cosma, G.L., Alexeev, V., Gonye, G.E., Yeo, C.J., Sawicki, J.A., Winter, J.M., and Brody, J.R. (2015) *Targeting the MRNA-Binding Protein HuR Impairs Malignant Characteristics of Pancreatic Ductal Adenocarcinoma Cells*. 6 (29)

Johnson, D.G. and Walker, C.L. (1999) 'Cyclins and Cell Cycle Checkpoints.' *Annual review of pharmacology and toxicology* 39, 295–312

Johnson, D.R., Fogh, S.E., Giannini, C., Kaufmann, T.J., Raghunathan, A., Theodosopoulos, P. V., and Clarke, J.L. (2015) 'Case-Based Review: Newly Diagnosed Glioblastoma'. *Neuro-Oncology Practice*

Joseph, B., Orlian, M., and Furneaux, H (1998) 'P21(Waf1) MRNA Contains a Conserved Element in Its 3'-Untranslated Region That Is Bound by the Elav-like MRNA-Stabilizing Proteins.' *The Journal*

of biological chemistry 273 (32), 20511–20516

Kakuguchi, W., Kitamura, T., Kuroshima, T., Ishikawa, M., Kitagawa, Y., Totsuka, Y., Shindoh, M., and Higashino, F. (2010) 'HuR Knockdown Changes the Oncogenic Potential of Oral Cancer Cells'. *Molecular Cancer Research* 8 (4), 520–528.

Kanaji, N., Watanabe, N., Kita, N., Bandoh, S., Tadokoro, A., Ishii, T., Dobashi, H., and Matsunaga, T. (2014) 'Paraneoplastic Syndromes Associated with Lung Cancer.' *World journal of clinical oncology* 5 (3), 197–223

Kanasty, R., Dorkin, J.R., Vegas, A., and Anderson, D. (2013) 'Delivery Materials for SiRNA Therapeutics.' *Nature materials* 12 (11), 967–77.

Kang, M.J., Abdelmohsen, Kotb, Hutchison, E.R., Mitchell, S.J., Grammatikakis, I., Guo, R., Noh, J.H., Martindale, Jennifer L., Yang, Xiaoling, Lee, E.K., Faghihi, M.A., Wahlestedt, C., Troncoso, J.C., Pletnikova, O., Perrone-Bizzozero, N., Resnick, S.M., deCabo, R., Mattson, M.P., and Gorospe, Myriam (2014) 'HuD Regulates Coding and Noncoding RNA to Induce APP→Aβ Processing'. *Cell Reports* 7 (5)

Kasashima, K, Terashima, K., Yamamoto, K., Sakashita, E, and Sakamoto, H (1999) 'Cytoplasmic Localization Is Required for the Mammalian ELAV-like Protein HuD to Induce Neuronal Differentiation.' *Genes to cells : devoted to molecular & cellular mechanisms* 4 (11), 667–683

Kasashima, Katsumi, Sakashita, Eiji, Saito, K., and Sakamoto, Hiroshi (2002) *Complex Formation of the Neuron-Speci ® c ELAV-like Hu RNA-Binding Proteins*. 30 (20), 4519–4526

Katahira, J. (2015) 'Nuclear Export of Messenger RNA'. *Genes* 6 (2), 163–184.

Kawagishi, H., Hashimoto, M., Nakamura, Hideaki, Tsugawa, T., Watanabe, A., Kontoyiannis, D.L., and Sugimoto, M. (2013) 'HuR Maintains a Replicative Life Span by Repressing the ARF Tumor Suppressor.' *Molecular and cellular biology* 33 (10), 1886–900.

Kazarian, M., Calbo, J., Proost, N., Carpenter, C.L., Berns, A., and Laird-Offringa, I. a. (2009) 'Immune Response in Lung Cancer Mouse Model Mimics Human Anti-Hu Reactivity'. *Journal of Neuroimmunology* 217 (1–2), 38–45.

Kazarian, M. and Laird-Offringa, I. a (2011) 'Small-Cell Lung Cancer-Associated Autoantibodies: Potential Applications to Cancer Diagnosis, Early Detection, and Therapy.' *Molecular cancer* 10 (1), 33.

Keene, J D (1999) 'Why Is Hu Where? Shuttling of Early-Response-Gene Messenger RNA Subsets.' *Proceedings of the National Academy of Sciences of the United States of America* 96 (1), 5–7

Keene, Jack D (2007) 'RNA Regulons: Coordination of Post-Transcriptional Events.' *Nature reviews. Genetics* 8 (7), 533–43.

Khabar, Khalid S A (2017) 'Hallmarks of Cancer and AU-Rich Elements'. *Wiley Interdisciplinary Reviews: RNA* 8 (1)

Kim-Ha, J., Kim, J., and Kim, Y.J. (1999) 'Requirement of RBP9, a Drosophila Hu Homolog, for Regulation of Cystocyte Differentiation and Oocyte Determination during Oogenesis.' *Molecular and cellular biology* 19 (4), 2505–2514

Kim, E.K. and Choi, E.-J. (2010) 'Pathological Roles of MAPK Signaling Pathways in Human Diseases'. *Biochimica et Biophysica Acta (BBA) - Molecular Basis of Disease* 1802 (4), 396–405.

Kim, H.H. and Gorospe, Myriam (2008) 'Phosphorylated HuR Shuttles in Cycles.' *Cell cycle* Georgetown: Texas 7 (20), 3124–3126

King, A. and Broggio, J. (2018) *Cancer Registration Statistics , England : 2016*. 1–22. available from <https://www.ons.gov.uk/peoplepopulationandcommunity/healthandsocialcare/conditionsanddiseases/bulletins/cancerregistrationstatisticsengland/final2016>

King, P H (2000) 'RNA-Binding Analyses of HuC and HuD with the VEGF and c-Myc 3'-Untranslated Regions Using a Novel ELISA-Based Assay.' *Nucleic acids research* 28 (7), 20.

King, Peter H. (1997) 'Differential Expression of the Neuroendocrine Genes Hel-NI and HuD in Small-Cell Lung Carcinoma: Evidence for down-Regulation of HuD in the Variant Phenotype'. *International Journal of Cancer* 74 (4), 378–382

King, Peter H (1994) 'Hel-N2: A Novel Isoform of Hel-N1 Which Is Conserved in Rat Neural Tissue and Produced in Early Embryogenesis'. *Gene* 151 (1), 261–265.

Kirkin, V., Joos, S., and Zörnig, M. (2004) 'The Role of Bcl-2 Family Members in Tumorigenesis'. *Biochimica et Biophysica Acta (BBA) - Molecular Cell Research* 1644 (2), 229–249.

Kleihues, P and Ohgaki, H (1999) 'Primary and Secondary Glioblastomas: From Concept to Clinical Diagnosis'. *Neuro-oncology* 1 (1), 44–51.

Koljonen, V., Böhling, T., Haglund, C., and Ristimäki, A. (2008) 'Expression of HuR in Merkel Cell Carcinoma and in Normal Skin.' *Journal of cutaneous pathology* 35 (1), 10–4.

Kreso, A. and Dick, J.E. (2017) 'Evolution of the Cancer Stem Cell Model'. *Cell Stem Cell* 14 (3), 275–291.

Krohn, A., Ahrens, T., Yalcin, A., Plones, T., Wehrle, J., Taromi, S., Wollner, S., Follo, M., Brabletz, T., Mani, S.A., Claus, R., Hackanson, B., and Burger, M. (2014) 'Tumor Cell Heterogeneity in Small Cell Lung Cancer (SCLC): Phenotypical and Functional Differences Associated with Epithelial-Mesenchymal Transition (EMT) and DNA Methylation Changes.' *PloS one* 9 (6),

Kurosu, T., Ohga, N., Hida, Y., Maishi, N., Akiyama, K., Kakuguchi, W., Kuroshima, T., Kondo, M., Akino, T., Totsuka, Y., Shindoh, M., Higashino, F., and Hida, K. (2011) 'HuR Keeps an Angiogenic Switch on by Stabilising MRNA of VEGF and COX-2 in Tumour Endothelium'. *British Journal Of Cancer* 104, 819.

Kuyumcu-Martinez, N.M., Wang, G.-S., and Cooper, T.A. (2007) 'Increased Steady-State Levels of CUGBP1 in Myotonic Dystrophy 1 Are Due to PKC-Mediated Hyperphosphorylation'. *Molecular cell* 28 (1), 68–78.

Kwak, E.L., Bang, Y.-J., Camidge, D.R., Shaw, A.T., Solomon, B., Maki, R.G., Ou, S.-H.I., Dezube, B.J., Jänne, P.A., Costa, D.B., Varella-Garcia, M., Kim, W.-H., Lynch, T.J., Fidias, P., Stubbs, H., Engelman, J.A., Sequist, L. V., Tan, W., Gandhi, L., Mino-Kenudson, M., Wei, G.C., Shreeve, S.M., Ratain, M.J., Settleman, J., Christensen, J.G., Haber, D.A., Wilner, K., Salgia, R., Shapiro, G.I., Clark, J.W., and Iafrate, A.J. (2010) 'Anaplastic Lymphoma Kinase Inhibition in Non–Small-Cell Lung Cancer'. *New England Journal of Medicine*

Lal, A., Kawai, T., Yang, Xiaoling, Mazan-Mamczarz, K., and Gorospe, Myriam (2005) 'Antiapoptotic Function of RNA-Binding Protein HuR Effected through Prothymosin Alpha'. *The EMBO Journal* 24, 1852–1862.

Lampaki, S., Zarogoulidis, P., Lagoudi, K., Tsavlis, D., Kioumis, I., Papakala, E., Lazaridis, G., Huang, H.,

Hohenforst-Schmidt, W., Pavlidis, P., Darwiche, K., Barbetakis, N., Karapantzos, I., Karapantzou, C., Rapti, A., Karavasilis, V., and Zarogoulidis, K. (2016) 'Small Cell Lung Cancer: Current and Future Strategies'. *Oncomedicine* 1 (Ld), 4–13.

Lange, A., Mills, R.E., Lange, C.J., Stewart, M., Devine, S.E., and Corbett, A.H. (2007) 'Classical Nuclear Localization Signals: Definition, Function, and Interaction with Importin Alpha.' *The Journal of biological chemistry* 282 (8), 5101–5105

Lazarova, D.L., Spengler, B. a, Biedler, J.L., and Ross, R. a (1999) 'HuD, a Neuronal-Specific RNA-Binding Protein, Is a Putative Regulator of N-Myc Pre-MRNA Processing/Stability in Malignant Human Neuroblasts.' *Oncogene* 18, 2703–2710

Leandersson, K., Riesbeck, K., and Andersson, T. (2006) 'Wnt-5a MRNA Translation Is Suppressed by the Elav-like Protein HuR in Human Breast Epithelial Cells'. *Nucleic Acids Research* 34 (14), 3988–3999

Lee, E.K., Kim, W., Tominaga, Kumiko, Martindale, Jennifer L, Yang, Xiaoling, Subaran, S.S., Carlson, O.D., Mercken, E.M., Kulkarni, R.N., Akamatsu, W., Okano, H., Perrone-bizzozero, N.I., Cabo, R. De, Egan, J.M., and Gorospe, Myriam (2012) 'Hud, Rna-Binding Protein Controls Insulin Translation'. *Molecular Cell* 45 (6), 1–10.

Lee, J.E. and Cooper, T.A. (2009) 'Pathogenic Mechanisms of Myotonic Dystrophy'. *Biochemical Society transactions* 37 (Pt 6), 1281–1286.

Letai, A.G. (2008) 'Diagnosing and Exploiting Cancer's Addiction to Blocks in Apoptosis.' *Nature reviews. Cancer* 8 (2), 121–132.

Levine, T.D., Gao, F., King, P H, Andrews, L.G., and Keene, J D (1993) 'Hel-N1: An Autoimmune RNA-Binding Protein with Specificity for 3' Uridylate-Rich Untranslated Regions of Growth Factor MRNAs.' *Molecular and cellular biology* 13 (6), 3494–504.

Levy, N.S., Chung, S, Furneaux, H, and Levy, A.P. (1998) 'Hypoxic Stabilization of Vascular Endothelial Growth Factor MRNA by the RNA-Binding Protein HuR.' *The Journal of biological chemistry* 273 (11), 6417–6423

Liang, P.-I., Li, W.-M., Wang, Y.-H., Wu, T.-F., Wu, W.-R., Liao, A.C., Shen, K.-H., Wei, Y.-C., Hsing, C.-H., Shiue, Y.-L., Huang, H.-Y., Hsu, H.-P., Chen, L.-T., Lin, C.-Y., Tai, C., Lin, C.-M., and Li, C.-F. (2012) 'HuR Cytoplasmic Expression Is Associated with Increased Cyclin A Expression and Poor Outcome with Upper Urinary Tract Urothelial Carcinoma.' *BMC cancer* 12 (1), 611.

Little, C.D., Nau, M.M., Carney, D.N., Gazdar, A.F., and Minna, J D (1983) 'Amplification and Expression of the C-Myc Oncogene in Human Lung Cancer Cell Lines.' *Nature* 306 (5939), 194–196

Liu, J., Dalmau, J, Szabo, A., Rosenfeld, M., Huber, J., and Furneaux, H (1995) 'Paraneoplastic Encephalomyelitis Antigens Bind to the AU-Rich Elements of MRNA'. *Neurology* 45 (3), 544 – 550.

Loffreda, A., Rigamonti, A., Barabino, S.M.L., and Lenzken, S.C. (2015) 'RNA-Binding Proteins in the Regulation of MiRNA Activity: A Focus on Neuronal Functions'. *Biomolecules* 5 (4), 2363–2387

López de Silanes, I., Fan, J., Yang, Xiaoling, Zonderman, A.B., Potapova, O., Pizer, E.S., and Gorospe, Myriam (2003) 'Role of the RNA-Binding Protein HuR in Colon Carcinogenesis.' *Oncogene* 22 (46), 7146–7154

López de Silanes, I., Lal, A., and Gorospe, Myriam (2005) 'HuR: Post-Transcriptional Paths to Malignancy.' *RNA biology* 2 (1), 11–13

López de Silanes, I., Zhan, M., Lal, A., Yang, Xiaoling, and Gorospe, Myriam (2004) 'Identification of a Target RNA Motif for RNA-Binding Protein HuR.' *Proceedings of the National Academy of Sciences of the United States of America* 101 (9), 2987–2992

Lopez, J. and Tait, S.W.G. (2015) 'Mitochondrial Apoptosis: Killing Cancer Using the Enemy Within'. *British journal of cancer* 112 (6), 957–962.

Louis, C.U. and Shohet, J.M. (2015) 'Neuroblastoma: Molecular Pathogenesis and Therapy'. *Annual Review of Medicine* 66 (1), 49–63.

Lovén, J., Zinin, N., Wahlström, T., Müller, I., Brodin, P., Fredlund, E., Ribacke, U., Pivarcsi, A., Påhlman, S., and Henriksson, M. (2010) *MYCN-Regulated MicroRNAs Repress Estrogen Receptor- (ESR1) Expression and Neuronal Differentiation in Human Neuroblastoma*. vol. 107

Lovly, C.M. and Carbone, D.P. (2011) 'Lung Cancer in 2010: One Size Does Not Fit All'. *Nat Rev Clin Oncol* 8 (2), 68–70.

Lukong, Kiven E, Chang, K., Khandjian, E.W., and Richard, Stéphane (2008) 'RNA-Binding Proteins in Human Genetic Disease.' *Trends in genetics : TIG* 24 (8), 416–425

Lunde, B.M., Moore, C., and Varani, G. (2007) 'RNA-Binding Proteins: Modular Design for Efficient Function.' *Nature reviews. Molecular cell biology* 8 (6), 479–90.

Ma, W J, Cheng, S, Campbell, C., Wright, A., and Furneaux, H (1996) 'Cloning and Characterization of HuR, a Ubiquitously Expressed Elav-like Protein.' *The Journal of biological chemistry* 271 (14), 8144–8151

Ma, Wei J. and Furneaux, Henry (1997) 'Localization of the Human HuR Gene to Chromosome 19p13.2'. *Human Genetics* 99 (1), 32–33

Mahner, S., Baasch, C., Schwarz, J., Hein, S., Wölber, L., Jänicke, F., and Milde-Langosch, K. (2008) 'C-Fos Expression Is a Molecular Predictor of Progression and Survival in Epithelial Ovarian Carcinoma'. *British journal of cancer* 99 (8), 1269–1275.

Mamula, M.J., Gee, R.J., Elliott, J.I., Sette, A., Southwood, S., Jones, P.J., and Blier, P.R. (1999) 'Isoaspartyl Post-Translational Modification Triggers Autoimmune Responses to Self-Proteins.' *The Journal of biological chemistry* 274 (32), 22321–22327

Maniatis, T. and Reed, R. (2002) 'An Extensive Network of Coupling among Gene Expression Machines.' *Nature* 416 (6880), 499–506

Manley, G.T., Smitt, P.S., Dalmau, Josep, and Posner, Jerome B. (1995) 'Hu Antigens: Reactivity with Hu Antibodies, Tumor Expression, and Major Immunogenic Sites'. *Annals of Neurology* 38 (1), 102–110

Mansfield, K.D. and Keene, Jack D. (2012) 'Neuron-Specific ELAV/Hu Proteins Suppress HuR MRNA during Neuronal Differentiation by Alternative Polyadenylation'. *Nucleic Acids Research* 40 (6), 2734–2746

Maris, C., Dominguez, C., and Allain, F.H.-T. (2005) 'The RNA Recognition Motif, a Plastic RNA-Binding Platform to Regulate Post-Transcriptional Gene Expression.' *The FEBS journal* 272 (9), 2118–2131

Maris, J.M., Hogarty, M.D., Bagatell, R., and Cohn, S.L. (2007) 'Neuroblastoma'. in *Lancet*. vol. 369 (9579). 2106–2120

Martin, K.C. and Ephrussi, A. (2009) 'MRNA Localization: Gene Expression in the Spatial Dimension'. *Cell* 136 (4), 719–730.

Marusich, M.F., Furneaux, H M, Henion, P.D., and Weston, J. a (1994) 'Hu Neuronal Proteins Are Expressed in Proliferating Neurogenic Cells.' *Journal of neurobiology* 25 (2), 143–155

Matsumoto, T., Ryuge, S., Kobayashi, M., Kageyama, T., Hattori, M., Goshima, N., Jiang, S.X., Saegusa, M., Iyoda, A., Satoh, Y., Masuda, N., and Sato, Y. (2012) 'Anti-HuC and -HuD Autoantibodies Are Differential Sero-Diagnostic Markers for Small Cell Carcinoma from Large Cell Neuroendocrine Carcinoma of the Lung'. *International Journal of Oncology* 40, 1957–1962

McKee, Adrienne E, Minet, E., Stern, C., Riahi, S., Stiles, C.D., and Silver, P.A. (2005) 'A Genome-Wide in Situ Hybridization Map of RNA-Binding Proteins Reveals Anatomically Restricted Expression in the Developing Mouse Brain.' *BMC developmental biology* 5, 14

Merlo, A., Gabrielson, E., Mabry, M., Vollmer, R., Baylin, S.B., and Sidransky, D. (1994) 'Homozygous Deletion on Chromosome 9p and Loss of Heterozygosity on 9q, 6p, and 6q in Primary Human Small Cell Lung Cancer.' *Cancer research* 54 (9), 2322–2326

Milne, A.N. a, Carvalho, R., Morsink, F.M., Musler, A.R., de Leng, W.W.J., Ristimäki, A., and Offerhaus, G.J. a (2006) 'Early-Onset Gastric Cancers Have a Different Molecular Expression Profile than Conventional Gastric Cancers.' *Modern pathology : an official journal of the United States and Canadian Academy of Pathology, Inc* 19, 564–572

Miyata, Y., Watanabe, S., Sagara, Y., Mitsunari, K., Matsuo, T., Ohba, K., and Sakai, H. (2013) 'High Expression of HuR in Cytoplasm, but Not Nuclei, Is Associated with Malignant Aggressiveness and Prognosis in Bladder Cancer.' *PloS one* 8 (3)

Mobarak, C.D., Anderson, K.D., Morin, M., Beckel-Mitchener, A., Rogers, S.L., Furneaux, Henry, King, P., and Perrone-Bizzozero, N.I. (2000) 'The RNA-Binding Protein HuD Is Required for GAP-43 MRNA Stability, GAP-43 Gene Expression, and PKC-Dependent Neurite Outgrowth in PC12 Cells'. *Molecular Biology of the Cell* 11 (9), 3191–3203.

Monclair, T., Brodeur, G.M., Ambros, P.F., Brisse, H.J., Cecchetto, G., Holmes, K., Kaneko, M., London, W.B., Matthay, K.K., Nuchtern, J.G., Von Schweinitz, D., Simon, T., Cohn, S.L., and Pearson, A.D.J. (2009) 'The International Neuroblastoma Risk Group (INRG) Staging System: An INRG Task Force Report'. *Journal of Clinical Oncology* 27 (2), 298–303

Mossé, Y.P., Laudenslager, M., Longo, L., Cole, K.A., Wood, A., Attiyeh, E.F., Laquaglia, M.J., Sennett, R., Lynch, J.E., Perri, P., Laureys, G., Speleman, F., Kim, C., Hou, C., Hakonarson, H., Torkamani, A., Schork, N.J., Brodeur, G.M., Tonini, Gian P, Rappaport, E., Devoto, M., and Maris, J.M. (2008) 'Identification of ALK as a Major Familial Neuroblastoma Predisposition Gene'. *Nature* 455, 930.

Muresu, R., Baldini, A., Gress, T., Posner, J B, Furneaux, H M, and Siniscalco, M. (1994) 'Mapping of the Gene Coding for a Paraneoplastic Encephalomyelitis Antigen (HuD) to Human Chromosome Site 1p34'. *Cytogenet Cell Genet* 65 (3), 177–178

Nabors, L.B., Gillespie, G.Y., Harkins, L., and King, Peter H (2001) 'HuR, a RNA Stability Factor, Is Expressed in Malignant Brain Tumors and Binds to Adenine- and Uridine-Rich Elements within the 3' Untranslated Regions of Cytokine and Angiogenic Factor MRNAs.' *Cancer research* 61 (5), 2154–2161

Nabors, L.B., Suswam, E., Huang, Yuanyuan, Yang, Xiuhua, Johnson, M.J., and King, Peter H (2003) 'Tumor Necrosis Factor Alpha Induces Angiogenic Factor Up-Regulation in Malignant Glioma Cells: A Role for RNA Stabilization and HuR.' *Cancer research* 63, 4181–4187

NCBI (2017) *Primer-BLAST A Tool for Finding Specific Primers* available from <https://www.ncbi.nlm.nih.gov/tools/primer-blast/>

Newton, A.C. (1995) 'Protein Kinase C: Structure, Function, and Regulation'. in *Journal of Biological Chemistry*. 270, 28495-28498.

Niesporek, S., Kristiansen, G., Thoma, A., Weichert, W., Noske, A., Buckendahl, A.C., Jung, K., Stephan, C., Dietel, M., and Denkert, C. (2008) 'Expression of the ELAV-like Protein HuR in Human Prostate Carcinoma Is an Indicator of Disease Relapse and Linked to COX-2 Expression'. *International Journal of Oncology* 32, 341–347

NLM (2018) *U.S National Libary of Medicine* available from <https://www.nlm.nih.gov/> [3 September 2019]

Nunez, G. and Clarke, M.F. (1994) 'The Bcl-2 Family of Proteins: Regulators of Cell Death and Survival.' *Trends in cell biology* 4 (11), 399–403

Oft, M. (2014) 'IL-10: Master Switch from Tumor-Promoting Inflammation to Antitumor Immunity'. *Cancer Immunology Research* 2 (3), 194 LP – 199.

Ogawa, Y., Kakumoto, K., Yoshida, T., Kuwako, K., Miyazaki, T., Yamaguchi, J., Konno, A., Hata, J., Uchiyama, Y., Hirai, H., Watanabe, M., Darnell, Robert B, Okano, H., and Okano, Hirotaka James (2018) 'Elavl3 Is Essential for the Maintenance of Purkinje Neuron Axons'. *Scientific Reports* 8 (1), 2722.

Ohgaki, Hiroko and Kleihues, Paul (2007) 'Genetic Pathways to Primary and Secondary Glioblastoma'. *The American journal of pathology* 170 (5), 1445–1453.

Okamoto, H., Watanabe, K., Kunikane, H., Yokoyama, A., Kudoh, S., Asakawa, T., Shibata, T., Kunitoh, H., Tamura, T., and Saijo, N. (2007) 'Randomised Phase III Trial of Carboplatin plus Etoposide vs Split Doses of Cisplatin plus Etoposide in Elderly or Poor-Risk Patients with Extensive Disease Small-Cell Lung Cancer: JCOG 9702.' *British journal of cancer* 97 (2), 162–169

Okano, H J and Darnell, R B (1997) 'A Hierarchy of Hu RNA Binding Proteins in Developing and Adult Neurons.' *The Journal of neuroscience : the official journal of the Society for Neuroscience* 17 (9), 3024–3037

Onganer, P.U., Seckl, M.J., and Djamgoz, M.B.A. (2005) 'Neuronal Characteristics of Small-Cell Lung Cancer.' *British journal of cancer* 93 (11), 1197–1201

Orphanides, G. and Reinberg, D. (2002) 'A Unified Theory of Gene Expression.' *Cell* 108 (4), 439–451

Pagliarini, V., Naro, C., and Sette, Claudio (2015) 'Splicing Regulation: A Molecular Device to Enhance Cancer Cell Adaptation'. *BioMed Research International*

Pavlova, N.N. and Thompson, C.B. (2016) 'The Emerging Hallmarks of Cancer Metabolism'. in *Cell Metabolism*.

Peirce, S.K. and Findley, H.W. (2015) *High Level MycN Expression in Non- MYCN Amplified Neuroblastoma Is Induced by the Combination Treatment Nutlin-3 and Doxorubicin and Enhances Chemosensitivity*. 1443–1449

Pereira, B., Billaud, M., and Almeida, R. (2017) 'RNA-Binding Proteins in Cancer: Old Players and New Actors'. in *Trends in Cancer*. vol. 3 (7) 506-528

Perrone-Bizzozero, N. and Bird, C.W. (2013) 'Role of HuD in Nervous System Function and Pathology.' *Frontiers in bioscience (Scholar edition)* 5, 554–563

Pham, T.N.D., Perez White, B.E., Zhao, H., Mortazavi, F., and Tonetti, D.A. (2017) 'Protein Kinase C α Enhances Migration of Breast Cancer Cells through FOXC2-Mediated Repression of P120-Catenin'. *BMC Cancer* 17 (1), 832.

Phillips, H.S., Kharbanda, S., Chen, Ruihuan, Forrest, W.F., Soriano, R.H., Wu, T.D., Misra, A., Nigro, J.M., Colman, H., Soroceanu, L., Williams, P.M., Modrusan, Z., Feuerstein, B.G., and Aldape, K. (2006) 'Molecular Subclasses of High-Grade Glioma Predict Prognosis, Delineate a Pattern of Disease Progression, and Resemble Stages in Neurogenesis'. *Cancer Cell*

Plateroti, M., De Araujo, P.R., Da Silva, A.E., and Penalva, Luiz O F (2012) 'The RNA-Binding Protein Musashi1: A Major Player in Intestinal Epithelium Renewal and Colon Cancer Development'. *Current Colorectal Cancer Reports* 8 (4), 290–297

Polyak, K. (1996) 'Negative Regulation of Cell Growth by TGFβ'. in *Biochimica et Biophysica Acta - Reviews on Cancer*. 1242(3):185-99.

Posner, J B and Dalmau, J (1997) 'Paraneoplastic Syndromes.' *Current opinion in immunology* 9 (5), 723–729

Prasanna, K., Johnson, R., Erin, L., Gangjian, Q., W., L.D., and Raj, K. (2009) 'IL-10 Inhibits Inflammation and Attenuates Left Ventricular Remodeling After Myocardial Infarction via Activation of STAT3 and Suppression of HuR'. *Circulation Research* 104 (2),

Pratt, A.J. and MacRae, I.J. (2009) 'The RNA-Induced Silencing Complex: A Versatile Gene-Silencing Machine'. *The Journal of biological chemistry* 284 (27), 17897–17901.

Prislei, S., Martinelli, E., Mariani, M., Raspaglio, G., Sieber, S., Ferrandina, G., Shahabi, S., Scambia, G., and Ferlini, C. (2013) 'MiR-200c and HuR in Ovarian Cancer.' *BMC cancer* 13 (1), 72.

Prochazka, P., Hrabeta, J., Vicha, A., Cipro, S., Stejskalova, E., Musil, Z., Vodicka, P., and Eckschlager, T. (2013) 'Changes in MYCN Expression in Human Neuroblastoma Cell Lines Following Cisplatin Treatment May Not Be Related to MYCN Copy Numbers.' *Oncology reports* 29 (6), 2415–2421

Puccini, J., Dorstyn, L, and Kumar, S (2013) 'Caspase-2 as a Tumour Suppressor'. *Cell death and differentiation* 20 (9), 1133–1139.

Pulido, M.A., DerHartunian, M.K., Qin, Z., Chung, E.M., Kang, D.S., Woodham, A.W., Tsou, J.A., Klooster, R., Akbari, O., Wang, L., Kast, W.M., Liu, S. V., Verschuuren, J.J.G.M., Aswad, D.W., and Laird-Offringa, I.A. (2016) 'Isoaspartylation Appears to Trigger Small Cell Lung Cancer-Associated Autoimmunity against Neuronal Protein ELAVL4'. *Journal of Neuroimmunology* 299, 70–78.

Pullmann, R., Kim, H.H., Abdelmohsen, Kotb, Lal, A., Martindale, Jennifer L, Yang, Xiaoling, and Gorospe, Myriam (2007) 'Analysis of Turnover and Translation Regulatory RNA-Binding Protein Expression through Binding to Cognate MRNAs '. *Molecular and Cellular Biology* 27 (18), 6265–6278.

Ramanathan, A., Robb, G.B., and Chan, S.-H. (2016) 'MRNA Capping: Biological Functions and Applications'. *Nucleic acids research* 44 (16), 7511–7526.

Ray, P.D. and Fry, R.C. (2015) *Chapter 2 - The Cell: The Fundamental Unit in Systems Biology*. ed. by Fry, R.C.B.T.-S.B. in T. and E.H. Boston: Academic Press, 11–42.

Re, A., Waldron, L., and Quattrone, Alessandro (2016) 'Control of Gene Expression by RNA Binding Protein Action on Alternative Translation Initiation Sites'. *PLOS Computational Biology* 12 (12),

Reck, M., Heigener, D.F., Mok, T., Soria, J.-C., and Rabe, K.F. (2013) 'Management of Non-Small-Cell Lung Cancer: Recent Developments'. *The Lancet* 382 (9893), 709–719.

Reed, J.C. (2000) 'Mechanisms of Apoptosis.' in *The American Journal of Pathology*. vol. 157 (5). United States, 1415–1430

Reeve, J.G., Rabbitts, P.H., and Twentyman, P.R. (1989) 'Amplification and Expression of Mdr1 Gene in a Multidrug Resistant Variant of Small Cell Lung Cancer Cell Line NCI-H69.' *British journal of cancer* 60 (3), 339–342

Rekhtman, N. (2010) 'Neuroendocrine Tumors of the Lung An Update'. *Arch Pathol Lab Med* 134, 1628–1638

Richard, S, Vogel, G., Huot, M.-E., Guo, T., Muller, W.J., and Lukong, K E (2008) 'Sam68 Haploinsufficiency Delays Onset of Mammary Tumorigenesis and Metastasis.' *Oncogene* 27 (4), 548–556

Robinow, S. (1988) 'The Locus Elav Of> Drosophila Melanogaster Is Expressed in Neurons at All Developmental Stages'. *Developmental biology* 126(2):294-303

Roméria da Silva, M., Moreira, G.A., Goncalves da Silva, R.A., Barbosa, É.D.A.A., Siqueira, R.P., Teixera, R.R., Almeida, M.R., Júnior, A.S., Fietto, J.L.R., and Bressan, G.C. (2015) *Splicing Regulators and Their Roles in Cancer Biology and Therapy*. 2015, 12

Roodhouse Gloyne, S. (1936) 'A Case of Oat Cell Carcinoma of the Lung Occurring in Asbestosis'. *Tubercle* 18 (3), 100–101.

Rosell, Rafael, Carcereny, E., Gervais, R., Vergnenegre, A., Massuti, B., Felip, E., Palmero, R., Garcia-Gomez, R., Pallares, C., Sanchez, J.M., Porta, R., Cobo, M., Garrido, P., Longo, F., Moran, T., Insa, A., De Marinis, F., Corre, R., Bover, I., Illiano, A., Dansin, E., de Castro, J., Milella, M., Reguart, N., Altavilla, G., Jimenez, U., Provencio, M., Moreno, M.A., Terrasa, J., Muñoz-Langa, J., Valdivia, J., Isla, D., Domine, M., Molinier, O., Mazieres, J., Baize, N., Garcia-Campelo, R., Robinet, G., Rodriguez-Abreu, D., Lopez-Vivanco, G., Gebbia, V., Ferrera-Delgado, L., Bombaron, P., Bernabe, R., Bearz, A., Artal, A., Cortesi, E., Rolfo, C., Sanchez-Ronco, M., Drozdowskyj, A., Queralt, C., de Aguirre, I., Ramirez, J.L., Sanchez, J.J., Molina, M.A., Taron, M., and Paz-Ares, L. (2012) 'Erlotinib versus Standard Chemotherapy as First-Line Treatment for European Patients with Advanced EGFR Mutation-Positive Non-Small-Cell Lung Cancer (EURTAC): A Multicentre, Open-Label, Randomised Phase 3 Trial'. *The Lancet Oncology* 13 (3), 239–246.

Ross, J. (1995) 'MRNA Stability in Mammalian Cells.' in *Microbiological Reviews*. vol. 59 (3). 423–450

Saito, K., Fujiwara, T., Katahira, J., Inoue, K., and Sakamoto, Hiroshi (2004) 'TAP/NXF1, the Primary MRNA Export Receptor, Specifically Interacts with a Neuronal RNA-Binding Protein HuD'. *Biochemical and Biophysical Research Communications* 321 (2), 291–297

Salvati, M., Frati, A., Russo, N., Caroli, E., Polli, F.M., Minniti, G., and Delfini, R. (2003) 'Radiation-Induced Gliomas: Report of 10 Cases and Review of the Literature.' *Surgical neurology* 60 (1), 60–7; discussion 67

Samson, M.-L. (2008) 'Rapid Functional Diversification in the Structurally Conserved ELAV Family of Neuronal RNA Binding Proteins'. *BMC Genomics* 9, 392.

Samson, M.-L. and Chalvet, F. (2003) 'Found in Neurons, a Third Member of the Drosophila Elav Gene Family, Encodes a Neuronal Protein and Interacts with Elav.' *Mechanisms of development* 120 (3), 373–383

Schaeffer, H.J. and Weber, M.J. (1999) 'Mitogen-Activated Protein Kinases: Specific Messages from Ubiquitous Messengers.' *Molecular and cellular biology* 19 (4), 2435–2444

Scheiba, R.M., de Opakua, A.I., Díaz-Quintana, A., Cruz-Gallardo, I., Martínez-Cruz, L.A., Martínez-Chantar, M.L., Blanco, F.J., and Díaz-Moreno, I. (2014) 'The C-Terminal RNA Binding Motif of HuR Is a Multi-Functional Domain Leading to HuR Oligomerization and Binding to U-Rich RNA Targets.' *RNA biology* 11 (10)

Scherr, A.-L., Gdynia, G., Salou, M., Radhakrishnan, P., Duglova, K., Heller, A., Keim, S., Kautz, N., Jassowicz, A., Elssner, C., He, Y.-W., Jaeger, D., Heikenwalder, M., Schneider, M., Weber, A., Roth, W., Schulze-Bergkamen, H., and Koehler, B.C. (2016) 'Bcl-XL Is an Oncogenic Driver in Colorectal Cancer.' *Cell death & disease* 7 (8), e2342

Schiavone, N., Rosini, P., Quattrone, A, Donnini, M., Lapucci, A., Citti, L., Bevilacqua, A., Nicolin, A., and Capaccioli, S. (2000) 'A Conserved AU-Rich Element in the 3' Untranslated Region of Bcl-2 MRNA Is Endowed with a Destabilizing Function That Is Involved in Bcl-2 down-Regulation during Apoptosis.' *FASEB journal : official publication of the Federation of American Societies for Experimental Biology* 14 (1), 174–184

Schwartzbaum, J. a, Fisher, J.L., Aldape, K.D., and Wrensch, M. (2006) 'Epidemiology and Molecular Pathology of Glioma.' *Nature clinical practice. Neurology* 2 (9), 494–503; quiz 1 p following 516.

Schwerk, C. and Schulze-Osthoff, K. (2005) 'Regulation of Apoptosis by Alternative Pre-MRNA Splicing'. in *Molecular Cell*. vol. 19 (1). 1–13

Sekido, Y.S., Bader, S.A., Carbone, D.P., Johnson, B.E., and Minna, John D (1994) *Molecular Analysis of the HuD Gene Encoding a Paraneoplastic Encephalomyelitis Antigen in Human Lung Cancer Cell Lines1*. 4988–4992

Shan, L., Liu, Yuanyi, and Wang, P. (2013) 'Recombinant Immunotoxin Therapy of Solid Tumors: Challenges and Strategies'. *Journal of basic and clinical medicine* 2 (2), 1–6.

Sigma-Aldrich (2017a) *Cor-L88* available from <http://www.sigmaaldrich.com/catalog/product/sigma/92031917?lang=en&region=GB>

Sigma-Aldrich (2017b) *NCI-H322 Cell Line Human* available from <http://www.sigmaaldrich.com/catalog/product/sigma/95111734?lang=en&region=GB>

Soller, M. and White, Kalpana (2004) 'ELAV.' *Current biology : CB* 14 (2), R53

Stamm, S., Ben-Ari, S., Rafalska, I., Tang, Y., Zhang, Zhaiyi, Toiber, D., Thanaraj, T.A., and Soreq, H. (2005) 'Function of Alternative Splicing.' *Gene* 344, 1–20

Stockhausen, M.-T., Kristoffersen, K., and Poulsen, H.S. (2010) 'The Functional Role of Notch Signaling in Human Gliomas'. *Neuro-oncology* 12 (2), 199–211.

Stoppoloni, D., Cardillo, I., Verdina, A., Vincenzi, B., Menegozzo, S., Santini, M., Sacchi, A., Baldi, A.,

and Galati, R. (2008) 'Expression of the Embryonic Lethal Abnormal Vision-like Protein HuR in Human Mesothelioma: Association with Cyclooxygenase-2 and Prognosis'. *Cancer* 113 (October), 2761–2769

Stupp, R., Hegi, M.E., Mason, Warren P., van den Bent, M.J., Taphoorn, M.J., Janzer, R.C., Ludwin, S.K., Allgeier, A., Fisher, B., Belanger, K., Hau, P., Brandes, A.A., Gijtenbeek, J., Marosi, C., Vecht, C.J., Mokhtari, K., Wesseling, P., Villa, S., Eisenhauer, E., Gorlia, T., Weller, M., Lacombe, D., Cairncross, J.G., and Mirimanoff, R.O. (2009) 'Effects of Radiotherapy with Concomitant and Adjuvant Temozolomide versus Radiotherapy Alone on Survival in Glioblastoma in a Randomised Phase III Study: 5-Year Analysis of the EORTC-NCIC Trial'. *The Lancet Oncology*

Sulman, E.P., Guerrero, M., and Aldape, K. (2009) 'Transcription Profiling of Brain Tumors: Tumor Biology and Treatment Stratification'. in *CNS Cancer: Models, Markers, Prognostic Factors, Targets, and Therapeutic Approaches* ed. by Meir, E.G. Totowa, NJ: Humana Press, 529–551.

Sundstrom, S., Bremnes, R.M., Kaasa, S., Aasebo, U., Hatlevoll, R., Dahle, R., Boye, N., Wang, M., Vigander, T., Vilsvik, J., Skovlund, E., Hannisdal, E., and Aamdal, S. (2002) 'Cisplatin and Etoposide Regimen Is Superior to Cyclophosphamide, Epirubicin, and Vincristine Regimen in Small-Cell Lung Cancer: Results from a Randomized Phase III Trial with 5 Years' Follow-Up.' *Journal of clinical oncology : official journal of the American Society of Clinical Oncology* 20 (24), 4665–4672

Szabo, a, Dalmau, J, Manley, G., Rosenfeld, M., Wong, E., Henson, J., Posner, J B, and Furneaux, H M (1991) 'HuD, a Paraneoplastic Encephalomyelitis Antigen, Contains RNA-Binding Domains and Is Homologous to Elav and Sex-Lethal.' *Cell* 67 (2), 325–333

Tarter, M. (2013) *The Neuronal RNA Binding Protein HuB as a Potential Tumor Suppressor in Glioblastoma*. PhD thesis. Italy:University of Trento

Thakkar, J.P., Dolecek, T.A., Horbinski, C., Ostrom, Q.T., Lightner, D.D., Barnholtz-Sloan, J.S., and Villano, J.L. (2014) 'Epidemiologic and Molecular Prognostic Review of Glioblastoma'. in *Cancer Epidemiology Biomarkers and Prevention*.

Theresa Phillips (2008) 'Regulation of Transcription and Gene Expression in Eukaryotes'. *Nature Education* 1(1):199 .

Thiery, J.P., Acloque, H., Huang, R.Y.J., and Nieto, M.A. (2009) 'Epithelial-Mesenchymal Transitions in Development and Disease'. *Cell* 139 (5), 871–890.

Thorgeirsson, T.E., Geller, F., Sulem, P., Rafnar, T., Wiste, A., Magnusson, K.P., Manolescu, A., Thorleifsson, G., Stefansson, H., Ingason, A., Stacey, S.N., Bergthorsson, J.T., Thorlacius, S., Gudmundsson, J., Jonsson, T., Jakobsdottir, M., Saemundsdottir, J., Olafsdottir, O., Gudmundsson, L.J., Bjornsdottir, G., Kristjansson, K., Skuladottir, H., Isaksson, H.J., Gudbjartsson, T., Jones, G.T., Mueller, T., Gottsater, A., Flex, A., Aben, K.K.H., de Vegt, F., Mulders, P.F.A., Isla, D., Vidal, M.J., Asin, L., Saez, B., Murillo, L., Blondal, T., Kolbeinsson, H., Stefansson, J.G., Hansdottir, I., Runarsdottir, V., Pola, R., Lindblad, B., van Rij, A.M., Dieplinger, B., Haltmayer, M., Mayordomo, J.I., Kiemeney, L.A., Matthiasson, S.E., Oskarsson, H., Tyrfingsson, T., Gudbjartsson, D.F., Gulcher, J.R., Jonsson, S., Thorsteinsdottir, U., Kong, A., and Stefansson, K. (2008) 'A Variant Associated with Nicotine Dependence, Lung Cancer and Peripheral Arterial Disease.' *Nature* 452 (7187), 638–642

Van Tine, B.A., Knops, J F, Butler, A., Deloukas, P., Shaw, G.M., and King, P H (1998) 'Localization of HuC (ELAVL3) to Chromosome 19p13.2 by Fluorescence in Situ Hybridization Utilizing a Novel Tyramide Labeling Technique.' *Genomics* 53 (3), 296–299

Topisirovic, I., Siddiqui, N., and Borden, K.L.B. (2009) 'The Eukaryotic Translation Initiation Factor 4E (EIF4E) and HuR RNA Operons Collaboratively Regulate the Expression of Survival and Proliferative Genes'. *Cell Cycle*

Travis, W. D., Colby, T. V., Corrin, B., Shimosato, Y., and Brambilla, E. (1999) *Histological Typing of Lung and Pleural Tumours* Berlin, Heidelberg: Springer Berlin Heidelberg. available from <http://link.springer.com/10.1007/978-3-642-60049-4>

Travis, William D., Brambilla, Elisabeth, Nicholson, A.G., Yatabe, Y., Austin, J.H.M., Beasley, M.B., Chirieac, L.R., Dacic, S., Duhig, E., Flieder, D.B., Geisinger, K., Hirsch, F.R., Ishikawa, Y., Kerr, K.M., Noguchi, M., Pelosi, G., Powell, C.A., Tsao, M.S., and Wistuba, I. (2015) 'The 2015 World Health Organization Classification of Lung Tumors'. *Journal of Thoracic Oncology* 10 (9), 1243–1260.

Uren, P.J., Burns, S.C., Ruan, J., Singh, K.K., Smith, A.D., and Penalva, Luiz O F (2011) 'Genomic Analyses of the RNA-Binding Protein Hu Antigen R (HuR) Identify a Complex Network of Target Genes and Novel Characteristics of Its Binding Sites'. *Journal of Biological Chemistry* 286 (43), 37063–37066

Van Meerbeeck, J.P., Fennell, D. a., and De Ruysscher, D.K.M. (2011) 'Small-Cell Lung Cancer'. *The Lancet* 378 (9804), 1741–1755.

Veas-Perez de Tudela, M., Delgado-Esteban, M., Cuende, J., Bolanos, J.P., and Almeida, A. (2010) 'Human Neuroblastoma Cells with MYCN Amplification Are Selectively Resistant to Oxidative Stress by Transcriptionally Up-Regulating Glutamate Cysteine Ligase.' *Journal of neurochemistry* 113 (4), 819–825

Venables, J.P., Klinck, R., Koh, C., Gervais-Bird, J., Bramard, A., Inkel, L., Durand, M., Couture, S., Froehlich, U., Lapointe, E., Lucier, J.F., Thibault, P., Rancourt, C., Tremblay, K., Prinos, P., Chabot, B., and Elela, S.A. (2009) 'Cancer-Associated Regulation of Alternative Splicing'. *Nature structural & molecular biology* 16 (6), 670–676.

Virolle, T., Krones-Herzig, A., Baron, V., De Gregorio, G., Adamson, E.D., and Mercola, D. (2003) 'Egr1 Promotes Growth and Survival of Prostate Cancer Cells: Identification of Novel Egr1 Target Genes'. *Journal of Biological Chemistry*

Vo, D. T., Abdelmohsen, K., Martindale, J. L., Qiao, M., Tominaga, K., Burton, T.L., Gelfond, J. a. L., Brenner, a. J., Patel, V., Trageser, D., Scheffler, B., Gorospe, M., and Penalva, L. O. F. (2012) 'The Oncogenic RNA-Binding Protein Musashi1 Is Regulated by HuR via MRNA Translation and Stability in Glioblastoma Cells'. *Molecular Cancer Research* 10 (1), 143–155

Wang, Hong, Zeng, F., Liu, Qiao, Liu, H., Liu, Z., Niu, L., Teng, M., and Li, X. (2013) 'The Structure of the ARE-Binding Domains of Hu Antigen R (HuR) Undergoes Conformational Changes during RNA Binding'. *Acta Crystallographica Section D: Biological Crystallography* 69 (3)

Wang, Huiwen, Molfenter, J., Zhu, Hui, and Lou, Hua (2010) 'Promotion of Exon 6 Inclusion in HuD Pre-MRNA by Hu Protein Family Members'. *Nucleic Acids Research* 38 (11), 3760–3770.

Wang, Jing, Liu, Qi, and Shyr, Y. (2015) 'Dysregulated Transcription across Diverse Cancer Types Reveals the Importance of RNA-Binding Protein in Carcinogenesis'. *BMC Genomics* 16 (7), 5.

Wang, Jun, Guo, Y., Chu, H., Guan, Y., Bi, J., and Wang, Baocheng (2013) 'Multiple Functions of the RNA-Binding Protein HuR in Cancer Progression, Treatment Responses and Prognosis'. *International Journal of Molecular Sciences* 14 (5), 10015–10041

Wang, Jun, Wang, Baocheng, Bi, J., and Zhang, Cong (2011) 'Cytoplasmic HuR Expression Correlates with Angiogenesis, Lymphangiogenesis, and Poor Outcome in Lung Cancer'. *Medical Oncology* 28, 577–585

Wang, Jun, Weipeng, Z., Guo, Y., Zhang, B., Xie, Q., Xiang, D., Gao, J., Wang, Baocheng, and Chen, Zhengtang (2009) *The Expression of RNA-Binding Protein HuR in Non-Small Cell Lung Cancer Correlates with Vascular Endothelial Growth Factor-C Expression and Lymph Node Metastasis*. vol. 76

Wang, W., Caldwell, M.C., Lin, S., Furneaux, H, and Gorospe, M (2000a) 'HuR Regulates Cyclin A and Cyclin B1 MRNA Stability during Cell Proliferation'. *The EMBO journal* 19 (10), 2340–2350.

Wang, W., Furneaux, H, Cheng, H., Caldwell, M.C., Hutter, D., Liu, Y, Holbrook, N., and Gorospe, M (2000b) 'HuR Regulates P21 MRNA Stabilization by UV Light.' *Molecular and cellular biology* 20 (3), 760–769

Wang, X. and Tanaka Hall, T.M. (2001) 'Structural Basis for Recognition of AU-Rich Element RNA by the HuD Protein'. *Nature Structural Biology* 8, 141.

Wang, Yang, Li, Yue, Toth, J.I., Petroski, M.D., Zhang, Zhaolei, and Zhao, J.C. (2014) 'N6-Methyladenosine Modification Destabilizes Developmental Regulators in Embryonic Stem Cells'. *Nature cell biology* 16 (2), 191–198.

Wang, Z., Bhattacharya, A., and Ivanov, D.N. (2015) 'Identification of Small-Molecule Inhibitors of the HuR/RNA Interaction Using a Fluorescence Polarization Screening Assay Followed by NMR Validation'. *PLoS ONE* 10 (9)

Ware, M.L., Berger, M.S., and Binder, D.K. (2003) 'Molecular Biology of Glioma Tumorigenesis'. *Histology and Histopathology* 18 (1), 207–216

Wennerberg, K., Rossman, K.L., and Der, C.J. (2005) 'The Ras Superfamily at a Glance'. *Journal of Cell Science* 118 (5), 843–846.

Westermark, U.K., Wilhelm, M., Frenzel, A., and Henriksson, M.A. (2011) 'The MYCN Oncogene and Differentiation in Neuroblastoma.' *Seminars in cancer biology* 21 (4), 256–266

Will, C.L. and Lührmann, R. (2011) 'Spliceosome Structure and Function'. in *Cold Spring Harbor Perspectives in Biology*. vol. 3 (7)

Wu, X., Lan, L., Smith, A., Marquez, R., Wilson, D., Rogers, S., Gao, P., Lovell, S., Karanicolas, J., Dixon, D., Aube, J., and Xu, L. (2015) 'Targeting an "Undruggable" RNA-Binding Protein: Discovery of Small Molecule Inhibitors of HuR for Novel Breast Cancer Therapy'. *Cancer Research* 75 (2449)

Wurth, L. (2012) 'Versatility of RNA-Binding Proteins in Cancer.' *Comparative and functional genomics* 2012 (June), 178525

Yamada, K., Iwayama, Y., Hattori, E., Iwamoto, K., Toyota, T., Ohnishi, T., Ohba, H., Maekawa, M., Kato, T., and Yoshikawa, T. (2011) 'Genome-Wide Association Study of Schizophrenia in Japanese Population'. *PLOS ONE* 6 (6),

Yaman, I., Fernandez, J., Sarkar, B., Schneider, R.J., Snider, M.D., Nagy, L.E., and Hatzoglou, M. (2002) 'Nutritional Control of MRNA Stability Is Mediated by a Conserved AU-Rich Element That Binds the Cytoplasmic Shuttling Protein HuR'. *Journal of Biological Chemistry* 277 (44), 41539–41546

Yan, C. and Higgins, P.J. (2013) 'Drugging the Undruggable: Transcription Therapy for Cancer.'

Biochimica et biophysica acta 1835 (1), 76–85.

Yan, W., Zhang, Y., Zhang, J., Cho, S.-J., and Chen, X. (2012) 'HuR Is Necessary for Mammary Epithelial Cell Proliferation and Polarity at Least in Part via ΔNp63'. *PLOS ONE* 7 (9),

Yang, Y.Y., Yin, G.L., and Darnell, R B (1998) 'The Neuronal RNA-Binding Protein Nova-2 Is Implicated as the Autoantigen Targeted in POMA Patients with Dementia.' *Proceedings of the National Academy of Sciences of the United States of America* 95 (22), 13254–13259

Yano, M., Hayakawa-Yano, Y., and Okano, H. (2016) 'RNA Regulation Went Wrong in Neurodevelopmental Disorders: The Example of Msi/Elav RNA Binding Proteins'. *International Journal of Developmental Neuroscience* 1–7.

Yao, K.M., Samson, M.L., Reeves, R., and White, K (1993) 'Gene Elav of Drosophila Melanogaster: A Prototype for Neuronal-Specific RNA Binding Protein Gene Family That Is Conserved in Flies and Humans.' *Journal of neurobiology* 24 (6), 723–739

Ye, J., Coulouris, G., Zaretskaya, I., Cutcutache, I., Rozen, S., and Madden, T.L. (2012) 'Primer-BLAST: A Tool to Design Target-Specific Primers for Polymerase Chain Reaction.' *BMC bioinformatics* 13, 134

Yi, R., Qin, Y., Macara, I.G., and Cullen, B.R. (2003) 'Exportin-5 Mediates the Nuclear Export of Pre-MicroRNAs and Short Hairpin RNAs'. *Genes and Development* 17 (24), 3011–3016

Zaharieva, E., Chipman, J.K., and Soller, M. (2012) 'Alternative Splicing Interference by Xenobiotics.' *Toxicology* 296 (1–3), 1–12.

Zaharieva, E., Haussmann, I.U., Bräuer, U., and Soller, M. (2015a) 'Concentration and Localization of Co-Expressed ELAV/Hu Proteins Control Specificity of MRNA Processing'. *Molecular and Cellular Biology* MCB.00473-15

Zaharieva, E., Haussmann, I.U., Bräuer, U., Soller, M., Brauer, U., and Soller, M. (2015b) 'Concentration and Localisation of Coexpressed ELAV/Hu Proteins Control Speicificity of MRNA Processing'. *Molecular and cellular biology* 35 (18), MCB.00473-15

Zhang, Cong, Xue, G., Bi, J., and Geng, M. (2014) *Cytoplasmic Expression of the ELAV-like Protein HuR as a Potential Prognostic Marker in Esophageal Squamous Cell Carcinoma*. 13277

Zhu, Haifeng, Berkova, Z., Mathur, R., Sehgal, L., Khashab, T., Tao, R.-H., Ao, X., Feng, L., Sabichi, A.L., Blechacz, B., Rashid, A., and Samaniego, F. (2015) 'HuR Suppresses Fas Expression and Correlates with Patient Outcome in Liver Cancer'. *Molecular Cancer Research* 13 (5), 809 LP – 818.

Zhu, Hui (2009) *A New Journey Of Hu Protein Family*. VDM Verlag Dr. Muller

Zhu, Hui, Hasman, R.A., Barron, V.A., Luo, G., and Lou, Hua (2006) *A Nuclear Function of Hu Proteins as Neuron-Specific Alternative RNA Processing Regulators*. 17 (December), 5105–5114

Zhu, Hui, Hinman, Melissa N, Hasman, R. a, Mehta, P., and Lou, Hua (2008) 'Regulation of Neuron-Specific Alternative Splicing of Neurofibromatosis Type 1 Pre-MRNA.' *Molecular and cellular biology* 28 (4), 1240–51.

Zhu, Hui, Zhou, H.-L., Hasman, R. a, and Lou, Hua (2007) 'Hu Proteins Regulate Polyadenylation by Blocking Sites Containing U-Rich Sequences.' *The Journal of biological chemistry* 282 (4), 2203–10.

Zong, F.Y., Fu, X., Wei, W.J., Luo, Y.G., Heiner, M., Cao, L.J., Fang, Z., Fang, R., Lu, D., Ji, H., and Hui, J. (2014) 'The RNA-Binding Protein QKI Suppresses Cancer-Associated Aberrant Splicing'. *PLoS Genetics* 10 (4)

Zuber, J., Tchernitsa, O.I., Hinzmann, B., Schmitz, A.-C., Grips, M., Hellriegel, M., Sers, C., Rosenthal, A., and Schäfer, R. (2000) 'A Genome-Wide Survey of RAS Transformation Targets'. *Nature Genetics* 24, 144.